4-1-2010

A Numerical Modeling Assessment for the Implementation of a Runoff Reduction Strategy Plan for the Restoration of Thalia Creek, Virginia Beach

Mac Sisson
Virginia Institute of Marine Science

Jian Shen
Virginia Institute of Marine Science

W. G. Reay
Virginia Institute of Marine Science

Eduardo J. Miles
Chesapeake Bay National Estuarine Research Reserve

Albert Y. Kuo
Virginia Institute of Marine Science

See next page for additional authors

Recommended Citation

Authors

Mac Sisson, Jian Shen, W. G. Reay, Eduardo J. Miles, Albert Y. Kuo, and Harry V. Wang

A NUMERICAL MODELING ASSESSMENT FOR THE IMPLEMENTATION OF A RUNOFF REDUCTION STRATEGY PLAN FOR THE RESTORATION OF THALIA CREEK, VIRGINIA BEACH
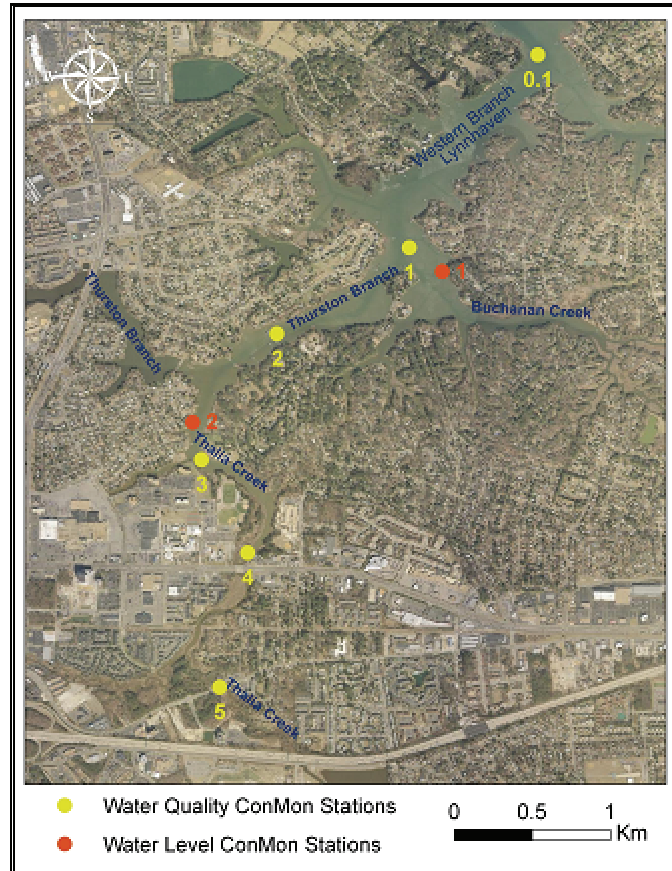
Mac Sisson, Jian Shen, William Reay, Eduardo Miles,
Albert Kuo, and Harry Wang

EXECUTIVE SUMMARY

1. The Norfolk District of the US Army Corps of Engineers and the City of Virginia Beach are working together on a cost-shared basis to identify and assess potential water quality problems in the Thurston Branch-Thalia Creek (TB-TC) system, a small tributary at the head of the Western Branch of the Lynnhaven River. In February 2009, these agencies contracted with the Virginia Institute of Marine Science (VIMS) for field monitoring surveys of TC and adjacent TB and the development of high-resolution hydrodynamic and water quality models for the TB-TC system capable of assessing the impact of nutrient and fecal coliform reductions from its watershed.

2. VIMS performed field surveys in summer 2009 spanning the TC-TB regions. High-frequency measurements of depth (surface elevation), salinity, water temperature, dissolved oxygen, chlorophyll, and turbidity were made at 5 locations in this region for periods of approximately ten days to two weeks each commencing in June, July, and August of 2009. Grab sample surveys were conducted at over 20 locations spanning this region on June 30, July 27, and August 27, 2009. These grab samples were each analyzed for water temperature, salinity, pH, dissolved oxygen, dissolved oxygen percent saturation, phosphate (PO_4), total dissolved phosphorus (TDP), ammonium (NH_4), nitrite (NO_2), nitrate-nitrite (NO_{23}), total dissolved nitrogen (TDN), the ratio of DIN:DIP, chlorophyll-a, pheo, fecal coliform, and *E. Coli*. It is noted that the parameters of dissolved organic phosphorus (DOP), nitrate (NO_3), dissolved inorganic nitrogen (DIN), and dissolved organic nitrogen (DON) were then calculated from these measurements. Two 30-day, high-frequency tide gauge deployments were conducted at locations in TC-TB in the latter part of 2009. All these data were added to the VIMS Lynnhaven River database. Additionally, sediment oxygen demand was measured and an additional grab sample survey was used to characterize the grain size distributions for more than 20 locations throughout the TB-TC system.

3. High (>20 to ≤ 60 ug·L^{-1}) to hyper-eutrophic (>60 ug·L^{-1}) concentrations of chl *a* were observed within the TB-TC system. Mean chl *a* concentrations and variability of measurements increased with distance upstream. High pheopigment to chl *a* ratios, particularly in the upper TC reaches, suggested a relatively degraded phytoplankton population possibly due to stress (e.g., light, salt) or elevated grazing pressures.

4. Dissolved oxygen patterns within the TB-TC system was highly dynamic and exhibited a strong diurnal signal driven by water temperature variation and biological activities. While most severe and chronic in the upper reaches, hypoxia (defined as $DO_{conc} \leq 2$ mg·L^{-1}) was observed throughout the TB-TC system. The duration of hypoxia ranged from 15 minutes to over 34 hours for a single event. The set-up and duration of severe hypoxia was influenced by solar insolation, timing of ebb-tide and freshwater input derived from storms. We have found that the oxygen and chlorophyll-a do not oscillate in the same frequency. DO is dominated by diurnal oscillations, while chlorophyll-a is more semi-diurnal. These observations indicate that benthic or attached algae may contribute to the DO diurnal oscillation which is less influenced by the tide.

4. All high-frequency monitoring stations exhibited negative mean net ecosystem metabolism (NEM) values ranging from -1.8 to -0.5 g O_2 m^{-2}·day^{-1} and respiration rates varying from

10.09-16.97 g O_2 m^{-2}·day^{-1}. Net summer heterotrophy increased with distance upstream and suggests that significant amounts of allochthonous sources of carbon are helping to fuel the high respiration rates. Sediment oxygen demand accounted for between 10-15% of open water respiration rates in the upper TC reach. Water column vertical light extinction coefficient (k_e) within the TB-TC system varied from 2.8 to 6.3 m^{-1} with corresponding $z_{1\%}$ depths (depths at which 1% of surface light is transmitted) ranging from 0.7 to 1.6 m, suggesting a limited role of benthic primary production in the channel regions in contrast to the shallower, broad shoal regions.

5. VIMS has completed a successful development of an integrated numerical modeling framework for the TB-TC system. This framework combines a high-resolution 3D hydrodynamic model (HEM-3D hydro) that provides the required transport for a water quality model (HEM-3D water quality) that, in turn, provides intra-tidal predictions of 23 water quality state variables. The hydrodynamic model underwent an extensive calibration for surface elevation, salinity, and temperature and the water quality model was calibrated for dissolved oxygen and chl-a.

6. Using the calibrated water quality model for the TB – TC system in the short-term (Julian Days 180 through 260 of 2009) simulations, several sensitivity tests were performed to assess the roles of non-point source (NPS) loadings and inputs from the bottom sediments. In these 80-day simulations, it was determined that even the total elimination of the NPS nutrients loadings could not bring the TC water quality for dissolved oxygen into compliance with state water quality standards within a short period due to high deposition of organics. An 80-day sensitivity test of a clean ("no sediment") river bottom was also conducted, and again DO levels often fell below the instantaneous criterion for DO (i.e., 4.3 mg·L^{-1}). The sensitivity test suggests that removal of sediment deposition without reducing nonpoint source loading will not solve the DO problem as nutrients can be quickly deposited to the bottom during high runoff events. Next, sensitivity tests were run that combined the clean river bottom and a 50% NPS reduction, and the results of these tests were that DO levels consistently exceeded the 4.3 mg·L^{-1} instantaneous minimum. Lastly, NPS loadings reductions were run as long-term (i.e., 4-year) simulations testing both 50% and 70% reductions from the TC watershed. It was determined that the DO criterion can be attained with approximately 70% reduction of nitrogen and carbon, and 40% reduction of phosphorus.

7. Fecal coliform bacteria (FCB) densities exceeded Commonwealth contact standards (> 200 MPN 100· ml^{-1}) in the upper reaches of TC on a routine basis while the lower and more open reaches of TB typically exhibited FCB densities between shellfish waters and recreational contact standards (> 14 MPN to ≤ 200 MPN·100 ml^{-1}). Findings are consistent with an increased "land effect" due to increases in the ratio of shoreline to water volume in the upper tidal reaches. Elevated FCB densities were also observed after periods of high rainfall. The relationship between FCB and *E. coli* density was strong ($r^2 \geq 0.95$) for two of the three surveys; heavy rainfall and loadings of ubiquitous FC positive microbes may explain discrepancies with the third survey. Sources of FCB to the TB-TC system would include nonpoint source runoff from urbanized and natural lands, and direct domestic and wild animal loadings. Additional study is required to source track and differentiate FCB loadings and to determine if true health concerns exist.

8. A fecal coliform model was also developed throughout the TB–TC system and simulations were performed for the fecal coliform load reductions. A long-term calibration was performed comparing model predictions with bi-monthly observations at VA-DEQ Station 7-THA000.76 for the period 2003-2006. Additionally, spatial comparisons were made between fecal coliform model predictions and the observations at more than 20 grab sample locations for two surveys (July 27, 2009 and August 30, 2009). The calibrated model was then used to assess fecal coliform loading reductions of 70%, 90%, 95% and 99%. It was determined that the swimming criterion (200 MPN·100 ml^{-1}) could be attained with approximately 90-95% reduction, whereas the shellfish harvesting criteria (14 MPN·100 ml^{-1} for 30-day geometric mean and 43 MPN·100 ml^{-1} for the 90th percentile) required a fecal coliform reduction of 99%.

Findings or recommendations contained herein do not constitute Corps of Engineers approval of any project(s) or eliminate the need to follow normal regulatory permitting processes.

TABLE OF CONTENTS

LIST OF TABLES

LIST OF FIGURES

xi

xv

CHAPTER I. INTRODUCTION

The Lynnhaven River includes the Eastern Branch, Western Branch, Long Creek, Broad Bay, Crystal Lake, Linkhorn Bay and all of the tributaries. A great deal of effort has been extended by the City of Virginia Beach and the US Army Corps of Engineers (Norfolk District) towards restoring and protecting the Lynnhaven River.

Thalia Creek (TC) is a small tidal subestuary at the head of the Western Branch that is connected to Thurston Branch (TB) directly downstream. Also downstream and located northeast of TC is Buchanan Creek (BC). These 3 water bodies are shown in Figure I.1. For purposes of this project, it should be noted that both the modeling domain and the field monitoring survey areas included TB as well as TC and their combined areas are hereby referred to as the TB-TC system.

TC is extremely narrow, ranging in width from 5 to 30 meters over its 4-km length. TB is much wider (150 to 250 m) over its 3-km length. Both water bodies are extremely shallow, with average depths between 1 and 2 meters. A navigable channel extends throughout all of TB, but only through a portion of TC identified as grab sample station 10 in Figure II.3. In the upstream portion of TC, there are two water bodies that are noteworthy. Lake Windsor is brackish water fed by TC. Lake Trashmore is a freshwater lake.

The Virginia Department of Environmental Quality (VA-DEQ) has bimonthly measured key water quality parameter at 16 primary Lynnhaven monitoring stations that span all branches. This monitoring program began in the 1980s, and therefore provides long-term records at these stations   Analysis of the data from the VA-DEQ station located in TC (i.e., 7-THA000.76) shows the highest long-term nutrient and fecal coliform bacteria (FCB) levels of any of the 16 stations in the Lynnhaven system.

Nutrient concentrations have led to eutrophic conditions in Thalia Creek during warmer months and subsequently to low dissolved oxygen levels (i.e., hypoxia), causing adverse impacts to benthic communities in Thalia Creek.

Many concerns regarding water quality conditions in the Thalia Creek area were described in the Lynnhaven River Restoration Reconnaissance Report (US ACE, 2002), particularly regarding tidal wetlands and siltation. A considerable acreage of marshland has been lost due to "dredging, filling, bulkheading, and channelization, and, to a lesser degree, natural erosional properties" (Malcolm Pirnie, 1980). It has been noted that siltation, such as is found in the Thalia Creek area, may be one of the causes of degraded water quality in these upstream reaches.

The agencies in charge of the present development efforts are the Norfolk District, U.S. Army Corps of Engineers (ACE), representing the Federal Government, and the City of Virginia Beach, acting as the Local Sponsor. These agencies signed a feasibility cost-sharing agreement and embarked on determining suitable and acceptable means for designing and implementing the environmental restoration of the Lynnhaven. During

discussions with personnel from VIMS and URS Corporation of Virginia Beach, it was resolved that a fully comprehensive system, including spatially high-resolution numerical modeling and watershed loading estimation, was required in order to address the issues cited in the reconnaissance report and to provide the management option of a control strategy of attaining the required endpoints for environmental restoration.

In February 2009, the ACE (Norfolk District) and the City of Virginia Beach contracted with VIMS for the development of hydrodynamic and water quality models for the TB-TC system receiving waters and with URS Corporation for an adapted version of its HSPF (Hydrological Simulation Program – FORTRAN) watershed model to provide both freshwater flows and nutrient and sediment loadings from the Lynnhaven River Watershed for this region.

This report provides the results of VIMS efforts as related to the collection of temporally high-resolution water quality data, grab sample surveys for key water quality parameters, sediment characterization and sediment oxygen demand (SOD) studies, and the physical-water quality integrated numerical modeling exercises. The objectives of these efforts were to assess the roles of non-point source and internal loadings of nutrients and FCB in support of efforts to reduce eutrophic and microbiological water quality issues within the TB-TC system.
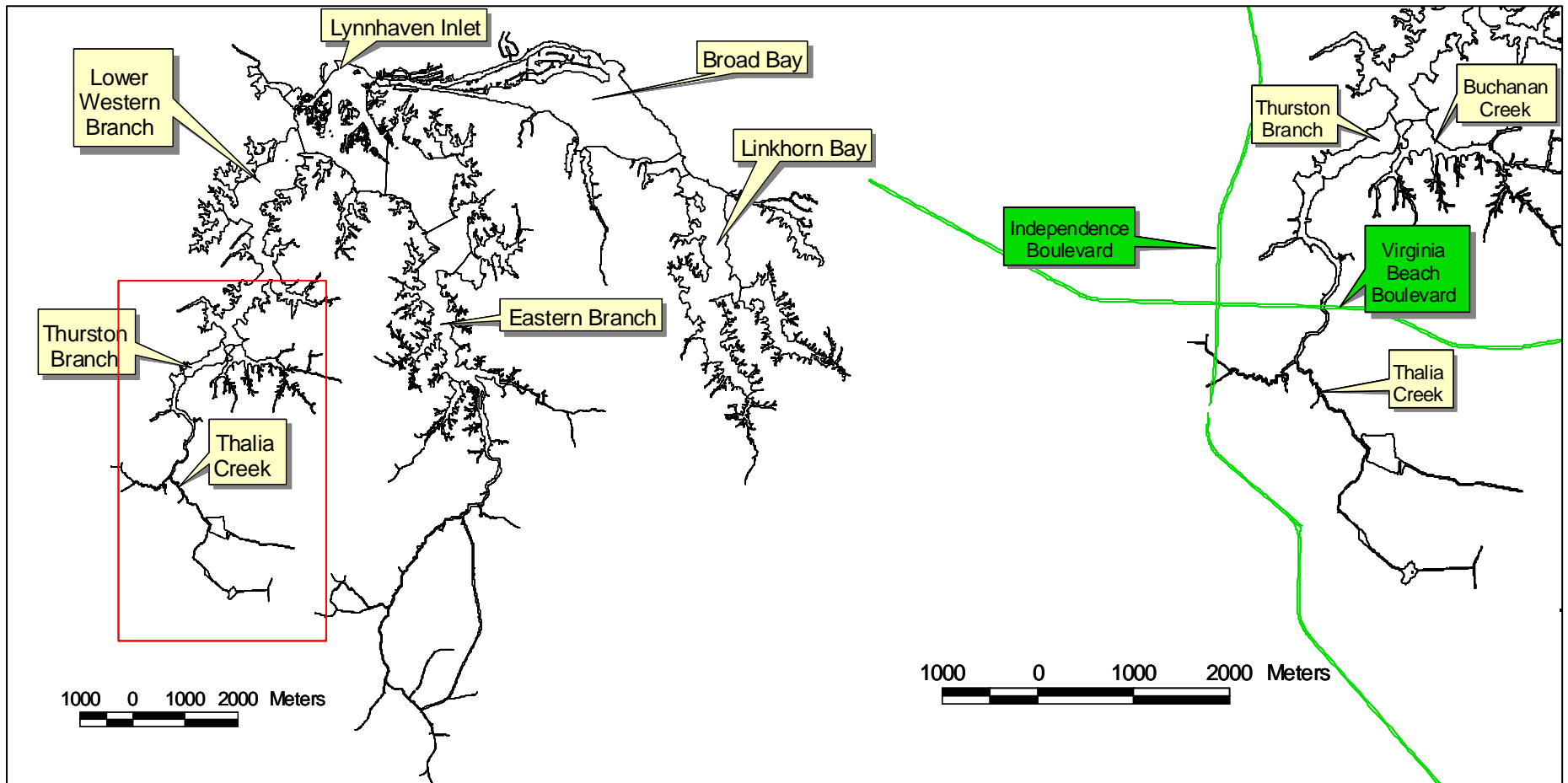
Figure I.1. Location of Thalia Creek, Thurston Branch, and Buchanan Creek in the upper Western Branch of the Lynnhaven River. Locations of major local road systems are shown in green on the right panel.

3

CHAPTER II. FIELD OBSERVATIONS

II-1 Introduction

Field studies were conducted in the tidal Thurston Branch - Thalia Creek (TB-TC) system to provide information on the current summertime water quality condition of this waterbody, to offer insight as to important controlling processes, and to be used for calibration and verification of both hydrodynamic and water quality models. Additional samples were collected in the upper Western Branch of Lynnhaven River and in Buchanan Creek (BC) which confluences with TB from the southeast. Prior to the present study, relatively few field observations were available for the TB-TC system. A previous study of BC by Ho et al. (1977) was conducted when the Birchwood Garden Sewage Treatment Plant was still operational. This study noted that both point and nonpoint source nutrient loads would have to be controlled in order to prevent the continuation of water quality problems in BC. Additionally, a long-term water quality station in the upper portion of TC has and continues to be monitored by Virginia's Department of Environmental Quality (VA-DEQ) for nutrients and bacteria parameters; VA-DEQ Station 7-THA000.76 coincides with the high-frequency ConMon water quality Station 4 of this report.   Field studies encompassed the following efforts: (1) high frequency observations of water level and water quality at fixed stations (ConMon stations), (2) three water quality grab sample surveys, (3) vertical water quality profiles, and (4) sediment studies that included both sediment characterization and benthic oxygen flux components. Sampling time periods for the studies are provided in Figure II.1. Sample station location maps for each effort are provided in Figure II.2 for ConMon stations and Figure II.3 for the grab sample survey stations. Sediment characterization sampling points coincided with the water quality grab sample stations, vertical profiles were collected at the ConMon station locations, and benthic flux studies were conducted at ConMon sampling Stations 4 and 5. Regional (Oceana NAS) precipitation and wind data over the duration of the field studies is provided in Figure II.4.
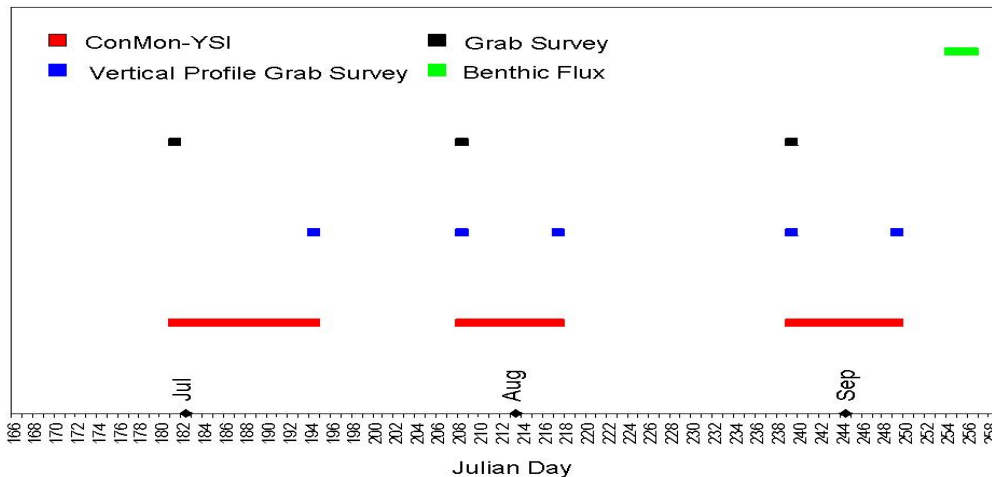
Figure II.1. Timeline for field data collection efforts in 2009.
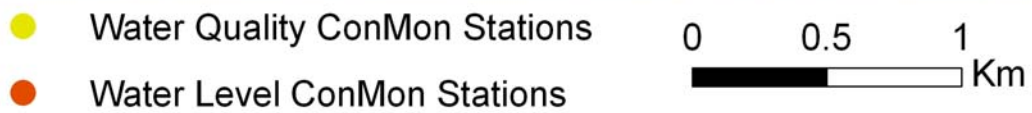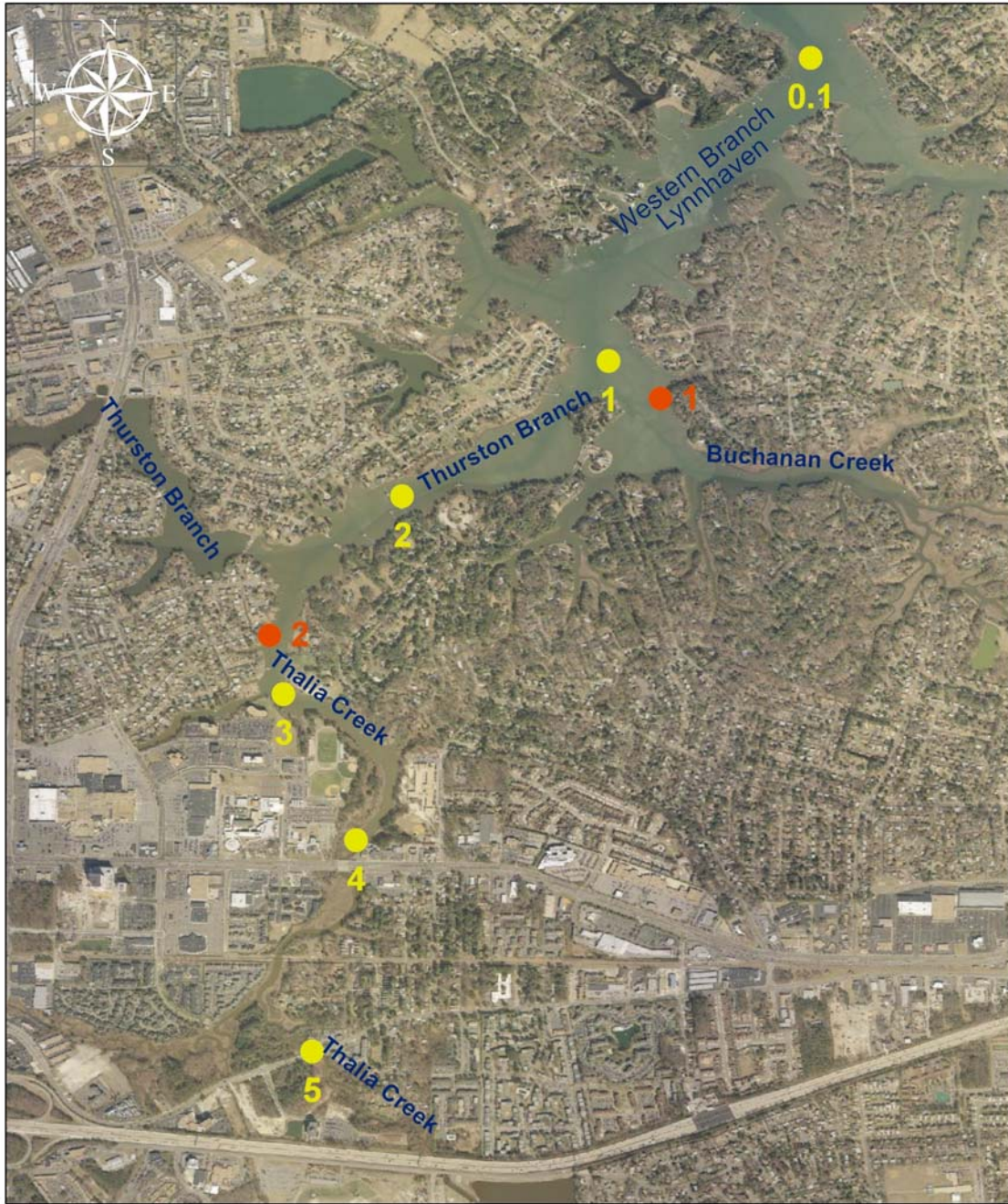
Figure II.2. Sampling station locations for high-frequency, ConMon water level and water quality measurements conducted in 2009. Note: ConMON water quality Stations 4 and 5 correspond to VA-DEQ water quality Stations 7-THA000.76 and THA001.39, respectively.
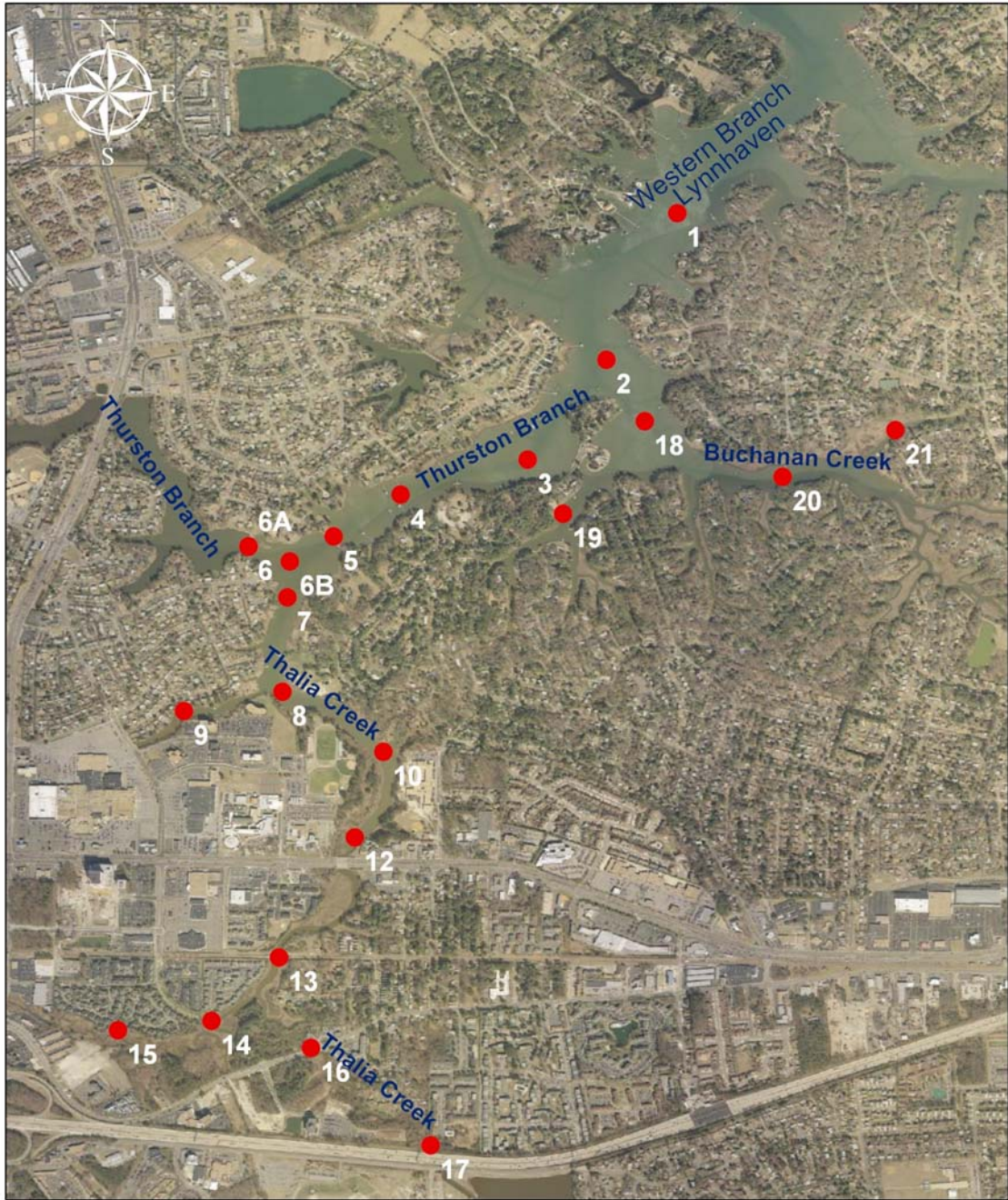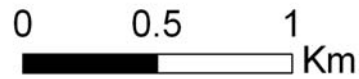
Figure II.3. Sampling station locations for water quality and sediment grab sampling surveys conducted in 2009. Note: Stations 12 and 16 correspond to VA-DEQ water quality Stations 7-THA000.76 and THA001.39, respectively.
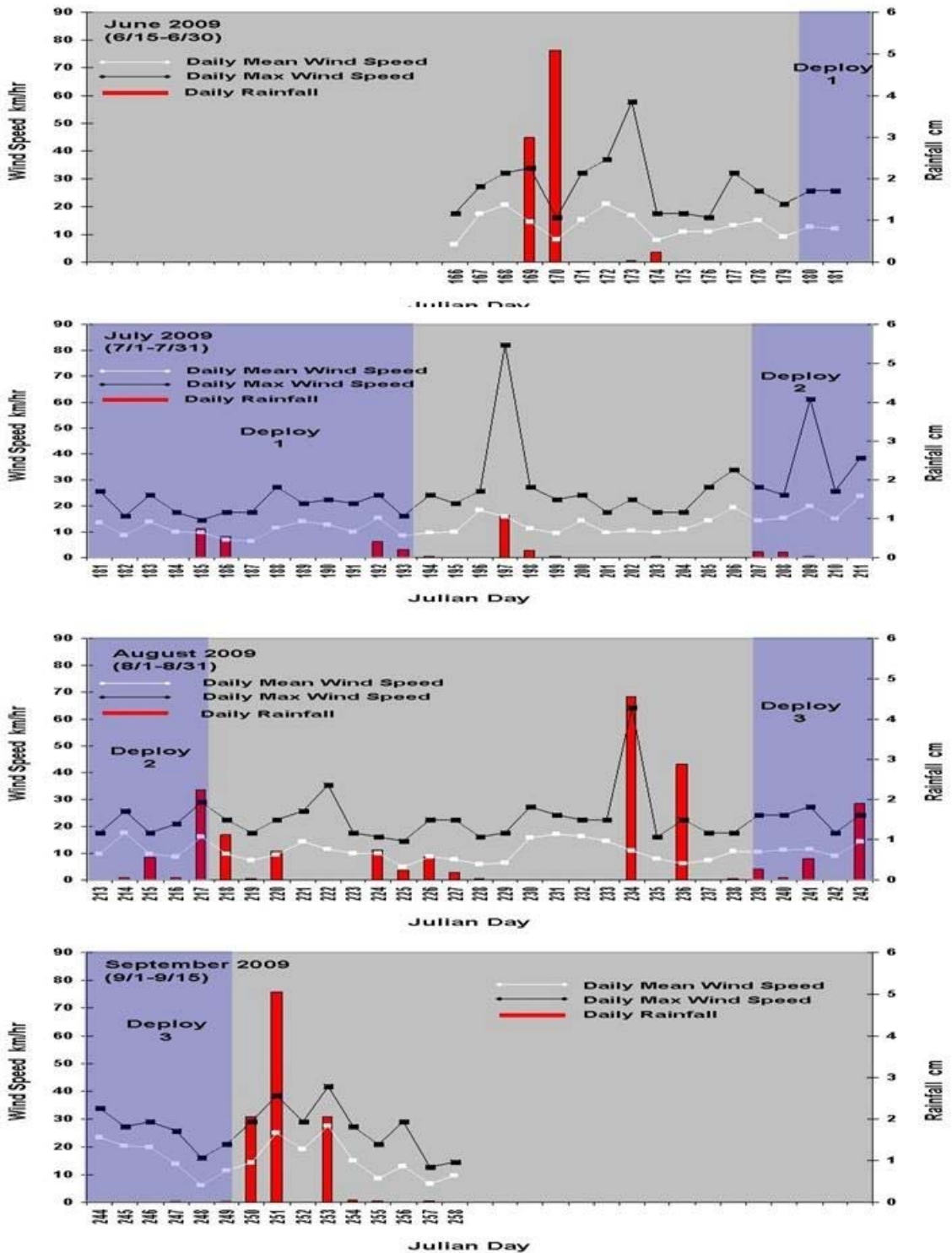
Figure II.4. Precipitation (cm) and wind speed (km/hr) data derived from Oceana
NAS (13769) NOAA National Weather Service station located in Oceana, VA.
(36.817N 76.033W). Blue shaded regions identify time periods when high
frequency water quality observations (ConMon stations) were being collected.
Data source: NOAA National Climatic Data Center. Note: Data is based on local
standard time.

7

II-2 High Frequency Observations at Fixed (ConMon) Stations

This study established synoptic, continuous monitoring (ConMon) stations in the TB-TC system to provide information on water level and water quality. Two ConMon water level stations, one near the mouth of TB (water level Station 1) and the other in the upper reaches of TC (Figure II.2), were established in order to determine tide characteristics over a single, 30^+ day period (October 15 – November 18, 2009). Five ConMon water quality stations were established within tidal portions of TB and TC along a main channel transect that captured the broad salinity regimes observed within the TB-TC system (Figure II.2). An additional station was established in the upper reaches of the Western Branch of the Lynnhaven River (ConMon Station 0.1) on the final deployment.

ConMon water quality stations were deployed on three separate occasions beginning in June and ending in September 2009. Deployment periods lasted between 10-13 days depending on the level of sensor biofouling (see Table II.1 for greater detail; Note: all times are referenced to Eastern Standard Time (EST)).

Table II.1. ConMon water quality station deployment time periods (June-September 2009).

Location	Deployment No.	Start date (time)	End date (time)	No. of Obs.
Station 1	1	06/30/09 (1515)	07/13/09 (1415)	1245
Station 2	1	06/30/09 (1530)	07/13/09 (1445)	1246
Station 3	1	06/30/09 (1600)	07/13/09 (1515)	1248
Station 4	1	06/30/09 (1145)	07/13/09 (1215)	1251
Station 5	1	06/30/09 (1330)	07/13/09 (1245)	1246
Station 1	2	07/27/09 (0845)	08/05/09 (1045)	873
Station 2	2	07/27/09 (0915)	08/05/09 (1130)	874
Station 3	2	07/27/09 (1000)	08/05/09 (1145)	872
Station 4	2	07/27/09 (1300)	08/05/09 (1345)	868
Station 5	2	07/27/09 (1430)	08/05/09 (1400)	863
Station 0.1	3	08/27/09 (1400)	09/06/09 (1000)	945
Station 1	3	08/27/09 (1130)	09/06/09 (1030)	957
Station 2	3	08/27/08 (1200)	09/06/09 (1045)	956
Station 3	3	08/27/09 (1230)	09/06/09 (1130)	957
Station 4	3	08/27/09 (0815)	09/06/09 (1115)	973
Station 5	3	08/27/09 (0915)	09/06/09 (1315)	977

ConMon water level stations were equipped with YSI 6600 data sondes outfitted with vented pressure sensors and the YSI 6560 Temperature/Specific Conductance sensor. ConMon water level station sondes were deployed at a fixed depth off homeowner piers and GPS located. ConMon water quality stations were equipped with YSI 6600 data sondes with the Clean Sweep Extended Deployment System and sampled at 15-minute intervals. Measured parameters included water depth (unvented pressure sensor), specific conductance (YSI 6560 sensor), percent dissolved oxygen saturation (%DO_{sat}; YSI 6150 ROX and 6562 Rapid Pulse sensor), pH (YSI 6561 sensor), turbidity (YSI 6136 sensor) and chlorophyll fluorescence (YSI 6025 sensor); salinity and dissolved oxygen concentrations (DO_{conc}) were calculated parameters.

At each station, a mooring anchor secured the instrument approximately 0.3-0.4 meters above the bottom substrate and a float immediately above the instrument kept the unit in a vertical position. All ConMon water quality stations were marked with a surface buoy and GPS located. All pre and post deployment calibrations and maintenance were completed in accordance with the YSI, Inc. operating manual methods (YSI 6-series Environmental Monitoring Systems Manual; YSI, Inc. Yellow Springs, OH).

II-2-1 30$^+$ Day Water Levels

Water level times series from the 30$^+$ day deployment (10/15 – 11/18/2009) are shown in Figure II.5 with extracted major tidal constituents presented in Table II.2. Tidal constituent information was generated through harmonic regression analysis using a least squares method. Results indicate that the tide exhibits standing wave characteristics as it propagates between the mouth of TB and the upper reaches of TC. Tidal range was on the order of 0.6 meters and phase differences for most constituents are within several minutes (exceptions: S_2, K_1, and O_1). It should be noted that the end of the deployment period was influenced by Tropical Storm Ida that re-intensified and stalled off the mid-Atlantic coast for three days resulting in strong onshore winds that subjected shorelines to strong storm tides and rainfall on the order of 15-20 cm.

II-2-2 Water Depth

Water depth time series plots for each ConMon water quality station are shown in Figures II.6, II.7, and II.8 for deployment periods 6/30-7/13/2009, 7/27-8/5/2009 and 8/27-9/6/2009, respectively. Water depths were calculated based on instrument height off the bottom. It should be noted that water level patterns suggest that mooring lines did not remain taut during selected periods of low tide. ConMon water quality Station 0.1 was not impacted due to elevated water depths as compared to ConMon water quality stations 2-4, as was ConMon water quality Station 5 which was secured directly to the mooring anchor due to shallow water conditions. From inspection of data not impacted by non-taut mooring lines, the system exhibited standing wave characteristic and a tidal range of approximately 0.5 meters; results are consistent with the 30$^+$-day water level study. These water depth data, as well as water level data from the 30$^+$-day study were used to support high-frequency model predictions of surface elevations presented in Chapter IV, Section IV-1-3 of this report.
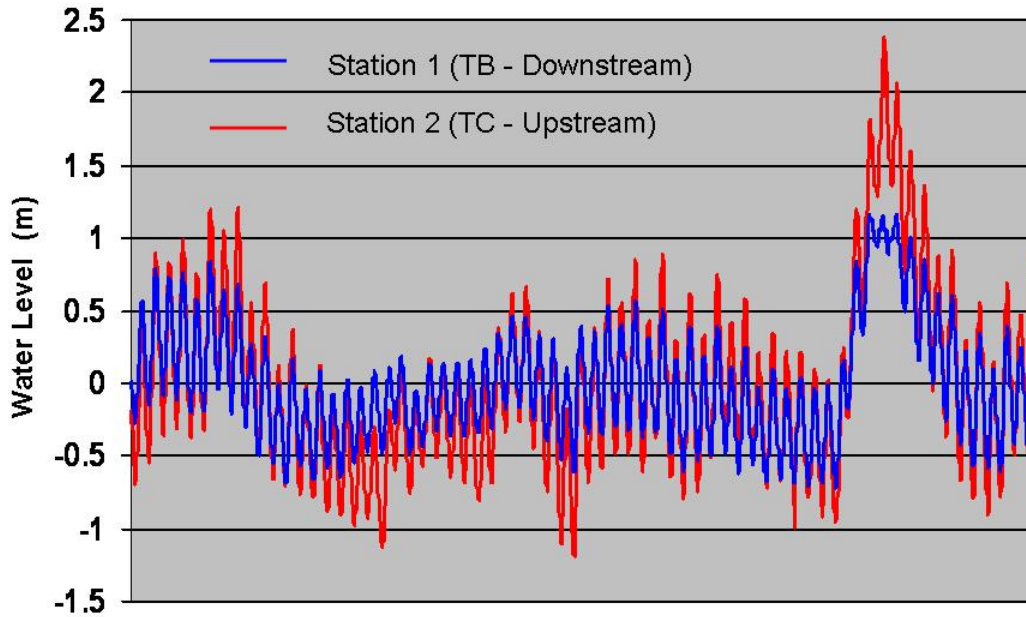
Figure II.5. Thurston Branch (Station 1) and Thalia Creek (Station 2) 30^+ day water levels relative to MWL at ConMon Stations 1-5.

Table II.2. Amplitudes and phases of major tidal constituents extracted from 30^+ day records of water level within the TB-TC system. Period of record: 10/15-11/18/2009.

	Station (Location)			
Constituent	**Station 1 (TB, downstream)**		**Station 2 (TC, upstream)**	
	Amplitude (cm)	**Phase (minutes)**	**Amplitude (cm)**	**Phase (minutes)**
M_2	29.6	165.0	29.6	169.2
S_2	5.8	-299.6	6.4	-336.1
N_2	3.3	273.1	4.5	276.4
K_1	6.4	-150.6	5.4	-239.5
M_4	2.5	97.2	2.5	95.9
O_1	2.4	580.2	2.3	518.5
M_6	1.6	-70.5	1.1	-82.5
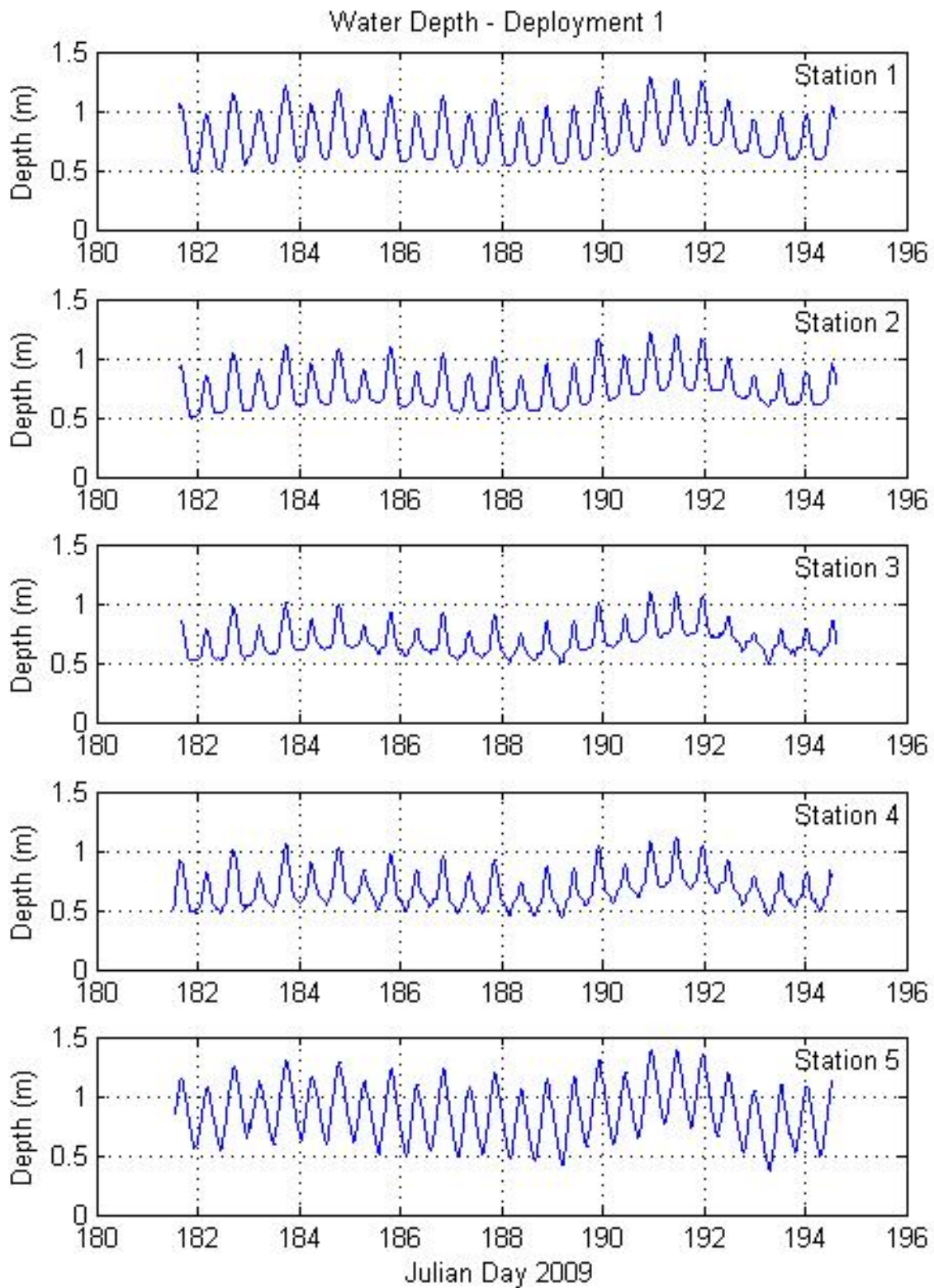
Figure II.6. ConMon water quality station water depth – Thurston Branch -
Thalia Creek Deployment 1 (June 30 – July 13, 2009).

11
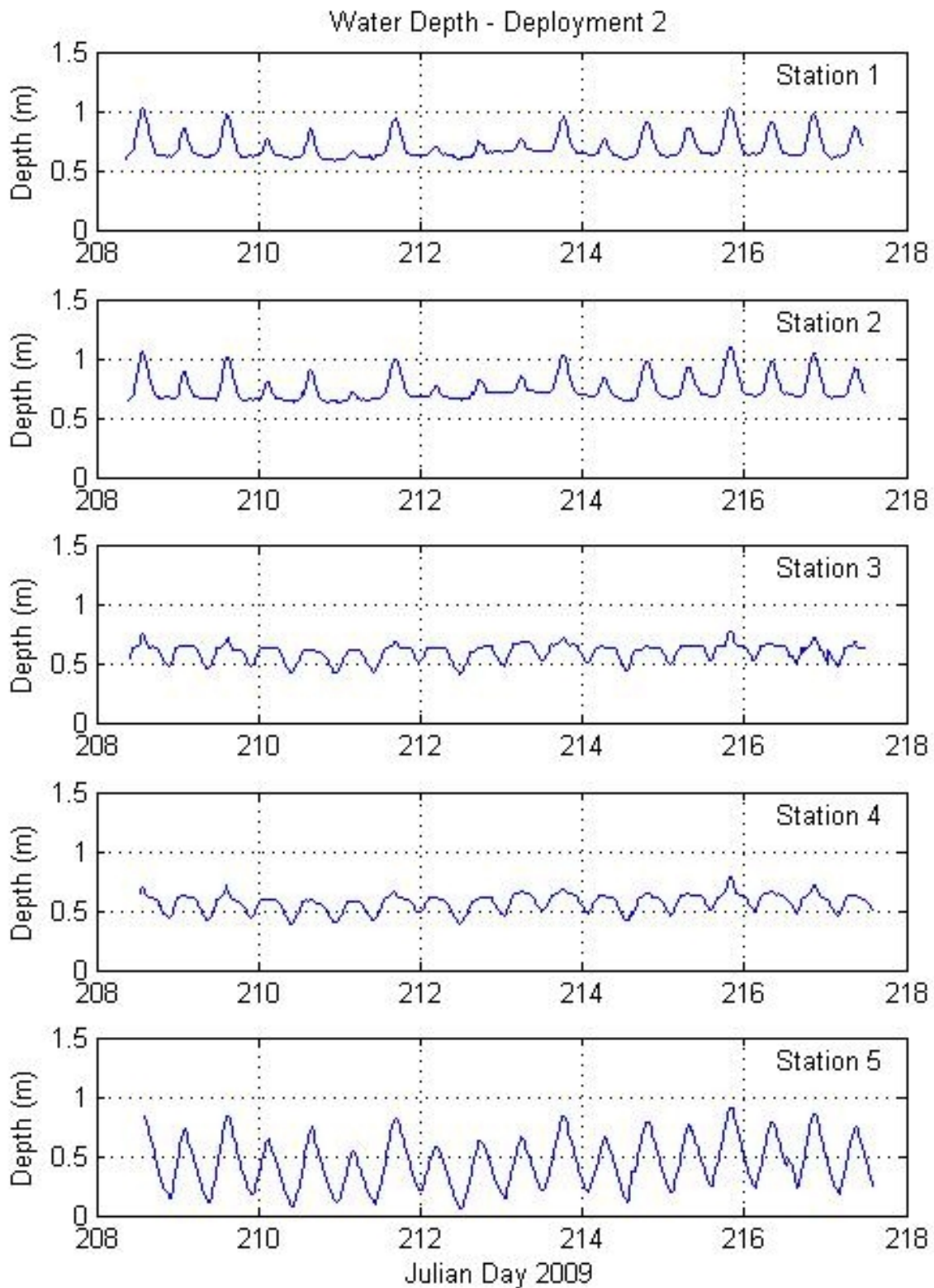
Figure II.7. ConMon water quality station water depth – Thurston Branch - Thalia Creek Deployment 2 (July 27 – August 5, 2009).
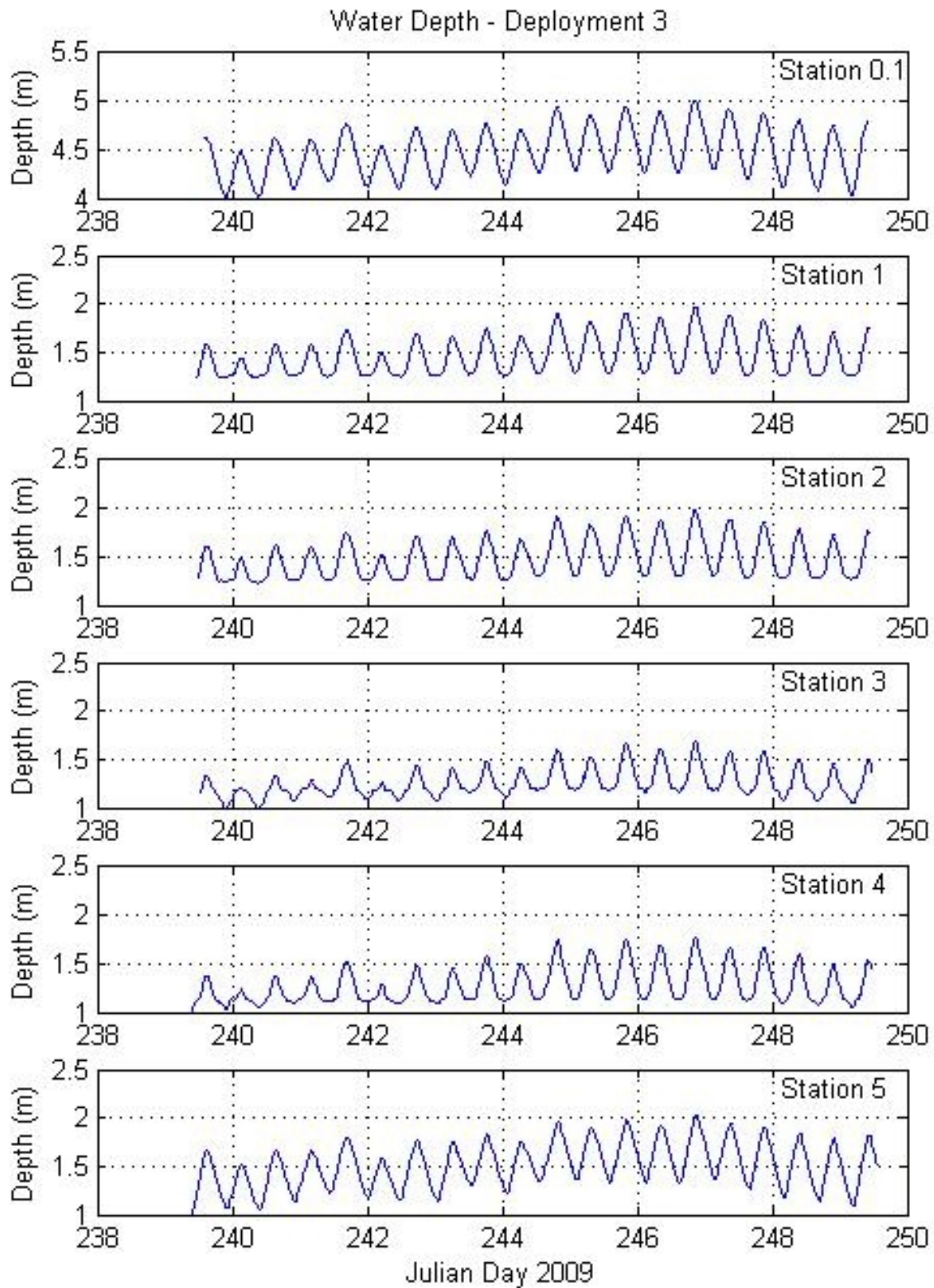
Figure II.8. ConMon water quality station water depth - Thurston Branch -Thalia
Creek Deployment 3 (August 27 – September 6, 2009).

II-2-3 Water Temperature

Water temperature time series plots for each ConMon water quality station are shown in Figures II.9, II.10, and II.11 for deployment periods 6/30-7/13/2009, 7/27-8/5/2009 and 8/27-9/6/2009, respectively. Summary statistics for individual stations by deployment period are provided in Table II.3. During periods of instrument deployment, water temperatures ranged between 22.4 and 33.6 ^{o}C. Mean water temperature over a deployment period was relatively similar between stations; average temperature for deployments 1 through 3 were on the order of 28, 29-30 and 26-27 ^{o}C, respectively. While overall mean deployment period temperatures were within 1 ^{o}C between all stations, the middle (ConMon water quality Stations 3 and 4) and upstream region (ConMon water quality station 5) generally exhibited greater variability in daily temperatures. Water temperatures showed a daily oscillation with higher temperature during daytime and lower temperature during the night with differences on the order of 2-2.5 ^{o}C in the lower reaches and 4-4.5 ^{o}C in the middle and upper reaches. When not influenced by storm events, the upper reaches generally exhibited higher daytime temperatures during the summer period, and in some cases, lower minimum temperatures during night time hours. This is presumably due to the shallower and narrower channel in the upper portions of TB-TC having a lower volume of water and thus being more susceptible to heating and cooling of water by ambient air.

Fluctuations in water temperature due to frontal systems with associated rainfall/runoff were also observed in the TB-TC system. This can be best exemplified by storm events that occurred during July 5-6, 2009 (Julian days: 186-187; 1.3 cm of rainfall; see Figure II.9) and August 3, 2009 (Julian day: 243; 1.9 cm of rainfall; see Figure II.11) where water temperatures dropped 3 and up to 7 ^{o}C, respectively. Recovery of diel temperature patterns within estuarine waters could take on the order of days following a significant rainfall event.

Water temperature is an important element of water quality through its influence on biological activity and water chemistry. However, for tidal waters of Virginia, water temperature standards are only established to control heated wastewater discharge and therefore would not apply to the TB-TC system. It should be noted that watershed development also has the potential to impact smaller-scale water bodies through clearing of riparian vegetation and the relative warming of storm runoff from hardened surfaces versus vegetative cover. In this study, water temperatures regularly exceeded 25 ^{o}C at all stations and maximum temperatures equal to or exceeding 30 ^{o}C were observed at all stations. These temperatures would support relatively high rates of algal productivity and microbial respiration and low dissolved oxygen saturation levels.
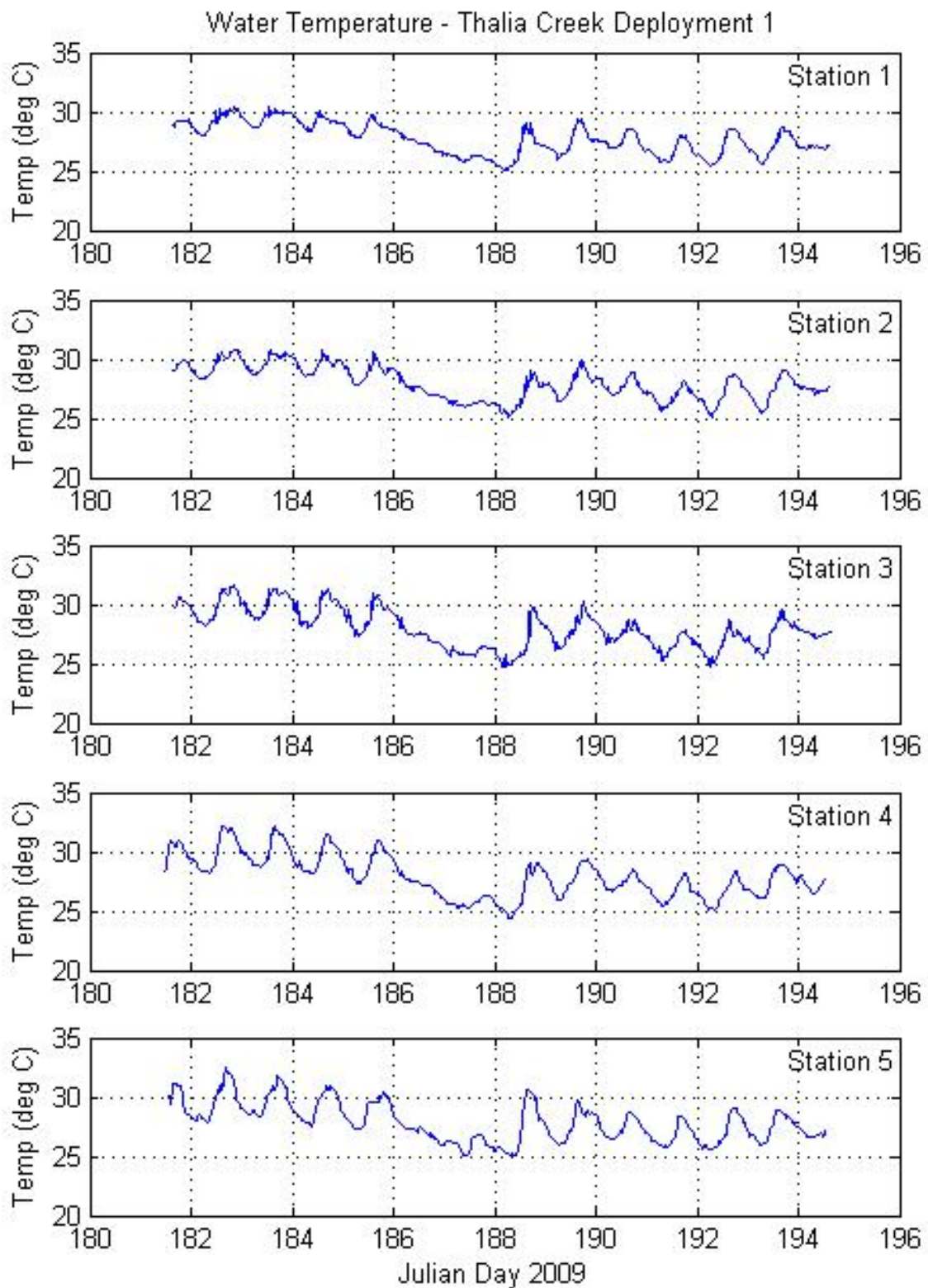
Figure II.9. ConMon water quality station temperature – Thurston Branch -
Thalia Creek Deployment 1 (June 30 to July 13, 2009).
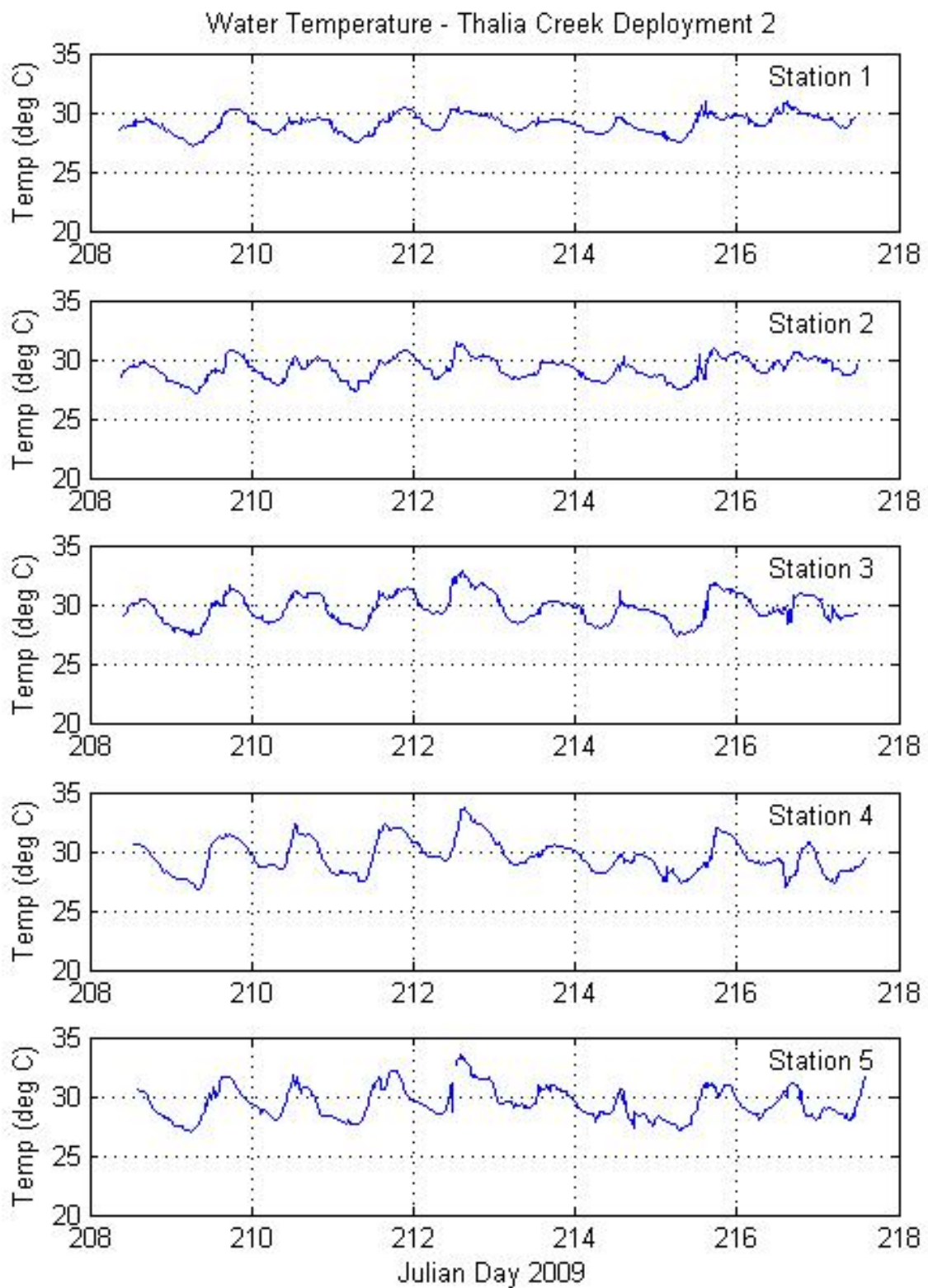
Figure II.10. ConMon water quality station temperature – Thurston Branch - Thalia Creek Deployment 2 (July 27 to August 5, 2009).
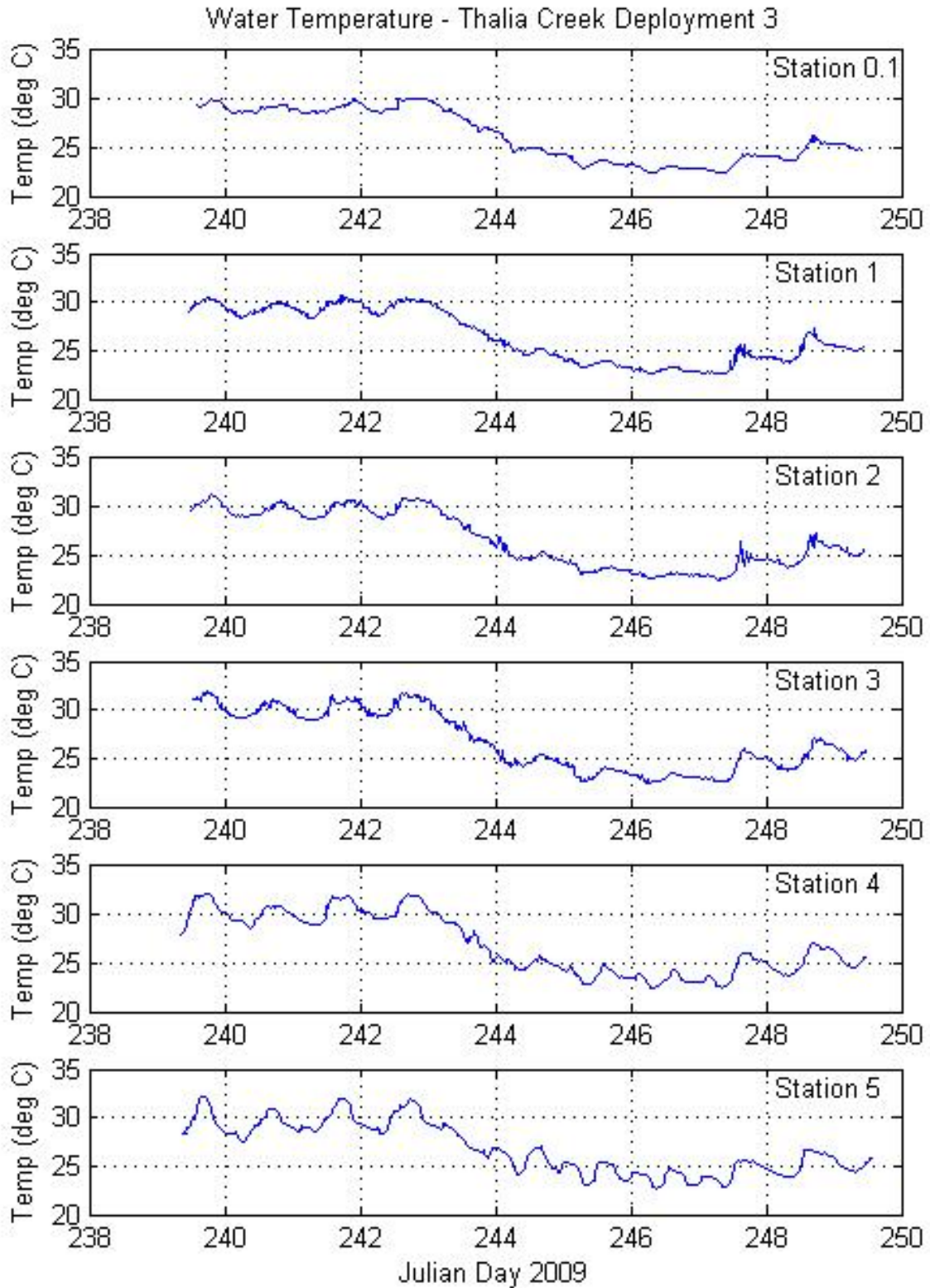
Figure II.11. ConMon water quality station temperature – Thurston Branch -
Thalia Creek Deployment 3 (August 27 to September 6, 2009).

17

Table II.3. Summary statistics for water temperature within the TB-TC system by ConMon water quality station and deployment period.

ConMon Station	Sampling Period 6/30-7/13/2009	Sampling Period 7/27-8/5/2009	Sampling Period 8/27-9/6/2009
0.1			Avg: 26.1 Min: 22.4 Max: 30.0 Std Dev: 2.6 N: 945
1	Avg: 27.7 Min: 25.1 Max: 30.5 Std Dev: 1.3 N: 1245	Avg: 29.1 Min: 27.2 Max: 30.9 Std Dev: 0.8 N: 873	Avg: 26.4 Min: 22.6 Max: 30.6 Std Dev: 2.7 N: 957
2	Avg: 28.0 Min: 25.1 Max: 30.9 Std Dev: 1.4 N: 1246	Avg: 29.2 Min: 27.1 Max: 31.4 Std Dev: 0.9 N: 874	Avg: 26.5 Min: 22.5 Max: 31.1 Std Dev: 2.8 N: 956
3	Avg: 28.0 Min: 24.7 Max: 31.6 Std Dev: 1.7 N: 1245	Avg: 29.7 Min: 27.3 Max: 32.8 Std Dev: 1.2 N: 871	Avg: 26.7 Min: 22.4 Max: 31.9 Std Dev: 3.0 N: 957
4	Avg: 27.9 Min: 24.2 Max: 32.2 Std Dev: 1.8 N: 1251	Avg: 29.6 Min: 26.8 Max: 33.6 Std Dev: 1.4 N: 868	Avg: 26.9 Min: 22.4 Max: 32.1 Std Dev: 3.0 N: 973
5	Avg: 27.9 Min: 25.0 Max: 32.4 Std Dev: 1.6 N: 1246	Avg: 29.5 Min: 27.0 Max: 33.5 Std Dev: 1.3 N: 860	Avg: 26.8 Min: 22.7 Max: 32.2 Std Dev: 2.6 N: 977

II-2-4 Salinity

Salinity time series plots for each ConMon water quality station are shown in Figures II.12, II.13, and II.14 for deployment periods 6/30-7/13/2009, 7/27-8/5/2009 and 8/27-9/6/2009, respectively. Summary statistics for individual stations by deployment period are provided in Table II.4. During the study periods, salinity values ranged between 0.9 and 22.5 psu, and as expected, decreased with distance up the TB-TC system. For this report, salinity regimes are defined as follows: tidal freshwater (range: 0-0.5 psu), oligohaline (range: 0.5-5 psu), mesohaline (range: 5-18 psu) and ployhaline (range: 18-27 psu). The upper Western Branch of the Lynnhaven River (ConMon water quality Station 0.1) was representative of polyhaline conditions, the lower reaches of the TB/TC system (ConMon water quality Stations 1 and 2) exhibited meso to polyhaline conditions, the middle reaches (ConMon water quality Stations 3 and 4) exhibited oligo to polyhaline conditions, and oligo to mesohaline conditions were observed at the most upper reach TC station (ConMon water quality Station 5). With exception to ConMon water quality Station 0.1, which was deployed on only one occasion, all stations exhibited relatively large variations in salinity over tidal and deployment periods. Tidal variations in salinity were on the order of 2-3 psu at ConMon water quality Station 1, 3-4 psu at ConMon water quality Station 2, 4-6 psu at ConMon water quality Station 3, and 6-9 psu at ConMon water quality Stations 4 and 5. Variations in salinity over deployment periods (between 10-13 days) was, in some cases, much greater than those observed over tidal cycles and exceeded 15 psu at ConMon water quality Stations 2 through 4. Depressions in salinity were observed following rainfall events with the most notable drops occurring on August 5, 2009 (Julian day 217; 2.2 cm of rainfall; see Figure II.13) at ConMon water quality Stations 2 through 4.
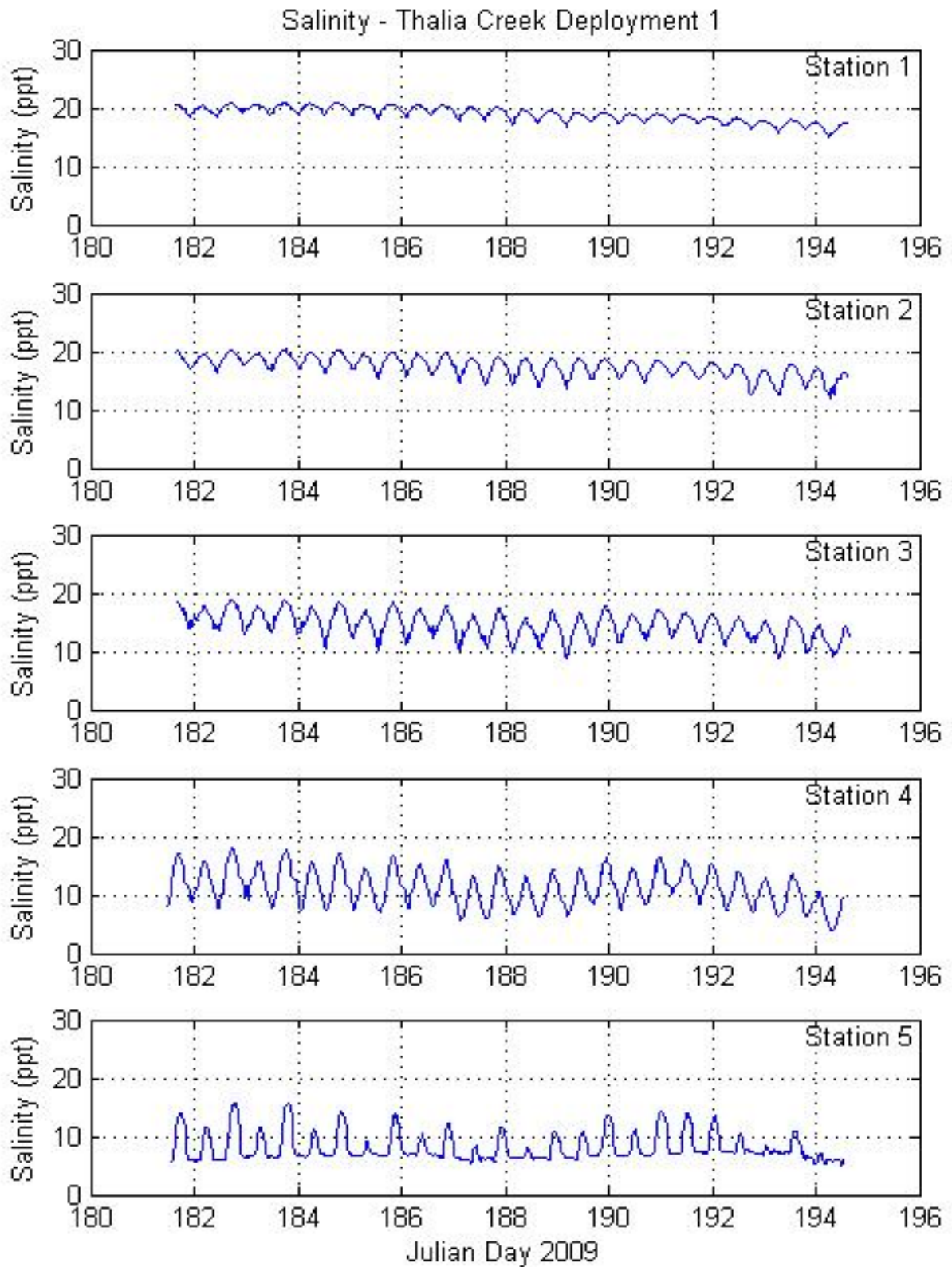
Figure II.12. ConMon water quality station salinity – Thurston Branch - Thalia Creek Deployment 1 (June 30 to July 6, 2009).
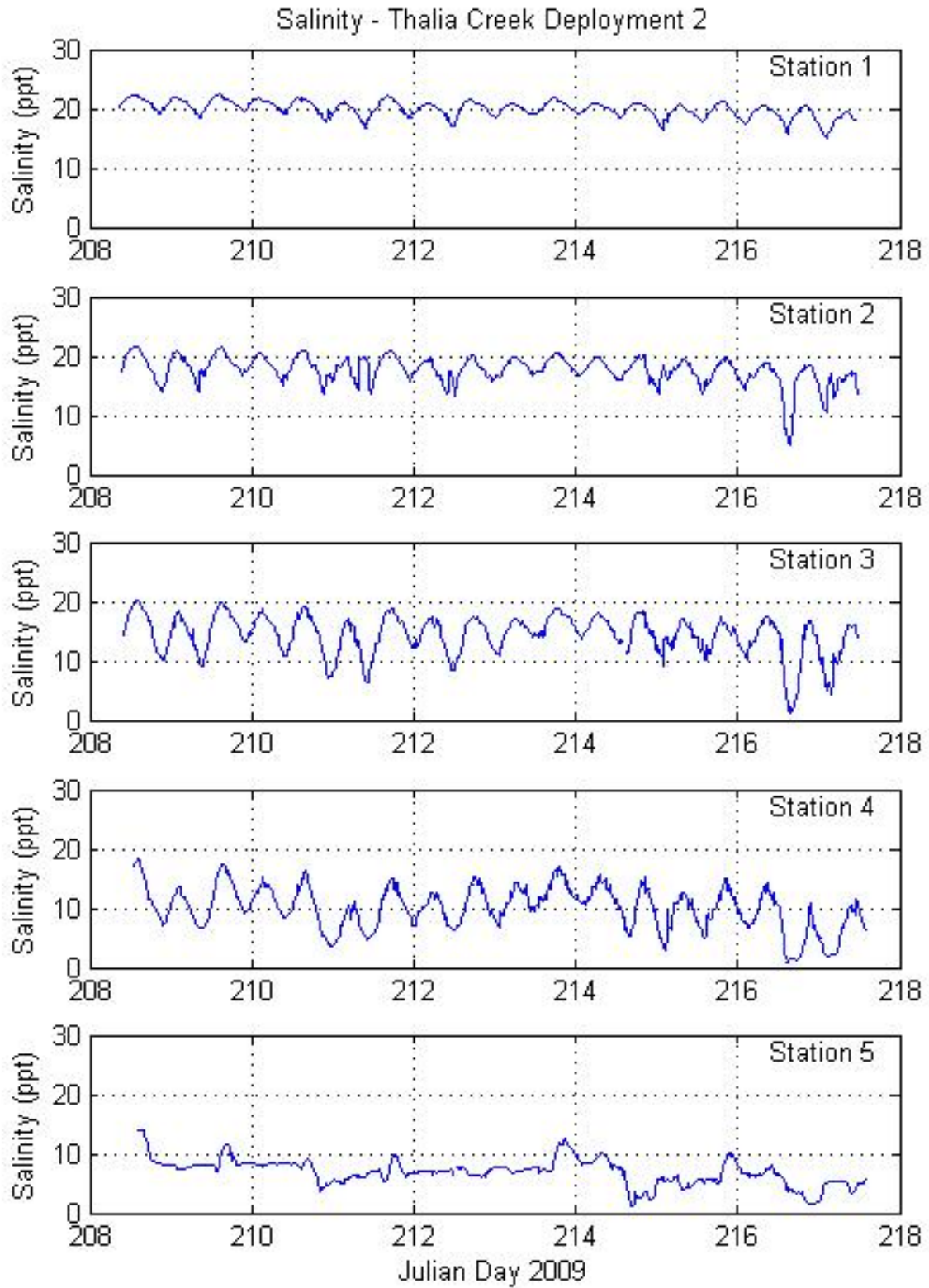
Figure II.13. ConMon water quality station salinity – Thurston Branch - Thalia Creek Deployment 2 (July 27 to August 5, 2009).

21
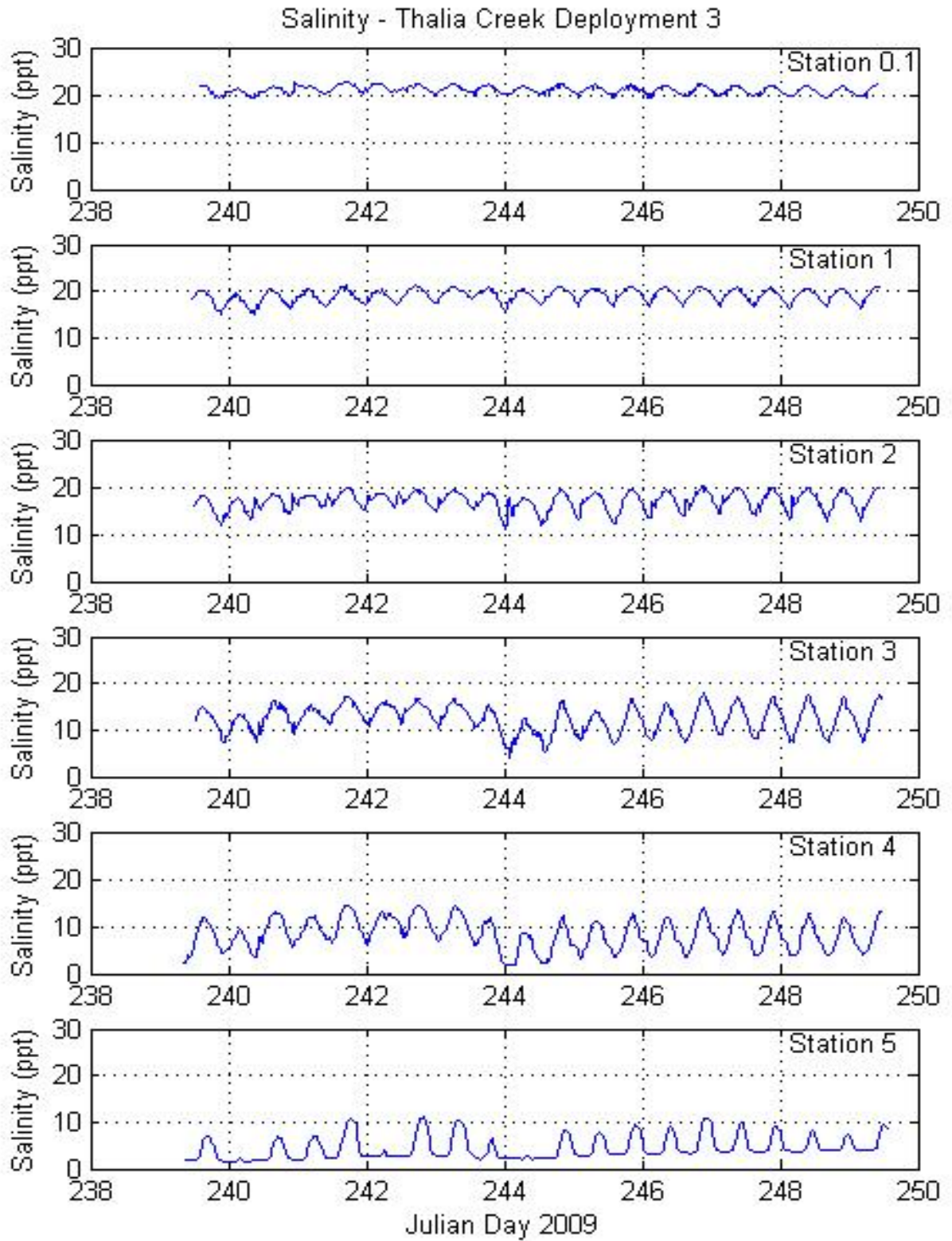
Figure II.14. ConMon water quality station salinity – Thurston Branch - Thalia
Creek Deployment 3 (August 27 to September 6, 2009).

Table II.4. Summary statistics for salinity within the TB-TC system by ConMon water quality station and deployment period.

ConMon Station	Sampling Period 6/30-7/13/2009	Sampling Period 7/27-8/5/2009	Sampling Period 8/27-9/6/2009
0.1			Avg: 21.05 Min: 19.18 Max: 22.78 Std Dev: 0.79 N: 945
1	Avg: 18.88 Min: 14.84 Max: 21.00 Std Dev: 1.22 N: 1245	Avg: 19.94 Min: 15.10 Max: 22.46 Std Dev: 1.33 N: 873	Avg: 19.03 Min: 15.20 Max: 21.22 Std Dev: 1.32 N: 957
2	Avg: 17.37 Min: 11.87 Max: 20.35 Std Dev: 1.68 N: 1246	Avg: 17.71 Min: 5.14 Max: 21.52 Std Dev: 2.24 N: 874	Avg: 16.99 Min: 11.23 Max: 20.02 Std Dev: 1.87 N: 956
3	Avg: 14.49 Min: 8.89 Max: 18.92 Std Dev: 2.16 N: 1245	Avg: 14.40 Min: 1.36 Max: 20.28 Std Dev: 3.35 N: 871	Avg: 12.46 Min: 3.84 Max: 17.76 Std Dev: 2.83 N: 957
4	Avg: 11.27 Min: 4.08 Max: 17.94 Std Dev: 2.99 N: 1251	Avg: 10.13 Min: 0.91 Max: 18.41 Std Dev: 3.60 N: 868	Avg: 8.35 Min: 1.84 Max: 14.52 Std Dev: 3.18 N: 973
5	Avg: 8.23 Min: 4.86 Max: 15.76 Std Dev: 2.45 N: 1246	Avg: 6.94 Min: 1.21 Max: 14.07 Std Dev: 2.17 N: 861	Avg: 4.51 Min: 1.54 Max: 11.00 Std Dev: 2.48 N: 977

II-2-5 Dissolved Oxygen

Dissolved oxygen concentration (DO_{conc}) time series plots for each ConMon water quality station are shown in Figures II.15, II.16, and II.17 for deployment periods 6/30-7/13/2009, 7/27-8/5/2009 and 8/27-9/6/2009, respectively. Summary statistics for individual stations by deployment period are provided in Table II.5. Figures II.18, II.19, and II.20 show times series of dissolved oxygen as a percent saturation ($DO_{\%sat}$) accounting for *in situ* salinity and temperature with summary statistics provided in Table II.6. Dissolved oxygen patterns within the TB-TC system were highly dynamic with concentrations ranging from anoxic to supersaturated conditions; minimum and maximum concentrations observed during the study were 0.0 and 13.1 mg·L^{-1} with corresponding $\%DO_{sat}$ of 0% and 183.3%. Deployment period mean DO_{conc} in the lower reaches (ConMon water quality stations 1 and 2; mean DO_{conc} range: 5.6-6.0 mg·L^{-1}; $DO_{\%sat}$ range: 76.7-87.9%) were generally elevated over mean values observed in the middle (ConMon water quality Stations 3 and 4; mean DO_{conc} range: 4.5-6.0 mg·L^{-1}; $DO_{\%sat}$ range: 63.4-79.9%) and upper reaches (ConMon water quality Station 5; mean DO_{conc} range: 3.7-5.2 mg·L^{-1}; $DO_{\%sat}$ range: 47.1-70.1%) of the TB/TC system. In addition to lower mean values, the middle and upper reaches exhibited greater variability in DO_{conc}.

In order to provide further insight of dissolved oxygen dynamics, harmonic regression analysis (method of least squares) was performed on the time series data to model periodicity driven by variations in solar energy (e.g., temperature and sunlight) and tidal advection. The two frequencies corresponding to the 24-hour (diurnal or diel) and 12.42 hour (principal M_2 tide or semi-diurnal) cycles were chosen for the analyses. The combined influence of the solar and tidal components accounted for 56-66%, 52-74 %, and 28-50 % of the DO_{conc} variability observed during the first, second, and third deployments, respectively. The lower accountability for the third deployment may be attributed to a significant storm event that occurred near the middle of the deployment period that disrupted the typical cyclic pattern observed in DO_{conc} levels (see Station 5, Figure II.17; Julian day: 243; 1.9 cm of rainfall). The strength or amplitudes of the two components derived from the harmonic analyses for each ConMon water quality station and deployment period are presented graphically in Figure II.21. Diurnal swings of DO_{conc} approached 7 mg·L^{-1} (twice of the amplitude) while maximum semi-diurnal swings were on the order of 2 mg·L^{-1}. The diurnal swing, which represented the combined result of diurnal water temperature variation and biological activities (e.g., photosynthesis of phytoplankton and benthic algae), was greatest in the upstream region (ConMon water quality Stations 4 and 5). The semi-diurnal variation, representing the combination effects of concentration gradient and tidal current strength, was greatest in the middle reach around ConMon water quality Stations 3 and 4.

Lowest DO_{conc} usually occurred in the early morning (~6:00-8:00 EST) with peak concentrations occurring in the late afternoon (~15:00-19:00 EST). When low tides preceded early morning hours, hypoxia could be observed as early as 2:00 EST. Severe hypoxia, defined as $DO_{conc} \leq 2$ mg·L^{-1}, was observed at all five TB-TC ConMon water quality stations during the study period. Detailed information, by station and deployment

period, regarding overall percent of time severe hypoxic conditions were observed, number of events and duration is provided in Tables II.7 through II.9. The set-up and duration of severe hypoxia was influenced by solar insolation, timing of ebb-tide and freshwater (and associated material) input derived from storms. These factors, along with temperature have been shown to trigger hypoxia in shallow Northeast and mid-Atlantic coastal bays (D'Avanzo and Kremer, 1994; Tyler et al., 2009). As with diel-cycling amplitudes of DO_{conc}, the number of hypoxia events and their duration increased as one moved from the lower (ConMon water quality Station 1) to the upper reaches (ConMon water quality Stations 4 and 5) of the TB-TC system. The duration of hypoxia ranged from 15 minutes to over 34 hours for a single event. Given the number of events and extended duration of some events, hypoxia was a chronic problem in the upper-middle (ConMon water quality Station 3) and upper reaches of TB-TC (ConMon water quality Stations 4 and 5). It should be noted that anoxic conditions, where DO_{conc} is completely depleted, were observed at ConMon water quality Station 5 following a significant rainfall event during the third deployment period (see Figure II.17; Julian day: 243; 1.9 cm of rainfall).

Figure II.15. ConMon water quality station dissolved oxygen concentration –
Thurston Branch - Thalia Creek Deployment 1 (June 30 to July 13, 2009).

26

Figure II.16. ConMon water quality station dissolved oxygen concentration –
Thurston Branch - Thalia Creek Deployment 2 (July 27 to August 5, 2009).

Figure II.17. ConMon water quality station dissolved oxygen concentration –
Thurston Branch - Thalia Creek Deployment 3 (August 27 to September 6, 2009).

Table II.5. Summary statistics for DO_{conc} $(mg \cdot L^{-1})$ within the TB-TC system by ConMon water quality station and deployment period.

ConMon Station	Sampling Period 6/30-7/13/2009	Sampling Period 7/27-8/5/2009	Sampling Period 8/27-9/6/2009
0.1			Avg: 5.6 Min: 2.8 Max: 8.5 Std Dev: 1.2 N: 945
1	Avg: 5.9 Min: 1.9 Max: 10.1 Std Dev: 1.5 N: 1245	Avg: 6.0 Min: 3.0 Max: 10.1 Std Dev: 1.5 N: 873	Avg: 6.0 Min: 2.6 Max: 10.7 Std Dev: 1.5 N: 957
2	Avg: 5.6 Min: 1.6 Max: 10.7 Std Dev: 1.9 N: 1246	Avg: 5.6[1] Min: 1.8[1] Max: 10.0[1] Std Dev: 1.9[1] N: 167[1]	Avg: 5.6 Min: 2.0 Max: 11.1 Std Dev: 1.8 N: 956
3	Avg: 5.6 Min: 0.4 Max: 11.7 Std Dev: 2.2 N: 1245	Avg: 5.0 Min: 0.1 Max: 10.7 Std Dev: 2.6 N: 871	Avg: 6.0 Min: 1.3 Max: 12.3 Std Dev: 2.4 N: 957
4	Avg: 5.5 Min: 0.6 Max: 11.4 Std Dev: 2.6 N: 1251	Avg: 4.5 Min: 0.5 Max: 11.3 Std Dev: 2.8 N: 868	Avg: 5.7 Min: 1.6 Max: 12.5 Std Dev: 2.5 N: 973
5	Avg: 5.2 Min: 0.5 Max: 13.1 Std Dev: 2.9 N: 1246	Avg: 4.6 Min: 0.2 Max: 11.7 Std Dev: 2.5 N: 859	Avg: 3.7 Min: 0.0 Max: 10.3 Std Dev: 2.4 N: 977

Note: (1) Significant amount of data was suspect due to possible sensor membrane puncture on 7/29/2009 (Julian day: 210; 3:00).

Figure II.18. ConMon water quality station percent saturation of dissolved oxygen – Thurston Branch - Thalia Creek Deployment 1 (June 30 to July 13, 2009).

30

Figure II.19. ConMon water quality station percent saturation of dissolved oxygen – Thurston Branch - Thalia Creek Deployment 2 (July 27 to August 5, 2009).

31

Figure II.20. ConMon water quality station percent saturation of dissolved oxygen – Thurston Branch - Thalia Creek Deployment 3 (August 27 to September 6, 2009).

32

Table II.6. Summary statistics for $DO_{\%sat}$ within the TB-TC system by ConMon water quality station and deployment period.

ConMon Station	Sampling Period 6/30-7/13/2009	Sampling Period 7/27-8/5/2009	Sampling Period 8/27-9/6/2009
0.1			Avg: 77.3 Min: 40.1 Max: 117.6 Std Dev: 16.1 N: 945
1	Avg: 83.1 Min: 26.0 Max: 145.7 Std Dev: 22.4 N: 1245	Avg: 87.9 Min: 42.1 Max: 149.6 Std Dev: 23.3 N: 873	Avg: 83.3 Min: 35.0 Max: 149.8 Std Dev: 21.9 N: 957
2	Avg: 79.4 Min: 21.5 Max: 153.2 Std Dev: 27.0 N: 1246	Avg: 81.2[1] Min: 25.3[1] Max: 148.3[1] Std Dev: 28.7[1] N: 167[1]	Avg: 76.7 Min: 27.5 Max: 149.8 Std Dev: 24.9 N: 956
3	Avg: 77.5 Min: 5.7 Max: 163.8 Std Dev: 31.6 N: 1245	Avg: 71.4 Min: 1.4 Max: 159.6 Std Dev: 38.4 N: 871	Avg: 79.9 Min: 16.5 Max: 161.1 Std Dev: 32.4 N: 957
4	Avg: 75.8 Min: 7.8 Max: 156.1 Std Dev: 36.3 N: 1251	Avg: 63.4 Min: 6.9 Max: 166.4 Std Dev: 41.0 N: 868	Avg: 74.9 Min: 20.5 Max: 159.7 Std Dev: 33.7 N: 973
5	Avg: 70.1 Min: 6.1 Max: 183.3 Std Dev: 40.3 N: 1246	Avg: 62.5 Min: 3.2 Max: 163.6 Std Dev: 35.5 N: 859	Avg: 47.1 Min: 0.0 Max: 144.6 Std Dev: 32.24 N: 977

Note: (1) Significant amount of data was suspect due to possible sensor membrane puncture on 7/29/2009 (Julian day: 210; 3:00).
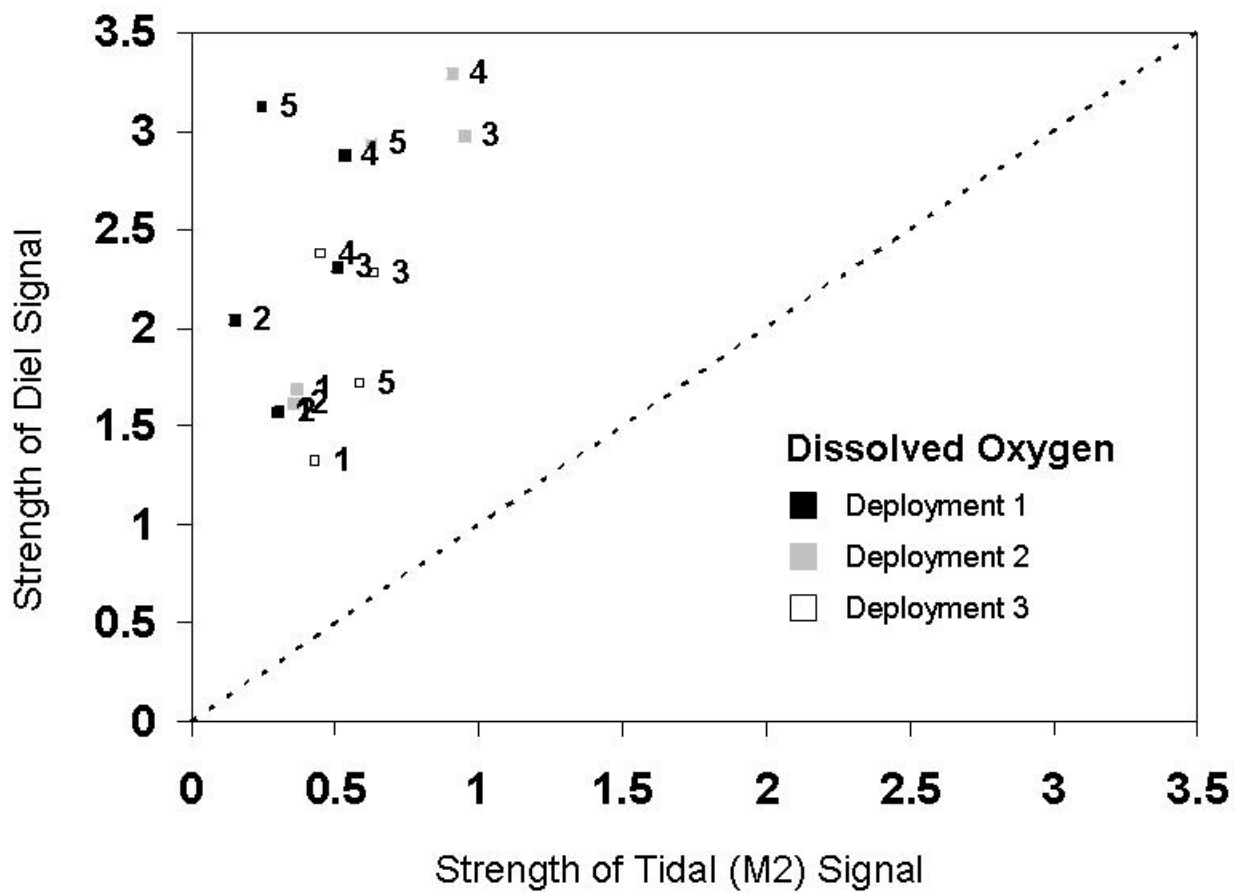
Figure II.21. Diel (24 hr) versus semi-diurnal (12.4 hr) influence on DO_{conc} by station and deployment period. Points plotting near the 45° or 1:1 line indicate diel (24 hr) and semi-diurnal (12.4 hr) forces equally influence DO_{conc} levels.

Table II.7. Percent of time that TB-TC ConMon water quality stations exhibited hypoxic conditions (hypoxia criteria: $DO_{\%sat} > 0$ to $< 30\%$ and $DO_{conc} \leq 2.0$ mg·L^{-1}) and exceeded Virginia open water DO_{conc} criteria for Chesapeake Bay and its tidal tributaries (Virginia instantaneous DO_{conc} standard: ≥ 4.3 mg·L^{-1} at ≥ 29 °C and ≥ 3.2 mg·L^{-1} at < 29 °C; VaSWCB 2009) during deployment period 1. Information on individual hypoxic events is also provided.

ConMon Station	% Time DO Met Hypoxia Criteria			Individual Hypoxia Events			
	DO_{sat}	DO_{conc}	VA Instant Stand	Event	Start Date (Julian Day)	Start Time EST	Duration hr:min
1	<0.1	<0.1	3.0	1	July 13 (194)	7:00	0:15
2	1.8	1.1	9.2	1	July 6 (187)	3:00	2:30
				2	July 6 (187)	9:00	0:15
				3	July 13 (194)	6:45	0:45
3	6.3	4.1	18.5	1	July 4 (185)	2:00	0:30
				2	July 5 (186)	3:45	0:15
				3	July 6 (187)	2:45	4:30
				4	July 6 (187)	9:00	0:15
				5	July 6 (187)	11:15	0:15
				6	July 6 (187)	14:45	0:45
				7	July 7 (188)	4:15	0:30
				8	July 11 (192)	6:45	0:15
				9	July 12 (193)	7:30	0:15
				10	July 13 (194)	6:00	3:45
4	11.4	8.8	27.0	1	July 4 (185)	3:00	1:30
				2	July 5 (186)	3:15	4:00
				3	July 5 (186)	9:00	3:15
				4	July 6 (187)	2:00	10:15
				5	July 7 (188)	3:45	3:00
				6	July 11 (192)	7:00	0:15
				7	July 13 (194)	4:45	5:30
5	19.7	14.4	31.5	1	July 2 (183)	7:15	0:15
				2	July 3 (184)	7:00	1:30
				3	July 4 (185)	2:45	6:15
				4	July 5 (186)	3:45	7:15
				5	July 6 (187)	0:15	11:30
				6	July 7 (188)	4:30	3:30
				7	July 10 (191)	3:45	5:15
				8	July 11 (192)	5:00	5:00
				9	July 12 (193)	3:30	0:45
				10	July 12 (193)	6:30	0:15
				11	July 12 (193)	9:30	0:30
				12	July 13 (194)	2:00	3:00

Table II.8. Percent of time that TB-TC ConMon water quality stations exhibited hypoxic conditions (hypoxia criteria: $DO_{\%sat}$ >0 to <30% and DO_{conc} <2.8 mg·L^{-1}) and exceeded Virginia open water DO_{conc} criteria for Chesapeake Bay and its tidal tributaries (Virginia instantaneous DO_{conc} standard: $\geq$ 4.3 mg·L^{-1} at $\geq$ 29 °C and $\geq$ 3.2 mg·L^{-1} at < 29 °C; VaSWCB 2009) during deployment period 2. Information on individual hypoxic events is also provided.

	% Time DO Met Hypoxia Criteria			Individual Hypoxia Events			
ConMon Station	DO_{sat}	DO_{conc}	VA Instant Stand.	Event	Start Date (Julian Day)	Start Time EST	Duration hr:min
1	0	0	3.1	-	-	-	-
2[1]	1.2[1]	1.2[1]	12.0[1]	1[1]	July 28 (209) [1]	8:30[1]	0:30[1]
3	11.6	9.8	44.2	1	July 28 (209)	4:00	4:30
				2	July 29 (210)	6:30	1:45
				3	July 29 (210)	23:15	1:00
				4	July 30 (211)	5:45	3:15
				5	July 31 (212)	7:15	0:30
				6	August 1 (213)	8:00	4:45
				7	August 3 (215)	2:15	0:30
				8	August 3 (215)	13:30	0:30
				9	August 4 (216)	3:15	0:30
				10	August 5 (217)	3:30	2:45
4	26.6	22.8	50.9	1	July 28 (209)	2:15	6:45
				2	July 29 (210)	4:45	4:00
				3	July 29 (210)	23:00	10:30
				4	July 31 (212)	6:00	3:15
				5	August 1 (213)	5:00	6:00
				6	August 1 (213)	11:30	1:00
				7	August 2 (214)	6:45	4:00
				8	August 3 (215)	1:45	5:30
				9	August 3 (215)	7:45	0:45
				10	August 3 (215)	9:15	2:45
				11	August 5 (217)	3:30	4:45
5	23.1	19.9	38.0	1	July 27 (208)	23:45	8:15
				2	July 29 (210)	1:45	6:45
				3	July 30 (211)	3:45	4:45
				4	July 31 (212)	5:45	1:45
				5	July 31 (212)	22:45	1:15
				6	August 1 (213)	1:30	7:45
				7	August 2 (214)	0:15	0:30
				8	August 2 (214)	2:15	7:15
				9	August 2 (214)	9:00	0:30
				10	August 3 (215)	5:30	4:00
				11	August 4 (216)	7:30	0:45

1. Deployment period only lasted 1.7 days due to suspected DO sensor membrane puncture.

Table II.9. Percent of time that TB-TC ConMon water quality stations exhibited hypoxic conditions (hypoxia criteria: $DO_{\%sat}$ >0 to <30% and DO_{conc} <2.8 mg·L^{-1}) and exceeded Virginia open water DO_{conc} criteria for Chesapeake Bay and its tidal tributaries (Virginia instantaneous DO_{conc} standard: $\geq$ 4.3 mg·L^{-1} at $\geq$ 29 °C and $\geq$ 3.2 mg·L^{-1} at < 29 °C; 9 VaSWCB 2009) during deployment period 3. Information on individual hypoxic events is also provided.

| ConMon Station | % Time DO Met Hypoxia Criteria | | | Individual Hypoxia Events | | | |
	DO_{sat}	DO_{conc}	VA Instant Stand.	Event	Start Date (Julian Day)	Start Time EST	Duration hr:min
1	0	0	1.3	-	-	-	-
2	0.6	0.3	16.4	1	August 28 (240)	8:45	0:30
3	3.0	1.2	24.1	1	August 28 (240)	10:30	0:15
				2	August 31 (243)	12:30	1:30
				3	September 1 (244)	2:15	1:00
4	9.9	7.3	27.6	1	August 28 (240)	7:15	4:00
				2	August 29 (241)	7:15	2:45
				3	August 30 (242)	6:15	5:45
				4	August 31 (243)	10:15	1:30
				5	August 31 (243)	16:00	0:30
				6	September 1 (244)	4:30	1:45
				7	September 1 (244)	8:45	1:15
5[1]	35.6[1]	31.6[1]	48.9[1]	1	August 29 (241)	5:15	4:00
				2	August 29 (241)	10:30	3:45
				3	August 30 (242)	3:00	1:15
				4	August 30 (242)	6:15	4:45
				5	August 30 (242)	12:15	4:00
				6	August 30 (242)	19:45	0:15
				7	August 30 (242)	20:45	34:15
				8	September 1 (244)	7:30	9:15
				9	September 2 (245)	4:30	0:15
				10	September 4 (247)	4:30	2:30
				11	September 5 (248)	5:15	2:15
				12	September 5 (248)	11:00	0:30
				13	September 5 (248)	18:30	0:30
				14	September 5 (248)	23:15	1:30
				15	September 6 (249)	4:15	9:15

1. Anoxic conditions were noted 1.1% of the deployment period.

II-2-6 Chlorophyll

Chlorophyll concentration (chl$_{fl}$; based on fluorescence) time series plots for each ConMon water quality station are shown in Figures II.22, II.23, and II.24 for deployment periods 6/30-7/13/2009, 7/27-8/5/2009 and 8/27-9/6/2009, respectively. Summary statistics for individual stations by deployment period are provided in Table II.10. As with dissolved oxygen, chl$_{fl}$ patterns within the TB-TC system were highly dynamic with concentrations ranging from 0.7 to 293.7 $\mu g \cdot L^{-1}$. In general, deployment period mean chl$_{fl}$ concentrations were lower in the downstream, higher salinity reaches (ConMon water quality Stations 1 and 2; mean chl$_{fl}$ range: 19.7 to 31.6 $\mu g \cdot L^{-1}$) than those observed in the middle (ConMon water quality Stations 3 and 4; mean chl$_{fl}$ range: 34.4 to 49.8 $\mu g \cdot L^{-1}$) and upper reaches (ConMon water quality station 5; mean chl$_{fl}$ range: 42.5 to 60.1 $\mu g \cdot L^{-1}$). Exception occurred at ConMon water quality Station 2 during the third deployment period (mean chl$_{fl}$: 62.7 $\mu g \cdot L^{-1}$) where elevated levels followed a significant rainfall event (1.9 cm) on August 31, 2009. Chl$_{fl}$ levels at other stations (e.g., ConMon stations 1, 5) exhibited a similar pattern but not to the degree as Station 2. In addition to overall elevated mean values, the middle and upper reaches generally exhibited greater variability in chl$_{fl}$ than observed in the lower reaches.

Harmonic analysis was conducted on the chl$_{fl}$ time series data to reveal any semi-diurnal and diurnal periodicity. The accountability of these components on chlorophyll variability was much lower than observed for DO$_{conc}$. The combined influence of the solar and tidal components accounted for 12-44%, 23-56, and 1-41 % of the chl$_{fl}$ variability observed at ConMon water quality Stations 1-4 during the first, second, and third deployments, respectively. Again, the lower accountability for the third deployment may be attributed to a significant storm event that occurred near the middle of the deployment period resulting in a disruption of the typical cyclic pattern observed in chl$_{fl}$ levels (see Station 2, Figure II.24; Julian day: 243; 1.9 cm of rainfall). For Station 5, the diurnal and semi-diurnal components accounted for less than 5 % of the variability for all three deployment periods. The strength or amplitudes of the two components derived from the harmonic analyses for each ConMon water quality station and deployment period are presented graphically in Figure II.25. Both diurnal and semi-diurnal swings of chl$_{fl}$ ranged from 4-18 $\mu g \cdot L^{-1}$; exception occurred for station 3 during the second deployment where the tidal signal approached 24 $\mu g \cdot L^{-1}$. The effect of tidal advection was slightly stronger at the downstream stations (ConMon water quality Stations 1 and 2), while the biological influence was stronger at the upstream stations (ConMon water quality Stations 4 and 5).
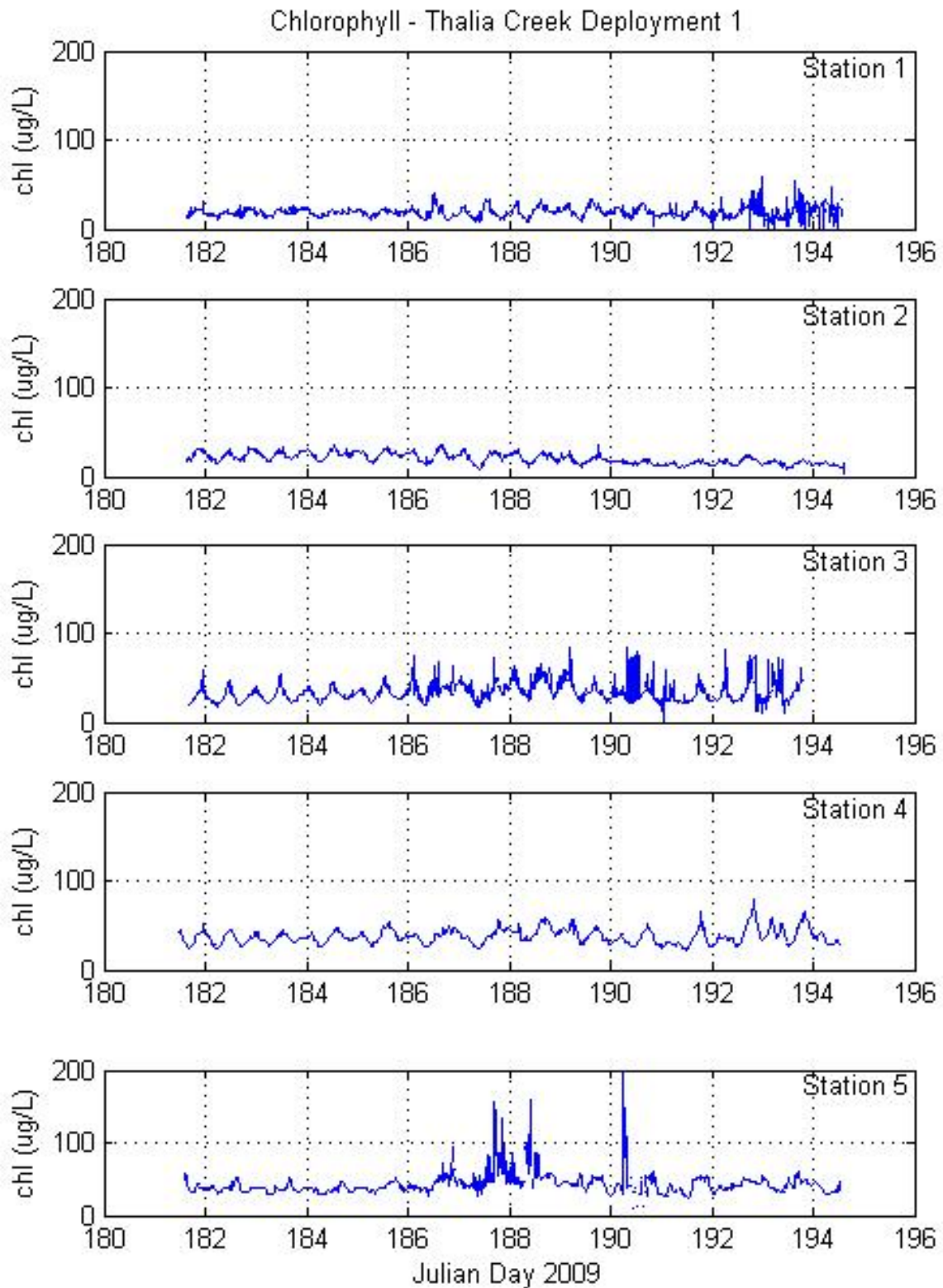
Figure II.22. ConMon water quality station chlorophyll (fluorescence) – Thurston Branch - Thalia Creek Deployment 1 (June 30 to July 13, 2009).

39
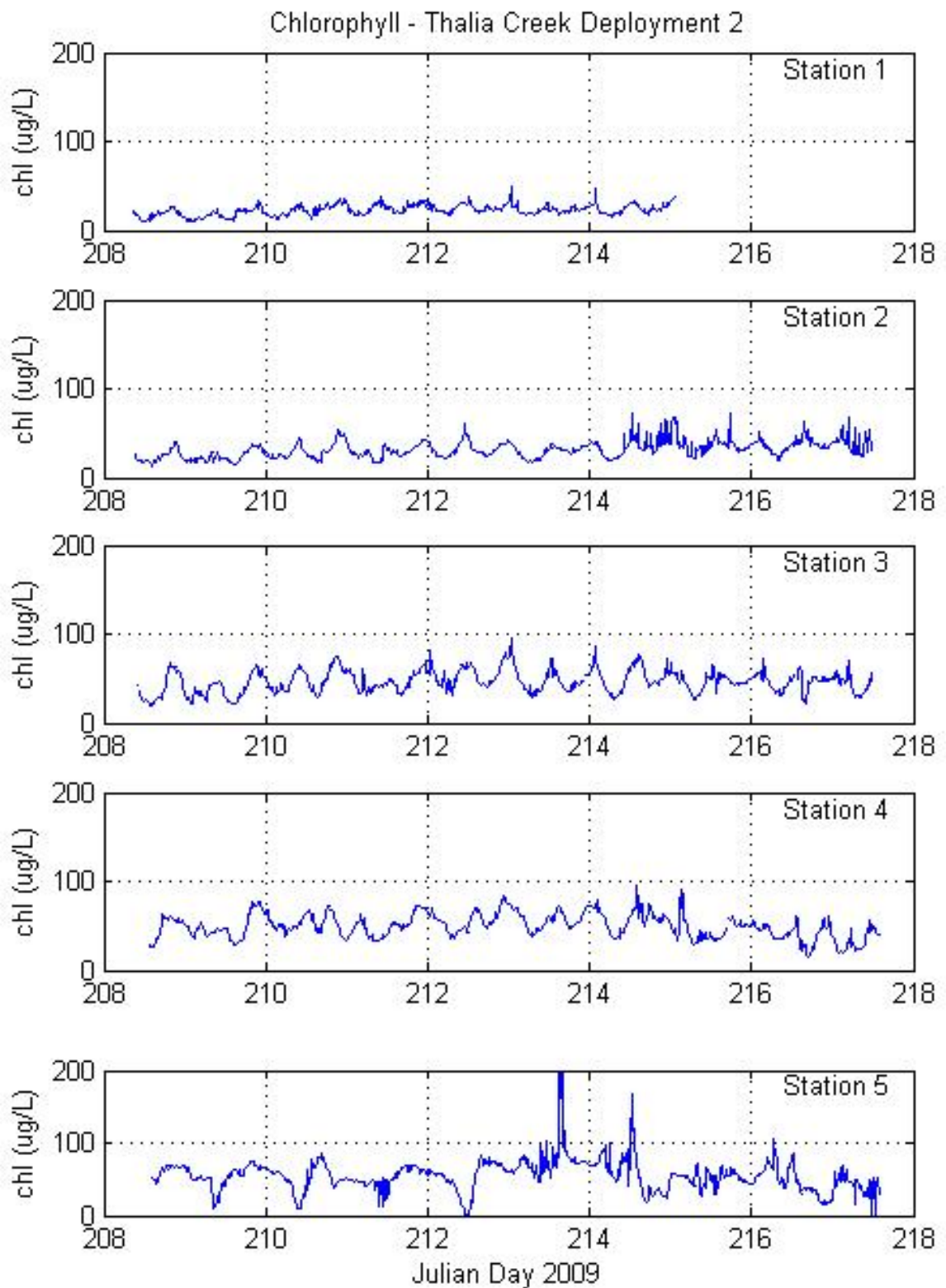
Figure II.23. ConMon water quality station chlorophyll (fluorescence) – Thurston Branch - Thalia Creek Deployment 2 (July 27 to August 5, 2009).

40
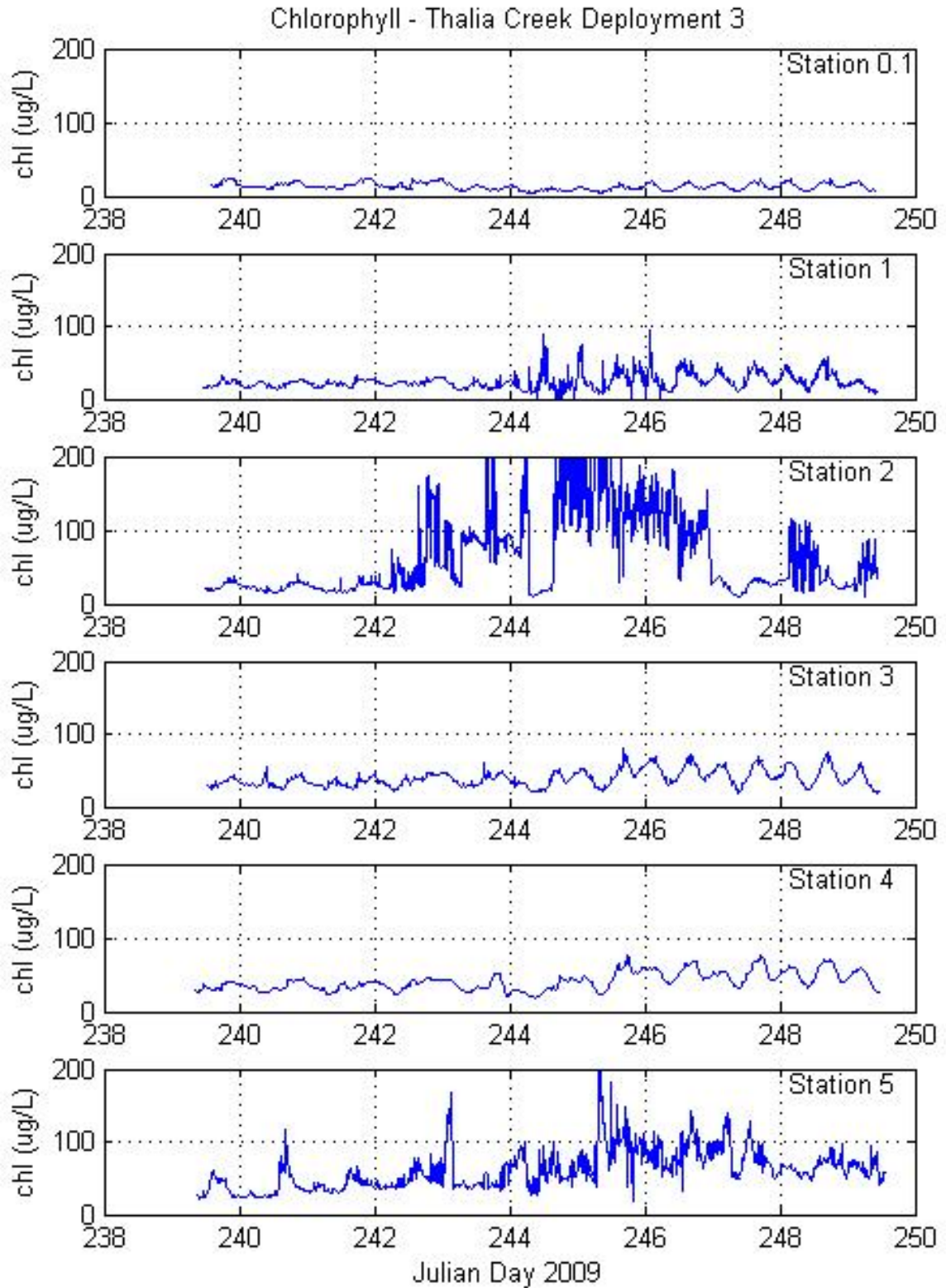
Figure II.24. ConMon water quality station chlorophyll (fluorescence) – Thurston Branch - Thalia Creek Deployment 3 (August 27 to September 6, 2009).

Table II.10. Summary statistics for chl_{fl} ($\mu g \cdot L^{-1}$) within the TB-TC system by ConMon water quality station and deployment period.

ConMon Station	Sampling Period 6/30-7/13/2009	Sampling Period 7/27-8/5/2009	Sampling Period 8/27-9/6/2009
0.1			Avg: 13.2 Min: 4.3 Max: 25.2 Std Dev: 4.6 N: 929
1	Avg: 19.1 Min: 0.7 Max: 57.9 Std Dev: 6.0 N: 1181	Avg: 23.7 Min: 6.2 Max: 49.6 Std Dev: 6.8 N: 869	Avg: 25.0 Min: 7.2 Max: 133.6 Std Dev: 11.9 N: 954
2	Avg: 20.2 Min: 8.7 Max: 36.6 Std Dev: 5.8 N: 1241	Avg: 31.6 Min: 13.7 Max: 73.2 Std Dev: 9.7 N: 871	Avg: 62.7 Min: 10.1 Max: 293.7 Std Dev: 57.8 N: 930
3	Avg: 34.4 Min: 1.3 Max: 178.9 Std Dev: 16.6 N: 1170	Avg: 46.5 Min: 19.8 Max: 95.4 Std Dev: 12.6 N: 865	Avg: 39.2 Min: 18.7 Max: 79.5 Std Dev: 11.4 N: 956
4	Avg: 37.5 Min: 21.8 Max: 78.6 Std Dev: 8.4 N: 1247	Avg: 49.8 Min: 14.5 Max: 94.9 Std Dev: 13.6 N: 867	Avg: 41.5 Min: 19.2 Max: 77.0 Std Dev: 12.2 N: 972
5	Avg: 42.5 Min: 9.1 Max: 157.8 Std Dev: 12.9 N: 1200	Avg: 55.7 Min: 2.8 Max: 246.5 Std Dev: 21.1 N: 851	Avg: 60.1 Min: 18.9 Max: 231.4 Std Dev: 27.7 N: 966
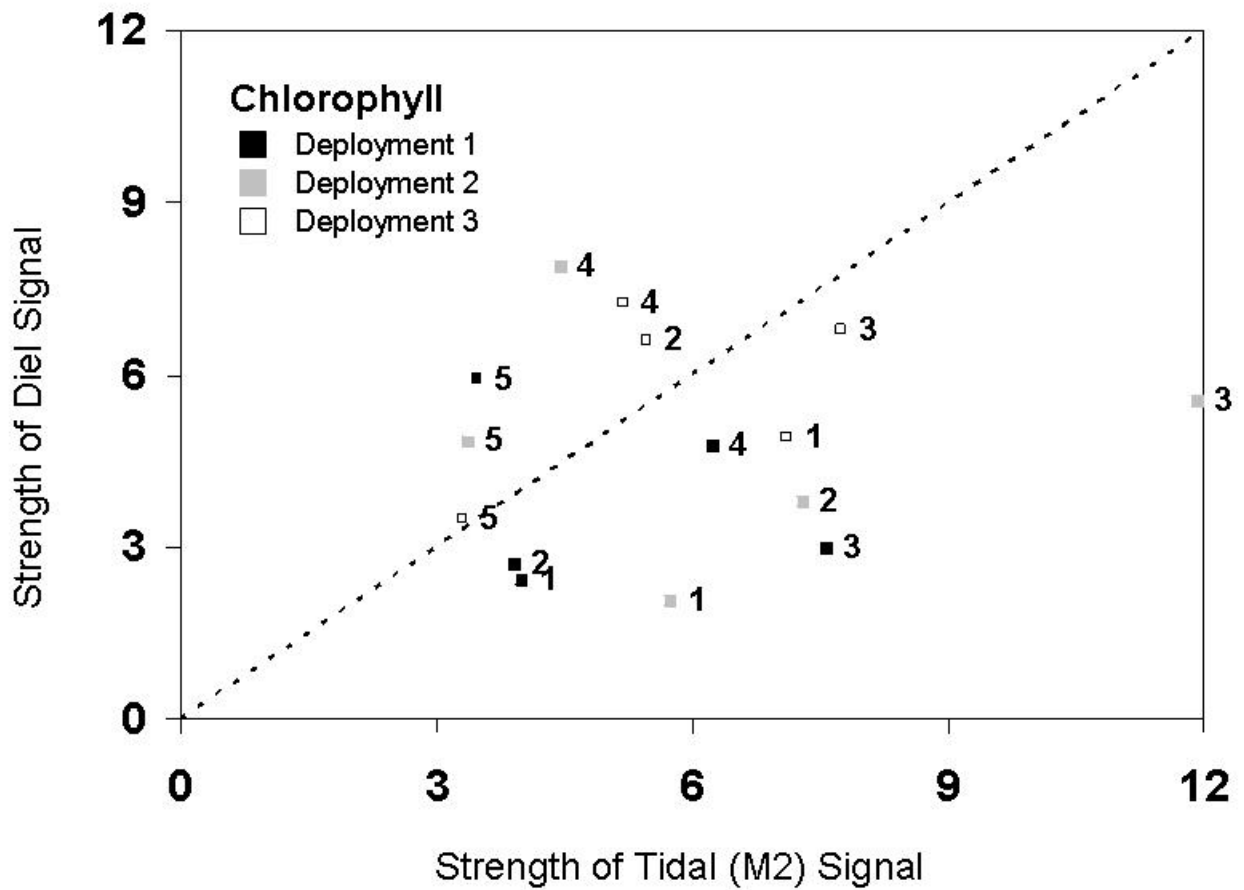
Figure II.25. Diel (24 hr) versus semi-diurnal (12.4 hr) influence on chl_{fl} levels by station and deployment period. Points plotting near the 45° or 1:1 line indicate diel (24 hr) and semi-diurnal (12.4 hr) forces equally influence chl_{fl} levels.

II-2-7 Turbidity

Turbidity level time series plots for each ConMon water quality station are shown in Figures II.26, II.27, and II.28 for deployment periods 6/30-7/13/2009, 7/27-8/5/2009 and 8/27-9/6/2009, respectively. Summary statistics for individual stations by deployment period are provided in Table II.11. Turbidity patterns within the TB-TC system were highly dynamic with NTU levels varying from 2.5 to greater than 500 NTUs. In general, average deployment period turbidity levels and associated variability decreased with distance upstream. At the mouth of TB-TC (ConMon water quality Station 1), mean deployment turbidity levels varied from 32.6 to 71.1 NTUs, compared to 30.4 to 44.3 NTU's within the mid-region (ConMon water quality Stations 2 and 3) and 22.0 to 32.4 NTUs within the upper region (ConMon water quality Stations 4 and 5).

Harmonic analyses were also performed on the time series data of turbidity. However, the results indicate much greater variability than could be accounted for with only the diurnal and semi-diurnal components. The inclusion of the M_4 component to account for tidal current strength did not improve the result. The strength or amplitudes of the two components derived from the harmonic analyses for each ConMon water quality station and deployment period are presented graphically in Figure II.29. The combined influence of the solar and tidal components accounted for 1-43 %, 1-59 %, and 4-52 % of the turbidity variability observed during the first, second, and third deployments, respectively. ConMon water quality Stations 1 and 4 generally showed equal diurnal (biological) and semi-diurnal (tidal advection) influence on turbidity levels, whereas the diurnal component dominated the upper reach (ConMon water quality Station 5) and the semi-diurnal component dominated in the middle reach (ConMon water quality Stations 2 and 3). It should be noted that sand represented a significant fraction in the most upper reach stations and may not be subject to resuspension via tidal currents. This is in contrast to the lower reaches which are characterized by broad and shallow shoal regions dominated by fine (silt-clay) sediments.
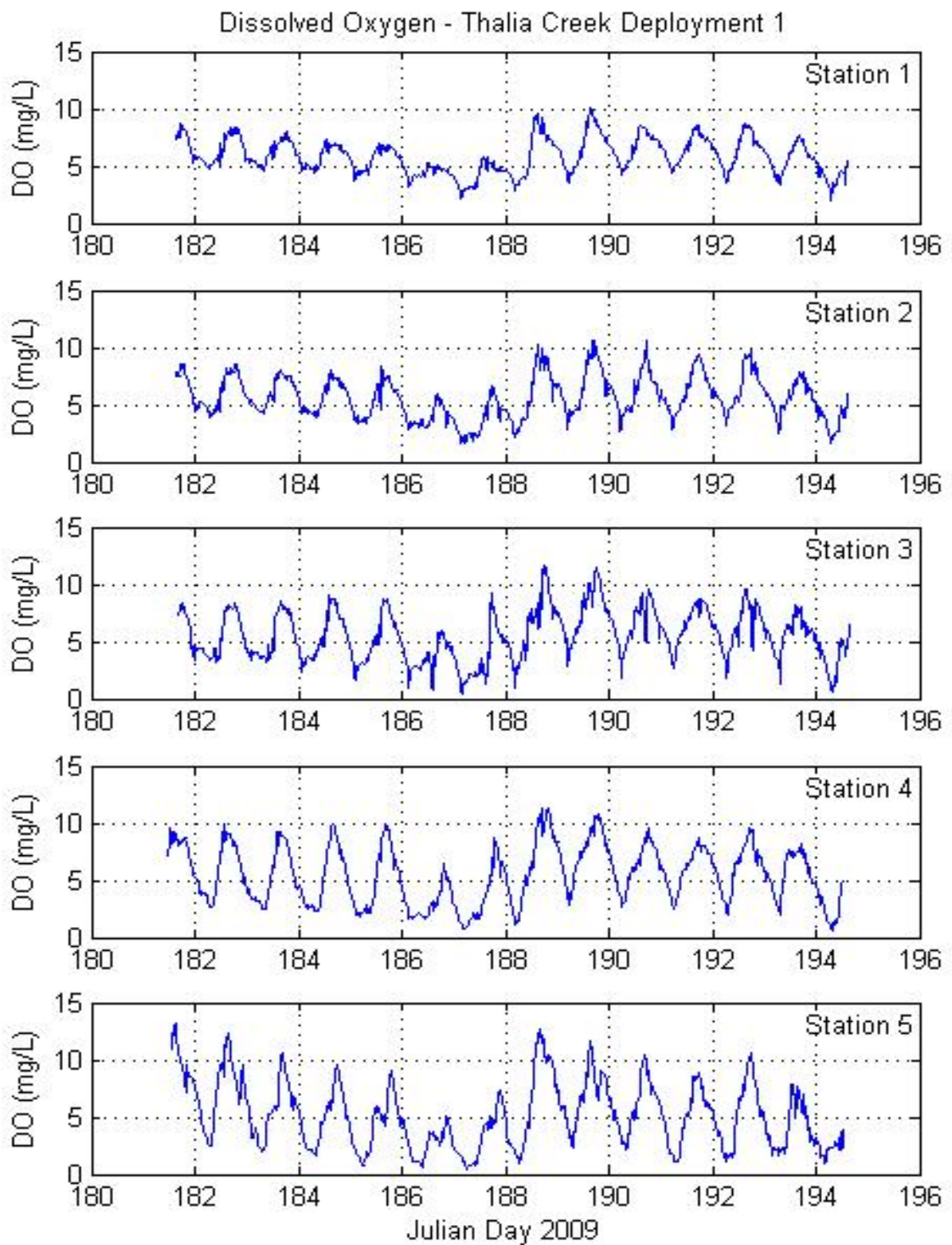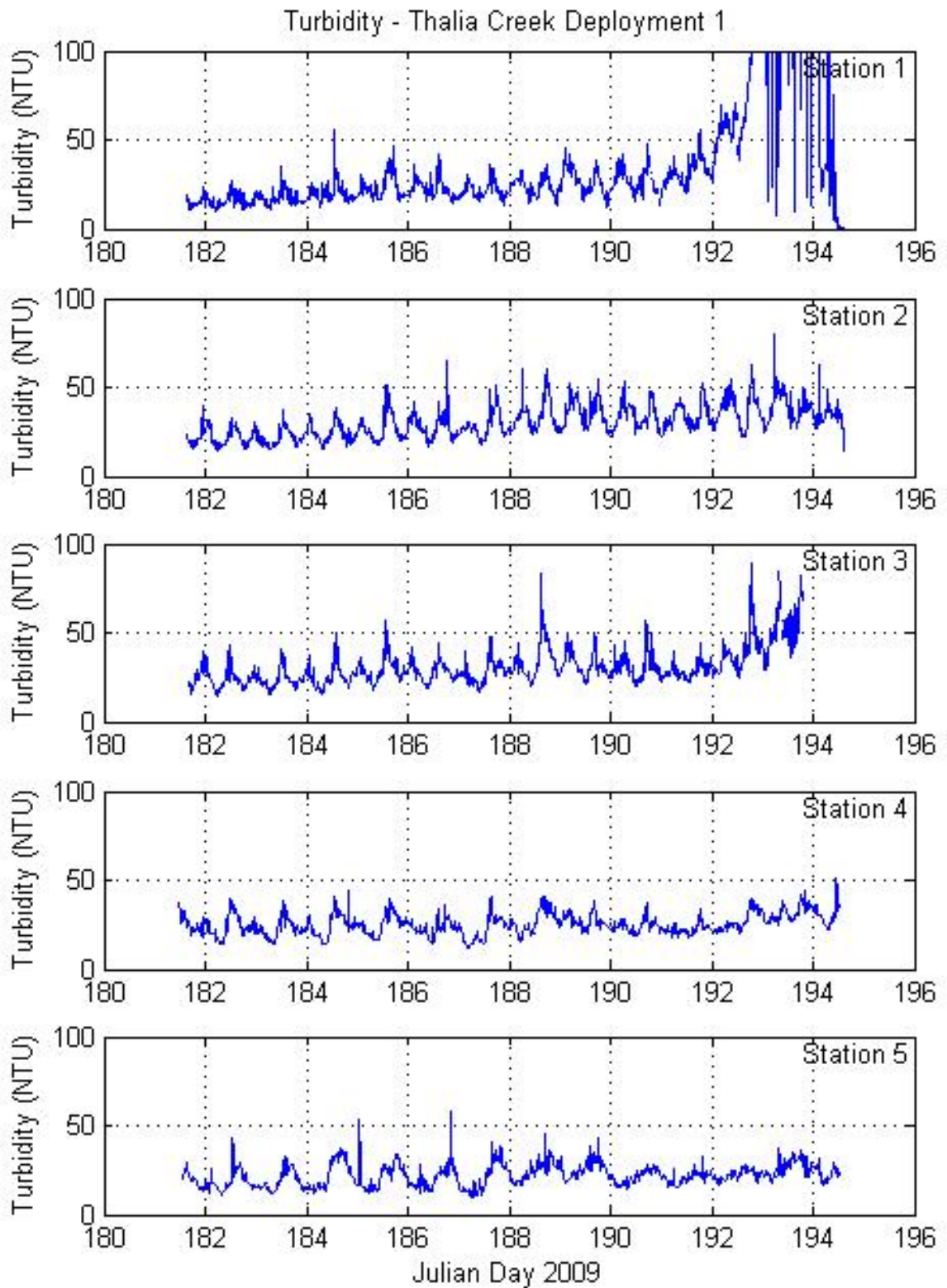
Figure II.26. ConMon water quality station turbidity – Thurston Branch - Thalia Creek Deployment 1 (June 30 to July 13, 2009).

45
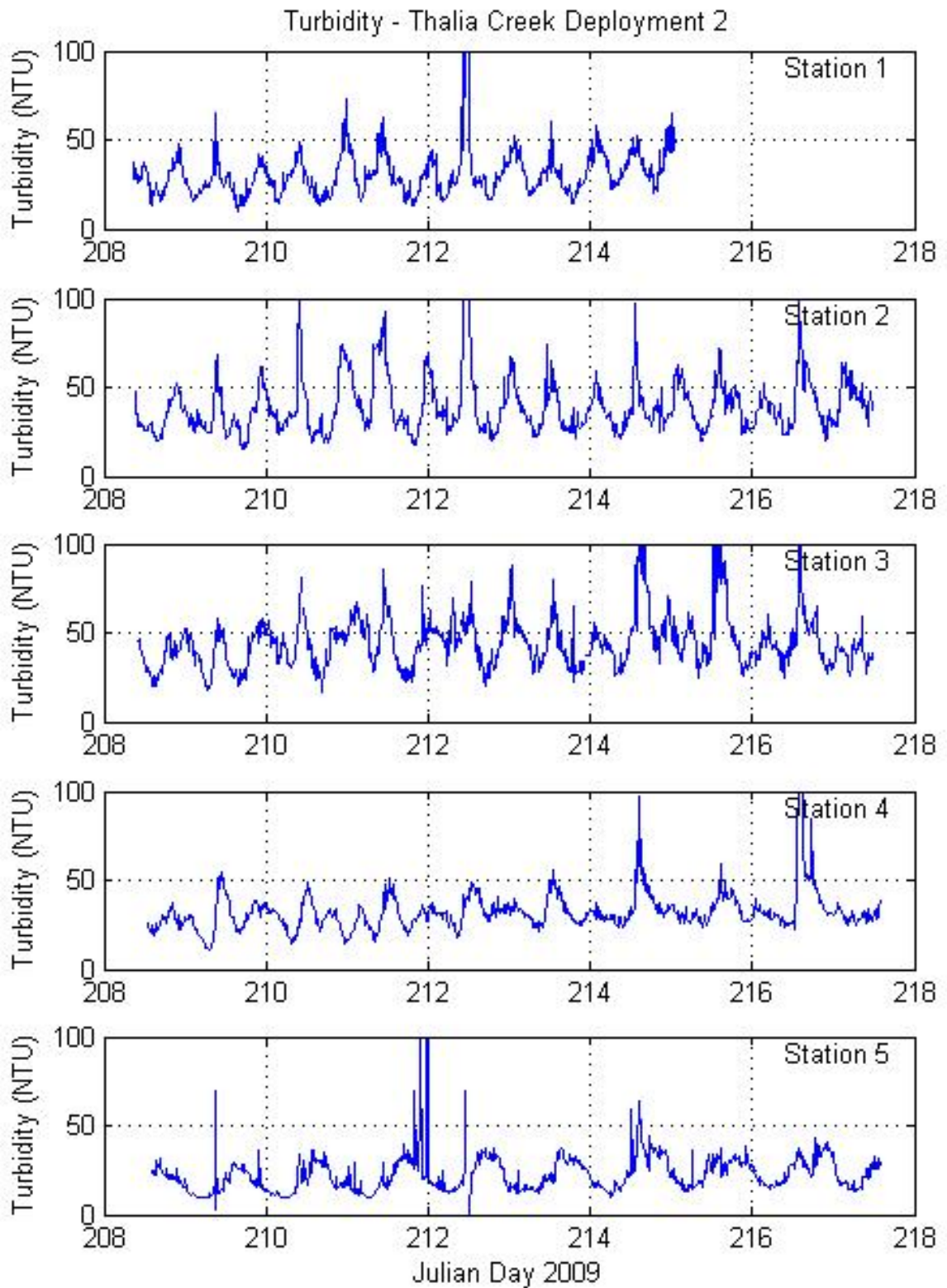
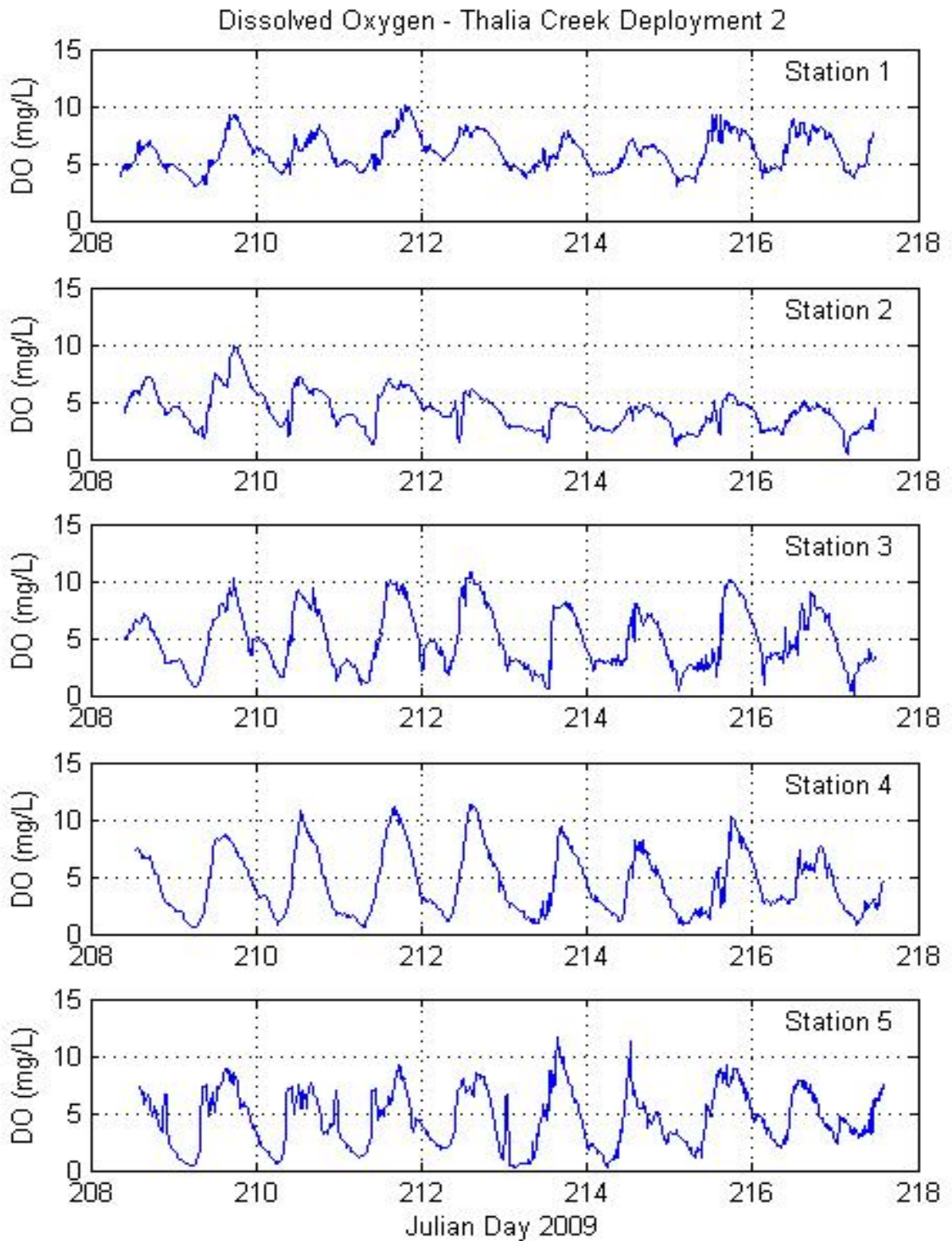Figure II.27. ConMon water quality station turbidity – Thurston Branch - Thalia
Creek Deployment 2 (July 27 to August 5, 2009).

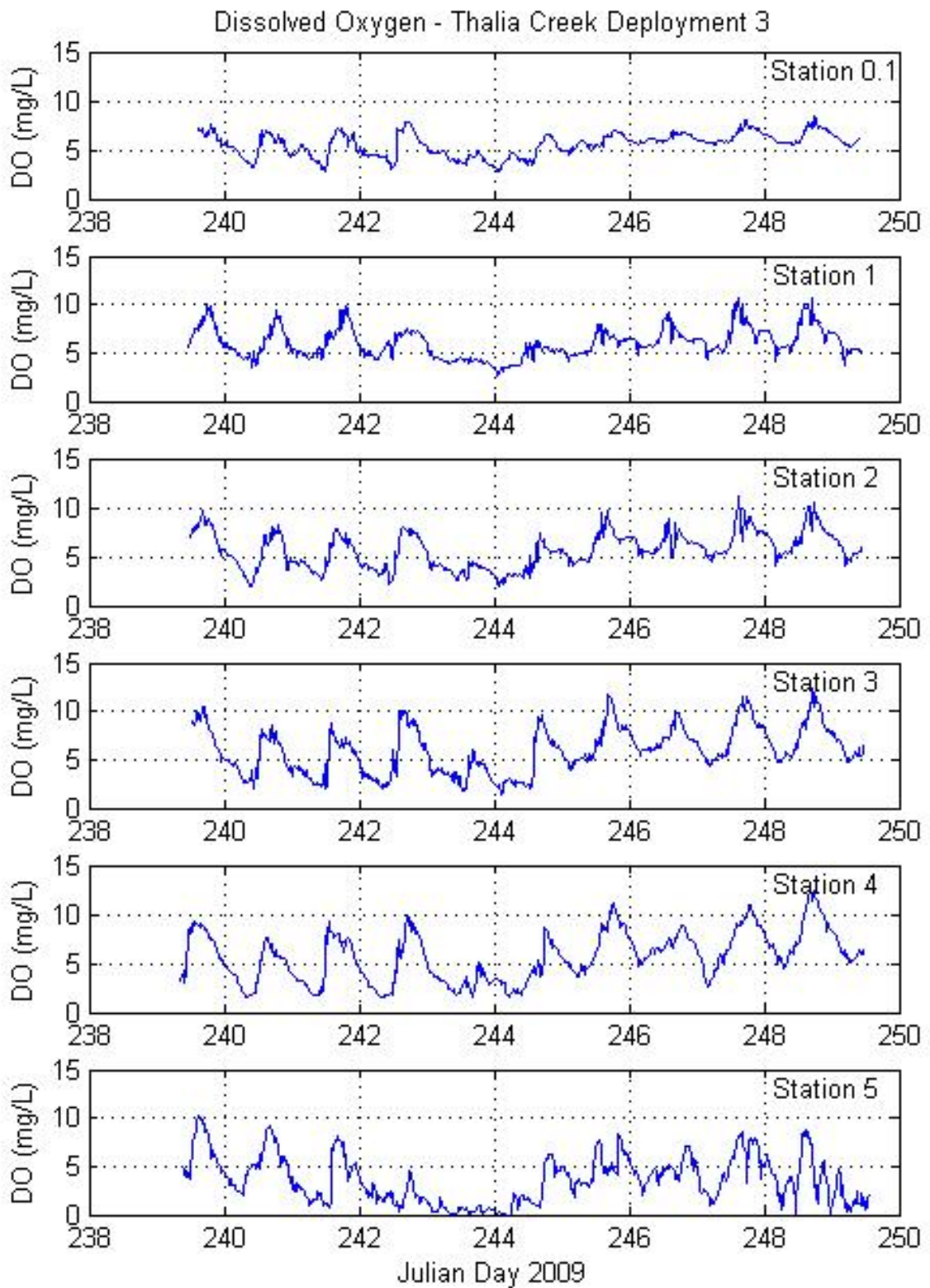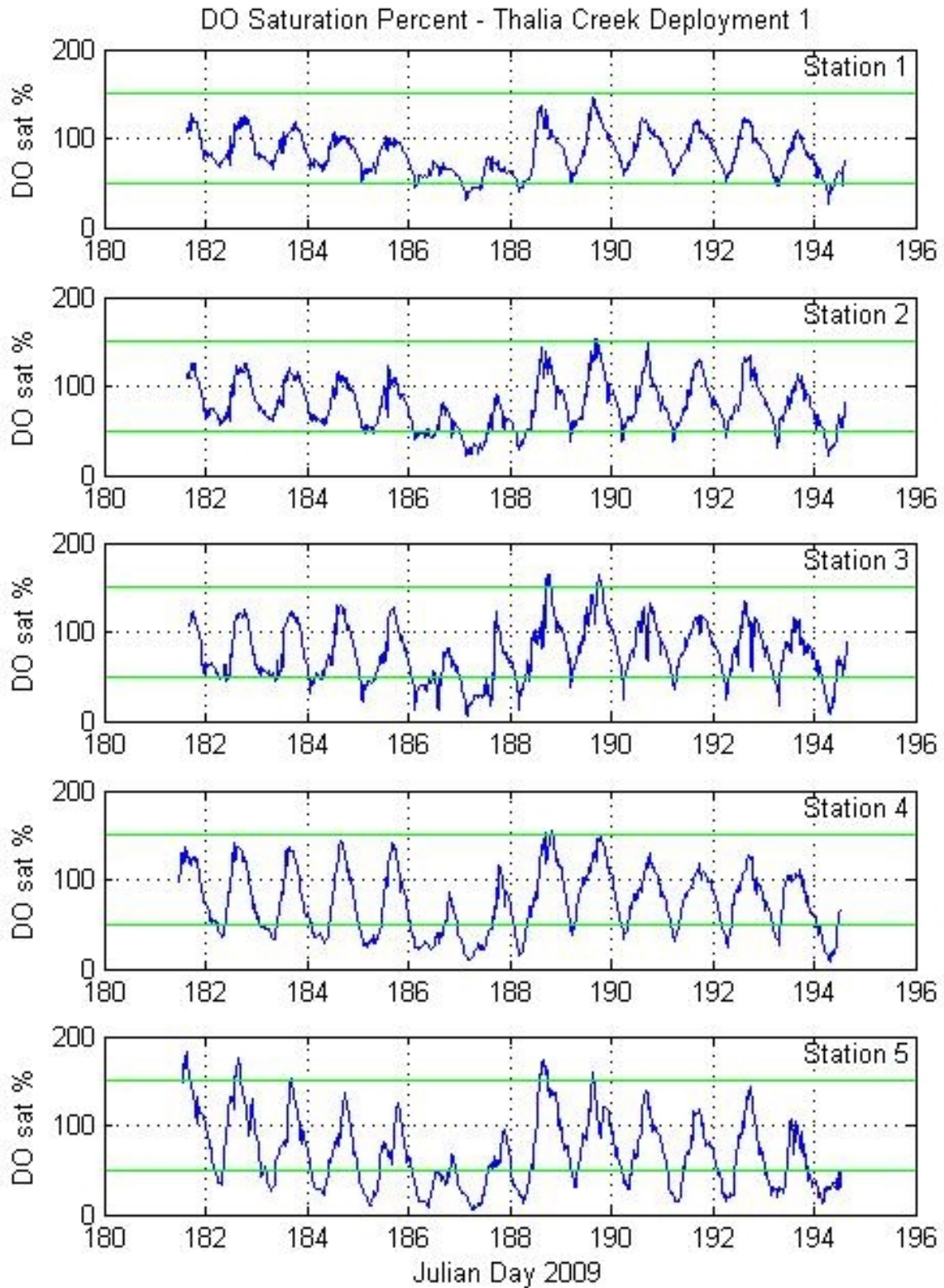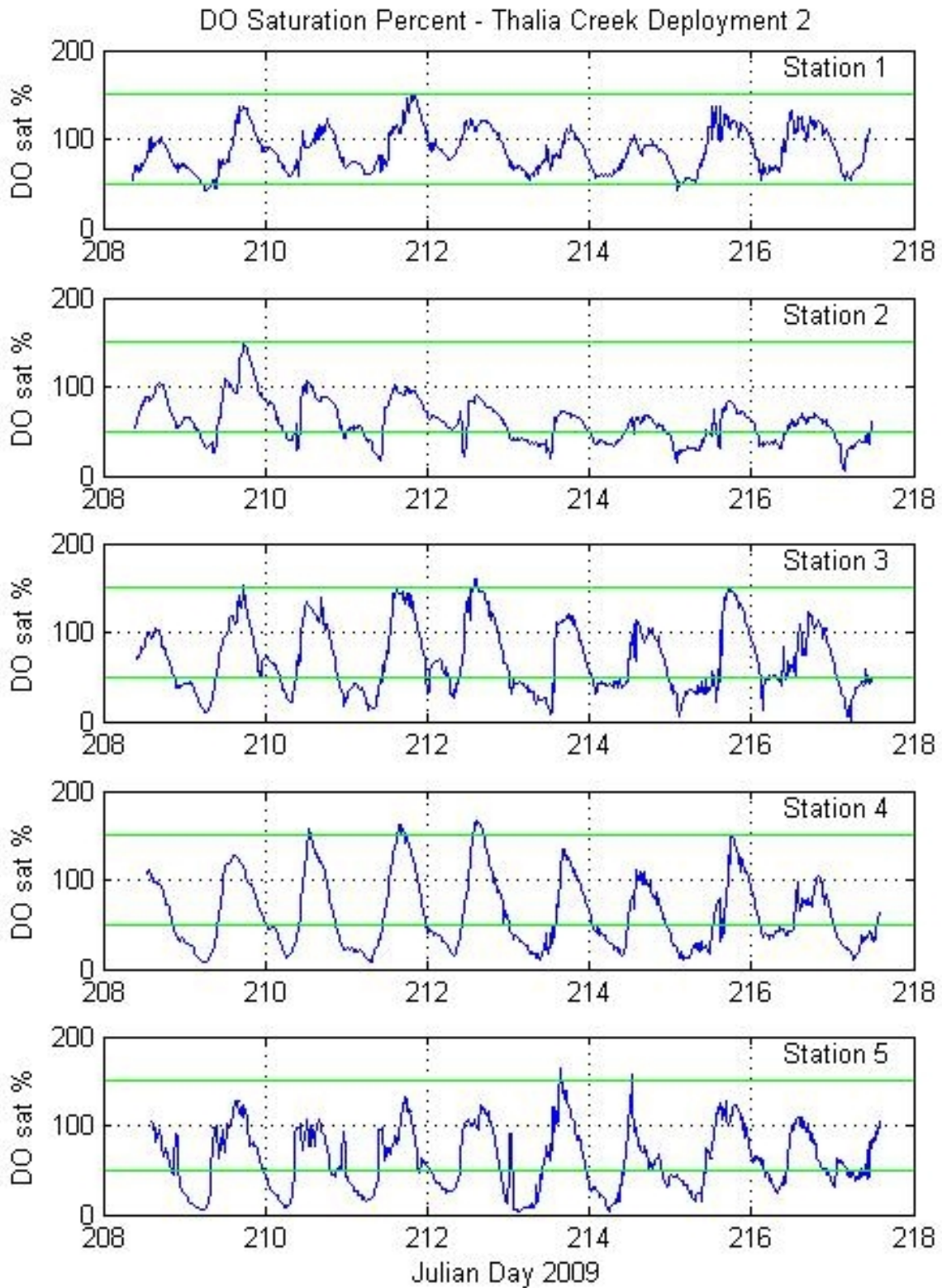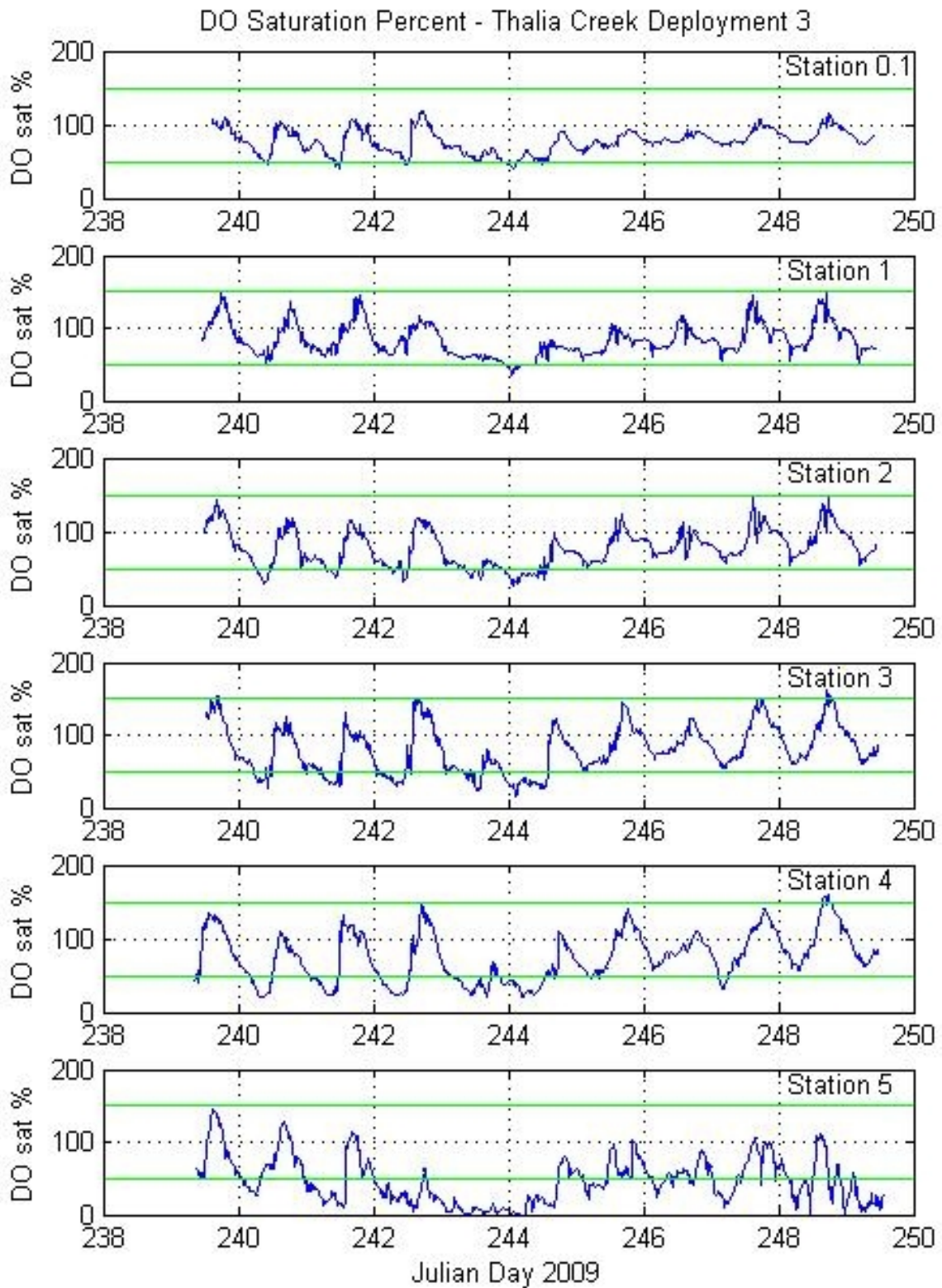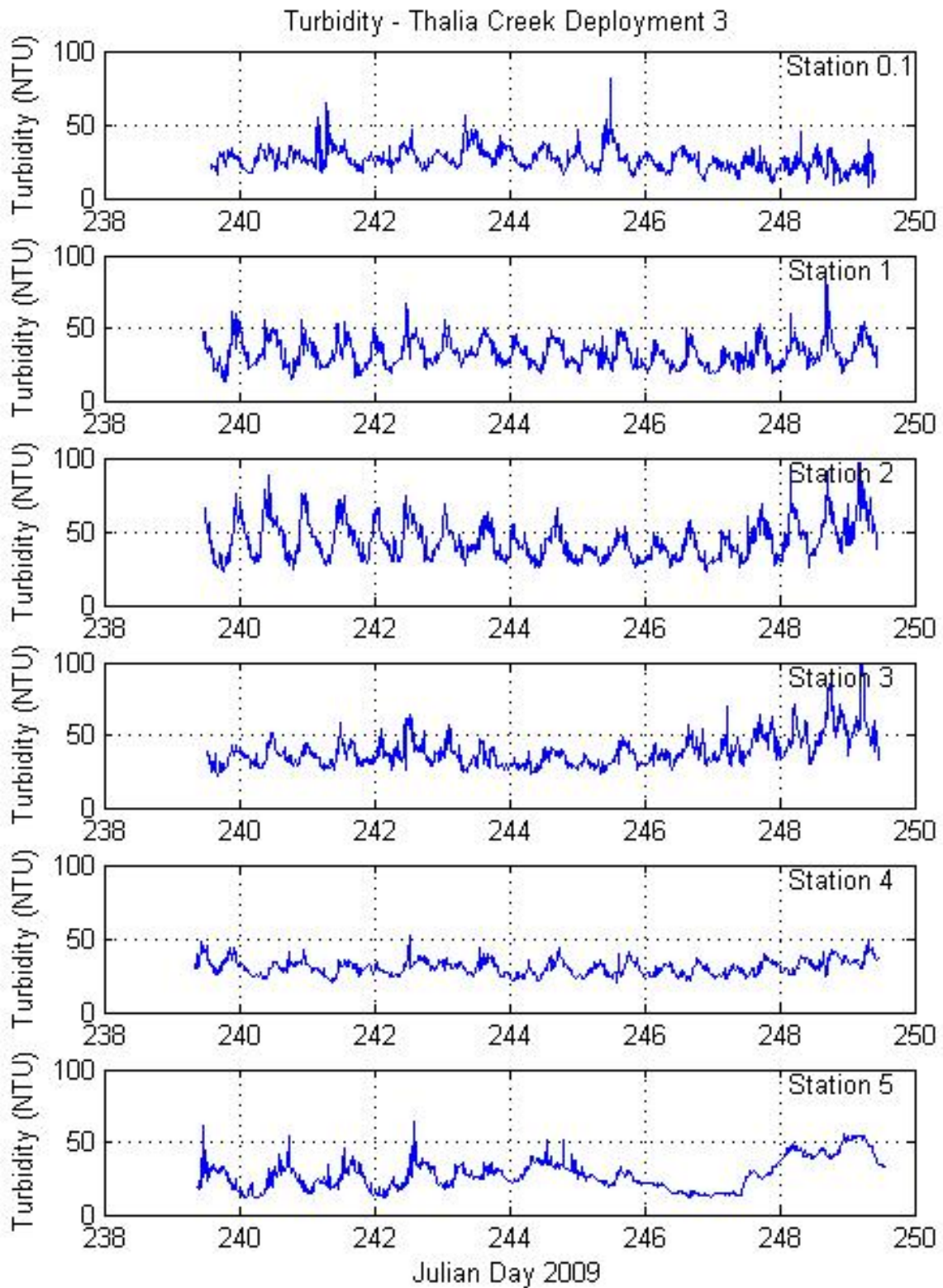Figure II.28. ConMon water quality station turbidity – Thurston Branch - Thalia Creek Deployment 3 (August 27 to September 6, 2009).

47

Table II.11. Summary statistics for turbidity (NTU) within the TB-TC system by ConMon water quality station and deployment period.

ConMon Station	Sampling Period 6/30-7/13/2009	Sampling Period 7/27-8/5/2009	Sampling Period 8/27-9/6/2009
0.1			Avg: 26.4 Min: 8.2 Max: 81.9 Std Dev: 7.5 N: 933
1	Avg: 50.0 Min: 3.5 Max: 782.5 Std Dev: 91.8 N: 1214	Avg: 71.1 Min: 7.9 Max: 587.5 Std Dev: 100.4 N: 856	Avg: 32.6 Min: 13.4 Max: 87.2 Std Dev: 9.2 N: 957
2	Avg: 30.4 Min: 13.9 Max: 79.4 Std Dev: 9.2 N: 1241	Avg: 39.2 Min: 15.0 Max: 185.3 Std Dev: 16.5 N: 869	Avg: 43.5 Min: 23.1 Max: 97.1 Std Dev: 12.6 N: 952
3	Avg: 39.4 Min: 14.7 Max: 539.6 Std Dev: 39.2 N: 1244	Avg: 44.3 Min: 17.1 Max: 156.1 Std Dev: 15.2 N: 863	Avg: 38.7 Min: 21.6 Max: 107.9 Std Dev: 10.7 N: 955
4	Avg: 25.3 Min: 11.7 Max: 51.4 Std Dev: 6.0 N: 1247	Avg: 32.4 Min: 10.9 Max: 136.1 Std Dev: 11.2 N: 867	Avg: 30.6 Min: 20.6 Max: 51.7 Std Dev: 5.1 N: 972
5	Avg: 22.0 Min: 10.3 Max: 57.5 Std Dev: 5.9 N: 1233	Avg: 22.2 Min: 2.5 Max: 64.3 Std Dev: 8.5 N: 846	Avg: 27.8 Min: 11.5 Max: 63.4 Std Dev: 10.4 N: 977
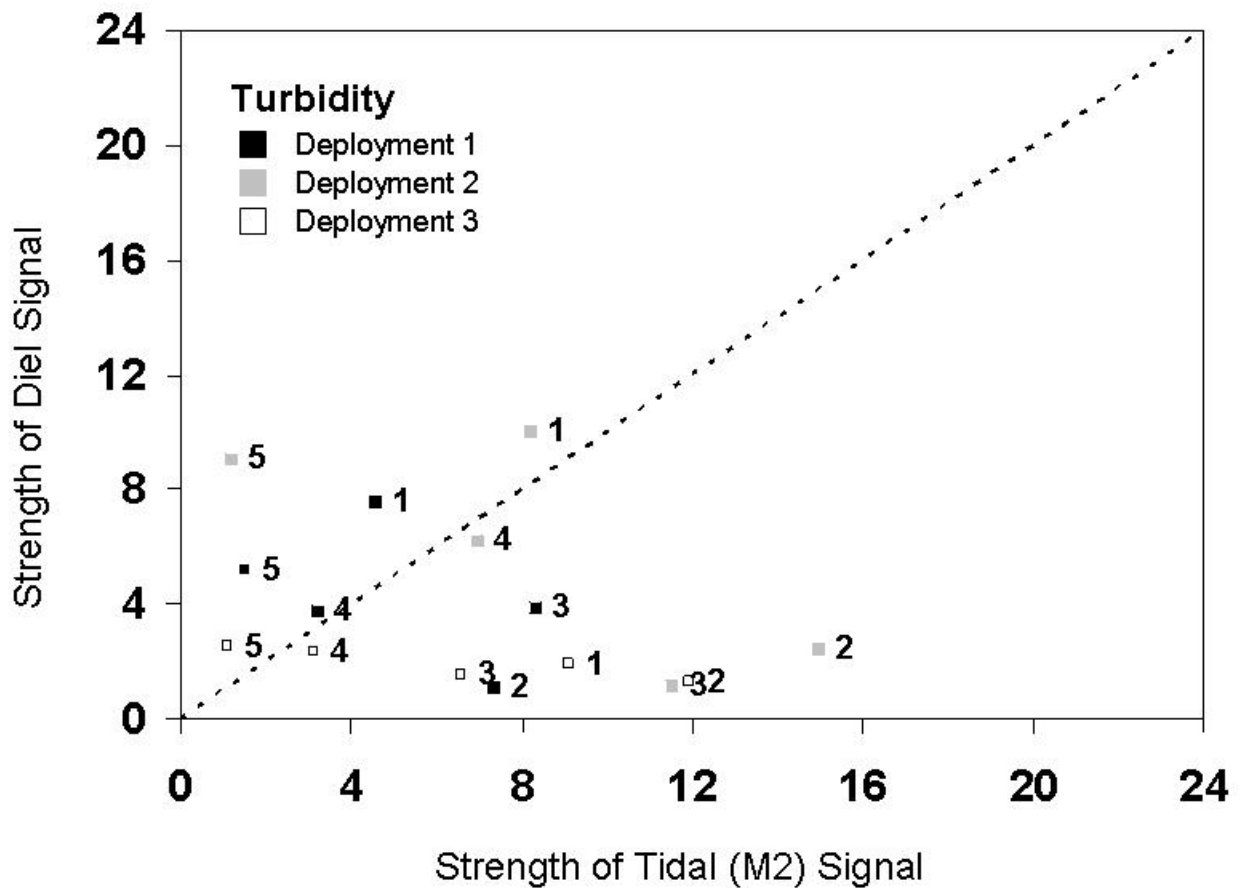
Figure II.29. Diel (24 hr) versus semi-diurnal (12.4 hr) influence on turbidity (NTU) levels by station and deployment period. Points plotting near the 45° or 1:1 line indicate diel (24 hr) and semi-diurnal (12.4 hr) forces equally influence turbidity (NTU) levels.

II-2-8 Estimation of Gross Primary Production and Community Respiration

High-frequency dissolved oxygen measurements were analyzed to provide estimates of ecosystem metabolism (e.g., gross photosynthesis and respiration) within the TB-TC system. This method utilizes a characteristic diurnal dissolved oxygen (DO) pattern exhibited in open waters where oxygen dynamics are dominated by biological processes rather than physical processes (Odum, 1956). In general, (1) DO levels rise from morning to mid-afternoon due to increasing photosynthetic oxygen production that is in excess of respiration rates, (2) beginning in late afternoon or evening, DO levels start to decline and continue to decrease as photosynthetic production rates approach zero at darkness, and (3) DO levels continue to decline through the evening due to continued

respiration with minimum DO levels being observed in the early morning hours. Open-water DO methods have been used in a range of estuarine studies to calculate ecosystem metabolism (Kemp et al., 1992; D'Avanzo et al., 1996; Caffrey, 2004).

For each 15 minute time interval, the DO_{conc} rate of change or flux (O_{flux}) within a defined area of water column was determined and adjusted for diffusion across the air-sea interface using equation II.1.

$$O_{flux} = [(DO_{t2} - DO_{t1}) \times z] - AS_{15\ minute\ exchange}$$ Equation II.1.

where:

   O_{flux} = Oxygen flux (g O_2 $m^{-2} \cdot$15 min^{-1})
   DO_{t2} = DO concentration at time interval 2 (g O_2 m^{-3})
   DO_{t1} = DO concentration at time interval 1 (g O_2 m^{-3})
   z = Water depth (m)
   $AS_{15\ minute\ exchange}$ = 15 minute Air-Sea exchange rate (g O_2 m^{-2})

Air-Sea exchange rate or net oxygen flux across the sea-water interface due to diffusion was estimated using hourly average wind speed (m·sec^{-1}) and 15-minute water column oxygen concentrations relative to saturation levels based on measured temperature and salinity (D'Avanzo et al., 1996) (Equation II.2).

$$AS_{15\ minute\ exchange} = 0.209 \left[\frac{(DO_{sat} - DO_{obs})}{DO_{sat}} \right] \times \frac{k_{O2}}{4}$$ Equation II.2.

where:

   $AS_{15\ minute\ exchange}$ = 15 minute Air-Sea exchange rate (g O_2 m^{-2})
   DO_{sat} = O_2 concentration calculated at atmospheric equilibrium (mg·L^{-1})
   DO_{obs} = Observed O_2 concentration (mg·L^{-1})
   k_{O2} = Gas exchange coefficient (g O_2 $m^{-2} \cdot hr^{-1}$)

The gas exchange coefficient (k_{O2}) was based on average hourly wind speed (W, m·sec^{-1}) measured at the Oceana NAS (13769) NOAA National Weather Service station following a logarithmic adjustment (D'Avanzo et al., 1996).

Net ecosystem metabolism (NEM) is a useful indicator of a water bodies' trophic status or condition. A positive NEM is indicative of an autotrophic system where internal production of organic matter dominates, whereas a negative NEM suggests that the system is heterotrophic and dependent on external sources of organic matter. To calculate daily net ecosystem metabolism (NEM), the 15-minute diffusion-corrected oxygen fluxes were summed over a 24-hour period based on site sunrise and sunset information. For example, the daily NEM calculation for July 1, 2009 would have summed 15-minute O_2 Flux values 05:00 July 1 to 05:00 July 2, 2009. Time estimates of sunrise and sunset for Virginia Beach, VA were determined via an online calculator (http://www.timeanddate.com/worldclock/sunrise.html) (Table II.12).

Table II.12. Time estimates of study site sunrise and sunset by sampling period and time and duration of daylight and nighttime hours. Day length is a function of site latitude and the day of the year and was defined as the time period when the upper limb of the sun's disk appears above the horizon (sunrise) to when the upper limb disappears below the horizon (sunset). Note: Time is referenced to EST.

Sampling Period	Time Estimates for Sunrise/Sunset (EST)	Daylight Hrs. (EST)	Night Hrs. (EST)
Start: 6/30/2009 End: 7/13/2009	Sunrise: 05:00 Sunset: 19:30	05:00 to 19:30 Hours: 14.5	19:30 to 05:00 (following day) Hours: 9.5
Start: 7/27/2009 End: 8/5/2009	Sunrise: 05:00 Sunset: 19:00	05:00 to 19:00 Hours: 14.0	19:00 to 5:00 Hours: 10.0
Start: 8/27/2009 End: 9/6/2009	Sunrise: 05:30 Sunset: 18:30	05:30 to 18:30 Hours: 13.0	18:30 to 5:30 Hours: 11.0

In addition to NEM, estimates of ecosystem total respiration (24 hr) and gross production were also calculated. Daily community total respiration (R_{com}), based on 15-minute night-time oxygen fluxes, was extrapolated over a 24-hour period according to Equation II.3. Multiplying nighttime oxygen fluxes by -1 was necessary in order to express respiration as a positive number.

$$R_{com} = \left[-1 \times \frac{\left(\sum_{Sunset}^{Sunrise} O_{flux} \right)}{dt_{night}} \right] \times 24$$

Equation II.3.

where:

R_{com} = Daily community respiration (g O_2 m^{-2}·day^{-1})
O_{flux} = Oxygen flux (g O_2 m^{-2}·15 min^{-1})
dt_{night} = night-time interval (hr)

Ecosystem gross production (P_{gross}) was calculated by adding the daytime ecosystem production (P_{net}) to the mean nighttime respiration rate multiplied by daytime hours as shown in equation II.4.

$$P_{gross} = \left[\left(-1 \times \frac{\left(\sum_{Sunset}^{Sunrise} O_{flux}\right)}{dt_{night}}\right) \times dt_{day}\right] + \sum_{Sunrise}^{Sunset} O_{flux}$$

Equation II.4.

where:

P_{gross} = Daily gross productivity (g O_2 m^{-2}·day^{-1})
O_{flux} = Oxygen flux (g O_2 m^{-2}·15 min^{-1})
dt_{night} = night-time interval (hr)
dt_{day} = daytime interval (hr)

Combined deployment summary statistics of net ecosystem metabolism, daily total respiration and daily gross production are shown in Figure II.30. Overall mean respiration rates varied from 10.09-16.97 g O_2 m^{-2}·day^{-1} with daily values ranging from 4.01-24.50 g O_2 m^{-2}·day^{-1}. In a survey of shallow mid-Atlantic estuarine systems, Caffrey (2004) reported mean summer respiration rates on the order of 9-26 g O_2 m^{-2}·day^{-1}; respiration rates were usually 1.5 to 2 times higher in the summer than any other season. Mean estimates of summer gross productivity ranged from 8.45- 15.51g O_2 m^{-2}·day^{-1} with daily values ranging from -0.69 to 25.44 g O_2 m^{-2}·day^{-1}. These values are also within the range (5-23 g O_2 m^{-2}·day^{-1}) reported by Caffrey (2004).

All stations exhibited an overall negative NEM with mean values ranging from -1.8 to -0.5 g O_2 m^{-2}·day^{-1} with daily values exhibiting both negative and positive values (range: -6.96 to 2.98 g O_2 m^{-2}·day^{-1}). While positive NEM values were observed, indicating some level of autotrophy, the overall negative mean NEM values indicates that the TB-TC system is primarily heterotrophic over the summer season. This suggests that a significant amount of carbon is being respired and that allochthonous sources of carbon are helping to fuel the high respiration rates. Potential "external" sources of organic carbon could include (1) terrestrial inputs during periods of freshwater inflow, (2) tidal marsh inputs, (3) benthic algal production in the shallow shoals regions and (4) inputs from the more marine Lynnhaven River system. A distinct spatial trend was observed along the salinity gradient of the TB-TC system with net heterotrophy increasing with distance upstream. This observation supports the premise that external loadings to the TB-TC system are more watershed or internally (e.g., marshes, benthic algae) based.
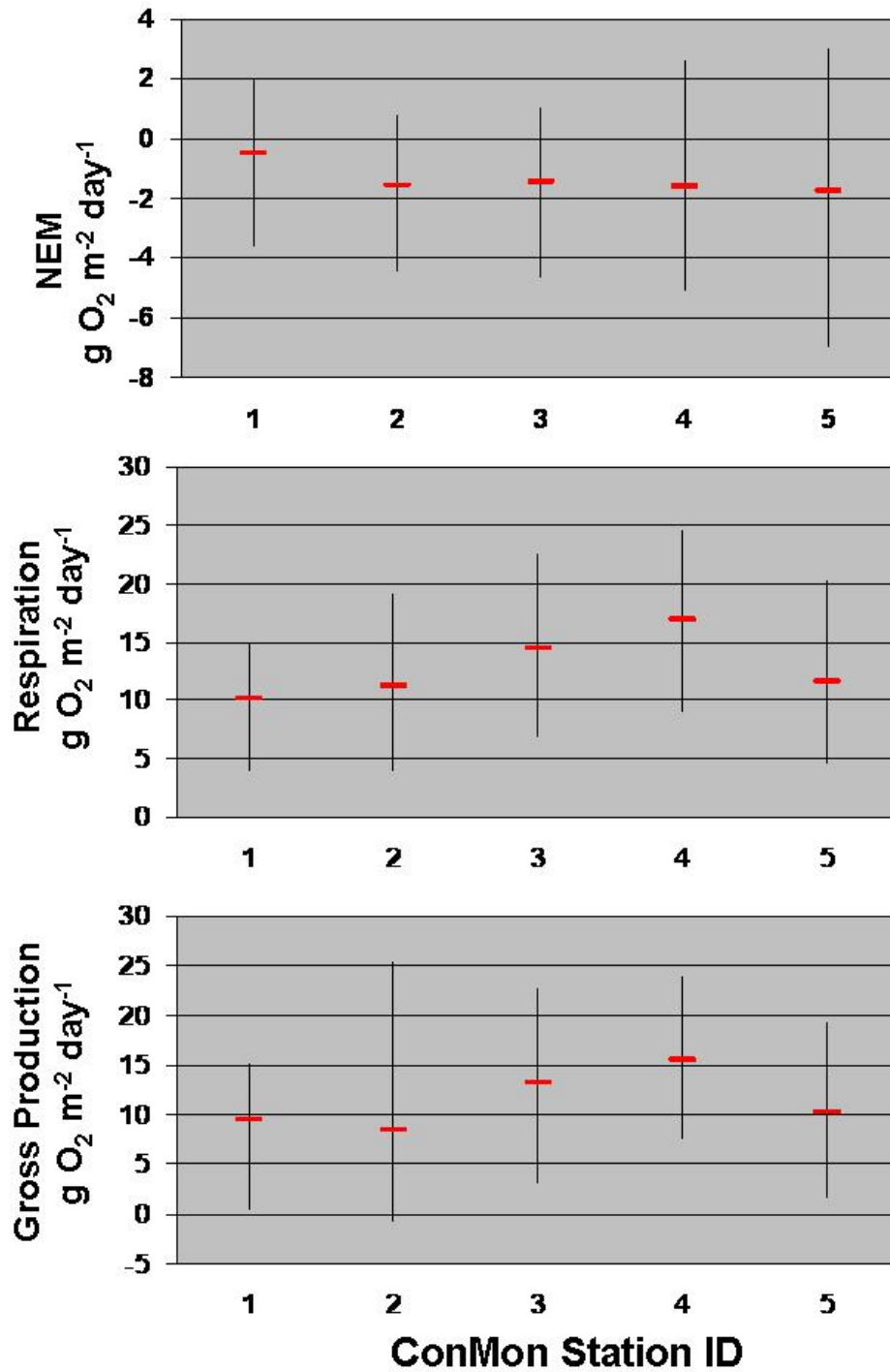
Figure II.30. Summary of net ecosystem metabolism (NEM), respiration and gross productivity rates within TB-TC. Red horizontal lines represent overall mean values based on all three deployment periods and error bars indicate minimum and maximum calculated rates.

II-3 Water Quality Grab Sample Surveys

In addition to the ConMon water quality stations, three water quality grab sampling surveys were conducted throughout the TB-TC and BC region in the summer of 2009. Each survey consisted of approximately 20 sampling stations with locations depicted in Figure II.3 and listed in Table II.13. Because sampling stations had to be accessed by a variety of means (i.e., vessel, vehicle and foot), long vessel transport times due to vessel ramp access and extensive no wake zones, and time required at each station, a near synoptic sampling of the system was not possible. It took typically between 5-6 hours to collect samples for each survey. On June 30th (high tide: 16:00 EST; sampling period: 11:36-16:37 EST), sampling order was headwater stations (Stations: 12-17), followed by TB-TC samples (Stations: 1-11) and then BC (Stations: 19-21). On July 27th (high tide: 13:45 EST; sampling period: 9:22-15:34 EST), sampling order was TB-TC, followed by BC and then headwater stations. On August 27th (high tide: 15:00 EST; sampling period: 8:10-13:16 EST), sampling order was headwater stations, followed by TB-TC and then BC.

The grab samples were taken at a depth of 0.25 m below the surface and during day-time hours. For each grab sample, the following parameters were measured: water temperature, salinity, pH, percent saturation of dissolved oxygen ($DO_{\%sat}$), dissolved inorganic phosphorus (PO_4; $mg \cdot L^{-1}$ as P), total dissolved phosphorus (TDP; $mg \cdot L^{-1}$ as P), ammonium (NH_4; $mg \cdot L^{-1}$ as N), nitrite (NO_2; $mg \cdot L^{-1}$ as N), nitrate + nitrite (NO_{23}; $mg \cdot L^{-1}$ as N), total dissolved nitrogen (TDN; $mg \cdot L^{-1}$ as N), chlorophyll-a ($\mu g \cdot L^{-1}$), pheopigment ($\mu g \cdot L^{-1}$), fecal coliform ($MPN \cdot 100\ ml^{-1}$), and *Escherichia coli* (*E. coli*; $MPN \cdot 100\ ml^{-1}$). Calculated parameters at each station included DO_{conc} (based on DO_{sat}; $mg \cdot L^{-1}$), dissolved organic phosphorus ($DOP = TDP-PO_4$; $mg \cdot L^{-1}$ as P), nitrate ($NO_3 = NO_{23}-NO_2$; $mg \cdot L^{-1}$ as N), dissolved inorganic nitrogen ($DIN = NH_4+NO_{23}$; $mg \cdot L^{-1}$ as N), dissolved organic nitrogen ($DON = TDN-DIN$; $mg \cdot L^{-1}$ as N) and DIN:DIP ratio. At each grab sampling point, vertical profiles of water temperature, salinity, pH, $DO_{\%sat}$ were field measured with a YSI 600 XL instrument; DO_{conc} was calculated. Sample depth intervals started at 10 cm below the surface, and continued at 25-cm intervals from the surface until the bottom was reached.

Nutrient samples were collected in acid washed, deionized rinsed nalgene bottles and stored on ice (4 °C) until return to the CBNERR laboratory located on the VIMS main campus in Gloucester Point, VA. Upon return to the laboratory, samples were immediately filtered with 0.45 μm membrane filters. Analysis of NH_4, NO_2 and PO_4 was conducted following sample filtration, whereas, samples for NO_3, TDN and TDP were stored frozen and analyzed at a later date. NH_4 was determined by a phenol hypochlorite method (Solorzano, 1969). NO_2 was determined by diazotizing with sulfanilamide and coupling with N-(1-naphthyl)-ethylenediamine to form an azo dye (U.S. EPA, 1983; Method 354.1). NO_3^- was determined after reduction to nitrite by use of Cu-Cd columns (U.S. EPA, 1983; Method 353.1). Dissolved inorganic phosphorus (PO_4) was determined by a single combined reagent ascorbic acid method (U.S. EPA, 1983; Method 365.2). TDP and TDN were determined using an alkaline potassium persulfate digestion method (modified from D'Elia (1977)); following digestion, TDP and TDN samples were

buffered and analyzed for NO_{23} and PO_4, respectively. Method detection limits (MDL) were 0.0015 mg·L^{-1} as P for PO_4, 0.0030 mg·L^{-1} as P for DOP and TDP, 0.0035 mg·L^{-1} as N for NH_4, 0.0002 mg·L^{-1} as N for NO_2, 0.0014 mg·L^{-1} as N for NO_3 and NO_{23}, and 0.0084 mg·L^{-1} as N for TDN and DON. Values below MDL were reported as ½ MDL.

Plant pigment samples were collected in deionized rinsed nalgene bottles and stored on ice until returned to the laboratory. Samples were then filtered with glass fiber filters, with filters being drawn dried, folded, sealed in an aluminum foil packet, and stored at – 20 °C until analysis; holding time was on the order of days. Chlorophyll *a* (Chl *a*) analysis followed a DMSO/acetone extraction procedure and quantified using a turner fluorometer (Jeffrey et al., 1996). For pheophytin measurements, samples were acidified and read again. Method detection limits were 0.5 µg·L^{-1} for Chl *a* and pheopigments.

Table II.13. Locations of grab samples taken in the TB-TC system with additional stations located in the upper Western Branch of Lynnhaven and Buchanan Creek.

Station	Location	Latitude	Longitude	June 30	July 27	August 27
1	Marker 33	36.85728	76.11212	x	x	x
2	YSI Station 1	36.86190	76.11472	x	x	x
3	Marker 40	36.85823	76.11760	x	x	x
4	Marker 43	36.85693	76.12227	x	x	x
5		36.85540	76.12473	x	x	x
6	Reservoir	36.85505	76.12787	x		
6A	Reservoir Runoff	36.85502	76.12786			x
6B	Embayment below Res.	36.85448	76.12634		x	x
7		36.85317	76.12643	x	x	x
8	Marker 53	36.84968	76.12662	x	x	x
9		36.84898	76.13023	x	x	x
10	Marker 57	36.84748	76.12290	x	x	x
11						
12	Church lot	36.84433	76.12395	x	x	x
13		36.83993	76.12673	x		x
14		36.83760	76.12922	x	x	x
15		36.83725	76.13265	x	x	x
16	Near bridge	36.83660	76.12557	x	x	x
17		36.83302	76.12117	x	x	x
18		36.85963	76.11330	x	x	x
19		36.85623	76.11630	x	x	x
20		36.85760	76.10823	x	x	x
21		36.85932	76.10410	x	x	x

Bacteriological samples were collected in sterile 100 ml bottles and stored at 4 °C until analysis that occurred within eight hours of collection. Fecal coliform bacteria (FCB) were enumerated by the Most Probable Number (MPN) procedure using A-1 medium (APHA, 1992; Method 9221 E). The standard 5-tube, three or four serial dilution MPN test was used. Because of the presence of ubiquitous fecal coliform positive organisms in aquatic environments, a fluorogenic confirmation assay for *E. coli* was run on all samples (Feng and Hartman, 1982). The lower and upper method detection limit for FCB MPN index were 2 and 1600 MPN·100 ml^{-1}, respectively.

II-3-1 Temperature, Salinity and Dissolved Oxygen

Grab sample data for temperature, salinity and dissolved oxygen are provided in Table II.14 for June 30, 2009, Table II.15 for July 27, 2009 and Table II.16 for August 27, 2009 sampling. Temperature varied between 28.4-31.88 °C during the June 30 survey, 28.5-31.2 °C during the July 27 survey and 25.6-32.7 °C during the August 27, 2009 survey. General spatial trends were not expected given the duration of the sampling period. Salinity varied between 1.90 and 19.63 psu, 9.09 and 20.69 psu and 0.25 and 17.03 psu throughout the tidal TB-TC system on June 30, July 27 and August 27, respectively. The non-tidal TB impoundment (Station 6) exhibited salinities (0.04-0.06 psu) characteristic of freshwater and discharged into TB-TC via a spillway throughout the study period. Measured salinity downstream from TB-TC varied from 16.8-20.8 psu in the upper reach of the Western Branch of the Lynnhaven River and 22.9-23.3 psu in Lynnhaven Bay near the Lynnhaven Inlet. Salinity signals indicated freshwater inputs from all smaller tidal creek systems within TB-TC. Near surface dissolved oxygen levels were strongly influenced by the time of day samples were collected. Day-time concentrations varied from 7.1-11.3 mg· L^{-1} on June 30, 4.4-11.3 mg· L^{-1} on July 27 and 3.4-10.5 mg· L^{-1} on August 27, 2009 within tidal portions of TB-TC.

II-3-2 Nutrients

Grab sample data for nutrients are provided in Table II.14 for June 30, 2009, Table II.15 for July 27 and Table II.16 for August 27, 2009. Spatial plots of ammonium (NH_4) concentrations for the three grab sample periods are provided in Figures II.31 through II.33. NH_4 concentrations varied from 0.0056 to 0.3488 mg·L^{-1} as N over the three grab sample periods. During the June 30 and July 27 samplings, maximum NH_4 concentrations observed were 0.1037 and 0.0378 mg·L^{-1} as N, respectively. During these samplings, NH_4 represented less than 5 percent of the TDN pool; exception occurred at the uppermost TC station (Station 17: 11%) on July 27. NH_4 levels were somewhat elevated in the upper reaches of TC (at and above Station 12) on the August 27, 2009 sampling as compared to the previous sampling dates. With a maximum observed concentration of 0.3488 mg·L^{-1} as N (Station 16) in the upper region, NH_4 represented a greater proportion of the TDN pool and was approximately 20% at Station 15, 30% at Stations 12, 13 and 17, and 50% at Station 16. It should be noted that samplings on June 30 and July 27, 2009 were preceded by at least five days of no significant rainfall as compared to the August 27, 2009 sampling where 4.6 cm and 2.9 cm was recorded at Oceana on August 22 and 24, 2009 respectively. Elevated NH_4 levels were generally

56

consistently higher in the upper portions of TC, particularly at Stations 16 and 17, than concentrations observed in TB, BC and the upper portion of the Western Branch of the Lynnhaven River.

Nitrite (NO_2) concentrations were below method detection limits for all sampling stations except 1 and 17 during the June 30 and July 27, 2009 samplings. While stations within the lower reaches of TC, TB, BC and the upper portion of the Western Branch of the Lynnhaven River exhibited below detection limit method concentrations of NO_2 on the August 27, 2009 sampling, concentrations up to 0.0154 mg·L^{-1} as N were observed in the upper reaches of TC (Stations 12-17). Even at its highest concentration, NO_2 only represented 2 percent of the TDN pool. Nitrification, the microbial mediated process that results in the oxidation of NH_4, could be responsible for the somewhat elevated NO_2 levels observed in the upper portions of TC during the August 27 sampling. As with NO_2, NO_3 concentrations were generally below method detection limits or low (< 0.0030 mg·L^{-1} as N) during the June 30 and July 27 samplings. Exception occurred at the uppermost TC station (Station 17) where NO_3 concentration of 0.0111 mg·L^{-1} as N was observed. During the August 27, 2009 sampling, measurable NO_3 levels were observed throughout the TB-TC system. Samples from upper western branch of the Lynnhaven River, BC and TB remained at method detection limits or low concentrations (≤ 0.0055 mg·L^{-1} as N) and increased up to 0.1541 mg·L^{-1} as N in the upper reaches of TC. While generally representing < 2% of the TDN pool, the maximum observed NO_3 value of 0.1541 mg·L^{-1} as N accounted for 22% of the TDN pool.

While soluble inorganic nitrogen salts (primarily NO_3 and NH_4) are generally recognized as the primary nitrogen source for the growth of phytoplankton and benthic algae, recent evidence shows that labile forms (e.g., urea, amino acids) of DON can stimulate productivity in estuarine phytoplankton and bacteria. Additionally, DON can be further broken down through microbial-mediated processes to release NH_4. Therefore, DON should be assessed in eutrophication studies of estuarine waters. Spatial plots of DON concentrations for the three grab sample periods are provided in Figures II.34 through II.36. DON concentrations varied from 0.2411 to 0.8312 mg·L^{-1} as N over the three grab sample periods. Within BC (Stations 18-21), DON concentrations varied from 0.2919 to 0.6584 mg·L^{-1} over the three samplings and with exception of Station 20 on August 27, 2009 comprised ≥ 96% of the TDN pool. Within tidal portions of TB-TC, DON concentrations ranged from 0.2455 to 0.8312 mg·L^{-1} as N over the three sampling periods and displayed a general inverse relationship with salinity resulting in elevated readings in headwater regions. By and large, DON accounted for ≥ 95% of the TDN pool within TB-TC. Exception occurred on the August 27, 2009 sampling when Station 12 and selected upper reach stations exhibited lower percentages (50-80%) due to elevated NH_4 levels contributing to the TDN pool. Given the limitations of inorganic nitrogen concentrations to assess eutrophic status of estuarine waters, TDN is generally considered a more useful index or metric. Spatial plots of TDN concentrations for the three grab sample periods are depicted in Figures II.37 through II.39. TDN concentrations varied from 0.2609 to 0.9191 mg·L^{-1} as N over the three grab sample periods. Within the TB-TC system, TDN showed a relatively consistent gradient with moderately high concentrations (> 0.6 mg·L^{-1} as N) in the upper reaches of TC and decreasing with distance downstream.

Spatial plots of dissolved inorganic phosphorus (PO_4) concentrations for the three grab sample periods are provided in Figures II.40 through II.42. PO_4 concentrations varied from 0.0065 to 0.0598 mg·L^{-1} as P over the three grab sample periods. PO_4 generally showed marginally elevated levels in headwater regions as compared to more open water down stream stations in TB-TC. Incorporating all stations, PO4 represented 43% (range: 30-60%) of the TDP pool on June 30, 28% (range: 19-46%) on July 27 and 63% (range: 45-84%) on August 27, 2009 samplings. As with PO_4 concentrations, its relative percent contribution to the TDP pool was greatest in the upper reaches of TC and BC where there existed extensive tidal marshes. DOP concentrations varied from 0.0052 to 0.0472 mg·L^{-1} as P within TB-TC over the three sampling period; the highest observed value, 0.0653 mg·L^{-1} as P, was observed in the upper Western Branch of Lynnhaven River (Station 1) on July 27, 2009. Spatial plots of TDP concentrations for the three grab sample periods are provided in Figures II.43 through II.45. TDP concentrations ranged from 0.0163 to 0.0802 mg·L^{-1} as P, which is representative of medium conditions based on national eutrophication assessment criteria (medium: ≥ 0.01 to ≤ 0.1 mg·L^{-1} as P; Bricker et al., 1999). There were no consistent spatial patterns associated with TDP within the TB-TC system.

Assuming that the molar uptake ratios of nitrogen and phosphorus by marine/estuarine phytoplankton are relatively constant (DIN:PO_4 = 16:1; Redfield et al., 1963), water column DIN: PO_4 ratios can provide insight into primary productivity limitation. Spatial plots of DIN: PO_4 ratios for the three grab sample periods are provided in Figures II.46 through II.48. DIN: PO_4 ratios ranged from 0.7-6.0 in tidal portions of TB-TC on June 30, 1.6-5.7 on July 27 and 0.7-57.9 on August 27, 2009. No clear DIN: PO_4 gradient patterns were observed for the June 30 and July 27, 2009 sampling. In contrast, August 27, 2009 DIN: PO_4 ratios showed an increasing trend with distance upstream in the upper portion of TC (Station 12 and above); exception to this occurred within the smaller western branch of TC. DIN: PO_4 ratios increased from 19.9:1 (Station 12) to 57.9:1 (Station 17), while ratios below the region were on the order of 2:1 or less. It should be noted that approximately 7 cm of rainfall occurred within 5 days preceding the August 27, 2009 sampling and 3 cm within 3 days of sampling. The increased in DIN: PO_4 ratios observed in the upper TC region on August 27, 2009 was a result of increases in both NH_4 and NO_3 levels. Results from June 30 and July 27, 2009 suggest nitrogen limitation of primary productivity throughout the TB-TC system. DIN: PO_4 ratios observed on August 27, 2009 are indicative of nitrogen limitation of primary productivity in the lower, high salinity reaches of TB-TC and phosphorus limitation, driven by potentially episodic runoff events, in portions of the upper, lower salinity TC. The sampled portions of Buchanan Creek exhibited DIN:PO_4 ratios reflective of nitrogen limitation throughout the summer sampling periods.

Table II.14. Grab sample data collected in Thurston Branch - Thalia Creek – Buchanan Creek on June 30, 2009.

Station	WT (°C)	Sal (ppt)	pH	DO (mg/L)	DO %sat	PO$_4$ (mg/L as P)	DOP (mg/L as P)	TDP (mg/L as P)	NH$_4$ (mg/L as N)	NO$_2$ (mg/L as N)	NO$_3$ (mg/L as N)	NO$_{23}$ (mg/L as N)	DIN (mg/L as N)	DON (mg/L as N)	TDN (mg/L as N)	DIN: DIP	Chla (µg/L)	Pheo (µg/L)	FC MPN/ 100 ml	E. coli MPN/ 100 ml
1	28.4	20.5	7.86	7.2	103.1	0.0137	0.0210	0.0347	0.0126	0.0001	0.0007	0.0007	0.0133	0.2829	0.2962	2.3	16.4	5.0	2	2
2	29.4	19.6	7.89	7.1	103.2	0.0170	0.0204	0.0374	0.0112	0.0001	0.0007	0.0007	0.0119	0.3698	0.3817	1.6	15.4	4.6	11	7
3	29.2	19.6	7.88	8.3	122.6	0.0153	0.0203	0.0356	0.0084	0.0001	0.0007	0.0007	0.0091	0.4021	0.4112	1.4	22.0	7.7	2	2
4	29.8	18.8	7.91	7.5	109.7	0.0186	0.0214	0.0400	0.0084	0.0001	0.0007	0.0007	0.0091	0.4228	0.4319	1.2	16.1	6.0	2	2
5	30.2	17.1	7.92	8.7	127.5	0.0170	0.0270	0.0440	0.0070	0.0001	0.0007	0.0007	0.0077	0.4284	0.4361	1.1	19.3	7.6	50	50
6	30.6	0.06	9.44	12.1	161.6	0.0170	0.0144	0.0314	0.0084	0.0001	0.0007	0.0007	0.0091	0.4650	0.4741	1.3	16.5	13.4	110	110
6A	*	*	*	*	*	*	*	*	*	*	*	*	*	*	*	*	*	*	*	*
6B	*	*	*	*	*	*	*	*	*	*	*	*	*	*	*	*	*	*	*	*
7	30.5	17.6	7.94	8.6	125.8	0.0170	0.0236	0.0406	0.0084	0.0001	0.0007	0.0007	0.0091	0.5635	0.5726	1.3	15.6	5.6	240	170
8	30.8	15.3	8.06	9.3	134.7	0.0186	0.0282	0.0468	0.0112	0.0001	0.0007	0.0007	0.0119	0.5229	0.5348	1.5	19.2	9.3	130	130
9	31.9	13.7	8.06	10.0	146.1	0.0120	0.0264	0.0384	0.0112	0.0001	0.0007	0.0007	0.0119	0.5305	0.5424	2.3	22.5	14.4	80	110
10	30.6	14.4	7.94	8.0	115.0	0.0220	0.0255	0.0475	0.0084	0.0001	0.0007	0.0007	0.0091	0.5247	0.5338	1.0	24.8	11.8	500	500
11	*	*	*	*	*	*	*	*	*	*	*	*	*	*	*	*	*	*	*	*
12	29.4	6.7	8.13	11.3	153.0	0.0253	0.0365	0.0618	0.0182	0.0001	0.0007	0.0007	0.0189	0.7077	0.7266	1.7	62.7	16.3	300	300
13	28.7	5.8	8.07	10.8	149.5	0.0236	0.0282	0.0518	0.0154	0.0001	0.0007	0.0007	0.0161	0.6517	0.6678	1.6	60.2	17.9	900	500
14	29.6	5.5	8.17	11.0	145.8	0.0186	0.0438	0.0624	0.0154	0.0001	0.0007	0.0007	0.0161	0.6218	0.6379	2.0	40.6	15.0	500	300
15	27.1	1.9	7.89	10.5	133.0	0.0485	0.0315	0.0800	0.0140	0.0001	0.0007	0.0007	0.0147	0.6346	0.6493	0.7	68.2	23.7	1600	1600
16	30.9	5.6	8.25	*	161.7	0.0319	0.0391	0.0710	0.0252	0.0001	0.0013	0.0014	0.0266	0.7788	0.8054	1.8	55.0	23.7	300	300
17	30.0	5.5	8.11	*	135.8	0.0402	0.0400	0.0802	0.1037	0.0014	0.0042	0.0056	0.1093	0.8098	0.9191	6.0	57.0	25.3	500	500
18	29.6	19.5	7.99	8.0	117.5	0.0170	0.0212	0.0382	0.0070	0.0001	0.0007	0.0007	0.0077	0.5688	0.5765	1.1	20.6	7.6	4	4
19	30.21	18.9	7.94	7.2	101.5	0.0170	0.0203	0.0373	0.0084	0.0001	0.0007	0.0007	0.0091	0.4286	0.4377	1.3	14.1	8.1	30	30
20	29.8	19.3	7.96	7.2	103.7	0.0153	0.0256	0.0409	0.0070	0.0001	0.0007	0.0007	0.0077	0.4772	0.4849	1.2	18.4	8.6	170	170
21	31.2	17.9	7.72	6.8	98.3	0.0186	0.0233	0.0419	0.0084	0.0001	0.0007	0.0007	0.0091	0.5168	0.5259	1.2	18.6	10.2	23	23

*: no sample collected; values in red represent samples below MDL and therefore assigned a value of ½ method detection limit.
WT: water temperature, Sal: salinity, DO: dissolved oxygen concentration, DO$_{\%sat}$: percent saturation of dissolved oxygen
PO$_4$: phosphate, DOP: dissolved organic phosphorus, TDP: total dissolved phosphorus
NH$_4$: ammonium, NO$_2$: nitrite, NO$_3$: nitrate, NO$_{23}$: nitrate-nitrite, DIN: dissolved inorganic nitrogen, DON: dissolved organic nitrogen
TDN: total dissolved nitrogen, DIN:DIP is ratio between dissolved inorganic nitrogen and dissolved inorganic phosphorus
Chla: chlorophyll-a, Pheo: pheophytin, FC: fecal coliform, E. coli: Escherichia coli

Table II.15. Grab sample data collected in Thurston Branch - Thalia Creek – Buchanan Creek on July 27, 2009

Station	WT (ºC)	Sal (ppt)	pH	DO (mg/L)	DO %sat	PO4 (mg/L as P)	DOP (mg/L as P)	TDP (mg/L as P)	NH4 (mg/L as N)	NO2 (mg/L as N)	NO3 (mg/L as N)	NO23 (mg/L as N)	DIN (mg/L as N)	DON (mg/L as N)	TDN (mg/L as N)	DIN: DIP	Chla (µg/L)	Pheo (µg/L)	FC MPN/ 100 ml	E. coli MPN/ 100 ml
1	28.6	20.8	7.72	4.5	64.4	0.0149	0.0653	0.0802	0.0182	0.0001	0.0013	0.0014	0.0196	0.6382	0.6578	2.9	15.6	6.3	17	17
2	28.6	19.4	7.48	4.4	63.1	0.0149	0.0319	0.0468	0.0126	0.0001	0.0007	0.0007	0.0133	0.5646	0.5779	2.1	23.8	10.0	80	50
3	28.5	18.0	7.44	4.4	61.9	0.0118	0.0403	0.0521	0.0126	0.0001	0.0007	0.0007	0.0133	0.5160	0.5293	2.6	18.8	9.9	80	80
4	28.5	16.2	7.42	4.6	65.5	0.0118	0.0472	0.0590	0.0224	0.0001	0.0007	0.0007	0.0231	0.6549	0.6780	4.5	27.6	13.7	140	140
5	28.8	15.7	7.49	4.6	65.0	0.0133	0.0355	0.0488	0.0168	0.0001	0.0013	0.0014	0.0182	0.7171	0.7353	3.0	31.4	17.6	300	170
6	*	*	*	*	*	*	*	*	*	*	*	*	*	*	*	*	*	*	*	*
6A	*	*	*	*	*	*	*	*	*	*	*	*	*	*	*	*	*	*	*	*
6B	28.9	14.5	7.50	5.3	75.0	0.0118	0.0433	0.0551	0.0154	0.0001	0.0027	0.0028	0.0182	0.7907	0.8089	3.4	35.0	18.5	900	900
7	29.0	14.4	7.49	5.6	78.4	0.0099	0.0369	0.0468	0.0168	0.0001	0.0007	0.0007	0.0175	0.6467	0.6642	4.1	33.1	18.2	500	500
8	29.4	13.1	7.55	6.3	89.7	0.0167	0.0386	0.0553	0.0182	0.0001	0.0013	0.0014	0.0196	0.6539	0.6735	2.6	42.6	22.7	240	240
9	29.1	14.2	7.52	6.0	86.2	0.0118	0.0384	0.0502	0.0126	0.0001	0.0013	0.0014	0.0140	0.6382	0.6522	2.6	36.7	21.1	240	240
10	26.6	12.3	7.52	6.2	88.1	0.0167	0.0412	0.0579	0.0196	0.0001	0.0027	0.0028	0.0224	0.7774	0.7998	3.0	50.4	27.7	220	220
11	*	*	*	*	*	*	*	*	*	*	*	*	*	*	*	*	*	*	*	*
12	31.2	16.1	9.37	11.2	137.9	0.0065	0.0382	0.0447	0.0140	0.0001	0.0027	0.0028	0.0168	0.5836	0.6004	5.7	37.5	16.9	50	50
13	*	*	*	*	*	*	*	*	*	*	*	*	*	*	*	*	*	*	*	*
14	30.5	11.5	7.75	8.3	118.0	0.0217	0.0410	0.0627	0.0140	0.0001	0.0013	0.0014	0.0154	0.6443	0.6597	1.6	55.2	28.0	240	240
15	30.4	13.7	7.80	9.1	125.6	0.0319	0.0367	0.0686	0.0210	0.0001	0.0027	0.0028	0.0238	0.8312	0.8550	1.7	84.8	39.2	1600	1600
16	30.7	13.1	7.74	8.1	117.1	0.0183	0.0416	0.0599	0.0140	0.0001	0.0013	0.0014	0.0154	0.5009	0.5163	1.9	48.6	25.4	110	110
17	30.1	9.1	7.64	6.3	98.0	0.0201	0.0360	0.0561	0.0378	0.0001	0.0111	0.0112	0.0490	0.7769	0.8259	5.4	59.7	36.3	300	300
18	29.1	20.7	7.49	5.1	74.2	0.0118	0.0326	0.0444	0.0168	0.0001	0.0007	0.0007	0.0175	0.6038	0.6213	3.4	22.5	8.5	80	80
19	29.2	20.3	7.42	5.0	73.9	0.0149	0.0383	0.0532	0.0224	0.0001	0.0027	0.0028	0.0252	0.6198	0.6450	3.8	22.5	9.6	30	30
20	29.4	19.9	7.46	5.1	75.2	0.0167	0.0244	0.0411	0.0112	0.0001	0.0007	0.0007	0.0119	0.6584	0.6703	1.7	22.3	12.2	70	70
21	29.5	20.1	7.47	5.6	80.5	0.0118	0.0289	0.0407	0.0140	0.0001	0.0007	0.0007	0.0147	0.4968	0.5115	2.9	21.3	11.3	50	50

*: no sample collected; values in red represent samples below MDL and therefore assigned a value of ½ method detection limit.

WT: water temperature, Sal: salinity, DO: dissolved oxygen concentration, DO%sat: percent saturation of dissolved oxygen

PO4: phosphate, DOP: dissolved organic phosphorus, TDP: total dissolved phosphorus

NH4: ammonium, NO2: nitrite, NO3: nitrate, NO23: nitrate-nitrite, DIN: dissolved inorganic nitrogen, DON: dissolved organic nitrogen

TDN: total dissolved nitrogen, DIN:DIP is ratio between dissolved inorganic nitrogen and dissolved inorganic phosphorus

Chla: chlorophyll-a, Pheo: pheophytin, FC: fecal coliform, E. coli: Escherichia coli

Table II.16. Grab sample data collected in Thurston Branch - Thalia Creek – Buchanan Creek on August 27, 2009

Station	WT (ºC)	Sal (ppt)	pH	DO (mg/L)	DO %sat	PO₄ (mg/L as P)	DOP (mg/L as P)	TDP (mg/L as P)	NH₄ (mg/L as N)	NO₂ (mg/L as N)	NO₃ (mg/L as N)	NO₂₃ (mg/L as N)	DIN (mg/L as N)	DON (mg/L as N)	TDN (mg/L as N)	DIN: DIP	Chla (µg/L)	Pheo (µg/L)	FC MPN/ 100 ml	E. coli MPN/ 100 ml
1	29.7	16.8	8.12	8.1	117.3	0.0319	0.0247	0.0566	0.0182	0.0001	0.0027	0.0028	0.0210	0.2411	0.2621	1.5	36.1	9.0	30	30
2	30.1	16.4	8.17	8.3	119.1	0.0269	0.0132	0.0401	0.0084	0.0001	0.0007	0.0007	0.0091	0.3996	0.4087	0.8	45.2	11.9	60	60
3	30.2	14.4	8.24	9.2	132.1	0.0319	0.0224	0.0543	0.0210	0.0001	0.0013	0.0014	0.0224	0.4216	0.4440	1.6	43.4	12.7	50	50
4	30.5	14.1	8.19	8.7	124.8	0.0304	0.0213	0.0517	0.0154	0.0001	0.0027	0.0028	0.0182	0.3205	0.3387	1.3	45.0	17.4	110	110
5	31.3	12.5	8.23	9.0	130.3	0.0285	0.0191	0.0476	0.0196	0.0001	0.0027	0.0028	0.0224	0.3468	0.3692	1.7	29.7	14.4	90	70
6	*	*	*	*	*	*	*	*	*	*	*	*	*	*	*	*	*	*	*	*
6A	31.1	0.0	9.77	11.8	159.1	0.0285	0.0142	0.0427	0.0266	0.0001	0.0055	0.0056	0.0322	0.3553	0.3875	2.5	22.7	15.8	60	30
6B	31.1	9.0	8.22	9.0	127.3	0.0508	0.0235	0.0743	0.0140	0.0001	0.0013	0.0014	0.0154	0.2455	0.2609	0.7	57.6	26.4	900	900
7	31.7	10.7	8.31	9.7	138.4	0.0269	0.0119	0.0388	0.0210	0.0001	0.0055	0.0056	0.0266	0.3073	0.3339	2.2	40.6	15.0	350	130
8	32.7	8.6	8.39	9.9	142.9	0.0269	0.0114	0.0383	0.0084	0.0001	0.0041	0.0042	0.0126	0.5468	0.5594	1.0	34.7	16.9	1600	1600
9	31.8	7.6	8.44	10.3	147.6	0.0254	0.0245	0.0499	0.0112	0.0001	0.0055	0.0056	0.0168	0.3745	0.3913	1.5	46.8	22.4	1600	240
10	32.4	8.6	8.39	10.5	151.2	0.0204	0.0249	0.0453	0.0084	0.0001	0.0069	0.0070	0.0154	0.4907	0.5061	1.7	43.0	15.3	1600	1600
11	*	*	*	*	*	*	*	*	*	*	*	*	*	*	*	*	*	*	*	*
12	27.5	2.3	7.32	3.4	44.6	0.0220	0.0083	0.0303	0.1779	0.0042	0.0154	0.0196	0.1975	0.4419	0.6394	19.9	60.2	18.4	1600	500
13	27.5	1.8	7.42	5.1	65.4	0.0235	0.0105	0.0340	0.2116	0.0042	0.0140	0.0182	0.2298	0.4241	0.6539	21.6	26.6	19.3	1600	300
14	28.3	1.0	7.62	8.7	111.6	0.0434	0.0165	0.0599	0.0182	0.0001	0.0041	0.0042	0.0224	0.4427	0.4651	1.1	32.7	21.2	1600	300
15	25.6	0.3	7.47	5.5	68.5	0.0598	0.0111	0.0709	0.1149	0.0154	0.1541	0.1695	0.2844	0.4050	0.6894	10.5	23.0	18.2	1600	300
16	27.8	2.1	7.38	5.1	65.3	0.0155	0.0052	0.0207	0.3488	0.0042	0.0154	0.0196	0.3684	0.3605	0.7289	52.6	30.1	28.5	1600	500
17	28.7	2.1	7.66	6.8	89.9	0.0087	0.0076	0.0163	0.2158	0.0014	0.0098	0.0112	0.2270	0.4295	0.6565	57.9	35.0	26.9	350	220
18	29.8	17.0	8.12	8.4	121.2	0.0350	0.0162	0.0512	0.0112	0.0001	0.0007	0.0007	0.0119	0.3694	0.3813	0.8	32.2	16.3	70	70
19	31.3	15.1	8.42	11.5	168.3	0.0350	0.0320	0.0670	0.0098	0.0001	0.0007	0.0007	0.0105	0.5810	0.5915	0.7	51.8	15.1	50	00
20	30.6	15.2	8.15	8.6	125.3	0.0319	0.0219	0.0538	0.0686	0.0001	0.0007	0.0007	0.0693	0.2919	0.3612	4.9	41.1	16.3	30	30
21	32.2	13.0	8.37	11.9	168.5	0.0285	0.0269	0.0554	0.0056	0.0001	0.0007	0.0007	0.0063	0.3659	0.3722	0.5	39.0	32.4	170	170

*: no sample collected; values in red represent samples below MDL and therefore assigned a value of ½ method detection limit.

WT: water temperature, Sal: salinity, DO: dissolved oxygen concentration, DO$_{\%sat}$: percent saturation of dissolved oxygen

PO₄: phosphate, DOP: dissolved organic phosphorus, TDP: total dissolved phosphorus

NH₄: ammonium, NO₂: nitrite, NO₃: nitrate, NO₂₃: nitrate-nitrite, DIN: dissolved inorganic nitrogen, DON: dissolved organic nitrogen

TDN: total dissolved nitrogen, DIN:DIP is ratio between dissolved inorganic nitrogen and dissolved inorganic phosphorus

Chla: chlorophyll-a, Pheo: pheophytin, FC: fecal coliform, E. coli: Escherichia coli

Figure II.31. Spatial plot of ammonium (NH_4) from Thurston Branch - Thalia Creek grab samples, June 30, 2009.
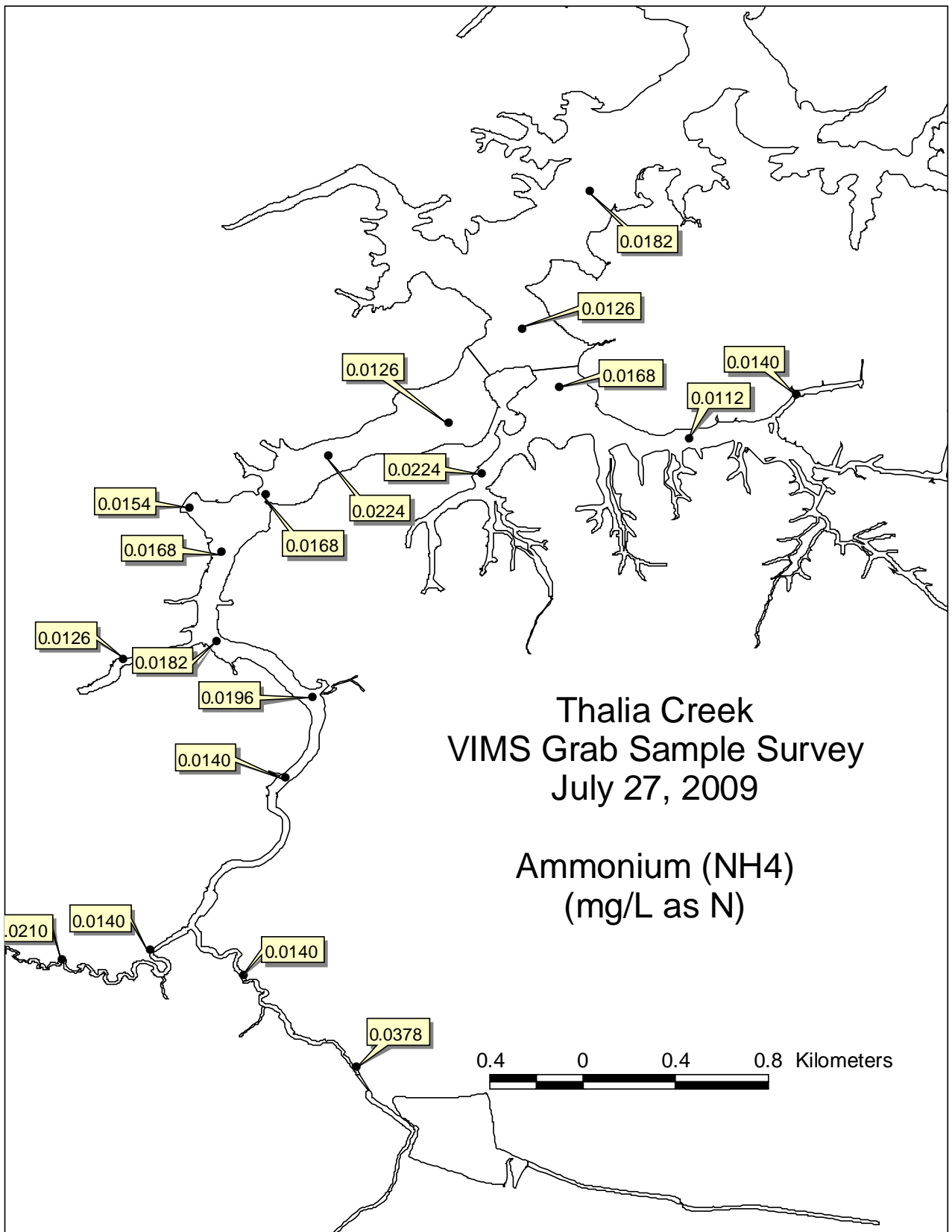
Figure II.32. Spatial plot of ammonium (NH$_4$) from Thurston Branch - Thalia Creek grab samples, July 27, 2009.

Figure II.33. Spatial plot of ammonium (NH_4) from Thurston Branch - Thalia Creek grab samples, August 27, 2009.
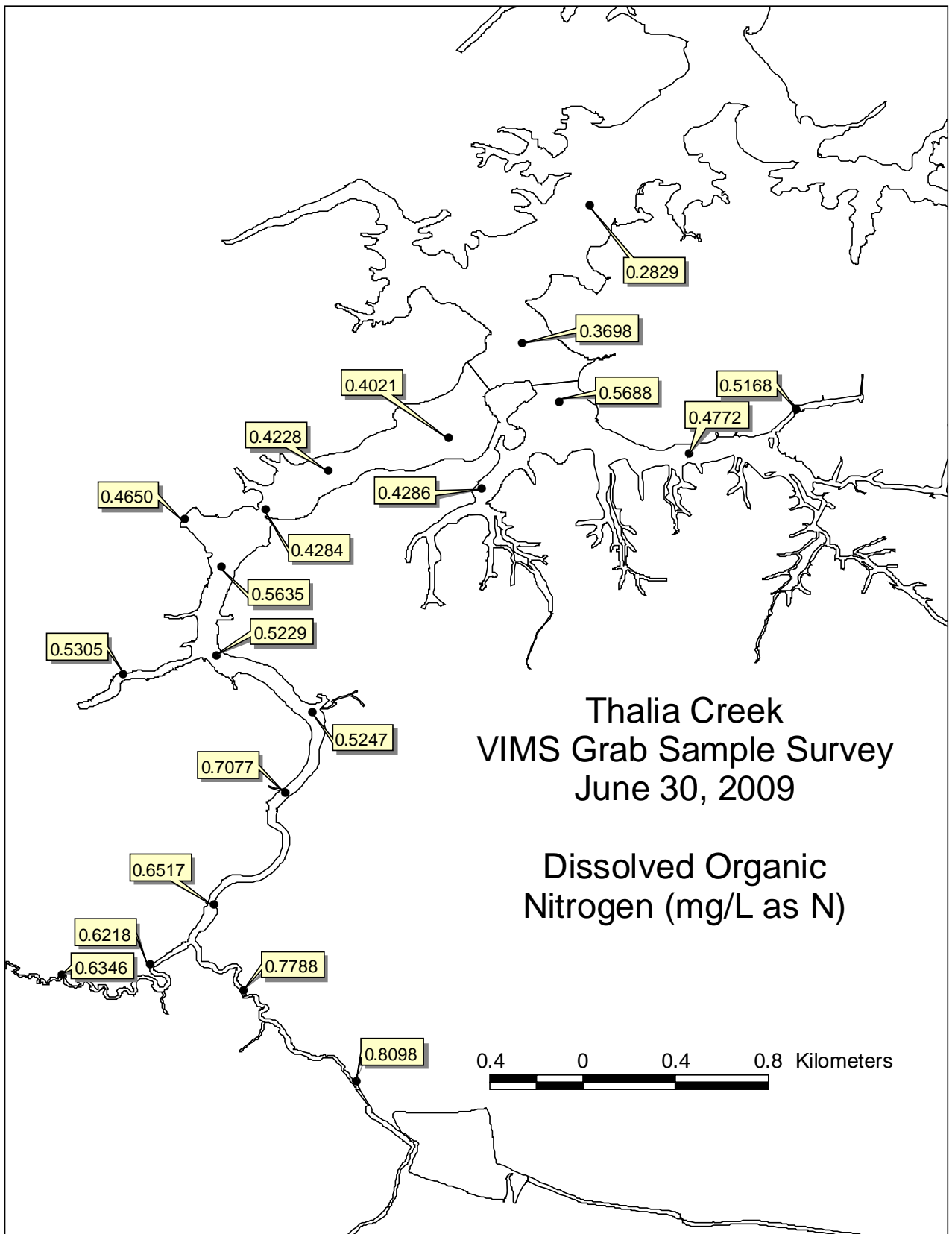
Figure II.34. Spatial plot of dissolved organic nitrogen (DON) from Thurston Branch -
Thalia Creek grab samples, June 30, 2009.
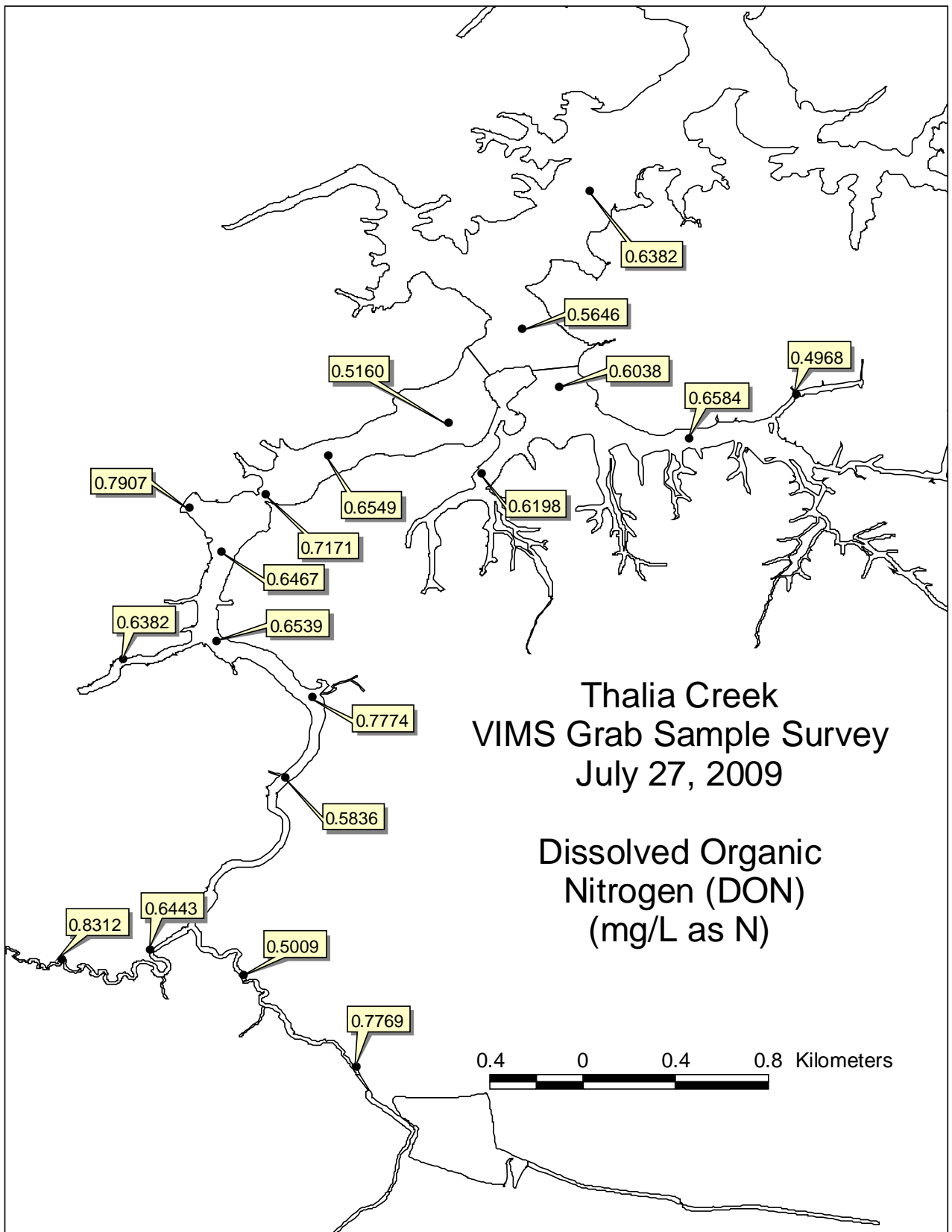
Figure II.35. Spatial plot of dissolved organic nitrogen (DON) from Thurston Branch - Thalia Creek grab samples, July 27, 2009.
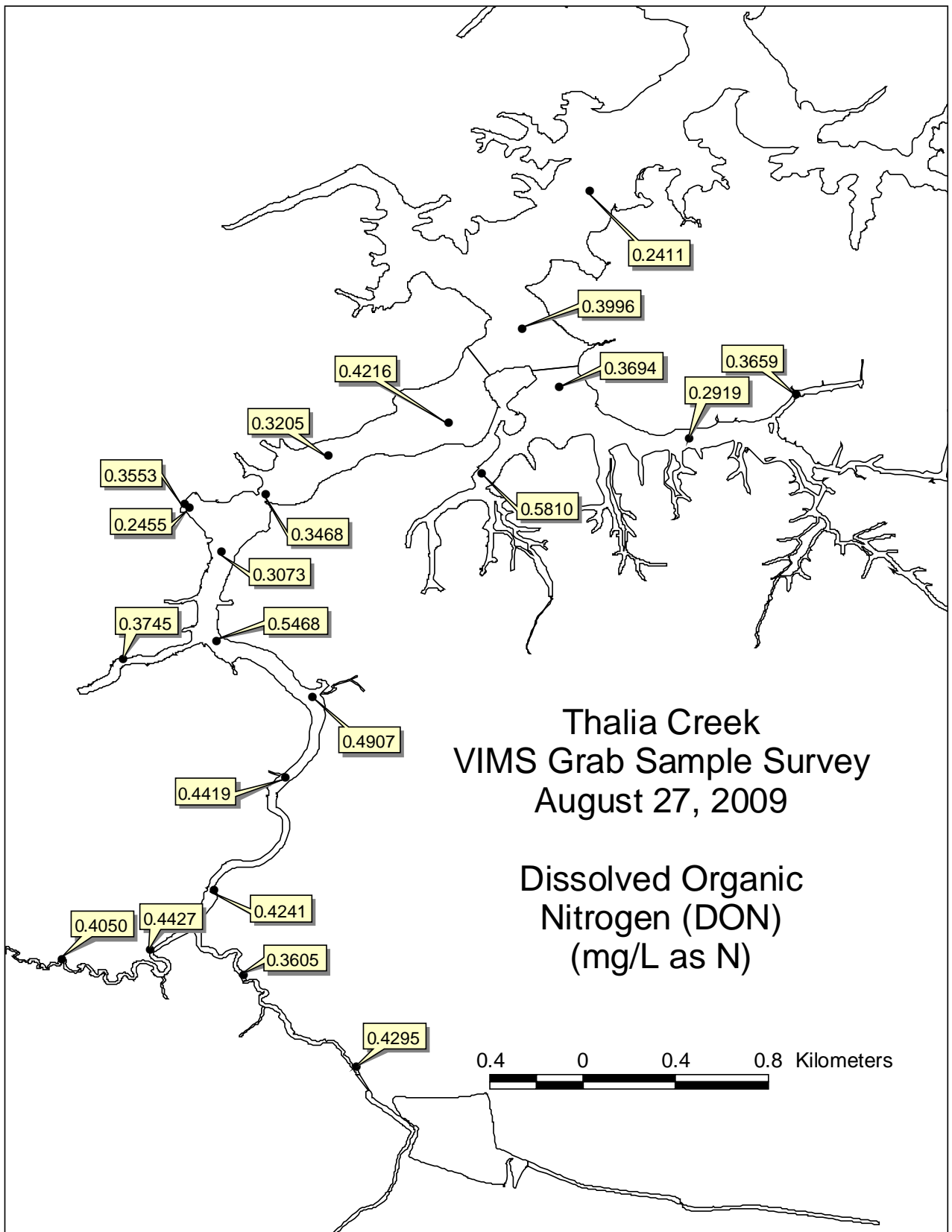
Figure II.36. Spatial plot of dissolved organic nitrogen (DON) from Thurston Branch - Thalia Creek grab samples, August 27, 2009.
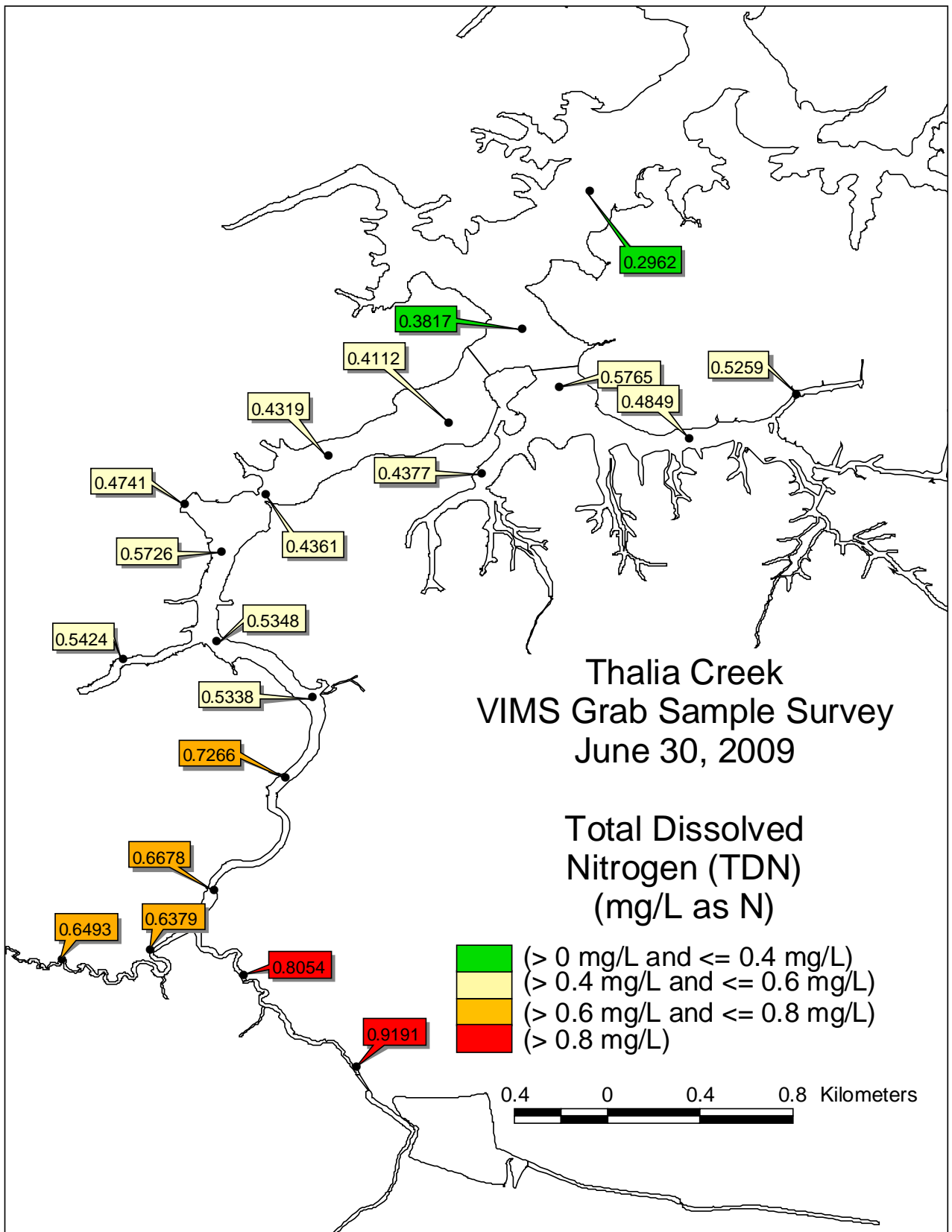
Figure II.37. Spatial plot of total dissolved nitrogen (TDN) from Thurston Branch - Thalia Creek grab samples, June 30, 2009.
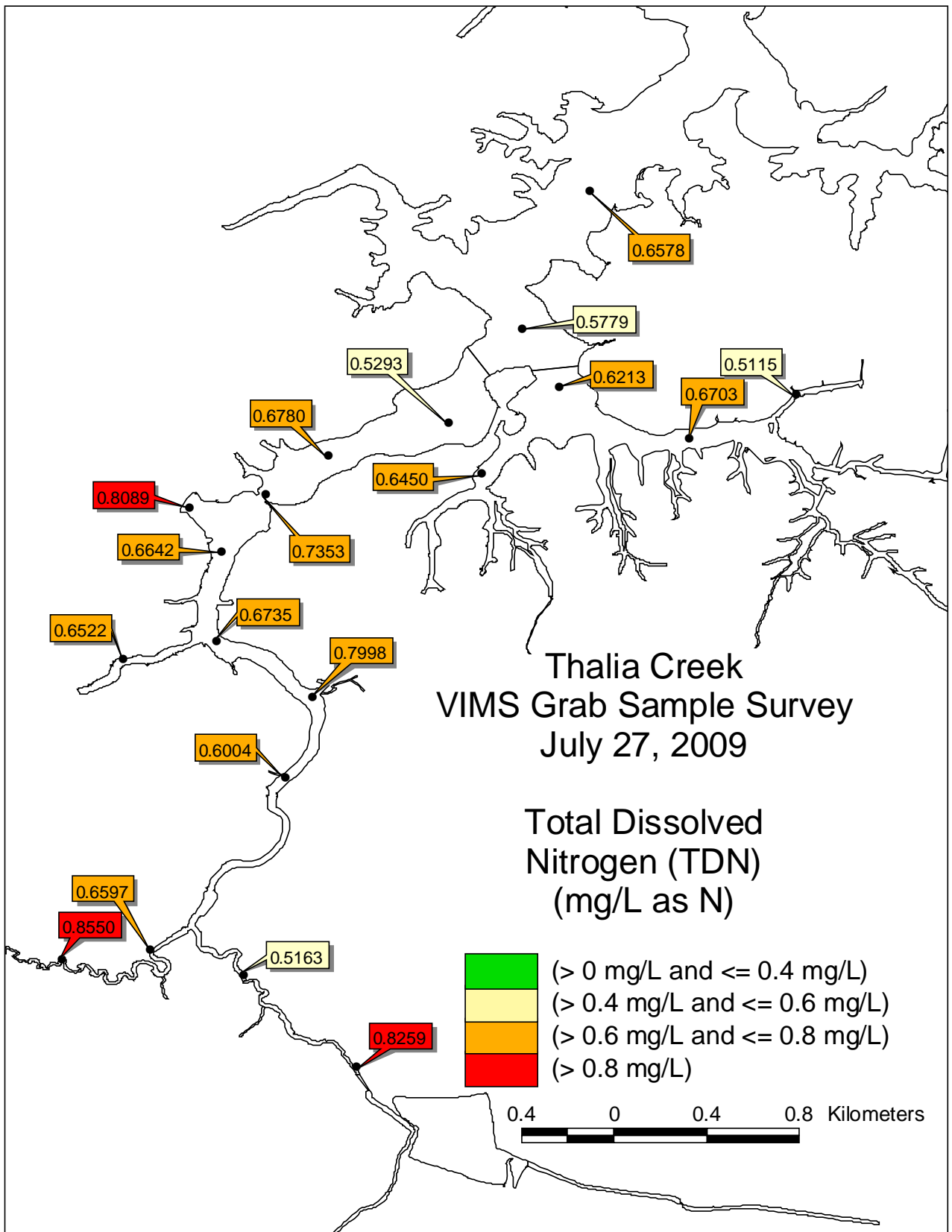
Figure II.38. Spatial plot of total dissolved nitrogen (TDN) from Thurston Branch - Thalia Creek grab samples, July 27, 2009.
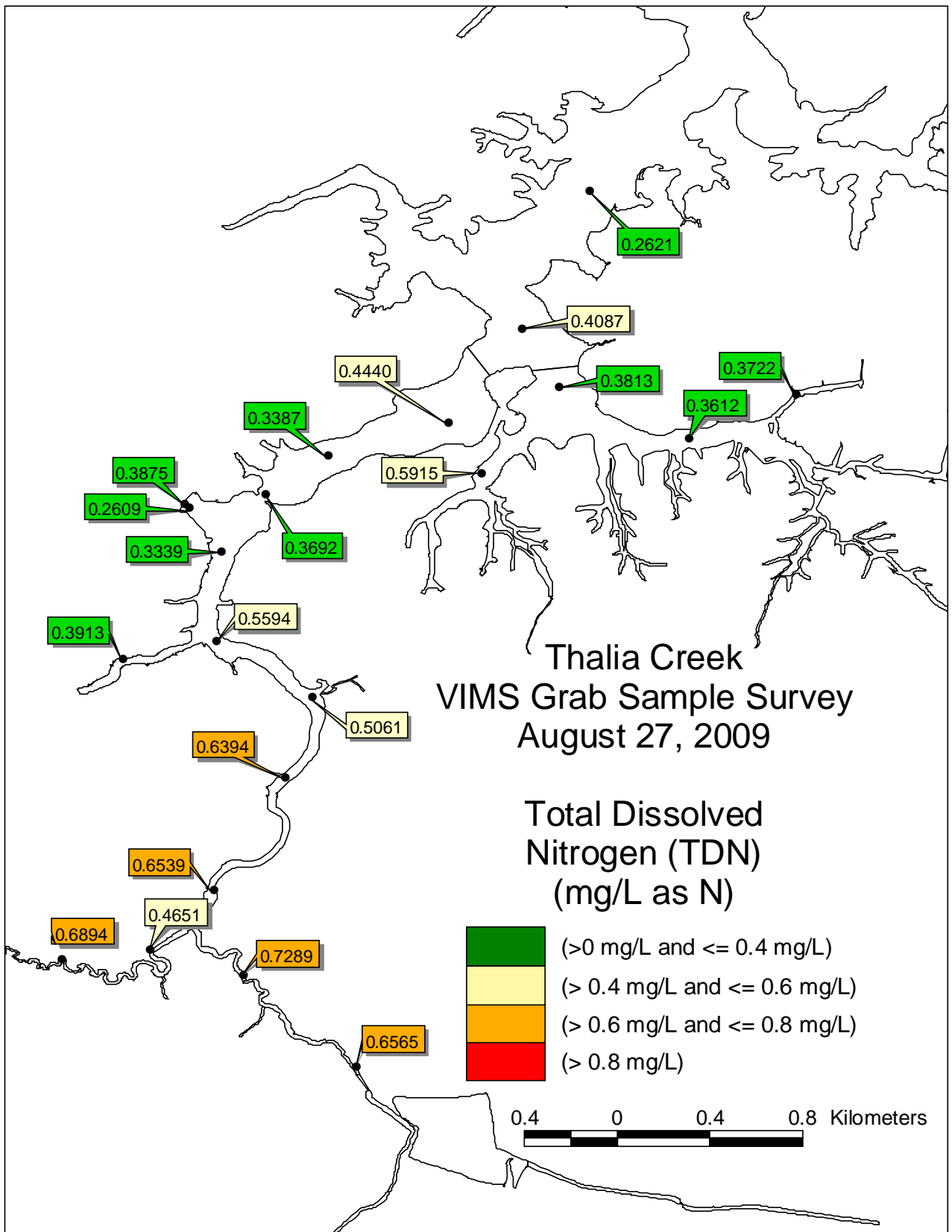
Figure II.39. Spatial plot of total dissolved nitrogen (TDN) from Thurston Branch - Thalia Creek grab samples, August 27, 2009.
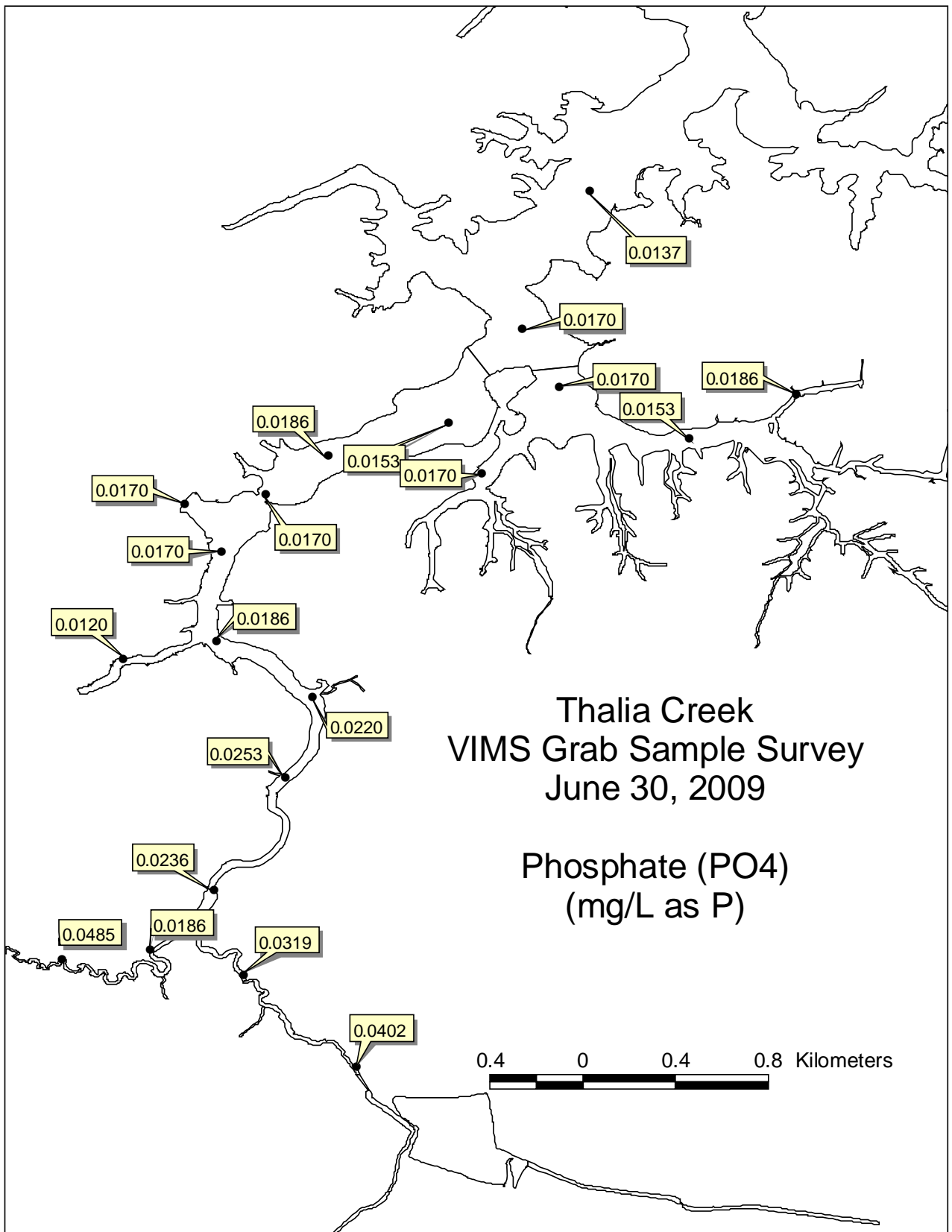
Figure II.40. Spatial plot of phosphate (PO$_4$) from Thurston Branch - Thalia Creek grab samples, June 30, 2009.
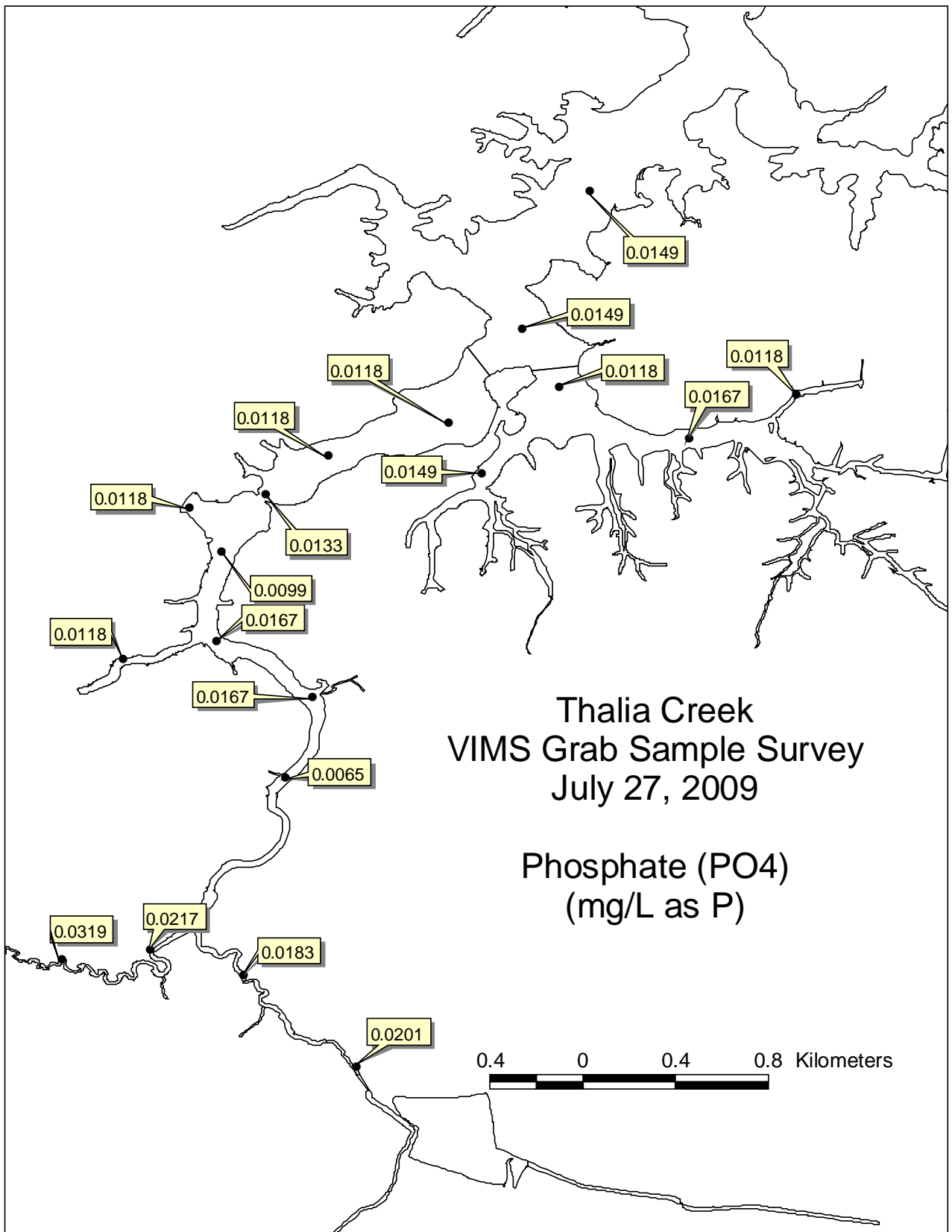
Figure II.41. Spatial plot of phosphate (PO$_4$) from Thurston Branch - Thalia Creek grab samples, July 27, 2009.
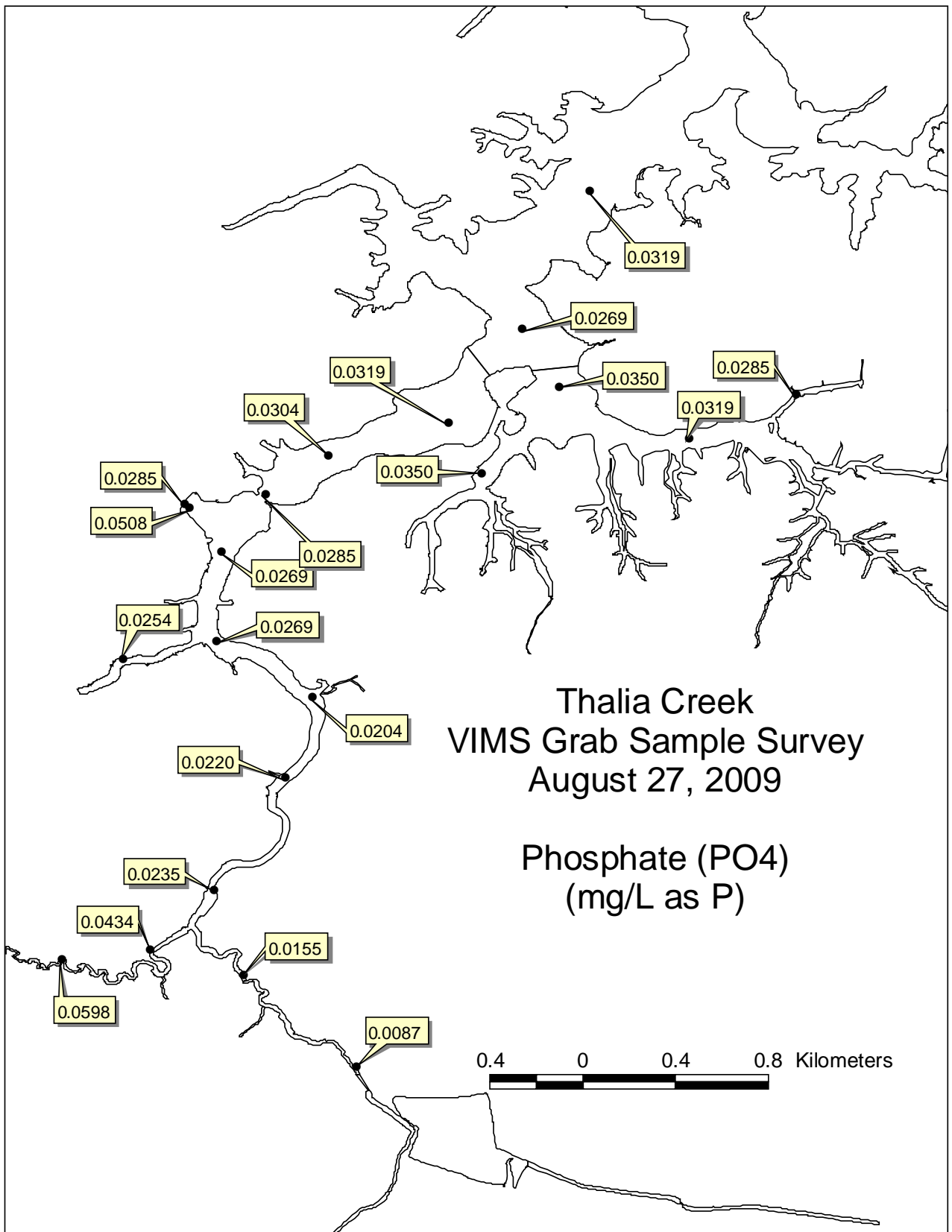
Figure II.42. Spatial plot of phosphate (PO$_4$) from Thurston Branch - Thalia Creek grab samples, August 27, 2009.
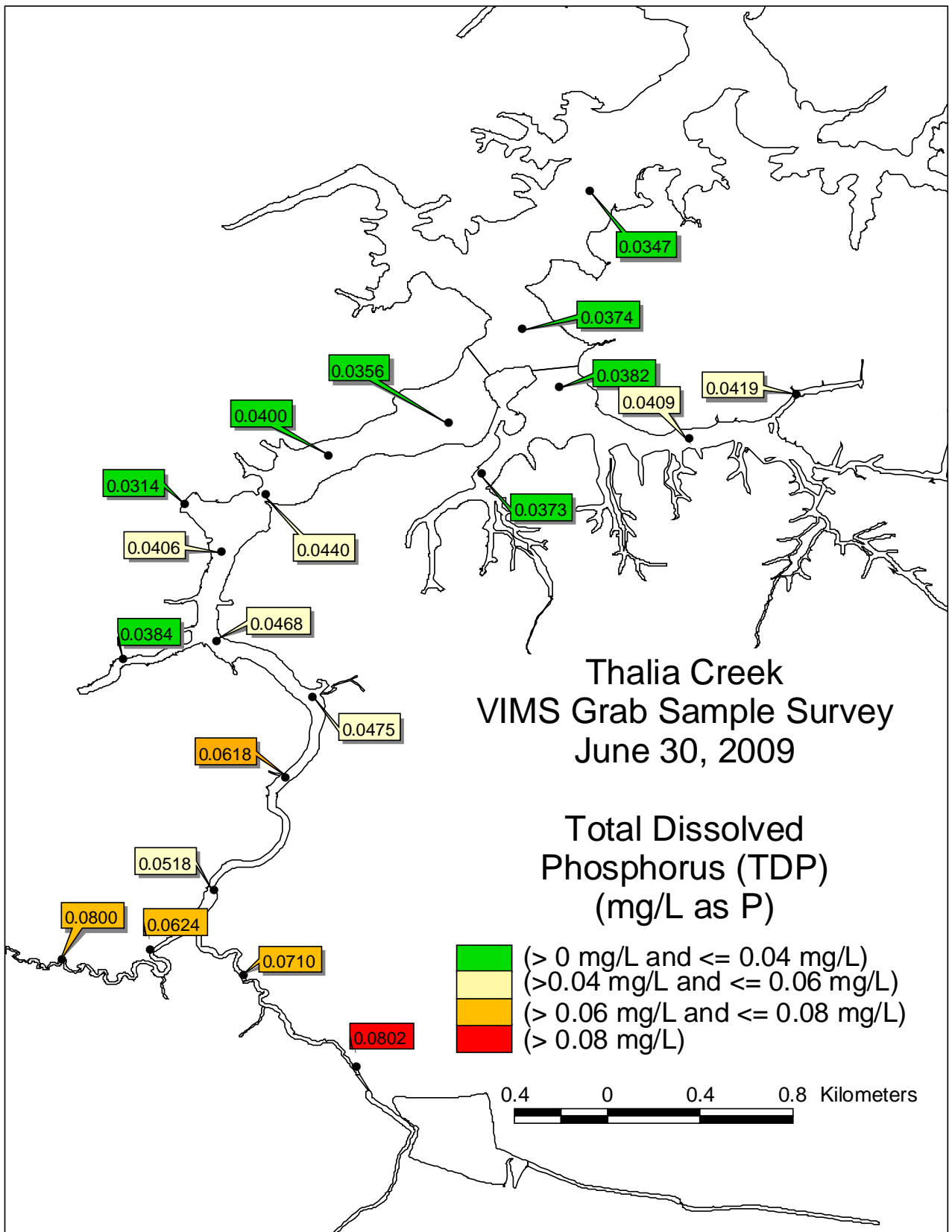
Figure II.43. Spatial plot of total dissolved phosphorus (TDP) from Thurston Branch - Thalia Creek grab samples, June 30, 2009.
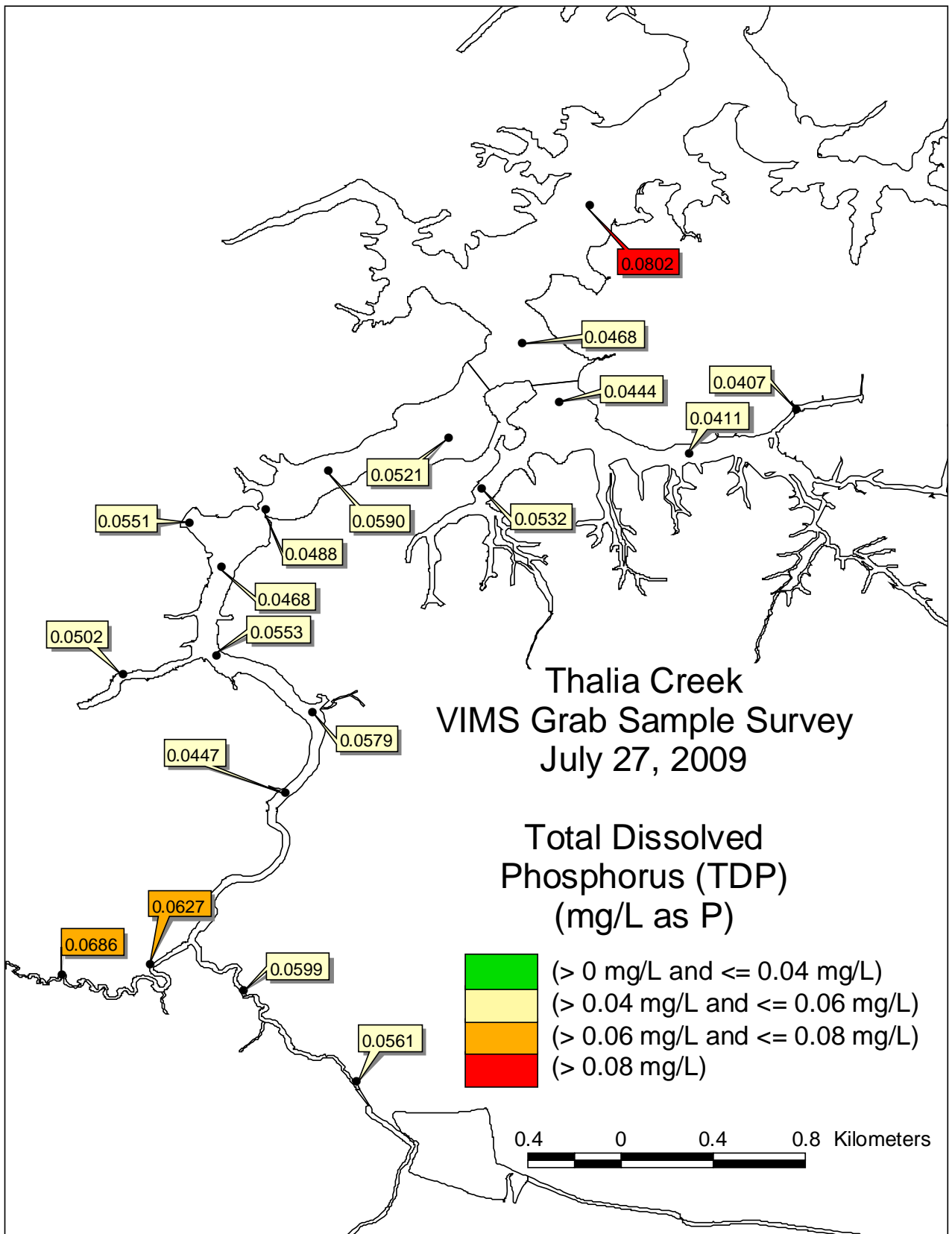
Figure II.44. Spatial plot of total dissolved phosphorus (TDP) from Thurston Branch - Thalia Creek grab samples, July 27, 2009.
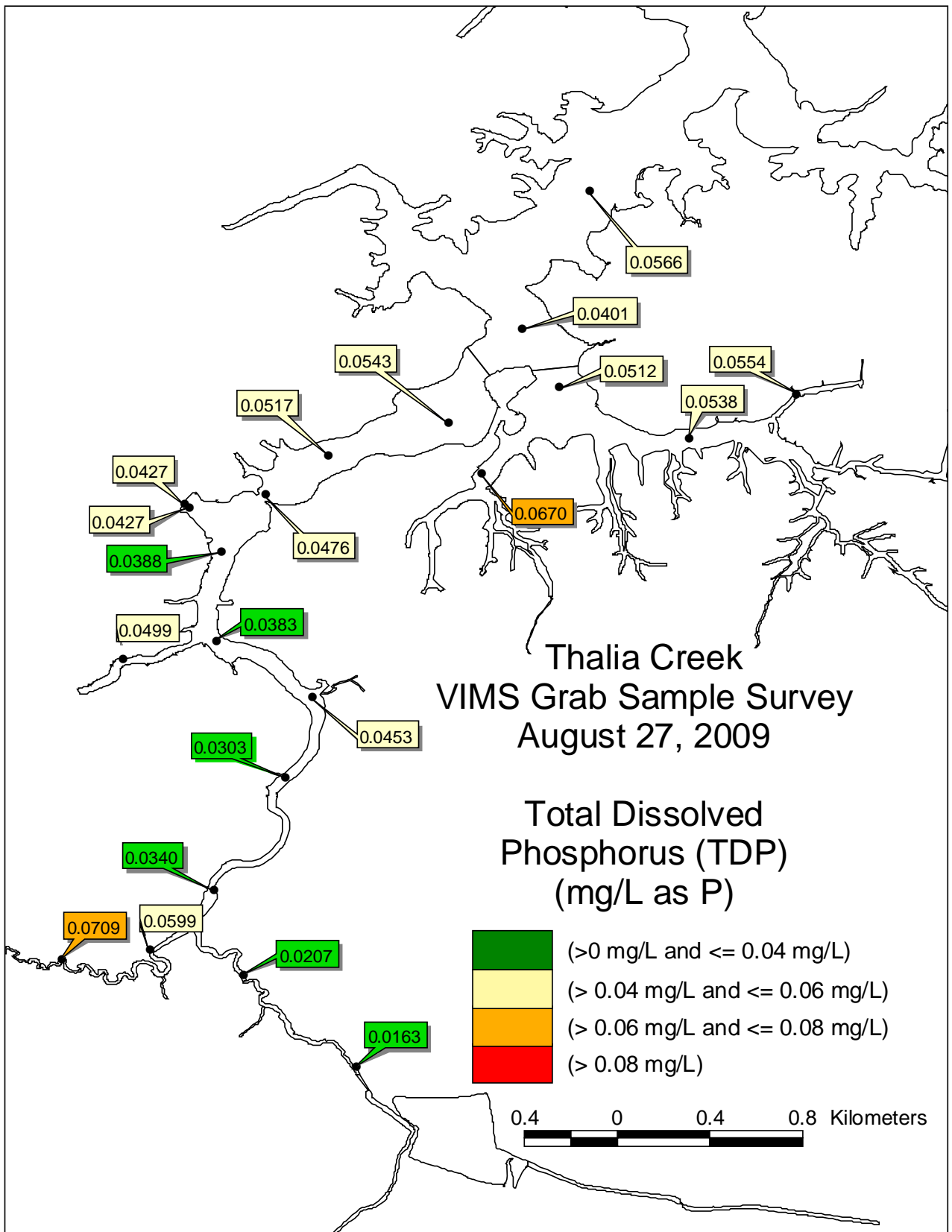
Figure II.45. Spatial plot of total dissolved phosphorus (TDP) from Thurston Branch - Thalia Creek grab samples, August 27, 2009.
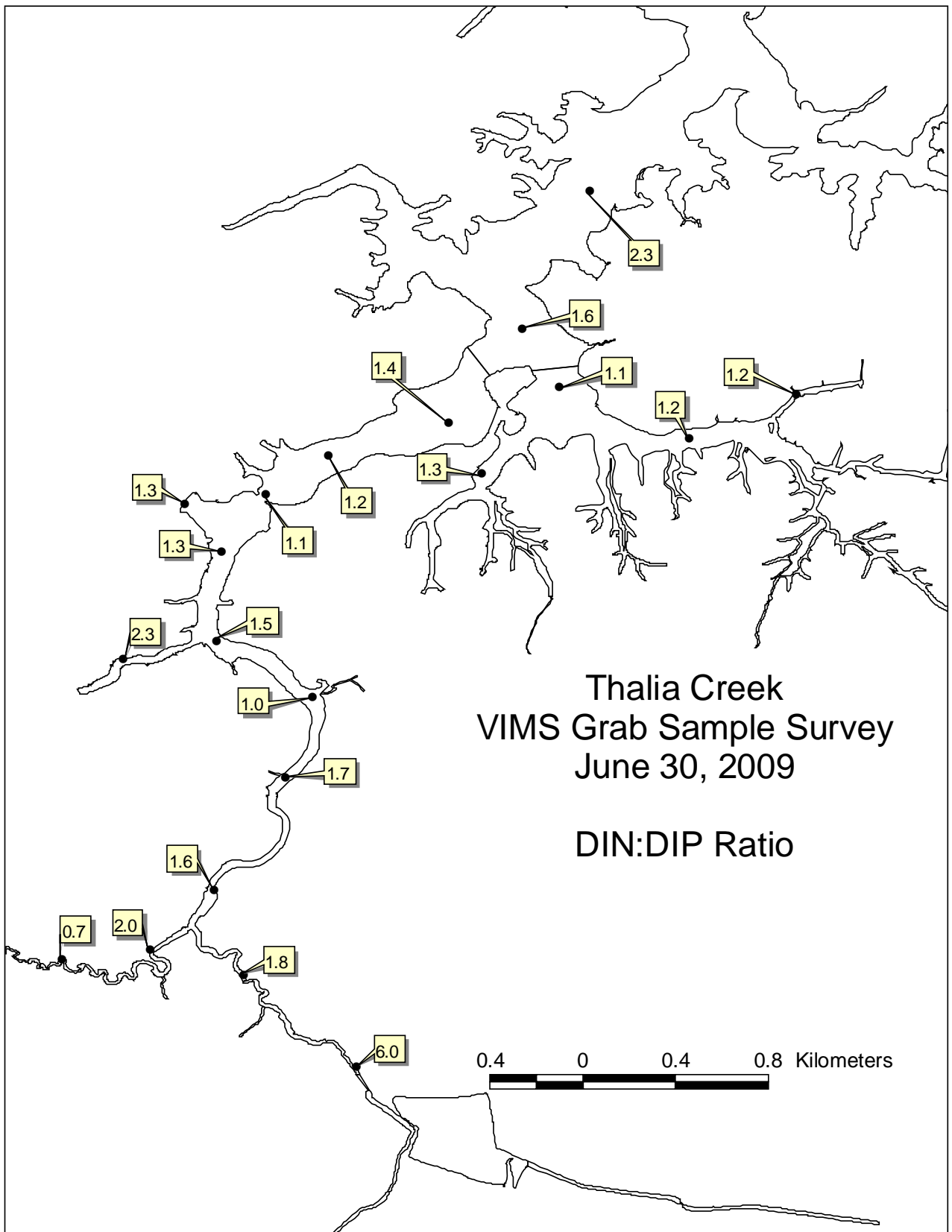
Figure II.46. Spatial plot of DIN:DIP ratio from Thurston Branch - Thalia Creek grab samples, June 30, 2009.

Thalia Creek
VIMS Grab Sample Survey
July 27, 2009
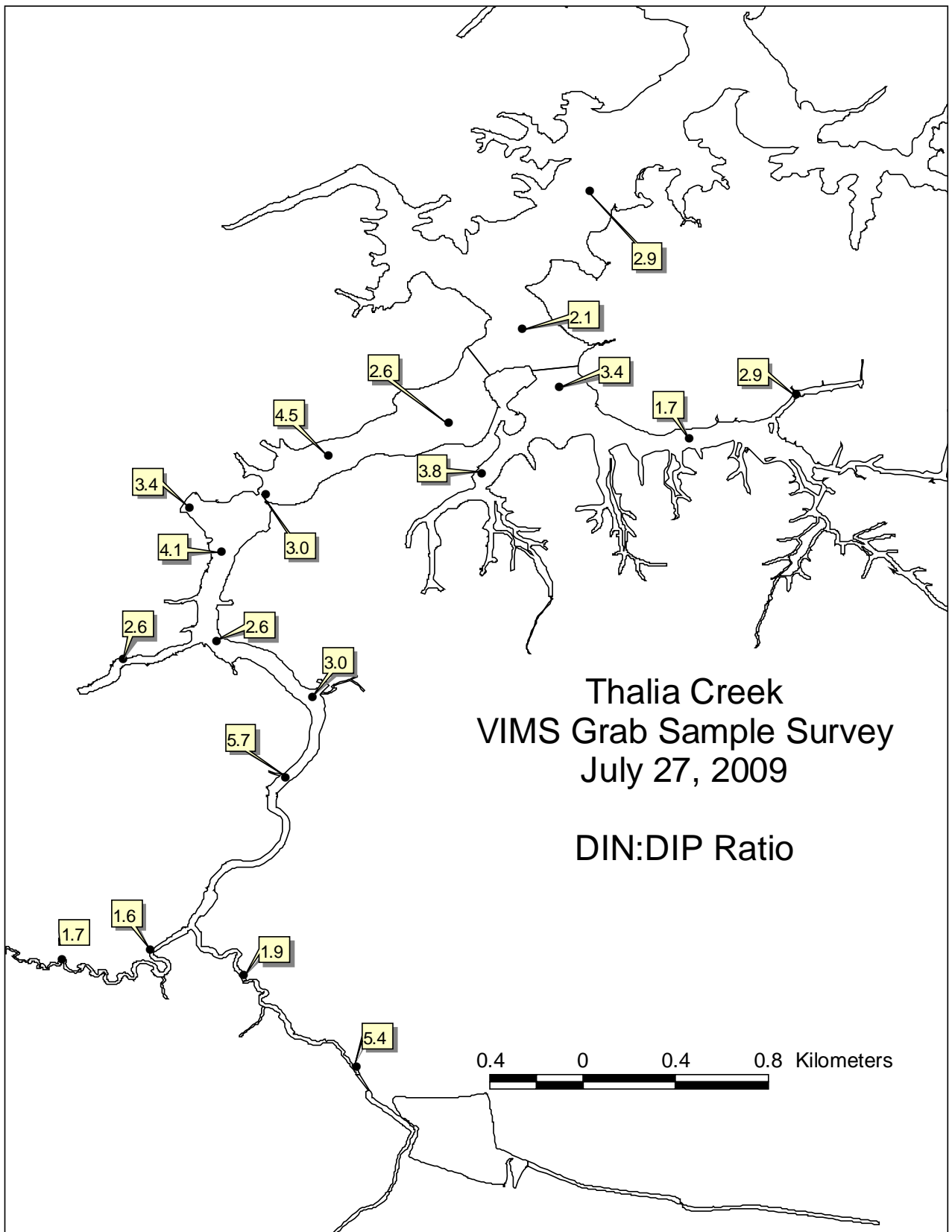
DIN:DIP Ratio

Figure II.47. Spatial plot of DIN:DIP ratio from Thurston Branch - Thalia Creek grab samples, July 27, 2009.
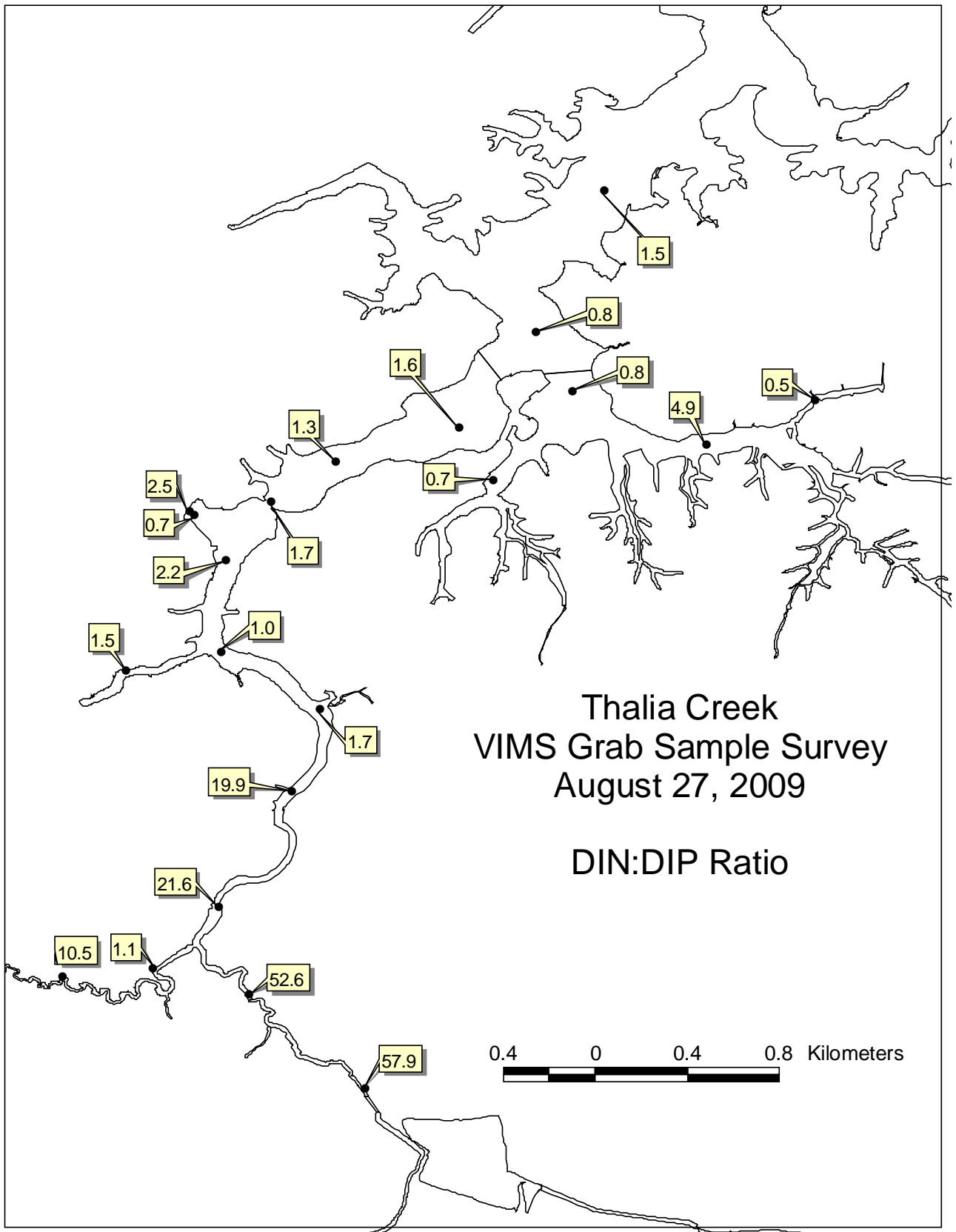
Figure II.48. Spatial plot of DIN:DIP ratio from Thurston Branch - Thalia Creek grab
samples, August 27, 2009.

II-3-3 Chlorophyll a

Plant pigment concentrations, both chlorophyll *a* (chl *a*) and pheopigments, for the three grab sample periods are provided in Tables II.14 to II.16 and spatial plots of chl *a* are presented in Figures II.49 through II.51. Chl *a* concentrations varied from 14.1-68.2 µg·L^{-1} on June 30, 15.6-84.8 µg·L^{-1} on July 27 and 22.7-60.2 µg·L^{-1} on the August 27, 2009 sampling. High (>20 to ≤ 60 µg·L^{-1}) to hyper-eutrophic (>60 µg·L^{-1}) concentrations of chl *a* were observed in the upper portion of TC (Stations 10 and above) on the June 30, 2009, from the middle reaches of TB (Station 4) and above on July 27, 2009 and throughout the entire TC-TB system including BC and the single station in the upper Western Branch of the Lynnhaven River on August 27, 2009. While still high, chl *a* levels observed in the upper portions of TC (Station 13 and above) on August 27, 2009 were relatively lower (on the order of 50%) than the two previous samplings. Mean chl *a* concentrations for the five stations were 56.2, 62.1 and 29.5 µg·L^{-1} for the June 30, July 27, and August 27, 2009 sampling, respectively. This observation may be indicative of enhanced flushing in the less saline portions due to recent rainfall events resulting in decreased residence time that could prevent accumulation of phytoplankton biomass in the upper, less saline reaches of TC. Alternately, this could simply indicate a die-back or enhanced grazing of the phytoplankton community.

Concentrations of pheopigments, which provide a measure degraded plant components, ranged from 4.6-25.3 µg·L^{-1}, 6.3-39.2 µg·L^{-1} and 9.0-28.5 µg·L^{-1} for the June 30, July 27 and August 27, 2009 sampling, respectively. Relatively high pheopigment to chl *a* ratios are a general indicator of degraded phytoplankton populations. Pheopigment : chl *a* varied from 0.3-0.4 in the upper and lower portions of TB-TC and 0.3-0.6 in the middle reaches on June 30, from 0.4-0.6 throughout TB-TC on July 27, and from 0.3-0.5 in the lower and middle reaches to 0.7 to almost 1.0 in the upper portion of TC. The increase in pheopigment : chl *a* in the upper reach of TC on August 27, 2009, was a result of both an increase in pheopigment and decrease in chl *a* concentrations. A possible suggestion for the high concentrations of pheopigments, particularly those observed in the upper portions of TC, is high phytoplankton mortality caused by osmotic stress from rapidly changing salinity levels (particularly following a storm event) or potentially elevated grazing pressures.
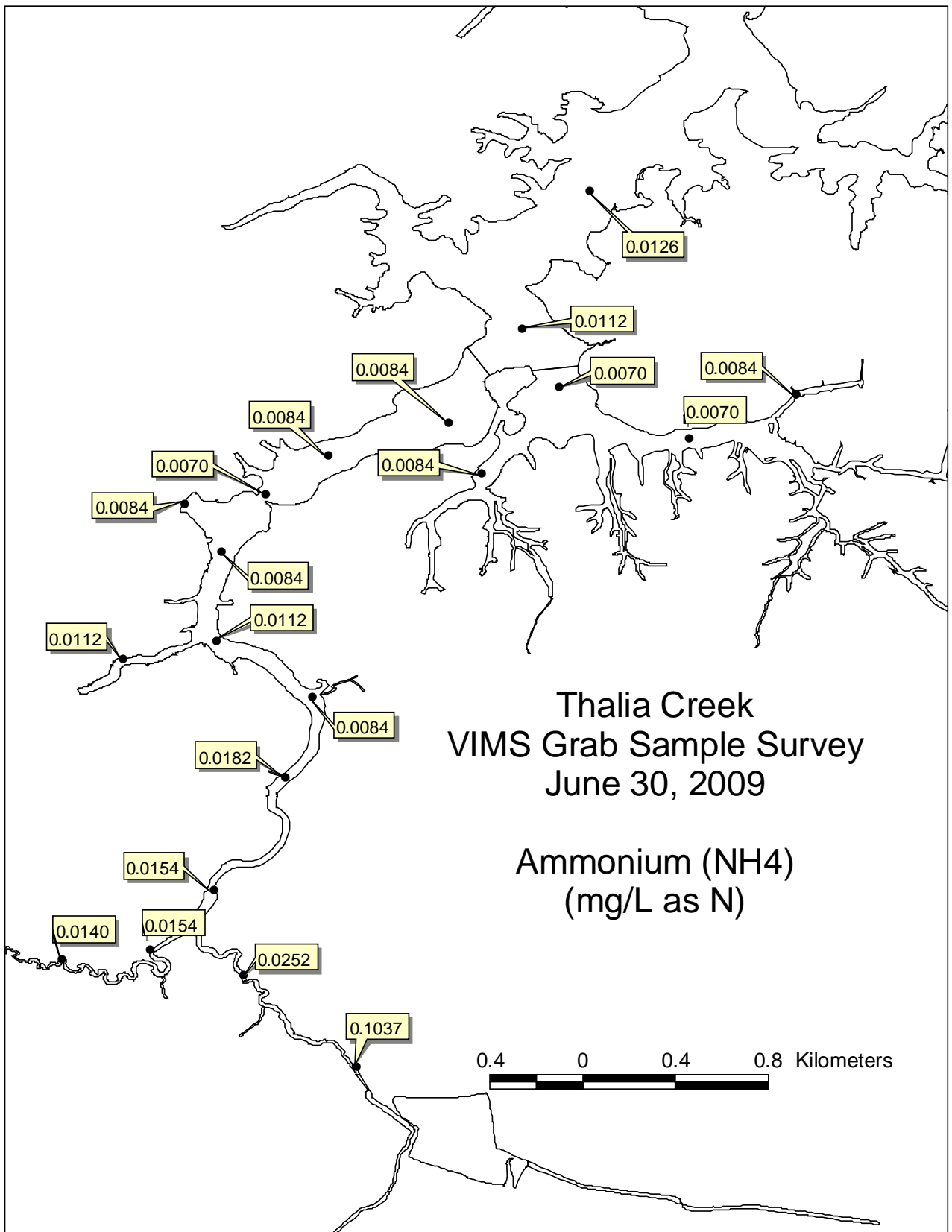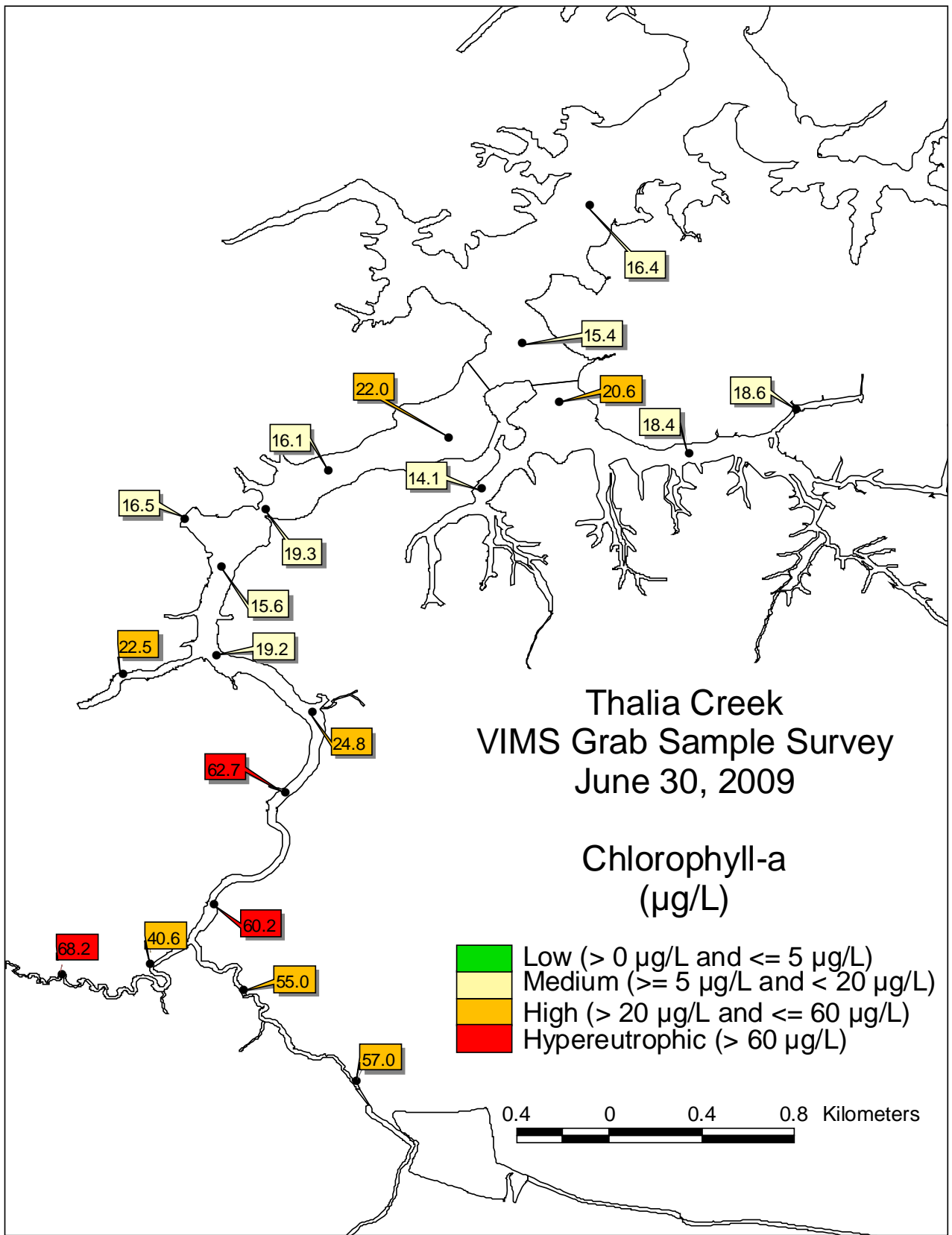
Figure II.49. Spatial plot of chlorophyll *a* from Thurston Branch - Thalia Creek grab samples, June 30, 2009.
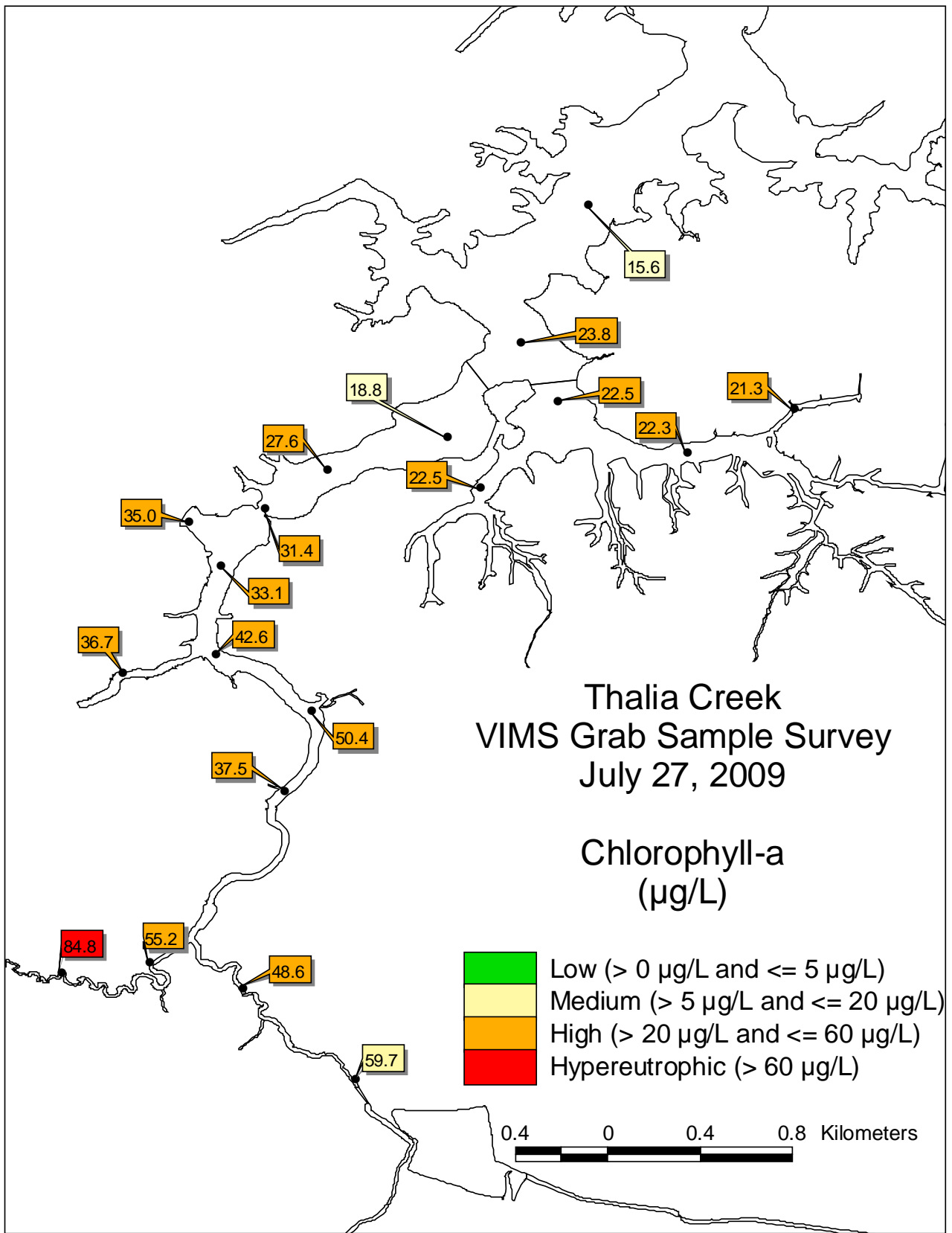
Figure II.50. Spatial plot of chlorophyll *a* from Thurston Branch - Thalia Creek grab
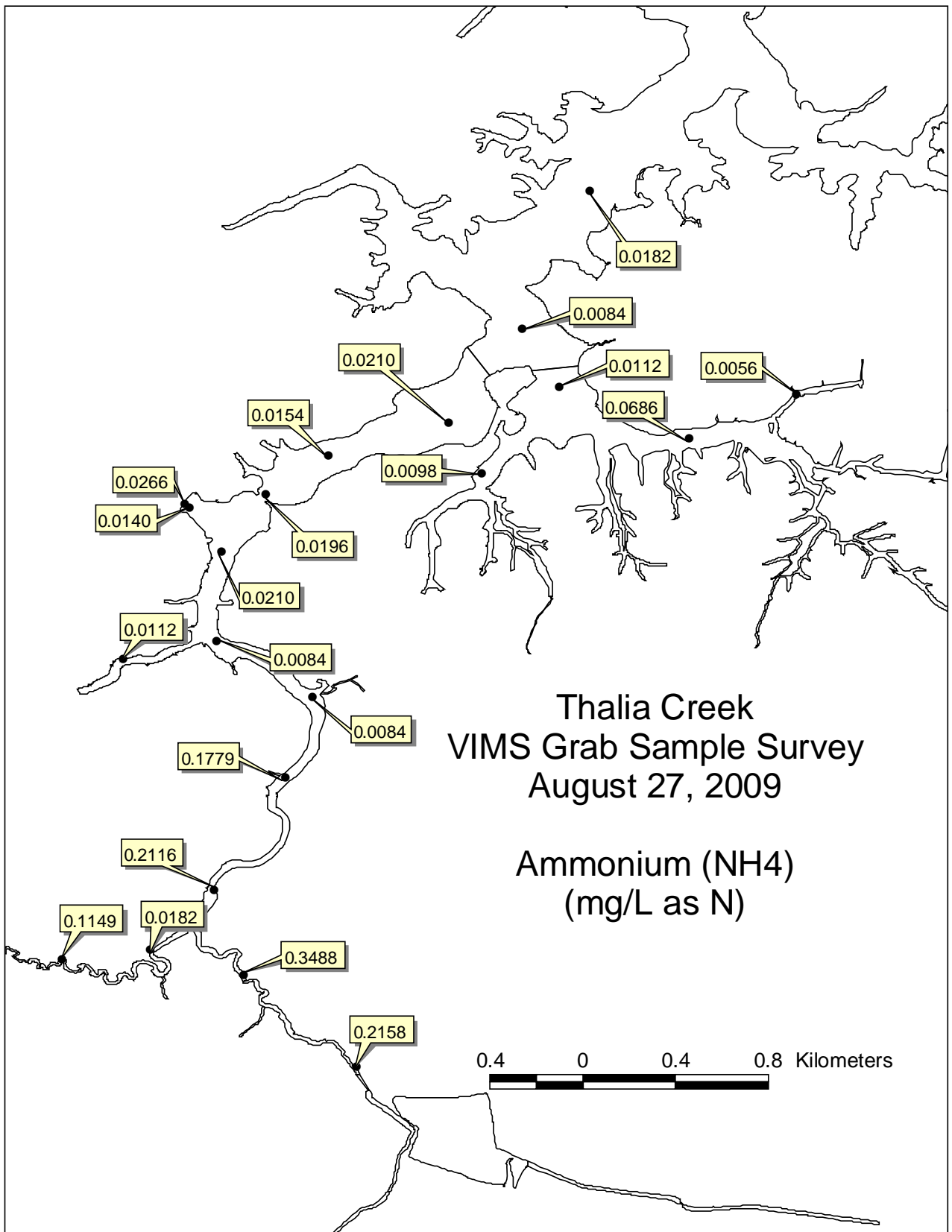samples, July 27, 2009.
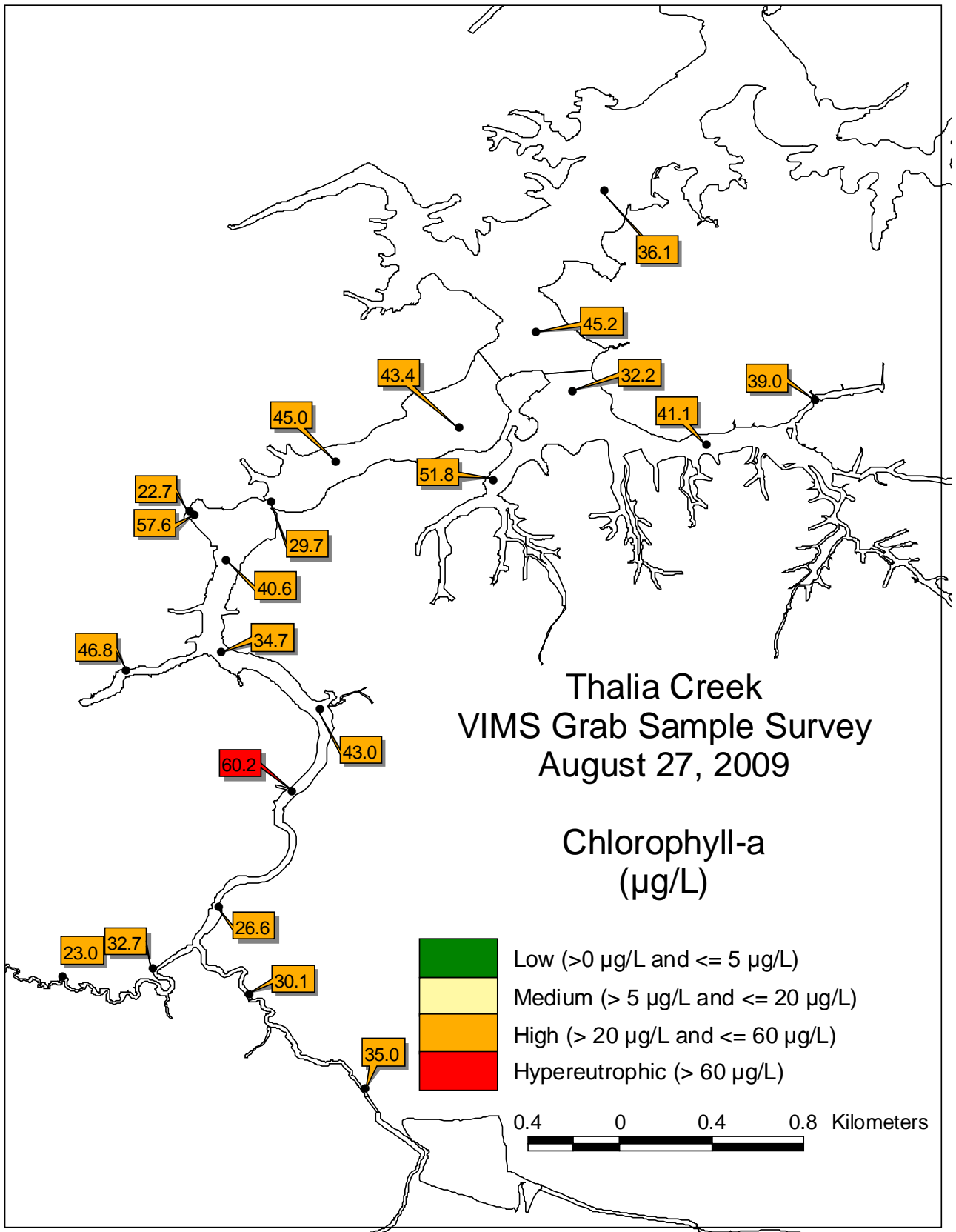
Figure II.51. Spatial plot of chlorophyll *a* from Thurston Branch - Thalia Creek grab samples, August 27, 2009.

2.3.4 Fecal Coliforms

The existence of pathogens has been the most cited water quality problem associated with nonpoint sources of pollution in Virginia (VA-DEQ, 2004) and currently the TB-TC system is impaired due to elevated fecal coliform densities. Fecal coliform bacteria (FCB) and *E. coli* densities for the three grab sample periods are provided in Tables II.14 to II.16 and spatial plots of FCB densities are presented in Figures II.52 through II.54. The relationship between FCB and *E. coli* density was strong exhibiting for two of the three surveys with r^2 values of 0.95 for June 30 and 0.99 for the July 27, 2009; r^2 value for August 27, 2009 was 0.38. The overall r^2 value for the entire 3-deployment data set was 0.54 and 0.97 if the five identified outliers were removed from analysis (see Figure II.55). The disagreement between FCB and *E. coli* densities was primarily isolated to the August 27, 2009 sampling, where heavy rainfall and subsequent runoff occurred days prior to the sampling, and several stations exhibited FCB densities exceeding the method limit of 1600 MPN·100 ml^{-1}. This discrepancy may be a result of ubiquitous fecal coliform positive microbes, such as *Klebsielia* and *Citrobacter*, or *E. coli* strains that do not produce β-glucuronidase, a requirement for the fluorogenic *E. coli* confirmation assay.

FCB samples varied from below 2 MPN·100 ml^{-1} to greater than 1600 MPN·100 ml^{-1} index detection limits. Elevated FCB densities exceeding Commonwealth contact standards (> 200 MPN 100· ml^{-1}) were observed in the upper reaches of TC (above Station 8) on a routine basis. The lower and more open reaches of TB and BC (a less developed and hardened watershed) typically exhibited FCB densities between shellfish waters and recreational contact standards (> 14 MPN to ≤ 200 MPN·100 ml^{-1}). With respect to shellfish water standards, only stations in the lower reaches of TB (Stations 2-4) and TC (Station 18), and upper Western Branch of Lynnhaven River (Station 1) met the standard of (≤ 14 MPN·100 ml^{-1}) during the June 30, 2009 sampling. It is a widespread observation with Virginia's coastal waters where FCB concentrations increase with distance upstream in tidal creeks where flushing rates may be reduced, suspended solids increase and the ratio of shoreline to water volume ("land effect") increases (Shima et al., 1994). Elevated FCB densities were also observed after periods of high rainfall. The August 27, 2009 sampling followed a significant period of rainfall (preceding 3 days: 2.9 cm; preceding 5 days: 7.45 cm) where FCB densities were generally elevated at all TC stations as compared to the three survey sampling geometric mean for each station. In several instances, density estimates exceeded the upper end of method detection limits (Stations 8, 12, 13, 14, 15 and 16). In conjunction with heavy rain on August 22, 2009, high winds could have resuspended muddy bottom sediments which have been shown to significantly impact water column FCB densities (Valiela et al., 1991). No rainfall occurred with 6 and 3 days of sampling on June 30 and July 17, 2009, respectively.

Sources of fecal indicator pathogens vary depending on the existence of relevant point sources and watershed characteristics. Given that there are no permitted sewage treatment discharges located within the survey area and that commercial and domestic wastewater is treated at the Chesapeake-Elizabeth Sewage Treatment Works (i.e., no

84

septic tanks or other on-site wastewater disposal systems), sources of FCB to the TB-TC system would include nonpoint source runoff from urbanized and natural lands, and direct domestic and wild animal loadings. The relatively large marsh systems in the upper reaches of TC and the large waterfowl population utilizing maintained lawn areas add complexity to the problem. In such developed areas, wildlife populations tend to migrate to the limited forested and marsh edge regions thereby increasing FCB loadings from such areas (Simmons et al., 1995; Siewicki et al., 2007). Regarding potential waterfowl sources, it was noted during field visits that a large number of waterfowl, in particular Canada geese (*Branta Canadensis*), inhabited the TB-TC area. Additionally, the spillway isolating the upper portion of TB from tidal influence was observed to be littered in waterfowl fecal matter and provided a consistent overland freshwater source to tidal waters of the TB-TC system. Grab samples from this area were extremely limited and additional sampling is recommended. FCB density in the reservoir sample was 110 MPN·100 ml^{-1} (Station 6, N=1), 60 MPN·100 ml^{-1} on the spillway (Station 6A, N=1), and 900 MPN·100 ml^{-1} (Station 6B, N=2) in the small tidal embayment adjacent to the spillway. While previous studies in other locations have demonstrated that large flocks of waterfowl can contribute to elevated FCB densities in a water body through direct defecation in the water or through runoff off dried fecal matter (Hussong et al., 1979; Valiela et al., 1991; Alderisio and DeLuca, 1999), source tracking is complex and more elaborate methodologies must be utilized to confirm the primary cause(s) of high FCB counts. It is important to note that the fecal coliform test is an indicator test and high densities alone do not constitute a human health threat. Harmful bacteria and/or viruses must also be present at specified levels. Hussong et al. (1979), reporting on waterfowl collected in northern Chesapeake Bay tributaries, found limited enterotoxin-producing E. coli isolated from birds at a single site and no *Salmonella* in either freshly collected fecal matter or aquatic roosting sites at multiple locations. Additional efforts are warranted in the TB-TC system to determine if true health concerns exist and, if so, what the primary sources of microbial contamination are.
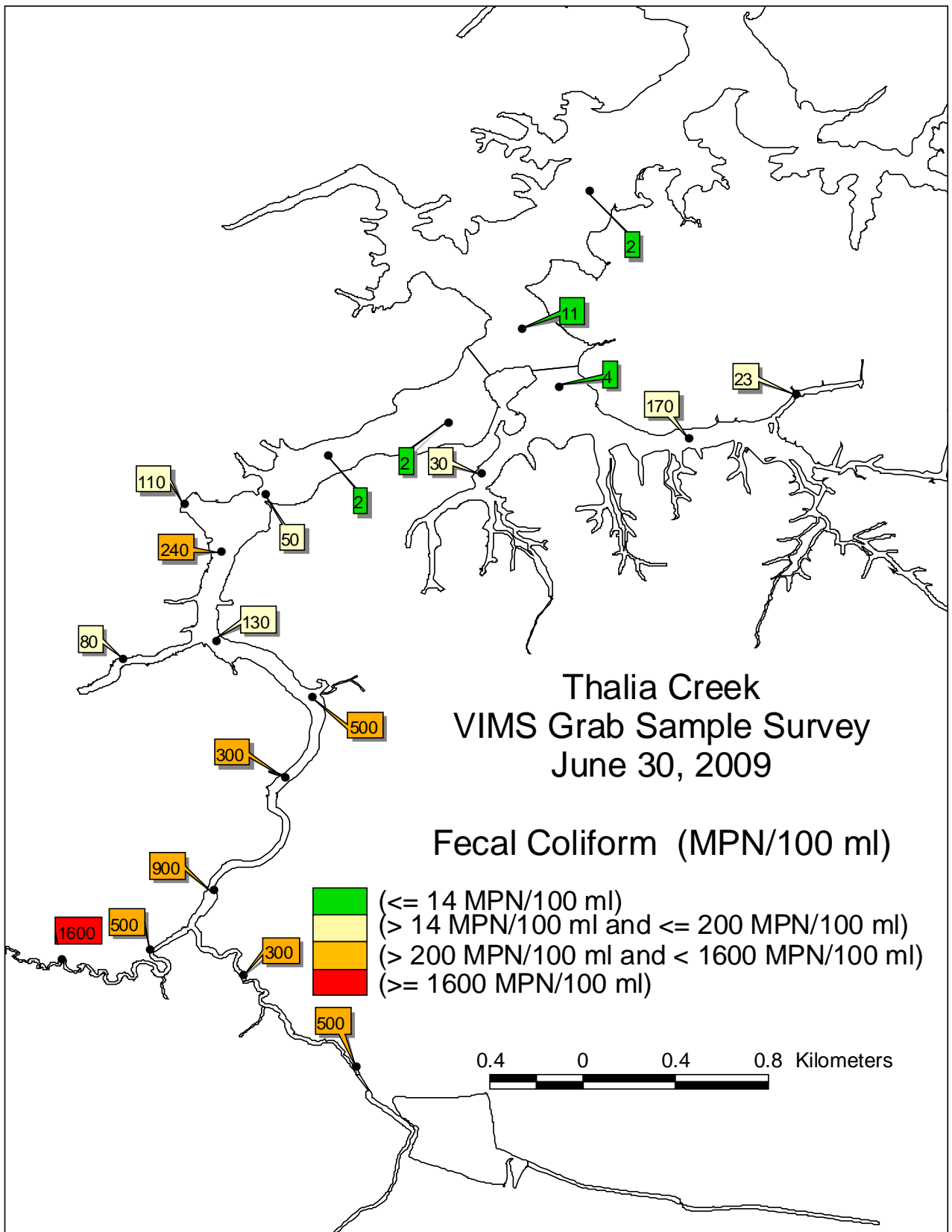
Figure II.52. Spatial plot of fecal coliform bacteria densities from Thurston Branch - Thalia Creek grab samples, June 30, 2009.
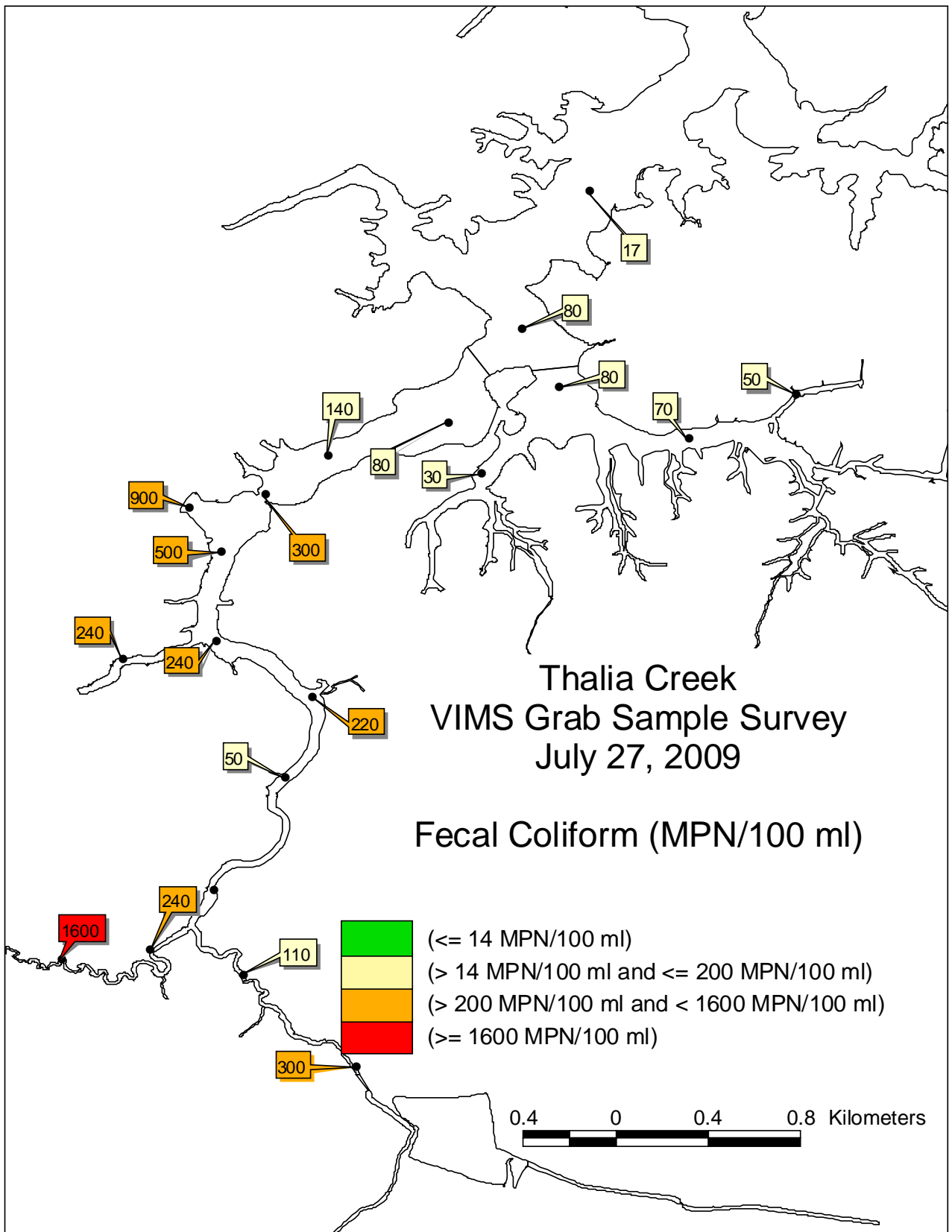
Figure II.53. Spatial plot of fecal coliform bacteria densities from Thurston Branch - Thalia Creek grab samples, July 27, 2009.

Thalia Creek
VIMS Grab Sample Survey
August 27, 2009

Fecal Coliform (MPN/100 ml)

- (<= 14 MPN/100 ml)
- (> 14 MPN/100 ml and <= 200 MPN/100 ml)
- (> 200 MPN/100 ml and <= 1600 MPN/100 ml)
- (>= 1600 MPN/100 ml)
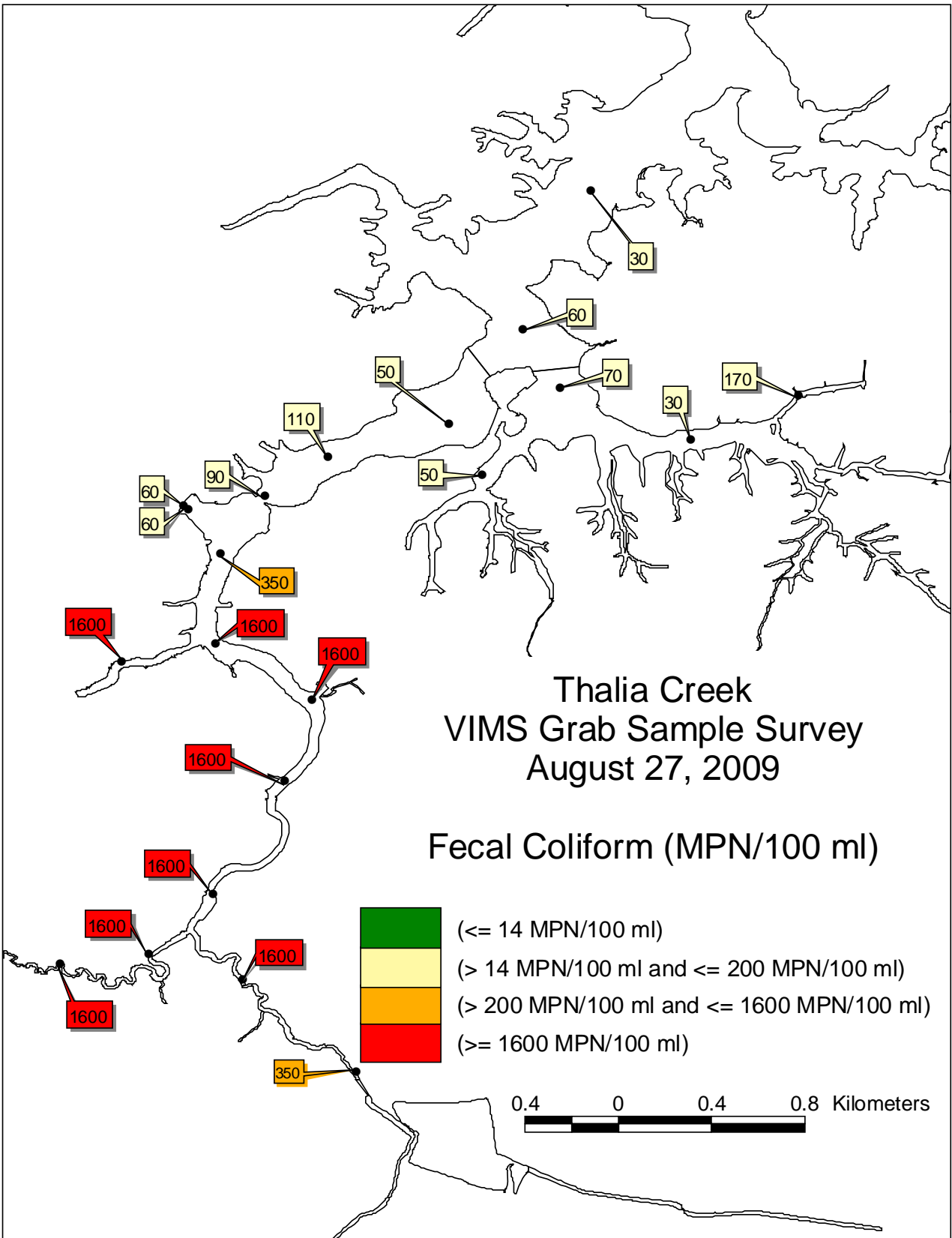
Figure II.54. Spatial plot of fecal coliform bacteria densities from Thurston Branch - Thalia Creek grab samples, August 27, 2009.
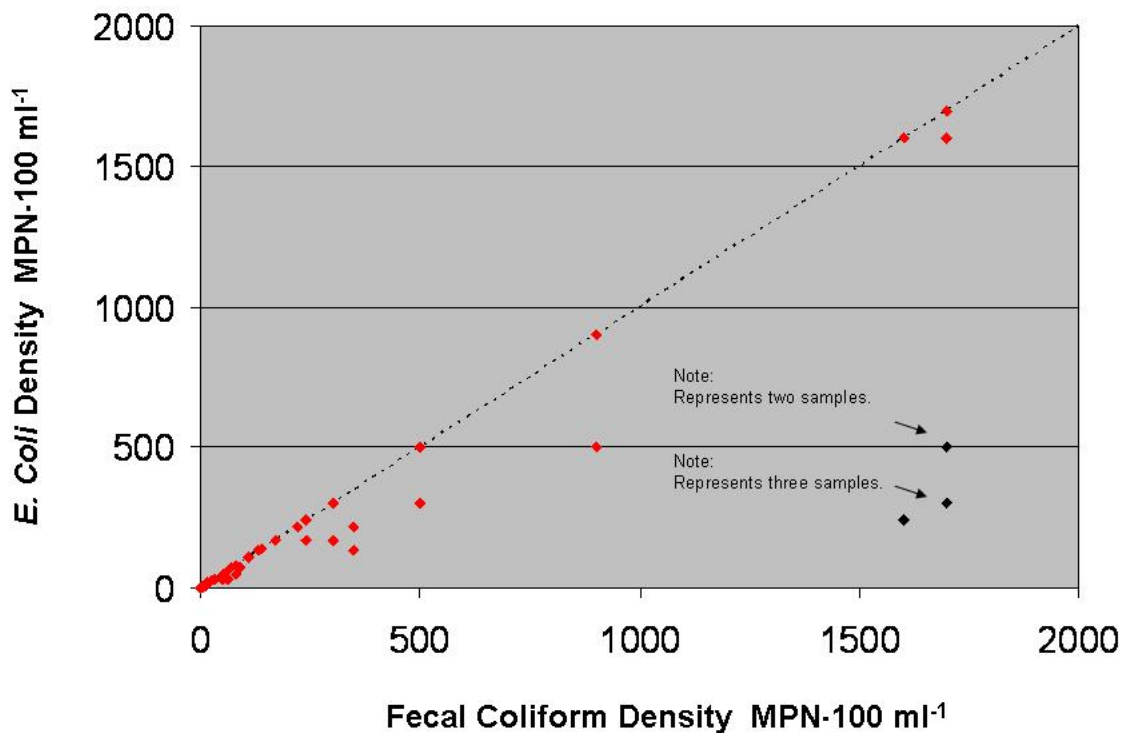
Figure II.55. Scatter plot of FCB density vs. *E. coli* density from TB-TC Creek samples. Data includes samples from June 30, July 27, and August 27, 2009 surveys. Note: Samples below detection limits (<2 MPN·100 ml^{-1}) were assigned a value of 1.9 MPN·100 ml^{-1} (N=1) and values exceeding method detection limits (>1600 MPN·100 ml^{-1}) were increased by one significant digit (>1600 MPN·100 ml^{-1} became 1700 MPN·100 ml^{-1}). Note: black points indicate visible outliers.

II-4 Vertical Water Quality Profiles

II-4-1 Temperature, Salinity, Density, and Dissolved Oxygen

Vertical water quality profiles for temperature, salinity, water density and DO_{conc} are provided in Figures II.56-II.59, respectively. Vertical profiles were collected when instrumentation for ConMon water quality stations were either deployed or collected. Profile data was collected on June 30, July 13 and 27, August 5 and 27 and September 6, 2009 under a variety of time of day and tidal stage conditions. ConMon water quality

89

Station 1, located at the mouth of TB, exhibited small density differences on the order of 1 kg·m^{-3} between surface and bottom water over depths of 0.5-1.5 meters; temperature decreased on the order of 1 °C from surface to bottom waters while salinity increases were typically 1ppt. Moving upstream, ConMon water quality Station 2 typically exhibited similar temperature, salinity and density variations as observed at ConMon water quality Station 1. The primary exception occurred on August 6, 2009 (JD: 218) when a strong density difference between surface and bottom waters (Δ density: 6 kg·m^{-3} over 1 meter depth; Δ temperature: 1.5 °C; Δ salinity: 6 ppt) was observed. This sampling followed a significant rainfall event (2.2 cm) the night prior to sampling. Vertical density differences at ConMon water quality Station 3 were typically 2 kg·m^{-3} (Δ temp: 1 °C; Δ salinity: 1-2 ppt) over depths of 0.5-1.25 meters with differences up to 7 kg·m^{-3} (Δ temp: 3 °C; Δ salinity: 9 ppt) over a 0.5 m depth when impacted by freshwater flow from the rainfall event described above. Vertical density differences at ConMon water quality Station 4 were relatively minimal at 1 kg·m^{-3} (Δ temp: 1 °C; Δ salinity: 1 ppt); note that no measurements were taken on August 5, 2009. ConMon water quality Station 5, the most upper reach TC station, remained relatively well-mixed throughout all samplings; Δ density, temperature and salinity were < 1 kg·m^{-3}, ≤ 2 °C and ≤ 1 ppt over the 0.5-0.9 meter profiles. Stratification of the water column can lead to or exacerbate water quality degradation by reducing mixing between surface and bottom waters. Stratification of the shallow water column in TB-TC was observed following significant rainfall events and impacted dissolved oxygen dynamics. This was most evident on the August 5, 2009 sampling, where DO$_{conc}$ levels decreased from 8.4 mg·liter-1 (DO$_{\%sat}$: 121) in surface waters to 1.2 mg·liter-1 (DO$_{\%sat}$: 22.1) over a 1.0 meter depth and 8.4 mg·liter-1 (DO$_{\%sat}$: 115) to 2.9 mg·liter-1 (DO$_{\%sat}$: 47) over 0.6 meters at ConMon water quality Stations 2 and 3, respectively.
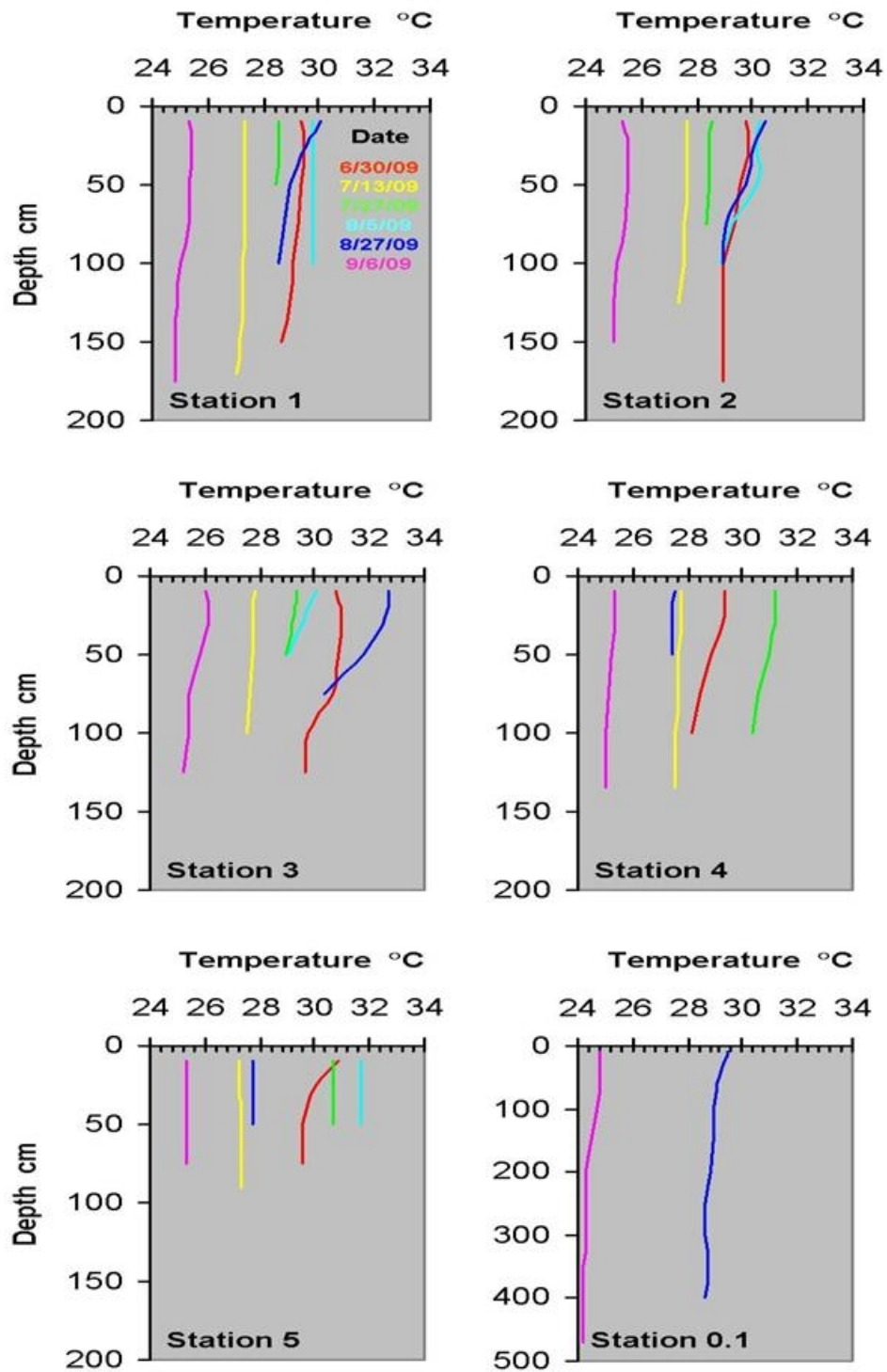
Figure II.56. Vertical profiles of water temperature (°C) for ConMon water quality stations during the June-September 2009 sampling period.
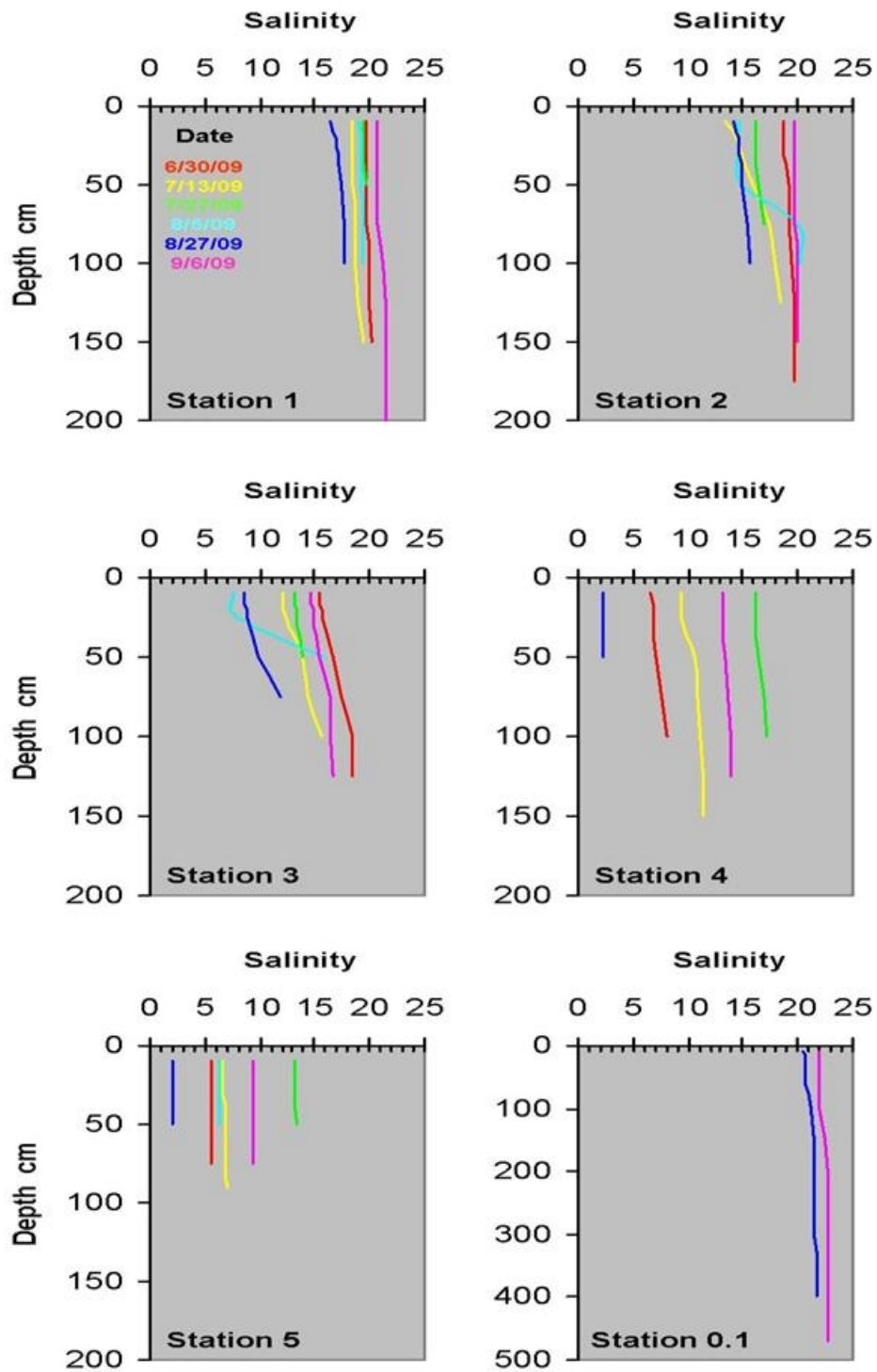
Figure II.57. Vertical profiles of salinity (psu) for ConMon water quality stations during the June-September 2009 sampling period.
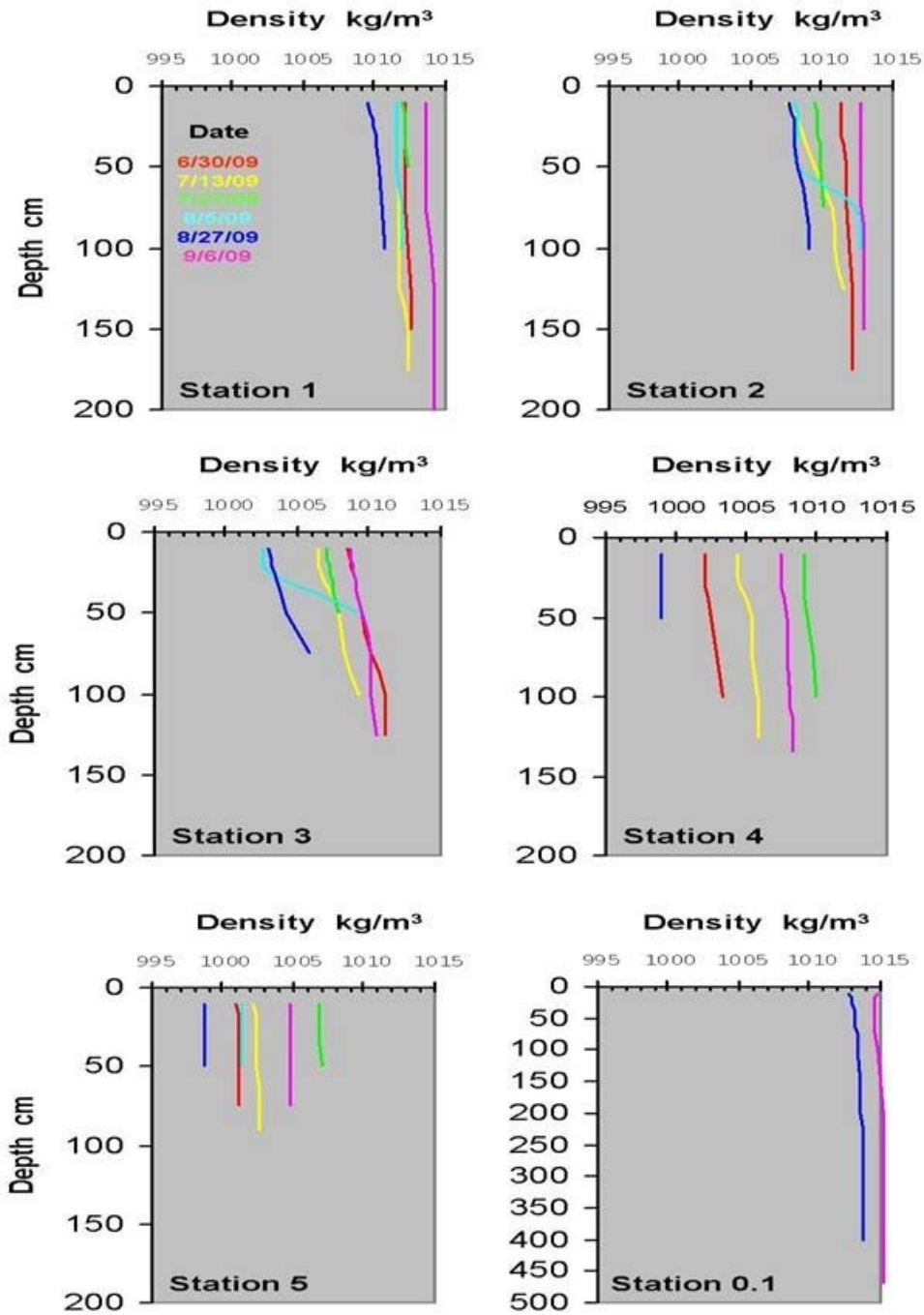
Figure II.58. Vertical profiles of calculated water density for ConMon water quality stations during the June-September 2009 sampling period.
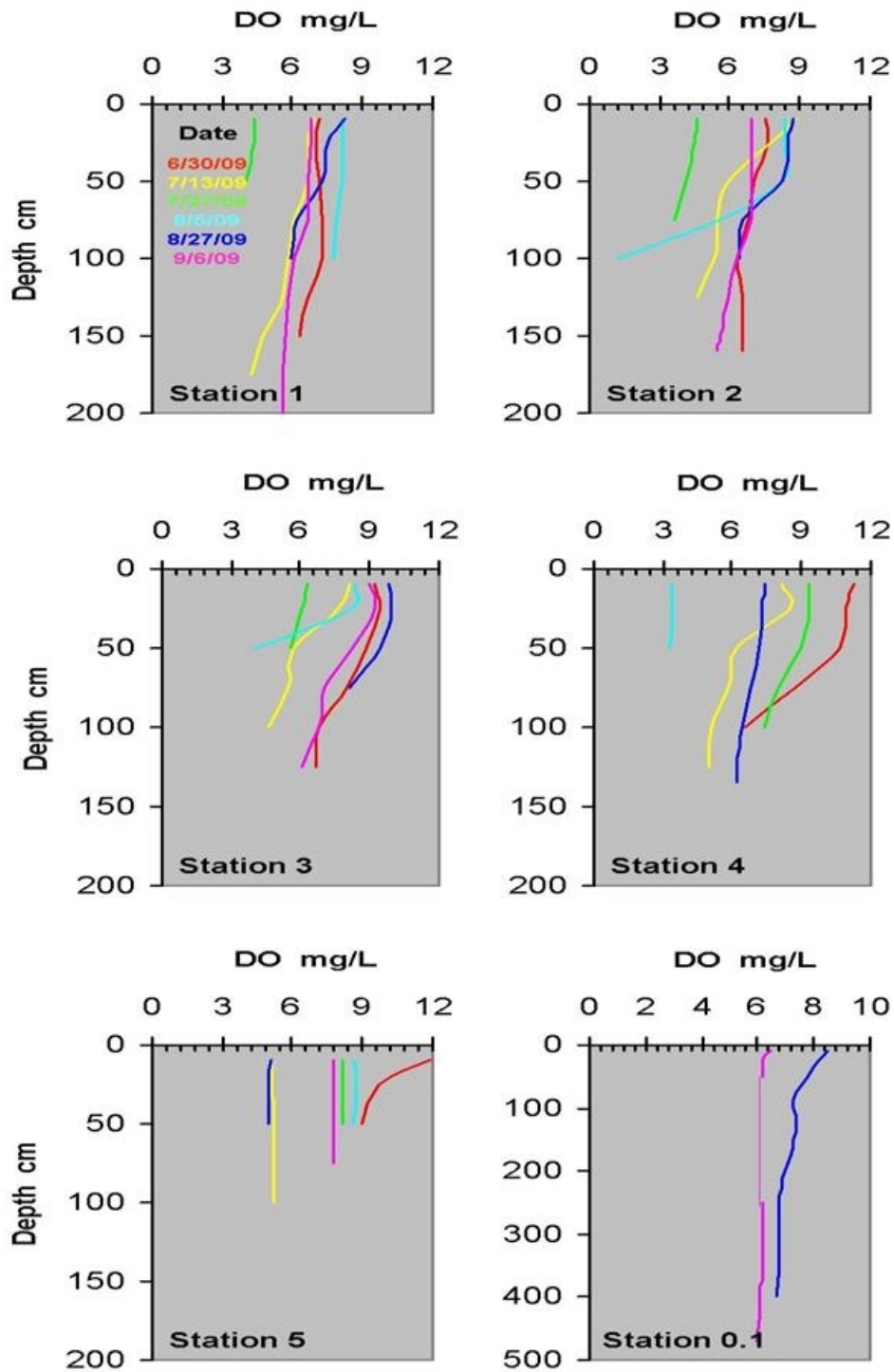
Figure II.59. Vertical profiles of DO_{conc} (mg·L^{-1}) for ConMon water quality stations during the June-September 2009 sampling period.

94

II-4-2 Solar Radiation

The photic zone or euphotic zone is the depth of the water in a waterbody where sufficient solar light penetration can support primary production. Light intensity within a water column is a function of many factors (e.g., water color, suspended solids, and phytoplankton abundance) and generally decreases exponentially with increasing depth. For phytoplankton, the photic zone can be approximated by the depth where 1% of the surface radiation still remains ($z_{1\%}$). For submerged aquatic vegetation (SAV), the minimum light requirements are on the order of 13% of surface light reaching the bottom for freshwater SAV and 22% for higher salinity species (Kemp et al., 2004). Below this depth, light becomes a limiting factor in primary production and biological activity is generally considered confined to the consumption of imported energy.

Solar radiation within the photosynthetic active range (PAR: 400-700 nm quantum response area) was measured with a LI-COR Model 1400 datalogger equipped with a LI-190 terrestrial quantum sensor and LI-192 underwater sensor. Water column depth measurement intervals were 0.10, 0.25, 0.50, 0.75 and 1.00 m. Vertical profiles of solar radiation were collected during the deployment and recovery of YSI instruments at the ConMon water quality stations.

 The depth of the phytoplankton photic zone was estimated based on direct observations of solar light penetration with depth which can be expressed in terms of the vertical light extinction coefficient (k_e)(Equation II.5). The slope of *ln* I/I_0 versus depth z provides an estimate of k_e.

$$I_z = I_0 e^{-k_e z}$$
Equation II.5.

where
I_z = Solar radiation at water depth z (μmol·sec^{-1}·m^{-2})
I_0 = Incoming surface solar radiation (z=0) (μmol·sec^{-1}·m^{-2})
k_e = Attenuation coefficient (m^{-1})
z = Depth of water column measurement (m)

The phytoplankton photic zone depth was determined from Equation II.6 (Thomann and Mueller, 1987).

$$z_{1\%} = \left(\frac{4.61}{k_e} \right)$$
Equation II.6.

where
$z_{1\%}$ = Depth at which 1% of surface radiation still remains (m)

Irradiance available for water column and benthic primary production is dependent on incident surface light, the water column attenuation coefficient and water depth. Calculated k_e and $z_{1\%}$ depths by station and date are provided in Table II.17. Water

column k_e within the TB-TC system, varying from 2.84 to 6.32 m^{-1} over the study period, was characteristic of relatively turbid water. K_e values exhibited a generally increasing trend with increasing distance upstream for three of the four samplings. Corresponding $z_{1\%}$ depths within the TB-TC system ranged from 0.7 to 1.6 m; a single sampling within the Western Branch of the Lynnhaven River was 1.8 m. Water depth generally exceeded $z_{1\%}$ for most (~75%) of the three deployment periods at ConMon water quality Stations 1 and 4, for all of the deployment periods at ConMon water quality Stations 2 and 3, and for approximately half the deployment periods at ConMon water quality Station 5 (see Figure II.60). This analysis suggests a limited role of benthic primary production in the channel regions of TB-TC, whereas the broad shoal region would be expected to have adequate light to support benthic algal communities.

Table II.17. Calculated light extinction coefficients (k_e) and photic zone ($z_{1\%}$) at ConMon water quality stations by sampling date.

Station	0.1		1		2		3		4		5	
Date	k_e (m^{-1})	$z_{1\%}$ (m)	k_e (m^{-1})	$z_{1\%}$ (m)	k_e (m^{-1})	$z_{1\%}$ (m)	k_e (m^{-1})	$z_{1\%}$ (m)	k_e (m^{-1})	$z_{1\%}$ (m)	k_e (m^{-1})	$z_{1\%}$ (m)
7/13/09	-	-	3.15	1.46	3.55	1.30	3.61	1.28	4.19	1.10	4.49	1.03
7/27/09	-	-	3.36	1.37	4.37	1.05	6.32	0.73	3.71	1.24	4.23	1.09
8/5/09	-	-	3.37	1.37	4.98	0.93	5.56	0.83	-	-	6.09	0.76
8/27/09	-	-	4.63	1.00	6.15	0.75	4.92	0.94	4.82	0.96	3.27	1.41
9/6/09	2.53	1.82	2.84	1.62	4.03	1.14	4.23	1.09	4.53	1.02	5.33	0.86
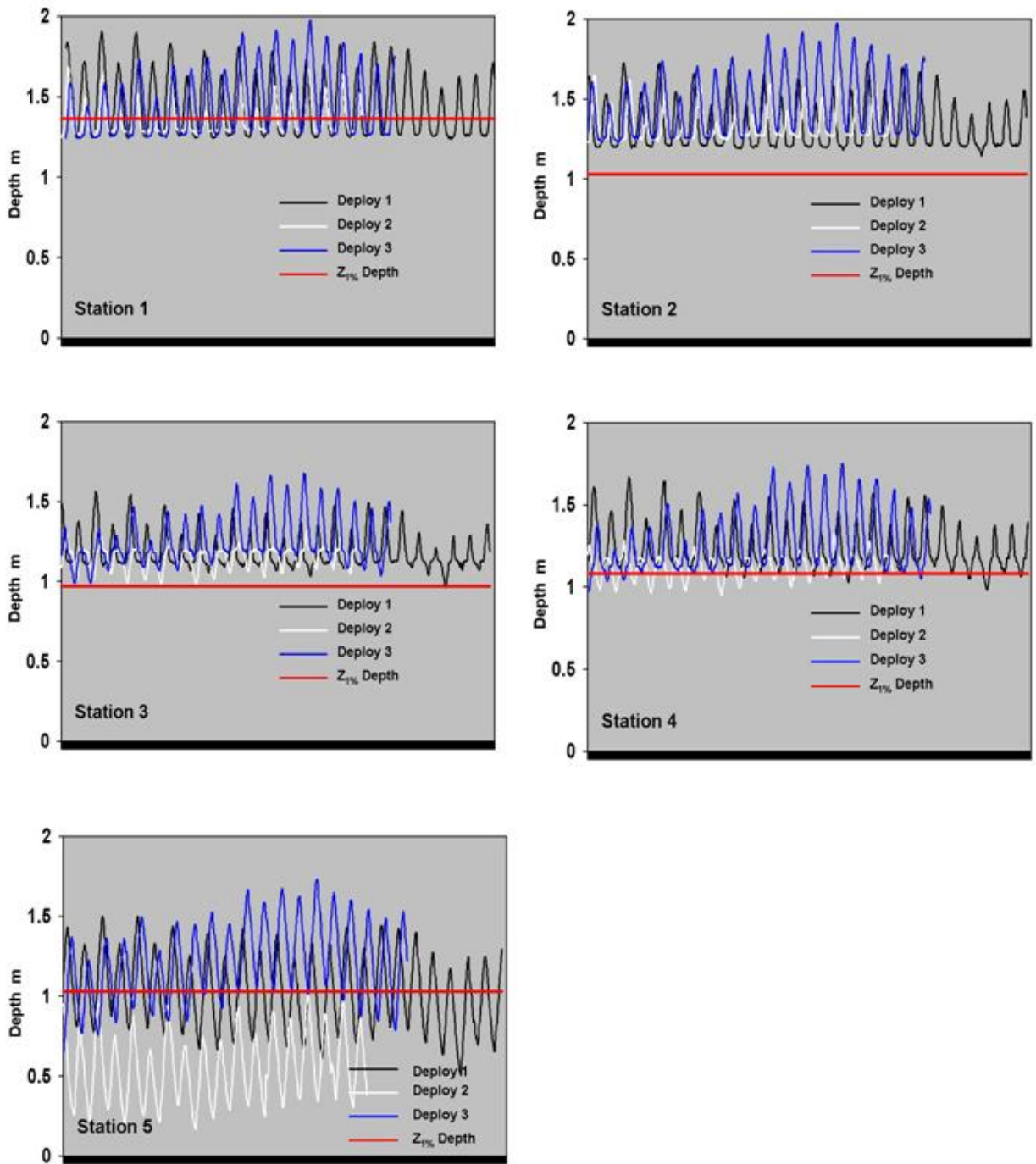
Figure II.60. Total water depth vesus $Z_{1\%}$ depth by ConMon station and deployment. $Z_{1\%}$ reference line based on average over the study period.

II-5 Sediment Studies

II-5-1 Physical Properties

Surficial (top 1 cm) sediment samples were collected on a one-time basis (August 2009) at the water quality grab sample stations within the main channel of the TB-TC system; additional samples were collected in Buchanan Creek and the upper portion of the Western Branch of the Lynnhaven River (see Figure II.3). Replicate sediment samples (N=3 or 4) were collected manually with a Wildco sediment corer with internal transparent plexiglass core liners (I.D.: 4.6 cm; Area sampled: 17.34 cm^2); all disturbed cores were discarded. Samples collected for texture analysis were homogenized into one composite sample, whereas samples for dry bulk density, porosity and % organic matter (%OM) were analyzed on an individual basis. Sediments were categorized into gravel, sand (coarse, medium, and fine), silt, and clay using the Wentworth scale following a wet-sieve and pipette analysis (Folk, 1980). Bulk density was expressed as the ratio between the mass of oven dried (105 °C) sediment and field volume of sediment. Sediment porosity, expressed as a percentage, was determined as the volume of water loss following oven drying (105 °C) per field condition volume. Percent OM was determined by percent weight loss following combustion (500 °C) of dried sediments (Dean, 1974).

Spatial distribution of coarse (i.e., sand) and fine or muddy (i.e., silt and clay) textured sediments within the TB-TC system, BC and the upper portion of the Western Branch of the Lynnhaven River are provided in Figures II.61 and II.62, respectively. Descriptive summary statistics for sediments are presented in Table II.18. Grain size distribution within the channels of TB, BC and the single station in the upper portion of the Western Branch of the Lynnhaven River were dominated (range: 93-100%) by silt/clay grain size fractions; exception occurred immediately below the impoundment (Station 6) where fines contributed 54% of the sediments mass. Sediments within TC exhibited a greater percent of coarse textured sand in the upper reaches ($\geq 30\%$) and graded to finer sediments in the lower reaches. These patterns of sediment grain size distribution suggest the importance of physical processes (transportation and deposition) and watershed runoff within the TB-TC system. Depending on flow rates, finer sediments can be retained in suspension and be transported downstream, whereas coarser sediment would tend to settle as lag deposits near entry points in the upper reaches.

Sediments within the muddy portions of the TB-TC system and BC generally showed an increasing trend of %OM with distance upstream. Within the TB-TC system, sediment %OM increased from 3-7% in TB (Stations 2-5) to 9-14% (Stations 7-13) in TC. In BC, sediment OM increased from 4-5% in the lower reaches (stations 18-19) to 8-9% in the upper reaches (Stations 20-21). Within the muddy channel sediments, OM was positively correlated to the percent silt content of the sediments. In the upper reaches of TC, the relationship between sediment texture and OM was more complex. In general, %OM generally decreases with increasing sediment texture size (i.e., gravel and sand) as exemplified by the most upstream station on TC (Station 17: OM = 2%; Sand: =97%).
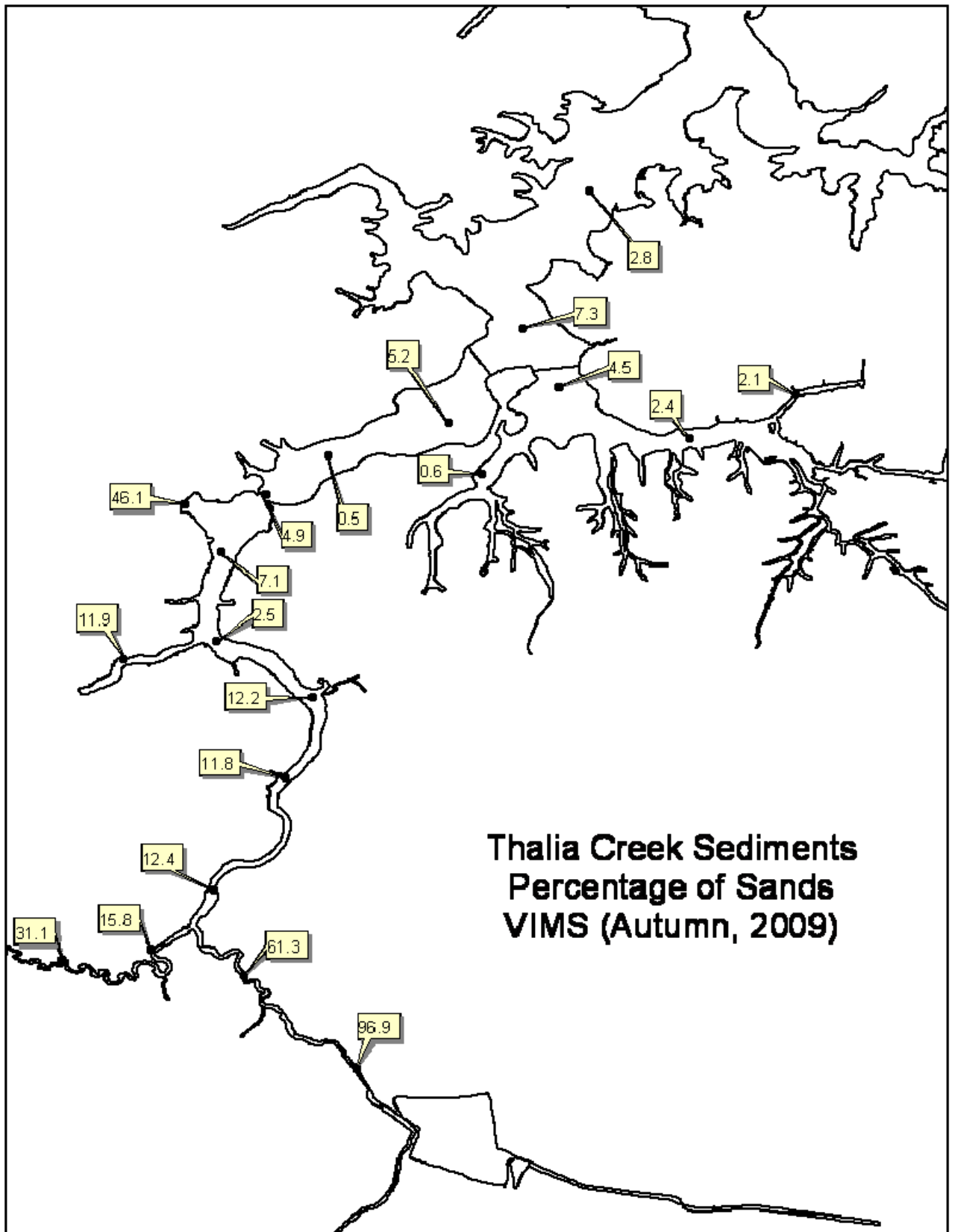
Figure II.61. Spatial plot of percent sand content of subtidal sediments from Thurston Branch - Thalia Creek grab samples, August, 2009.
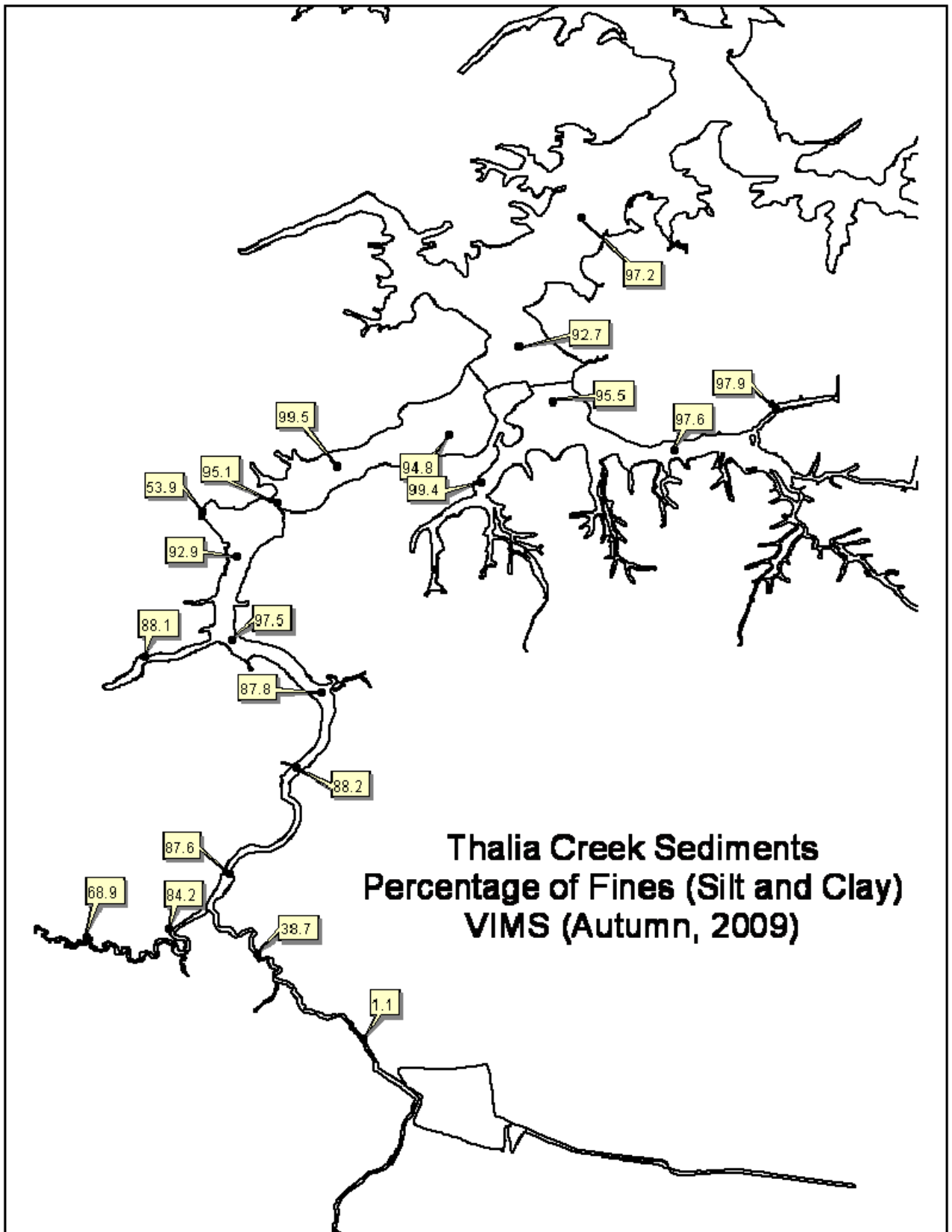
Figure II.62. Spatial plot of percent fines (silt and clay) content of subtidal
sediments from Thurston Branch - Thalia Creek grab samples, August, 2009.

Table II.18. Sediment properties from channel stations within the TB-TC system, Buchanan Creek, and the upper Western Branch of the Lynnhaven River. Standard deviation and sample size are presented parenthetically.

Station ID	Bulk Density ($g \cdot cm^{-3}$)	Porosity	% Organic Matter	Texture (gravel/sand/silt/clay)
1	0.62 (0.28,3)	0.81 (.18,3)	4.6 (2.9,3)	0.0 / 2.8 / 66.0 / 31.2
2	0.63 (0.19,2)	0.85 (0.18,3)	3.0 (0.3,3)	0.0 / 7.3 / 60.2 / 32.5
3	0.65 (0.04,4)	0.89 (0.01,4)	5.5 (2.1,4)	0.0 / 5.2 / 67.9 / 27.0
4	0.34 (0.02,2)	0.84 (0.06,2)	5.6 (3.3,4)	0.0 / 0.5 / 63.7 / 35.8
5	0.56 (0.29,2)	0.95 (0.01,2)	6.5 (3.4,4)	0.0 / 4.9 / 62.3 / 32.8
6	0.70 (0.07,3)	0.94 (0.02,3)	4.6 (1.4,4)	0.0 / 46.1 / 39.5 / 14.4
7	0.34 (0.04,2)	0.93 (0.03,2)	9.1 (1.8,4)	0.0 / 7.1 / 67.9 / 25.0
8	0.24 (0.06,4)	0.77 (0.10,4)	10.2 (4.3,4)	0.0 / 2.5 / 69.5 / 27.9
9	0.24 (0.00,2)	0.78 (0.00,2)	10.4 (2.1,4)	0.0 / 11.9 / 64.5 / 23.6
10	0.26 (0.08,2)	0.90 (0.13,2)	13.2 (2.4,4)	0.0 / 12.2 / 66.4 / 21.4
12	0.32 (0.01,2)	0.94 (0.05,2)	12.1 (0.5,3)	0.0 / 11.8 / 87.5 / 0.7
13	0.39 (0.09,3)	0.97 (0.01,3)	13.6 (3.0,4)	0.0 / 12.4 / 76.6 / 11.0
14	0.87 (0.38,3)	0.70 (0.11,3)	6.5 (5.6,4)	0.0 / 15.8 / 69.6 / 14.6
15	0.49 (0.08,4)	0.81 (0.09,4)	12.5 (1.0,4)	0.0 / 31.1 / 63.5 / 5.4
16	0.89 (0.31,3)	0.78 (0.16,3)	4.7 (3.8,3)	0.0 / 61.3 / 38.7 / 0.0
17	1.44 (0.20,4)	0.63 (0.12,4)	2.0 (1.8,4)	2.0 / 96.9 / 1.1 / 0.0
18	0.55 (0.17,2)	0.77 (0.13,2)	4.2 (2.1,4)	0.0 / 4.5 / 65.4 / 30.1
19	0.45 (-,1)	0.94 (-,1)	5.3 (2.6,4)	0.0 / 0.6 / 70.5 / 28.9
20	0.51 (0.13,3)	0.81 (0.14,3)	8.7 (1.7,4)	0.0 / 2.4 / 77.9 / 19.6
21	0.33 (0.01,3)	0.89 (0.08,3)	7.5 (2.7,4)	0.0 / 2.1 / 78.9 / 18.9

II-5-2 Sediment Oxygen Flux

Sediment and water column interactions are of significant ecological importance with respect to nutrient and oxygen dynamics in shallow coastal waters. *In situ* sediment oxygen flux measurements were conducted at three locations within TB-TC during September 2009. Study locations were located in the upper reaches of TC and corresponded to ConMon water quality Stations 4 and 5. A third study was conducted in the lower reaches of TB (between ConMon water quality Stations 1 and 2) but was disrupted by wave action from passing vessels. Studies began near noon and lasted approximated 2.5-3 hours under similar tidal conditions.

Benthic flux chambers were used in the studies and work on the basic principle of measuring change in chemistry of a known volume of isolated bottom water that remains in contact with a known area of sediment. Light (transparent) and dark (opaque) flux chambers were constructed of acrylic plastic, and enclosed 0.07 m^2 of sediment and 7.94 liters of ambient surface water. Flux chambers were fitted with a sharpened rim that assured a tight seal with the sediment (6-cm penetration) and uniform water volume

within chambers. To avoid stratification and allow for continuous (2-minute sampling intervals) measurement of DO_{conc}, water was gently and continuously recirculated between the flux chamber and flow-through chamber housing the datasonde sensors. Flow was sustained by controllable 12-volt bilge pumps installed within the flux chambers and a variable set of recirculation tubing. Blank water column chambers, similar to benthic chambers but sealed at the bottom to eliminate contact with sediment, were incubated concurrently with benthic chambers in order to account for water column processes affecting DO dynamics. Oxygen flux was estimated by calculating the rate of change in DO_{conc}, which was generally linear, over the incubation period.

Benthic daily respiration (R_{ben}), net production (P_{bennet}) and gross production ($P_{bengross}$) were estimated by Equations II.7, II.8 and II.9, respectively. In addition, daily estimates of NEM were also calculated by subtracted R_{ben} from $P_{bengross}$. Results are presented in Table II.19.

$$R_{ben} = \left(\frac{\overline{\Delta DO}_{concDC} - \overline{\Delta DO}_{concDC\,Control}}{hr} \right) \times \left(-\frac{24\,hr}{day} \right) \qquad \text{Equation II.7}$$

where:

R_{ben} = Daily benthic community respiration (g O_2 $m^{-2} \cdot day^{-1}$)
ΔDO_{concDC} = Mean hourly rate of DO_{conc} change in dark chamber (g O_2 $m^{-2} \cdot hr^{-1}$)
$\Delta DO_{concDC\,Control}$ = Mean hourly rate of DO_{conc} change in dark chamber control
     (g O_2 $m^{-2} \cdot hr^{-1}$)

$$P_{bennet} = \left(\frac{\overline{\Delta DO}_{concLC} - \overline{\Delta DO}_{concLC\,Control}}{hr} \right) \times dt_{day} \qquad \text{Equation II.8}$$

where:

P_{bennet} = Daily benthic net production (g O_2 $m^{-2} \cdot day^{-1}$)
ΔDO_{concLC} = Mean hourly rate of DO_{conc} change in light chambers (g O_2 $m^{-2} \cdot hr^{-1}$)
$\Delta DO_{concDC\,Control}$ = Mean hourly rate of DO_{conc} change in light chamber control
     (g O_2 $m^{-2} \cdot hr^{-1}$)
dt_{day} = Daytime interval or photoperiod (hr)

$$P_{bengross} = P_{bennet} + \left(\frac{R_{ben}}{24\,hr} x \, dt_{day} \right) \qquad \text{Equation II.9}$$

where:

$P_{bengross}$ = Daily gross productivity (g O_2 $m^{-2} \cdot day^{-1}$)
P_{bennet} = Daily benthic net production (g O_2 $m^{-2} \cdot day^{-1}$)
dt_{day} = Daytime interval or photoperiod (hr)

Table II.19. Mean benthic metabolic rates for upper Thalia Creek.

Station	Ecosystem Gross Productivity O_2 $g·m^{-2}·day^{-1}$	Daytime Ecosystem Production O_2 $g·m^{-2}·day^{-1}$	Respiration O_2 $g·m^{-2}·day^{-1}$	NEM O_2 $g·m^{-2}·day^{-1}$
ConMon 4	0.77	-0.31	1.99	-1.22
ConMon 5	0.12	-0.53	1.20	-1.08

II-6 Summary and Key Findings

(1) The TB-TC system, a tidal subestary connecting to the Western Branch of the Lynnhaven River, is relatively shallow with channel depths typically varying from 1.0 to 1.5 meters. The primary channel is flanked by broad shoals in the lower reaches that narrow with distance upstream. Channel sediments in TB and the lower reaches of TC were dominated (>85%) by silt/clay grain size fractions. Sediment %OM within this region increased with distance upstream from 3 to 14%. Channel sediments within the upper reaches of TC exhibited greater sand content, increasing with distance upstream from 15 to 31% in the west fork and 61 to 97% in the southeast fork signifying sandy lag deposits near the entry points.

(2) The tide had standing wave characteristics as it propagated between the mouth of TB and the upper reaches of TC. Tidal range was on the order of 0.6 meters and phase differences for most harmonic constituents were within several minutes. The studied portions of TB-TC displayed a broad range of salinity regimes ranging from oligohaline to polyhaline conditions. Tidal variations in salinity were on the order of 6-9 ppt in the upper reaches of TC and 2-3 ppt near the mouth of TB. Variations over a 10-day deployment period could be as high as 15 ppt. Depressions in salinity due to rainfall events were observed throughout the TB-TC system.

(3) Within the TB-TC system, TDN showed a relatively consistent gradient with moderately high concentrations (> 0.6 mg·L^{-1} as N) in the upper TC reaches and decreasing with distance downstream. DON typically accounted for ≥ 95% of the TDN pool. TDP exhibited moderate concentrations (≥ 0.01 to ≤ 0.1 mg·L^{-1} as P) with PO_4 representing between 30-60% of TDP pool. DIN: PO_4 ratios are reflective of nitrogen limitation of primary productivity throughout the TB-TC system with the potential for phosphorus limitation in the upper, low salinity reaches following significant rainfall events.

4) High (>20 to ≤ 60 μg·L^{-1}) to hyper-eutrophic (>60 μg·L^{-1}) concentrations of chl *a* were observed within the TB-TC system. Mean chl *a* concentrations and variability of measurements increased with distance upstream. High pheopigment to chl *a* ratios,

particularly in the upper TC reaches, suggested a relatively degraded phytoplankton population possibly due to stress (e.g., light, salt) or elevated grazing pressures.

(5) Dissolved oxygen patterns within the TB-TC system was highly dynamic and exhibited a strong diurnal signal driven by water temperature variation and biological activities. While most severe and chronic in the upper reaches, hypoxia (defined as $DO_{conc} \leq 2$ mg·L^{-1}) was observed throughout the TB-TC system. The duration of hypoxia ranged from 15 minutes to over 34 hours for a single event. The set-up and duration of severe hypoxia was influenced by solar insolation, timing of ebb-tide and freshwater input derived from storms.

(6) All ConMon stations exhibited negative mean NEM values ranging from -1.8 to -0.5 g O_2 m^{-2}·day^{-1} and respiration rates varying from 10.09-16.97 g O_2 m^{-2}·day^{-1}. Net summer heterotrophy increased with distance upstream and suggests that significant amounts of allochthonous sources of carbon are helping to fuel the high respiration rates. Sediment oxygen demand accounted for between 10-15% of open water respiration rates in the upper TC reach. Water column k_e within the TB-TC system varied from 2.8 to 6.3 m^{-1} with corresponding $z_{1\%}$ depths ranging from 0.7 to 1.6 m, suggesting a limited role of benthic primary production in the channel regions in contrast to the shallower, broad shoal regions.

(7) FCB densities exceeded Commonwealth contact standards (> 200 MPN 100· ml^{-1}) in the upper reaches of TC on a routine basis while the lower and more open reaches of TB typically exhibited FCB densities between shellfish waters and recreational contact standards (> 14 MPN to $\leq$ 200 MPN·100 ml^{-1}). Findings are consistent with an increased "land effect" due to increases in the ratio of shoreline to water volume in the upper tidal reaches. Elevated FCB densities were also observed after periods of high rainfall. The relationship between FCB and *E. coli* density was strong ($r^2 \geq 0.95$) for two of the three surveys; heavy rainfall and loadings of ubiquitous FC positive microbes may explain discrepancies with the third survey. Sources of FCB to the TB-TC system would include nonpoint source runoff from urbanized and natural lands, and direct domestic and wild animal loadings. Additional study is required to source track and differentiate FCB loadings and to determine if true health concerns exist.

CHAPTER III. NUMERICAL MODELING METHODOLOGY

III-1. Description of Numerical Modeling Framework

Numerical modeling, in a broad sense, is a process of building a mathematical abstraction of an actual system. In the estuarine and coastal environmental context, the system consists of physical, chemical, and biological components that are interactive and feed back on one another. The VIMS numerical modeling framework, as shown in Figure III.1, involves an integrated approach that combine several different processes such as hydrodynamic, water quality, nutrient, and sediment processes in order to fully simulate the water quality conditions. Whereas the water quality model is shown to be the central processing mechanism, it depends heavily upon the other models with which it interacts:

1) The hydrodynamic model for providing mass transport;
2) the HSPF watershed model for freshwater discharge and nutrient loadings; and
3) the sediment model for sediment flux information.
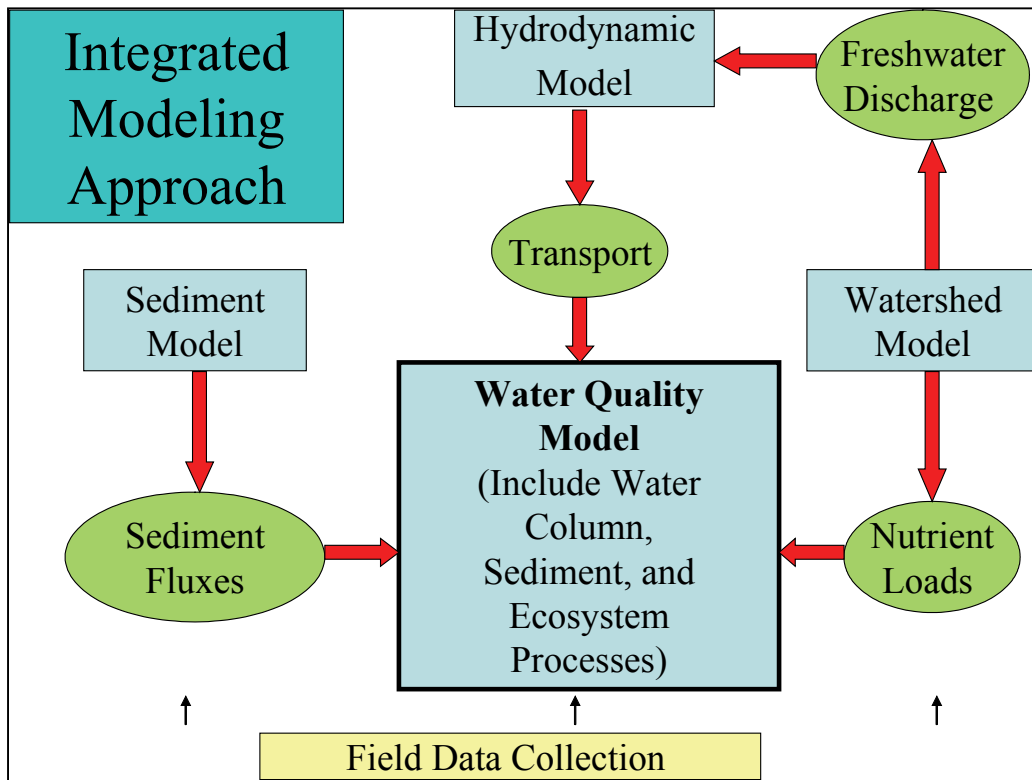
Figure III.1. The integrated modeling approach used for the VIMS water quality model

VIMS has several combined hydrodynamic and water quality models suitable for implementing within the model framework shown above. HEM-3D (hydrodynamic-

eutrophication model in 3 dimensions) was chosen for application to the Thurston Branch - Thalia Creek system because it was earlier selected for TMDL studies of Thalia Creek by VA-DEQ.

III-2. The HEM-3D hydrodynamic model

The Virginia Institute of Marine Science (VIMS) has worked with the Army Corps of Engineers and the City of Virginia Beach personnel to utilize the calibrated Hydrodynamic Eutrophication Model in 3 dimensions (HEM-3D) for the environmental assessment of the Thurston Branch - Thalia Creek system. The original HEM-3D model was developed and refined at VIMS over the period 1988-1995 (Hamrick, 1992; Park et al., 1995). It is a multi-parameter finite difference model representing estuarine flow and material transport in three dimensions. Wind stress and momentum transfer can also be represented as input at the air-water interface with salinity and freshwater discharge handled as input at the appropriate longitudinal boundary. Tidal input can be represented at the downstream open boundary by either a specific time history of water level or a simulated tide based on one or a combination of multiple tidal constituents of known amplitude and phase.

 The code is written in standard FORTRAN 77 and is highly portable to UNIX or DOS platforms. It is computationally efficient due to the programmer's avoidance of logical operators, and it economizes on required storage by maintaining only active water cell variables in memory. This code was written to be highly vectorizable, anticipating upcoming developments in parallel processing. Due to a well-designed user interface, the internal source code remains the same from application to application. The HEM-3D model can be quickly converted to a 2D model either horizontally or vertically for preliminary testing. The model's most unique features include the mass conservative scheme that it uses for drying and wetting in shallow areas. It also incorporates vegetation resistance formulations (Hamrick, 1994). The most valuable feature is the model's ability to couple with both water quality and sediment transport models. The model uses a stretched (i.e., "sigma") vertical coordinate system and a curvilinear-orthogonal horizontal coordinate system to solve vertically hydrostatic, free surface, variable density, and turbulent-averaged equations of motion. This solution is coupled with a solution of the transport equations for turbulent kinetic energy, solving the equations of motion. Integration over time involves an internal-external mode splitting procedure separating "the internal shear or baroclinic mode" from the external turbulent length scale, salinity, and temperature. A staggered grid provides the framework for the spatial finite differencing (second order accurate) used by the numerical scheme to "free surface gravity wave or barotropic mode" (Hamrick and Yang, 1995).

For a full description of the formulation of the governing equations and numerical solution techniques for both the equations of motion and the transport equations for salinity, temperature, and turbulence intensity, the reader is referred to Chapter III (methodology) of Sisson et al. (2008), available online at http://www.vims.edu/GreyLit/VIMS/sramsoe400.pdf.

III-3. Description of the watershed model for the Lynnhaven River Basin

As VIMS has developed the hydrodynamic and water quality models for the Lynnhaven River receiving waters, URS Corporation of Virginia Beach has developed a watershed model for the Lynnhaven River Basin. The watershed model used by URS is HSPF (Hydrological Simulation Program – FORTRAN), version 12 (URS Technical Memorandum, Hydrologic Concepts and Parameter Development, 2006).

The goal of the watershed modeling effort is to provide the freshwater discharge and nutrient and sediment loadings from the watershed at high spatial and temporal resolutions.   The Lynnhaven River Basin, consisting of 7 sub-watersheds, has been delineated into 1,079 catchments, ranging in size from approximately 40 acres, as shown in Figure III.2.

The landuse in the Lynnhaven Basin is 40% residential and 35% composed of streets, commercial and office space, and military use. In its watershed model development, URS selected a total of 23 land uses within the Lynnhaven River basin into which zoning codes could then be grouped. URS then assigned to each landuse a directly connected impervious percentage, as shown in Table III.1. Landuse was employed to develop effective impervious area percentages for the nearly 57,000 land parcels within the Lynnhaven Basin.

For each of these catchments, the URS model simulates the following 9 constituents:
- biochemical oxygen demand (BOD)
- total dissolved solids (TDS)
- chemical oxygen demand (COD)
- nitrate – nitrite (NO_3)
- total Kjeldahl nitrogen (TKN)
- ammonia (NH_3)
- total phosphorus (TP)
- dissolved phosphorus (DP)
- total suspended sediments (TSS)

The URS model was calibrated by comparing its predictions to monitoring data collected at 5 sites within and/or nearby the Lynnhaven basin (URS, 2007). The calibrated model was then used to provide multi-year datasets of its outputs of hourly nutrient loadings and freshwater discharge to the VIMS models.

Water quality conditions in the Thalia Creek portion of the Western Branch are worse than any other portion of the Lynnhaven River monitored bi-monthly by the VA-DEQ program. For this project, the Thalia Creek watershed spatial resolution was further delineated from that shown in Figure III.2. A total of 44 subwatershed areas were selected for daily specifications of nutrient and fecal coliform loadings and freshwater discharge, as shown in Figure III.3.
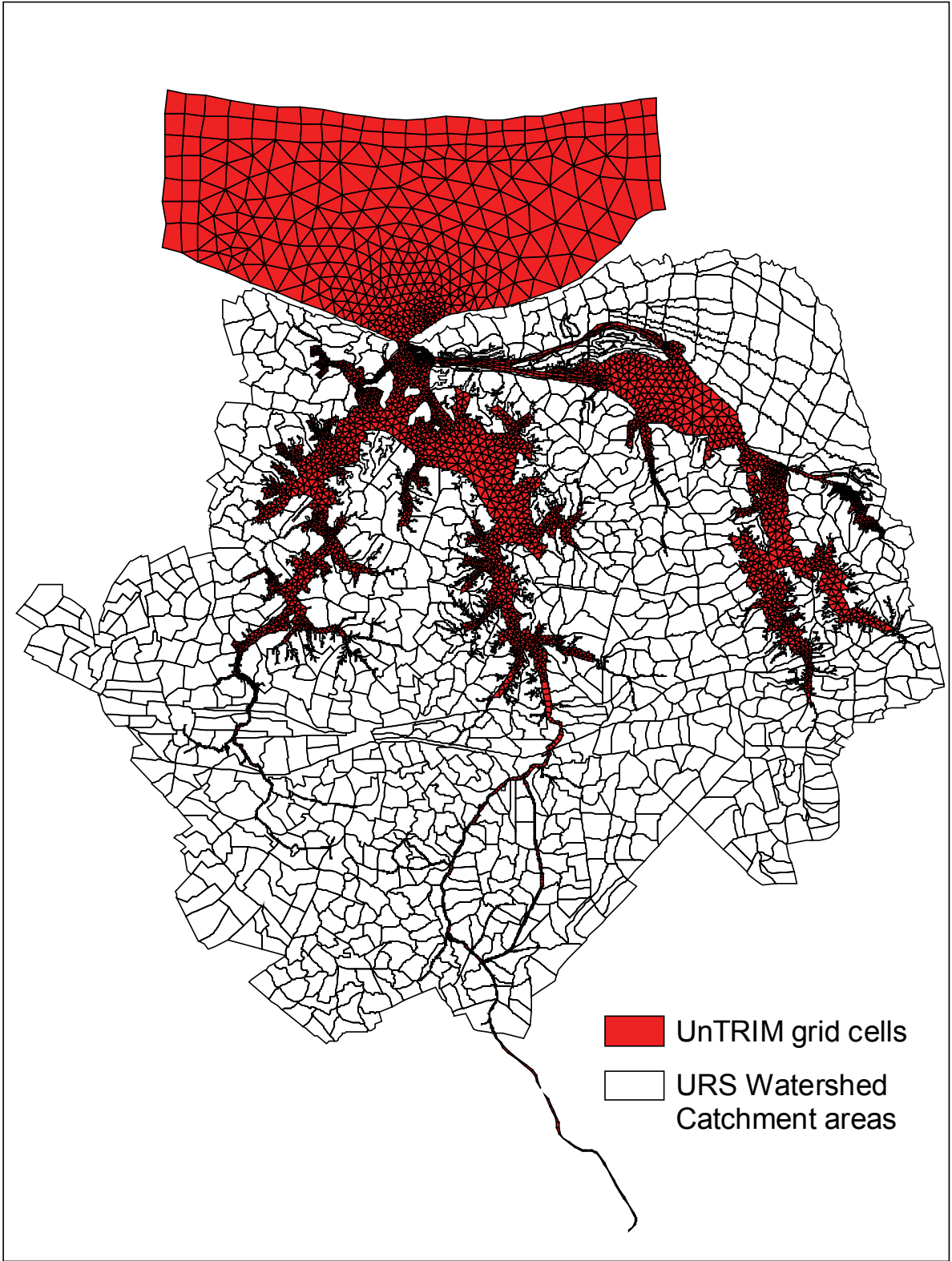
Figure III.2. The 1079 catchment areas delineated by the URS watershed model superimposed on the UnTRIM model grid.

Table III.1. Impervious percentages of Lynnhaven Basin Landuse Categories.

Landuse No.	Landuse	Landuse Description	Impervious Percentage
1	AG	Agricultural	15%
2	SFL	Single Family Low Density	16%
3	SFM	Single Family Medium Density	21%
4	SFH	Single Family High Density	24%
5	MFM	Multi-Family Medium Density	37 %
6	MFH	Multi-Family High Density	62%
7	PD	Planned Development	29%
8	O	Office	71%
9	NB	Neighborhood Business	39%
10	B	Business	73%
11	I	Industrial	45%
12	RT	Resort Tourist	71%
13	PK	Park	5%
14	GC	Golf Course	5%
15	OS	Open Space	0.5%
16	OF	Other facilities	8%
17	SC	School	47%
18	ST	Street	60%
19	CM	Cemetary	5%
20	CH	Church	47%
21	WT	Wetland	100%
22	BMP	Best Management Practice	100%
23	WAT	Water	100%
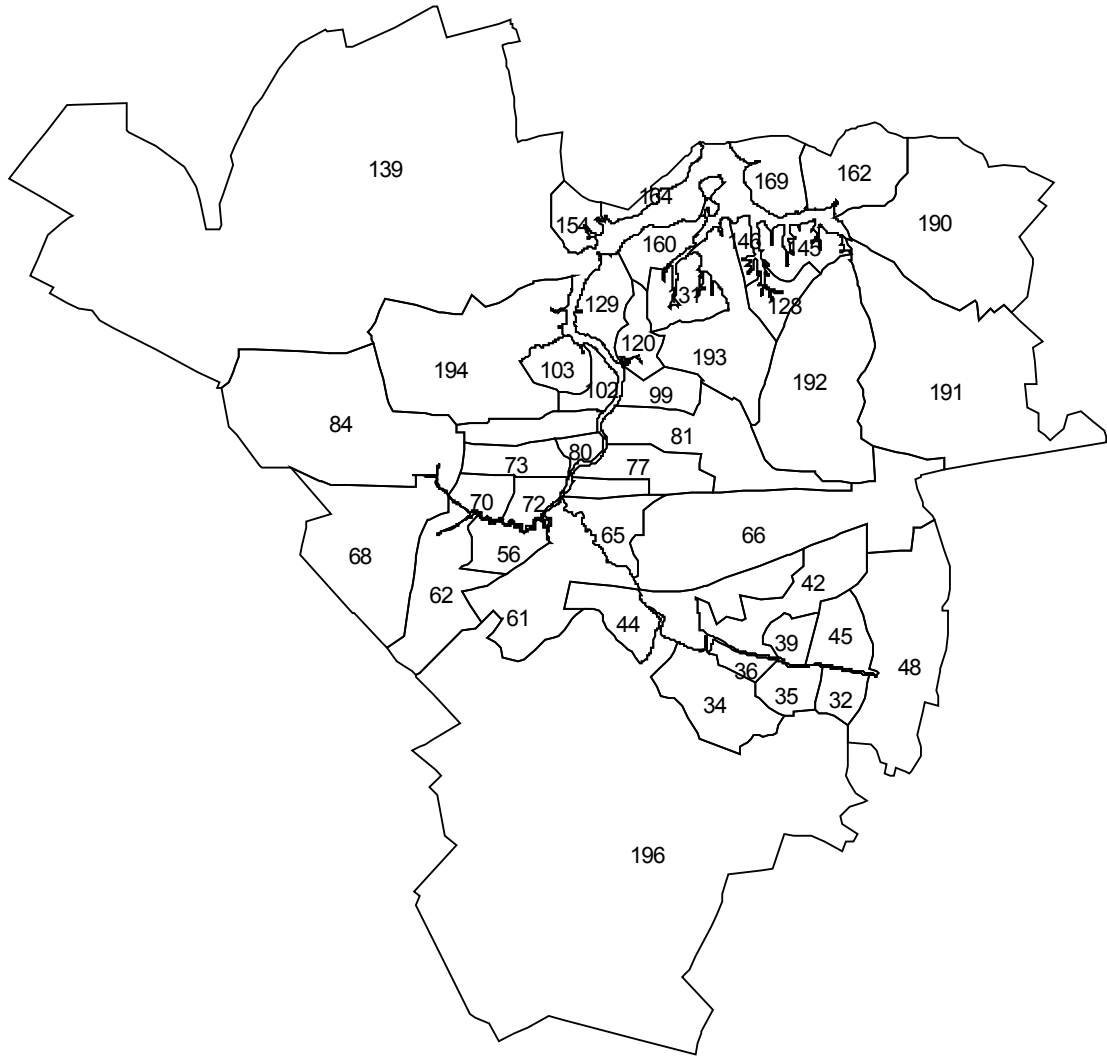
Figure III.3. Nonpoint source locations for the URS watershed model in Thalia Creek

III-4. The HEM-3D Water Quality Model

A water quality model with twenty-one state variables has been developed and integrated with the hydrodynamic model to form the three-dimensional VIMS Hydrodynamic-Eutrophication Model (HEM-3D) (Park et al., 1995). The information of physical transport processes, both advective and diffusive, simulated by the hydrodynamic model described in Section III-2, are used to account for the transport of passive substances including non-conservative water quality parameters. The model, upon receiving the physical transport from the hydrodynamic model, simulates the spatial and temporal distributions of water quality parameters including dissolved oxygen, suspended algae (3 groups), various components of carbon, nitrogen, phosphorus, and silica cycles, and fecal coliform bacteria.

The VIMS HEM-3D was used to simulate nutrients, algae, and DO dynamics for the Thurston Branch – Thalia Creek system. The model was calibrated and validated against DEQ's monitoring data for selected years. Once the model was calibrated and validated, the model was set up to run scenarios to assess the effects of nutrient load reductions.

The water quality model simulates 21 state variables in the water column and 23 state variables in the sediment together with the velocity field, suspended sediments, and temperature. The model has been updated to include benthic algae and macroalgae. For this application, only green algae were modeled. The effects of benthic algae were included in the model simulations. The following is a description of water quality processes modeled with the water quality portion of HEM-3D.

III-4-1. Dissolved oxygen process

(1) Effects of algae in water column on dissolved oxygen

Algae produce oxygen during photosynthesis and consume oxygen through respiration. The quantity produced during photosynthesis depends on the form of nitrogen taken up. Since oxygen is released in the reduction of nitrate (NO_3), more oxygen is produced, per unit of carbon fixed, when NO_3 is the algal nitrogen source than when ammonia NH_4 is the source. When NH_4 is the nitrogen source, one mole of oxygen is produced per mole carbon dioxide fixed. When NO_3 is the nitrogen source, 1.3 moles oxygen are produced per mole carbon dioxide fixed. The equation that describes the effect of algae photosynthesis on DO in the model is:

$$\frac{\delta DO}{\delta t} = \sum_{x} \left(\left(1.3 - 0.3 PN_x \right) P_x \right) AOCR \cdot B_x \qquad \text{(III-1)}$$

where:

PN_x = algal group x preference for ammonium in which

P_x = production rate of algal group x (day^{-1})
AOCR = DO-to-carbon ratio in respiration (2.67 g O_2 per g C)
B_x = algal biomass (g C m^{-3})

As employed here, basal metabolism is the sum of all internal processes that decrease algal biomass. A portion of the metabolism is respiration and may be viewed as a reversal of production. In respiration, carbon and nutrients are returned to the environment accompanied by the consumption of DO. Respiration cannot proceed in the absence of DO. Basal metabolism cannot decrease in proportion to oxygen availability.

Formulation of this process is described as:

$$\frac{\delta DO}{\delta t} = \sum_x \left(-\frac{DO}{KHR_x + DO} BM_x \right) AOCR \cdot B_x \qquad \text{(III-2)}$$

where:

KHR_x = half-saturation constant of DO for algal DOC exudation (g O_2 m^{-3})
BM_x = basal metabolism rates for algal group x (day^{-1})

(2) Effects of nitrification on dissolved oxygen

Nitrification is a process mediated by specialized groups of autotrophic bacteria that obtain energy through the oxidation of ammonia to nitrite and oxidation of nitrite to nitrate. A simplified expression for complete nitrification is:

$$NH_4^+ + 2O_2 \rightarrow NO_3^- + H_2O + 2H^{2+} \qquad \text{(III-3)}$$
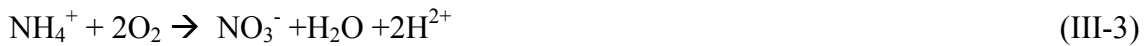
The equation indicates that two moles of oxygen are required to nitrify one mole of ammonia into nitrate. The simplified equation is not strictly true, however. Cell synthesis by nitrifying bacteria is accomplished by the fixation of carbon dioxide so that less than two moles of oxygen are consumed per mole ammonium utilized (Wezernak and Gannon, 1968). In this study, nitrification is modeled as a function of available ammonium, dissolved oxygen, and temperature:

$$NT = \frac{DO}{KHONT + DO} \frac{NH_4}{KHNNT + NH_4} f(T) \cdot NTM \qquad \text{(III-4)}$$

where:

NT = nitrification rate (gm N m^{-3} day^{-1})
NTM = maximum nitrification rate at optimal temperature (gm N m^{-3} day^{-1})
KHONT = half-saturation constant of DO required for nitrification (gm DO m^{-3})
KHNNT = half-saturation constant of NH_4 required for nitrification (gm N m^{-3})

Therefore, the effect of nitrification on DO is described as follows:

$$\frac{\delta DO}{\delta t} = - AONT \cdot NT \qquad \text{(III-5)}$$

where:

AONT = mass DO consumed per mass ammonia nitrified (4.33 gm DO gm^{-1} N)

(3) Effects of surface reaeration on dissolved oxygen

Reaeration occurs only in the model surface cells. The effect of reaeration is:

$$\frac{\delta DO}{\delta t} = \frac{K_R}{\Delta z_s} (DO_S - DO) \qquad \text{(III-6)}$$

where:

K_R = reaeration coefficient (m day $^{-1}$)
Δz_s = model layer thickness (m)
DO_S = dissolved oxygen saturation concentration (gm DO m^{-3})

Saturation dissolved oxygen concentration DO_S is computed (Genet et al., 1974):

$$\begin{aligned} DO_S = {}& 14.5532 - 0.38217 \cdot T + 0.0054258 \cdot T^2 \\ & - \frac{S}{1.80655} \left(0.1665 - 5.866 \cdot 10^{-3} \cdot T + 9.796 \cdot 10^{-5} \cdot T^2 \right) \end{aligned} \qquad \text{(III-7)}$$

where:

S = salinity (ppt)

(4) Effects of Chemical Oxygen Demand on dissolved oxygen

In the present model, chemical oxygen demand represents the reduced materials that can be oxidized through inorganic means. The kinetic equation showing the effect of chemical oxygen demand (bottom cells only) is:

$$\frac{\delta DO}{\delta t} = - \frac{DO}{KHO_{COD} + DO} K_{COD} \cdot COD \qquad \text{(III-8)}$$

113

where:

COD = chemical oxygen demand concentrations (g O_2-equivalents m^{-3})
KHO_{COD} = half-saturation constant of DO for oxidation of COD (g O_2 m^{-3})
K_{COD} = oxidation rate of COD (day^{-1})
BF_{COD} = sediment flux of COD (g O_2-equivalents m^{-2} day^{-1}).

$$K_{COD} = K_{CD} \cdot \exp(KT_{COD}[T - TR_{COD}]) \qquad \text{(III-9)}$$

where:

K_{CD} = oxidation rate of COD at reference temperature TR_{COD} (day^{-1})
KT_{COD} = effect of temperature on oxidation of COD ($°C^{-1}$)
TR_{COD} = reference temperature for oxidation of COD (°C).

Overall, the internal sources and sinks of dissolved oxygen include algal photosynthesis and respiration, atmospheric reaeration (surface cells only), heterotrophic respiration, nitrification, and oxidation of COD. The complete kinetic equation showing sediment oxygen demand (bottom cells only) is:

$$\frac{\delta DO}{\delta t} = \sum_x \left((1.3 - 0.3 \cdot PN_x)P_x - \frac{DO}{KHR_x + DO} BM_x \right) AOCR \cdot B_x$$

$$+ \lambda_1 \frac{K_R}{\Delta z_S}(DO_S - DO) - \frac{DO}{KHO_{DOC} + DO} AOCR \cdot K_{DOC} \cdot DOC \qquad \text{(III-10)}$$

$$- AONT \cdot NIT - \frac{DO}{KHO_{COD} + DO} K_{COD} \cdot COD + \lambda_2 \frac{SOD}{\Delta z}$$

III-4-2. Model Phytoplankton Kinetics

There are three functional groups for algae: cyanobacteria, diatoms, and green algae. This grouping is based upon the distinctive characteristics of each class and upon the significant roles these characteristics play in the ecosystem. Cyanobacteria are characterized by their bloom-forming characteristics in fresh water. They are characterized as having small settling velocity and are subject to low predation pressure. Diatoms are large phytoplankton that usually produce the spring bloom in the saline water. Settling velocity of diatoms is relatively large, so the diatoms settling into sediment may be a significant source of carbon for sediment oxygen demand. Diatoms are also distinguished by their requirement of silica as a nutrient. The green algae represent the mixture that characterizes blooming in saline waters during summer and autumn, and are subject to relatively high grazing pressure.

114

Equations governing the three algal groups are similar. Differences among groups are expressed through the magnitudes of parameters in the equations. Generic equations are presented below, except when group-specific relationships are required. Algal sources and sinks in the conservation equation include production, metabolism, predation, and settling. In the following equations, a subscript, **x**, is used to denote three algal groups: **c** for cyanobacteria, **d** for diatoms, and **g** for green algae. The internal sources and sinks included are growth (production), basal metabolism (respiration and exudation), predation, and settling. The following kinetic equations for algae are:

$$\frac{\delta B_x}{\delta t} = \left(P_x - BM_x - PR_x\right)B_x - WS_x\frac{\delta B_x}{\delta z} \qquad \text{(III-11)}$$

where:

B_x = algal biomass, expressed as carbon (g C m^{-3})
P_x = growth (production) of algae (day^{-1})
BM_x = basal metabolism of algae (day^{-1})
PR_x = predation rates of algae (day^{-1})
WS_x = algal settling velocity (m day^{-1})
z = vertical coordinate

(1) Growth (Production)

Algal growth depends on nutrient availability, ambient light, and temperature. The effects of these processes are considered to be multiplicative as follows:

$$P_x = PM_x \cdot f(N) \cdot f(I) \cdot f(T) \qquad \text{(III-12)}$$

where:

PM_x = maximum production rate under optimal conditions (day^{-1})
f(N) = effect of sub-optimal nutrient
f(I) = effect of light intensity
f(T) = effect of temperature

(2) Effect of nutrient on growth

Liebig's "law of the minimum" (Odum, 1971) is used, so that nutrient limitation is determined by the single most limiting nutrient:

$$f(N) = \text{minimium}\left\{\frac{NH_4 + NO_3}{KHN_x + NH_4 + NO_3}, \frac{PO_{4d}}{KHP_x + PO_{4d}}, \frac{SAd}{KHS_d + SAd}\right\} \qquad \text{(III-13)}$$

115

where:

NH_4, NO_3 = ammonium and nitrate nitrogen concentrations, respectively (g N m^{-3})
PO_4d = dissolved phosphate concentration (g P m^{-3})
SAd = dissolved silica concentration (g Si m^{-3})
KHN_x = half-saturation constant for algal nitrogen uptake (g N m^{-3})
KHP_x = half-saturation constant for algal phosphorus uptake (g P m^{-3})
KHS_d = half-saturation constant for silica uptake by diatoms (g Si m^{-3})

(3) Effects of light on growth

The influence of light on phytoplankton production is represented by a chlorophyll-specific production equation (Jassby and Platt, 1976):

$$P^B = P^Bm \frac{I}{\sqrt{I^2 + IK^2}}$$ (III-14)

where:

P^B = photosynthetic rate (g C g^{-1} Chl d^{-1})
P^Bm = maximum photosynthetic rate (g C g^{-1} Chl d^{-1})
I = irradiance (E m^{-2} d^{-1})

Parameter Ik is defined as the irradiance at which the initial slope of the production vs. irradiance relationship intersects the value of P^Bm:

$$IK = \frac{P^Bm}{\alpha}$$ (III-15)

where:

α = initial slope of production vs. irradiance relationship (g C g^{-1} Chl (E m^{-2})$^{-1}$)

Chlorophyll-specific production rate is readily converted to carbon specific growth rate, through division by the carbon-to-chlorophyll ratio:

$$G = \frac{P^B}{CChl}$$ (III-16)

where:

$CChl$ = carbon-to-chlorophyll ratio (g C g^{-1} chlorophyll-a)

(4) Effect of temperature on growth

The effect of temperature on algal production is represented by a function similar to a Gaussian probability curve:

$$f(T) = \exp\left(-KTG1_x\,[T - TM_x]^2\right) \quad \text{when } T \leq TM_x$$
$$ = \exp\left(-KTG2_x\,[TM_x - T]^2\right) \quad \text{when } T > TM_x$$

(III-17)

where:

TM_x = optimal temperature for algal growth (°C)
$KTG1_x$ = effect of temperature below TM_x on algal growth (°C^{-2})
$KTG2_x$ = effect of temperature above TM_x on algal growth (°C^{-2})

(5) Constructing the photosynthesis vs. irradiance curve

A production versus irradiance relationship is constructed for each model cell at each time step. First, the maximum photosynthetic rate under ambient temperature and nutrient concentrations is determined:

$$P^B m(N,T) = P^B m * f(T) * f(N)$$

(III-18)

where:

$P^B m(N,T)$ = maximum photosynthetic rate under ambient temperature and nutrient concentrations (g C g^{-1} Chl d^{-1})

The single most limiting nutrient is employed in determining the nutrient limitation. Next, parameter Ik is derived from Equation III-15. Finally, the production vs. irradiance relationship is constructed using $P^B m$ (N,T) and Ik.

(6) Water surface irradiance

Hourly surface irradiance measured at Gloucester Point was used for irradiance at the surface for the model simulations for this project.

Irradiance declines exponentially with depth below the surface. The attenuation coefficient, Ke, is computed as a function of background extinction and concentrations of chlorophyll-a and total suspended solids.

(7) The light attenuation model

The water quality model requires daily solar radiation intensity except fractional day length, in order to simulate the algal growth. The light attenuation model also requires

117

input of the light attenuation coefficient. It is assumed that the light extinction coefficient consists of three parts: background extinction, the light extinction due to suspended solids, and light extinction due to algae:

$$Ke = a_1 + a_2 * TSS + a_3 * CHL \qquad \text{(III-21)}$$

where:

a_1 = background attenuation (m^{-1})
a_2 = attenuation by inorganic suspended solids ($m^2 g^{-1}$)
a_3 = attenuation by organic suspended solids ($m^2 gm^{-1} CHL$)
TSS = total suspended solids concentration ($g m^{-3}$)
CHL = chlorophyll-a concentration ($mg\ CHL\ m^{-3}$)

The "background" attenuation term included attenuation from both water and dissolved organic matter. Individual parameters were determined from Park et al. (1995b). The value for a_1 used in the model is 0.735 m^{-1}, a_2 is 0.018 $m^2 g^{-1}$, and a_3 is 0.06 $m^2 mg^{-1}$ CHL.

(8) Basal metabolism

Basal metabolism is commonly considered to be an exponentially increasing function of temperature:

$$BM_x = BMR_x * \exp\left(KTB_x [T - TR_x]\right) \qquad \text{(III-22)}$$

where:

BMR_x = metabolic rate at reference temperature TR_x (day^{-1})
KTB_x = effect of temperature on metabolism ($C^{\circ-1}$)
TR_x = reference temperature for metabolism (C°)

(9) Predation

The predation formulation is identical to basal metabolism. The difference in predation and basal metabolism lies in the distribution of the end products of these processes.

$$PR_x = BPR_x \exp\left(KTB_x (T - TR_x)\right) \qquad \text{(III-23)}$$

where:

BPR_x = predation rate at TR_x (day^{-1})
KTB_x = effect of temperature on predation ($C^{\circ-1}$)
TR_x = reference temperature for predation (C°)

(10) Settling velocity

The algal settling rate employed in the model represents the total effect of all physiological and behavioral processes that result in the downward transport of phytoplankton. The settling rate employed, from 0.1 m d^{-1} to 0.2 m d^{-1}, was used in the model to optimize the agreement between predicted and observed algae.

(11) Effect of algae on phosphorus

Model phosphorus state variables include total phosphate (dissolved, sorbed, and algal), dissolved organic phosphorus, labile particulate organic phosphorus, and refractory particulate organic phosphorus. The amount of phosphorus incorporated in algal biomass is quantified through a stoichiometric ratio. Thus, total phosphorus in the model is expressed:

$$TotP = PO_4d \; + \; PO_4p + Apc*Bx + DOP + LPOP + RPOP \tag{III-24}$$

where:

TotP = total phosphorus (g P m^{-3})
PO$_4$d = dissolved phosphate (g P m^{-3})
PO$_4$p = particulate inorganic phosphate (g P m^{-3})
Apc = algal phosphorus-to-carbon ratio (g P g^{-1} C)
DOP = dissolved organic phosphorus (g P m^{-3})
LPOP = labile particulate organic phosphorus (g P m^{-3})
RPOP = refractory particulate organic phosphorus (g P m^{-3})

Algae take up dissolved phosphate during production and release dissolved phosphate and organic phosphorus through respiration. The fate of phosphorus released by respiration is determined by empirical distribution coefficients. The fate of algal phosphorus incorporated by zooplankton and lost through zooplankton mortality is determined by a second set of distribution parameters.

(12) Effect of algae on nitrogen

Model nitrogen state variables include ammonium, nitrate, dissolved organic nitrogen, labile particulate organic nitrogen, and refractory particulate organic nitrogen. The amount of nitrogen incorporated in algal biomass is quantified through a stoichiometric ratio. Thus, total nitrogen in the model is expressed:

$$TotN = NH_4 + NO_3 + Anc*Bx + DON + LPON + RPON \tag{III-25}$$

where:

TotN = total nitrogen (g N m^{-3})
NH$_4$ = ammonium (g N m^{-3})
NO$_3$ = nitrate (g N m^{-3})
Anc = algal nitrogen-to-carbon ratio (g N g^{-1} C)
DON = dissolved organic nitrogen (g N m^{-3})
LPON = labile particulate organic nitrogen (g N m^{-3})
RPON = refractory particulate organic nitrogen (g N m^{-3})

Algae take up ammonium and nitrate + nitrite during production and release ammonium and organic nitrogen through respiration. Nitrate + nitrite is internally reduced to ammonium before synthesis into biomass occurs (Parsons et al., 1984). Trace concentrations of ammonium inhibit nitrate reduction so that, in the presence of multiple nitrogenous nutrients, ammonium is utilized first. The "preference" of algae for ammonium is expressed by an empirical function (Thomann and Fitzpatrick, 1982):

$$PN = NH_4 * \frac{NO_x}{(KHn + NH_4)*(KHn + NO_x)}$$
$$+ NH_4 * \frac{KHn}{(NH_4 + NO_x)*(KHn + NO_x)}$$

(III-26)

where:

PN = algal preference for ammonium uptake (0 < Pn < 1)
KHn = half saturation concentration for algal nitrogen uptake (g N m^{-3})

When nitrate + nitrite is absent, the preference for ammonium is unity. When ammonium is absent, the preference is zero.

(13) Effect of algae on silica

The model incorporates two siliceous state variables: dissolved silica and particulate biogenic silica. The amount of silica incorporated in algal biomass is quantified through a stoichiometric ratio. Thus, total silica in the model is expressed:

TotSi = Dsil + Asc * Bx + PBS   (III-27)

where:

TotSi = total silica (g Si m^{-3})
Dsil = dissolved silica (g Si m^{-3})
Asc = algal silica-to-carbon ratio (g Si g^{-1} C)
PBS = particulate biogenic silica (g Si m^{-3})

As with the other nutrients, the fate of algal silica released by metabolism and predation is represented by distribution coefficients.

III-4-3. Benthic sediment process

Additionally, a benthic sediment process model developed by DiToro and Fitzpatrick (1993) was incorporated and coupled with HEM-3D for the present model application.

The sediments in this model are represented by two layers: the upper aerobic layer (Layer 1) and the lower anoxic layer (Layer 2). The sediment process model is coupled with the water column eutrophication model through depositional and sediment fluxes. First, the sediment model is driven by net settling of particulate organic matter from the overlying water column to the sediments (depositional flux). Then, the mineralization of particulate organic matter in the lower anoxic sediment layer produces soluble intermediates, which are quantified as diagenesis fluxes. The intermediates react in the upper oxic and lower anoxic layers, and portions are returned to the overlying water column as sediment fluxes. Computation of sediment fluxes requires mass-balance equations for ammonium, nitrate, phosphate, sulfide/methane, and available silica. Mass-balance equations are solved for these variables for both the upper and lower layers. Complete model documentation of the sediment flux model can be found in DiToro and Fitzpatrick (1993).

III-5. Fecal coliform model

Transport with first-order decay of fecal coliform is incorporated into the hydrodynamic prediction model and is treated by the model like a dissolved substance. The decay of fecal coliform, which is a combination of die-off, settling, and both salinity and temperature influences. The decay rate is estimated based on literature values and the field measurements conducted in the Lynnhaven in 2006. For the current application, neither the growth of bacteria in the sediment nor sediment re-suspension has been considered. The model is capable of handling both point and non-point sources.

CHAPTER IV. MODEL CALIBRATION AND VALIDATION

The hydrodynamic and water quality models applied to the TB–TC system were developed using the framework outlined in Chapter III. The calibration is a process by which the performance parameters are constrained by comparing the model predictions with the field measured observations. For example, the bottom friction parameters were adjusted during the calibration process. A calibration assures that the model will produce results that meet or exceed some defined criteria with a specified degree of confidence.

The hydrodynamic model was calibrated with observed surface elevations using VIMS survey data collected during the summer and autumn seasons of 2009. The water quality model was calibrated using the VIMS survey data collected in the summer of 2009, during which period both the freshwater discharge and the non-point source loading data were provided by the HSPF watershed model developed for the Lynnhaven by URS Corporation of Virginia Beach.

IV-1 Calibration of the Hydrodynamic Model

The calibration for the hydrodynamic model used for the Thalia Creek and Thurston Branch system consisted of comparison of model predictions and high-frequency observed water surface elevation, salinity and temperature data for a total of 15 time series each, with each deployment time series ranging from 10-16 days.

IV-1-1 Boundary conditions

For the application of the HEM-3D hydrodynamic model to the TB-TC system, it was necessary to specify the downstream boundary condition where Thurston Branch enters into the portion of the Western Branch downstream. The downstream boundary conditions consisted of specifications of time series of surface elevation and salinity along the exterior row of grid cells at the northern extent of the model grid, as shown in Figure IV.1. These data were derived from the water depth measurement as well as salinity measurements at the most downstream ConMon water quality stations (Stations 0.1 and 1), shown earlier in Figure II.2.

IV-1-2 Freshwater discharge

There are no USGS gauges recording freshwater inflow to any of the Lynnhaven branches. For this reason, as was the case for the primary VIMS hydrodynamic model developed for the entire Lynnhaven, the VIMS hydrodynamic model for the Thurston Branch – Thalia Creek system was dependent upon the URS watershed model for its freshwater discharge inputs. As discussed in Section III-3, the URS model included hourly freshwater discharge values derived from a total of 44 catchment areas surrounding Thalia Creek.
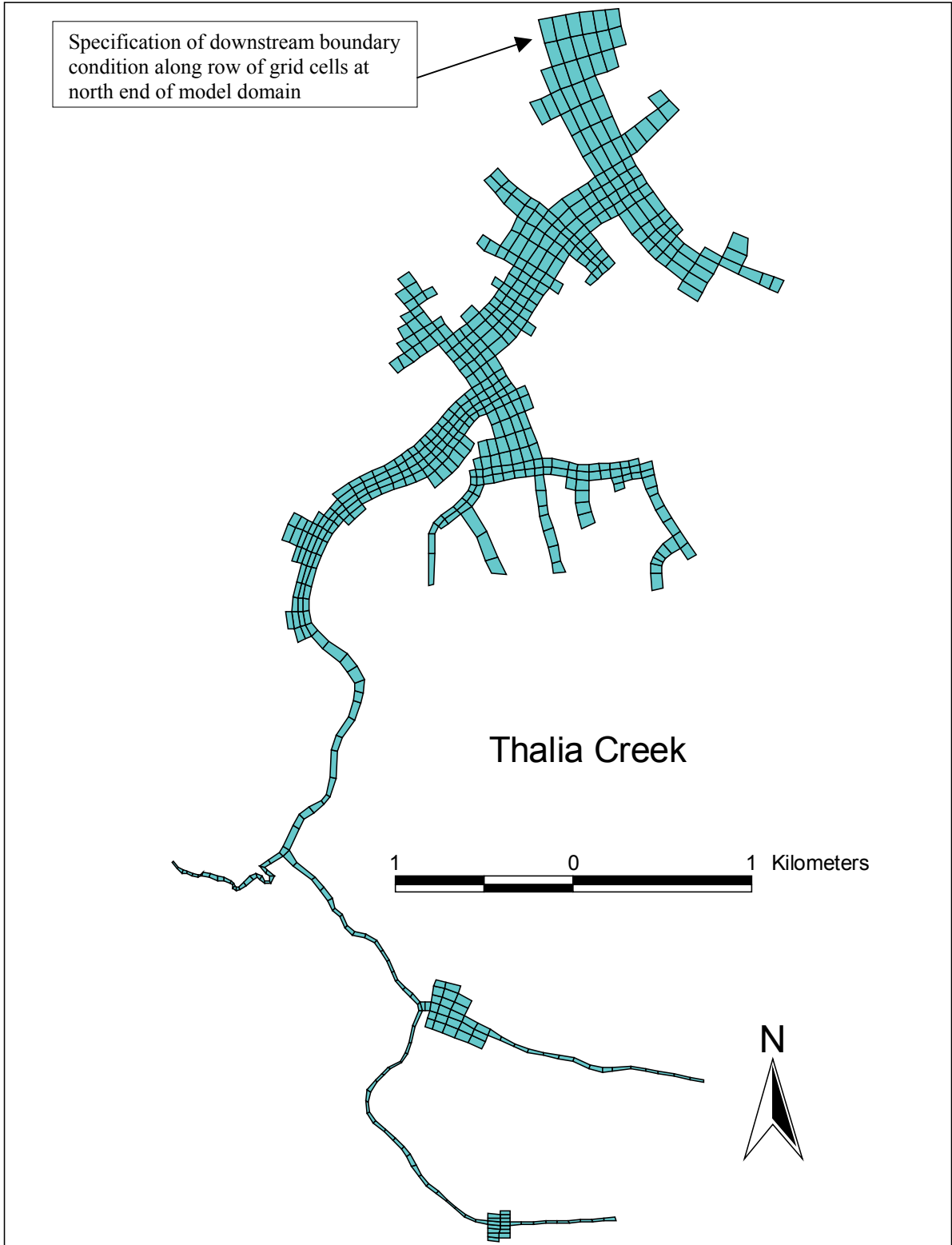
Specification of downstream boundary condition along row of grid cells at north end of model domain

Thalia Creek

1   0   1 Kilometers

N

Figure IV.1. Locations of boundary condition specifications for the Thalia Creek model.

IV-1-3 Calibration for surface elevation

For the calibration for water surface elevation in TB-TC, VIMS compared model predictions to observed high-frequency surface elevations for the first 3 deployments at 5 locations ranging from 10 to 16 days in duration. These deployments are listed in Table IV.1.

Table IV.1. Locations and dates of comparison for predicted vs. observed surface elevation in Thurston Branch and Thalia Creek.

Deployment	Locale	Survey Dates	Location Map	Results
1	ConMon Sta. 1	06/30-07/13/09	Figure II.1	Figure IV.2
1	ConMon Sta. 2	06/30-07/13/09	Figure II.1	Figure IV.2
1	ConMon Sta. 3	06/30-07/13/09	Figure II.1	Figure IV.2
1	ConMon Sta. 4	06/30-07/13/09	Figure II.1	Figure IV.2
1	ConMon Sta. 5	06/30-07/13/09	Figure II.1	Figure IV.2
2	ConMon Sta. 1	07/27-08/05/09	Figure II.1	Figure IV.3
2	ConMon Sta. 2	07/27-08/05/09	Figure II.1	Figure IV.3
2	ConMon Sta. 3	07/27-08/05/09	Figure II.1	Figure IV.3
2	ConMon Sta. 4	07/27-08/05/09	Figure II.1	Figure IV.3
2	ConMon Sta. 5	07/27-08/05/09	Figure II.1	Figure IV.3
3	ConMon Sta. 1	08/27-09/06/09	Figure II.1	Figure IV.4
3	ConMon Sta. 2	08/27-09/06/09	Figure II.1	Figure IV.4
3	ConMon Sta. 3	08/27-09/06/09	Figure II.1	Figure IV.4
3	ConMon Sta. 4	08/27-09/06/09	Figure II.1	Figure IV.4
3	ConMon Sta. 5	08/27-09/06/09	Figure II.1	Figure IV.4
4	Putnam Dr.	10/13-11/18/09	Figure II.5	Figure IV.11
4	Regal Court	10/13-11/18/09	Figure II.5	Figure IV.12

Real-time comparisons of predicted vs. observed surface elevations for Thurston Branch and Thalia Creek are shown in Figure IV.2 (June 30 to July 13, 2009), Figure IV.3 (July 27 to August 5, 2009), and Figure IV.4 (August 27 to September 6, 2009). It should be noted that some measurements only show water level variations during flood tide. The surface elevation becomes smooth or very small during low tide, which is mainly caused by the instrument deployment when water depths become shallow during low tide. The model captures the tidal variations during flood tide well at Stations 1-4 and the model simulations match the observations well at Station 5 where water elevations are properly measured. Overall, the model captured the semi-diurnal peaks and troughs and the phases of the observations quite well.
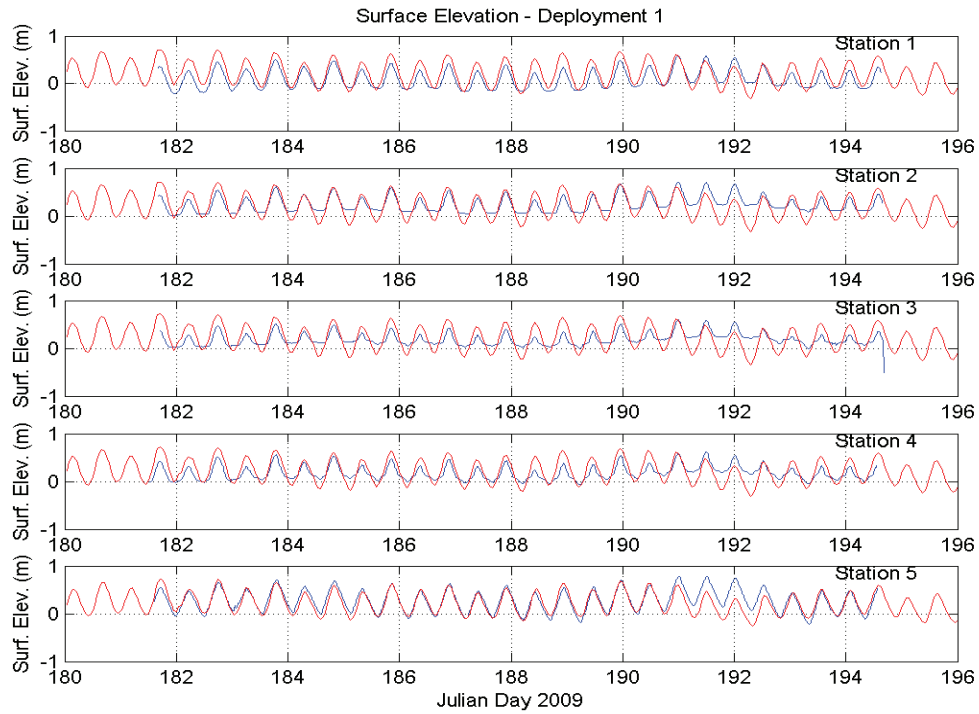
Figure IV.2. Predicted (red) vs. observed (blue) surface elevation – Thalia Creek Deployment 1, June 30 to July 6, 2009.
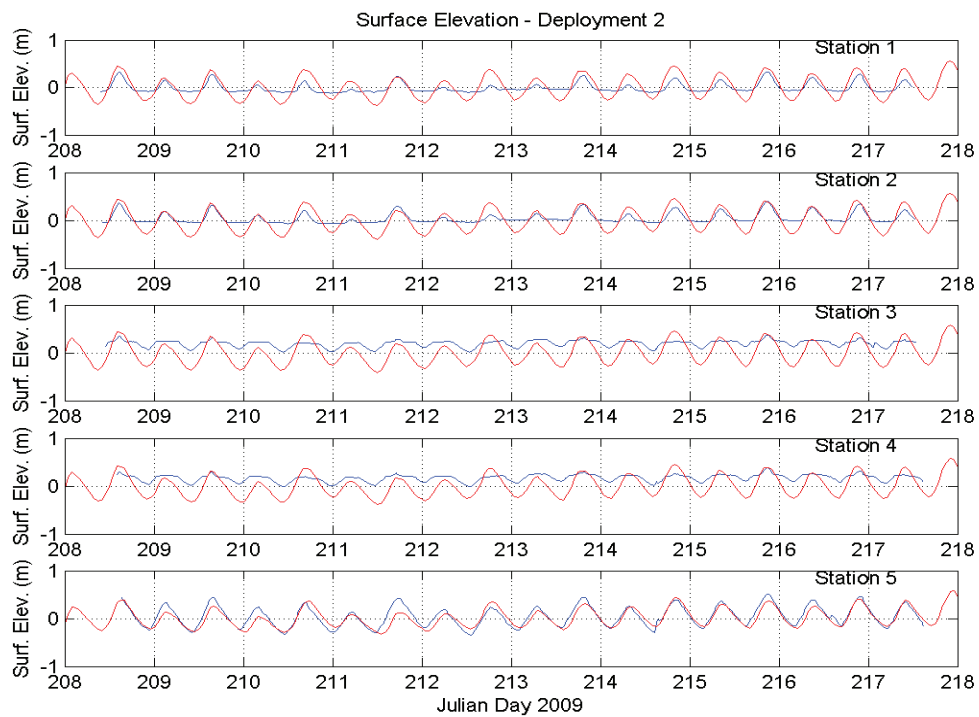

Figure IV.3. Predicted (red) vs. observed (blue) surface elevation in Thalia Creek Deployment 2, July 27 to August 5, 2009.
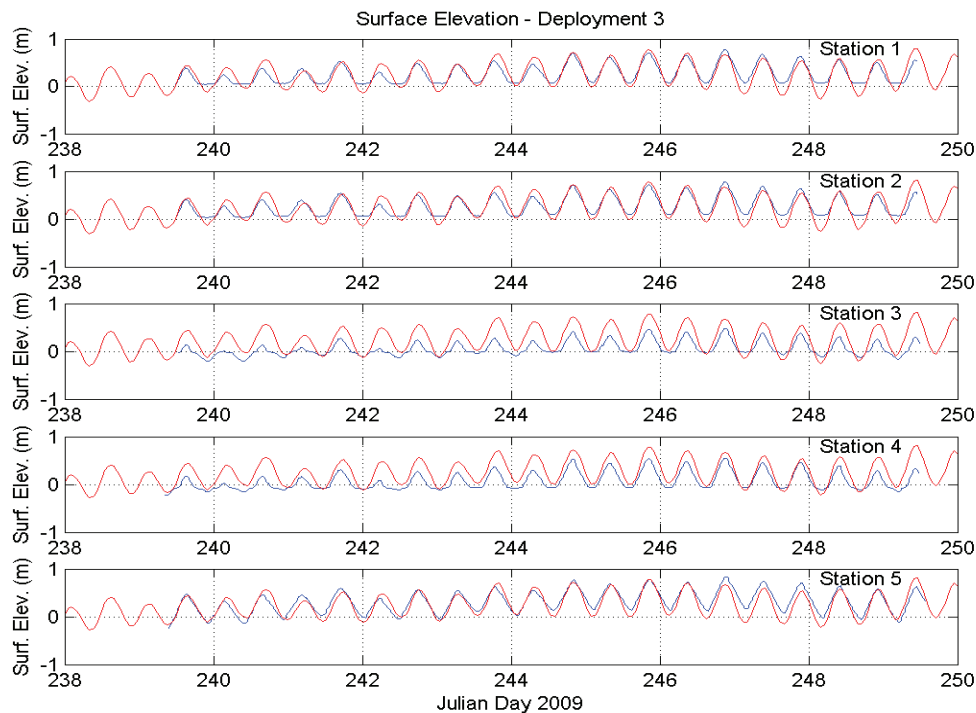
125

Figure IV.4. Predicted (red) vs. observed (blue) surface elevation - Thalia Creek Deployment 3, August 27 to September 6, 2009.

IV-1-4 Calibration for salinity

Real-time comparisons of predicted vs. observed salinity for TB-TC are shown in Figures IV.5 through IV.7 for all ConMon water quality stations for Deployments 1, 2, and 3, respectively. Because the system is shallow, it is very susceptible to the freshwater pulse. Any deviation of the freshwater discharge can affect the salinity. Therefore, the model may miss some events when the modeled freshwater discharge deviates from the actual freshwater discharge, particularly in the upstream. It can be seen that the model captures the general trend of salinity fluctuations and matches all stations to within approximately 2 ppt throughout the deployments.

IV-1-5 Calibration for temperature

Real-time comparisons of predicted vs. observed water temperature for TB-TC are shown in Figures IV.8 through IV.10 for all ConMon water quality stations for Deployments 1, 2, and 3, respectively. As there are no hourly solar radiation data available in Thalia Creek, hourly measurements from Gloucester Point were used. Because the system is shallow and the temperature is also affected by the inflow temperature that is estimated based on air temperature, some deviations of the model results from observations can be expected. Overall, the model results are suitable for the water quality simulations.
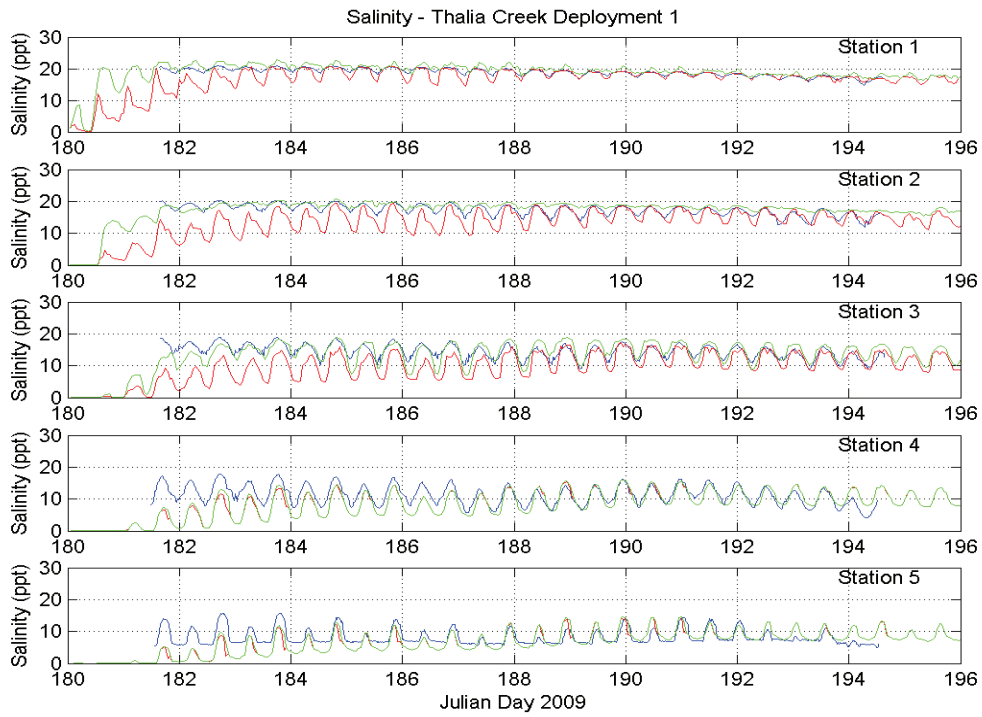
Figure IV.5. Predicted (red for surface, green for bottom) vs. observed (blue) salinity, Thalia Creek Deployment 1, June 30 to July 13, 2009.
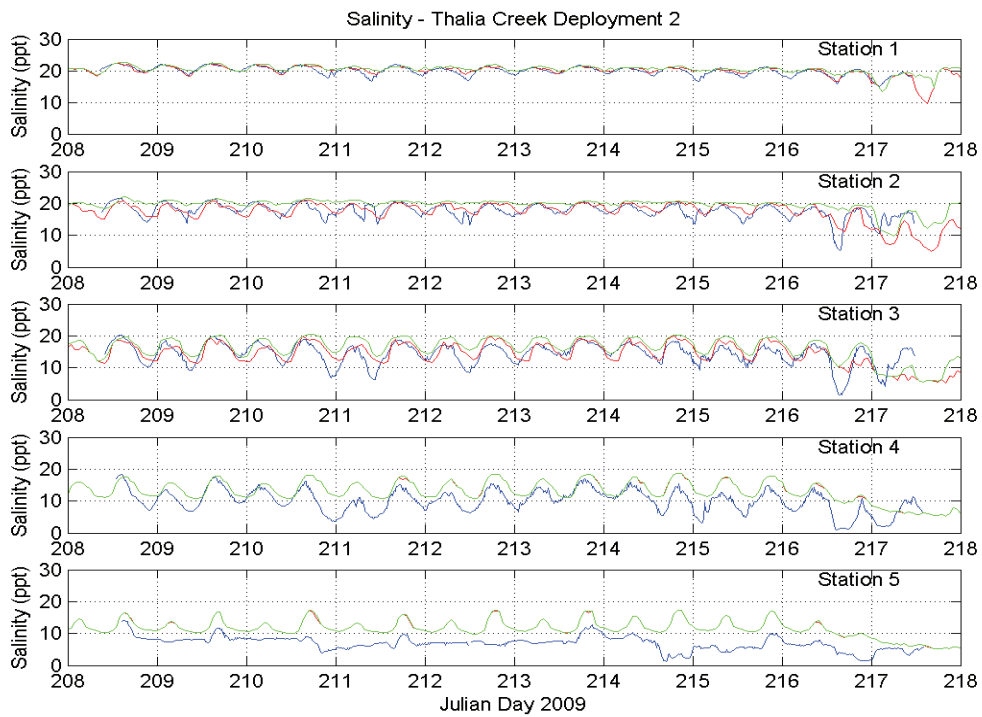

Figure IV.6. Predicted (red for surface, green for bottom) vs. observed (blue) salinity, Thalia Creek Deployment 2, July 27 to August 5, 2009.
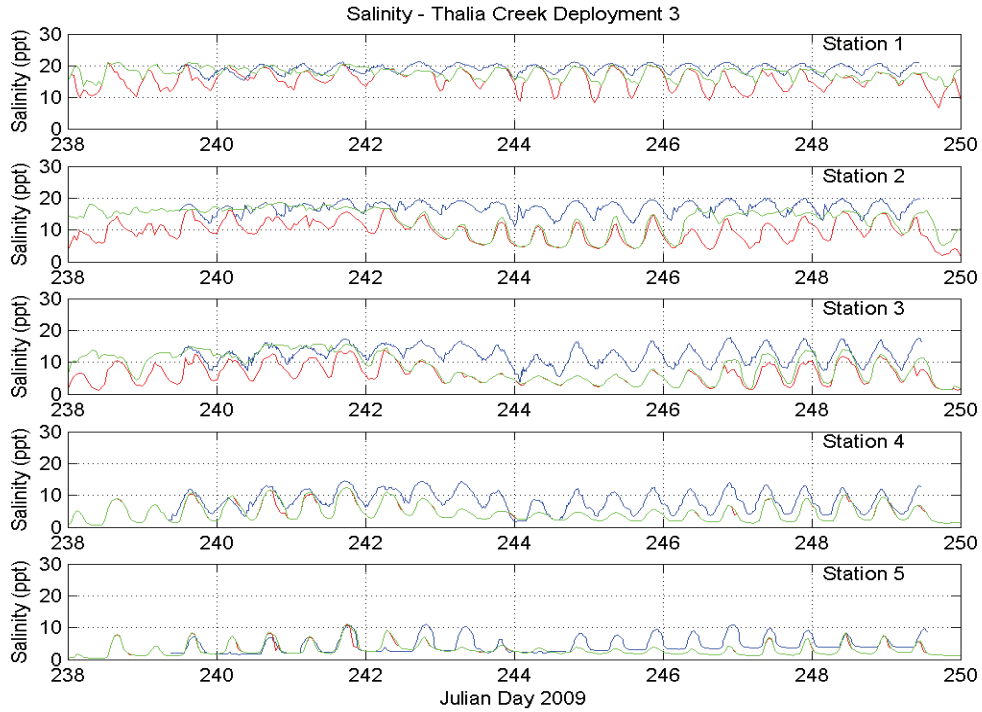
Figure IV.7 Predicted (red for surface, green for bottom) vs. observed (blue) salinity - Thalia Creek Deployment 3, August 27 to September 6, 2009.
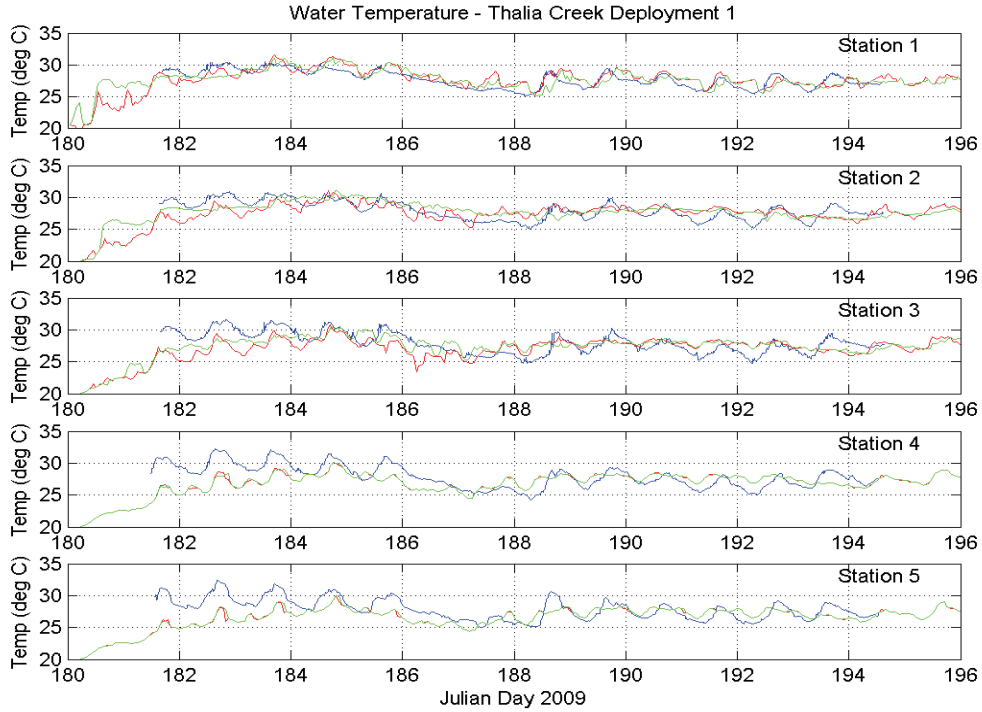

Figure IV.8. Predicted (red for surface, green for bottom) vs. observed (blue) water temperature - Thalia Creek Deployment 1, June 30 to July 13, 2009.
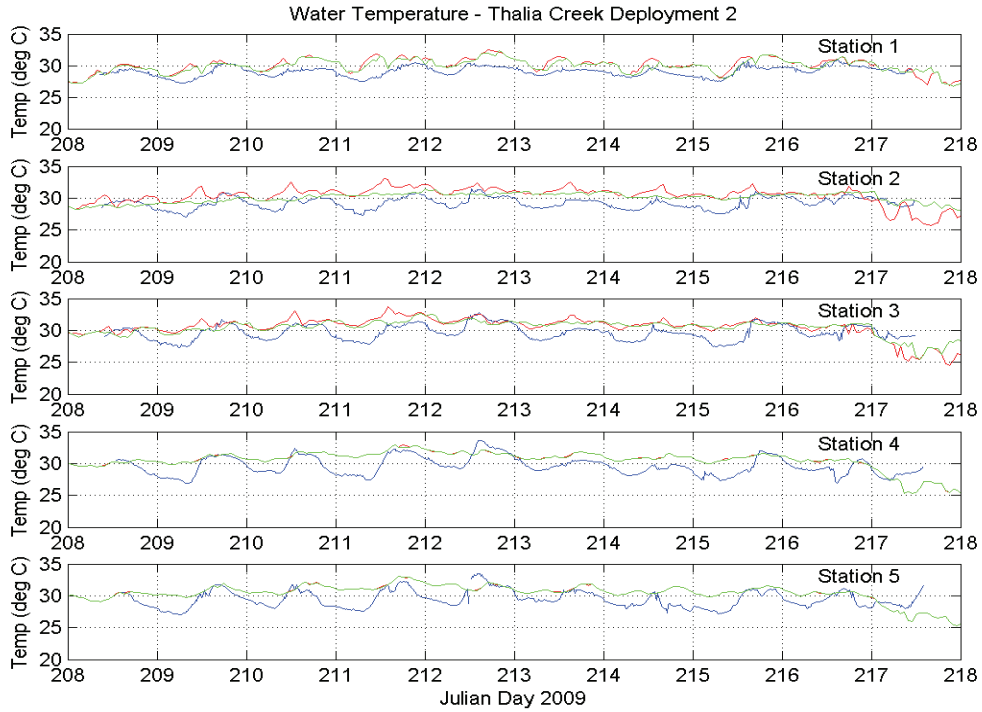
Figure IV.9. Predicted (red for surface, green for bottom) vs. observed (blue) water temperature -Thalia Creek Deployment 2, July 27 to August 5, 2009.
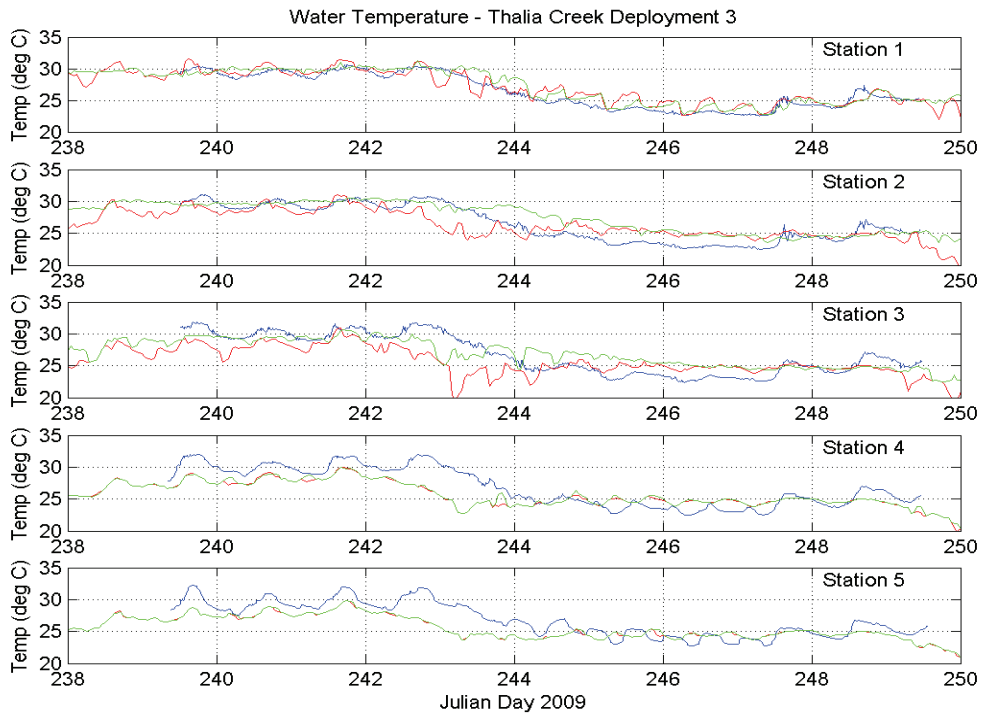

Figure IV.10. Predicted (red for surface, green for bottom) vs. observed (blue) water temperature - Thalia Creek Deployment 3, August 27 to September 6, 2009.

IV-1-6 Validation for surface elevation

Validation of the model's ability to predict water surface elevation was performed by comparing model results against the 30-day high-frequency observations at 2 locations in Thalia Creek and Thurston Branch. This deployment of tidal gauges at two locations occurred over the period from October 14 through November 18, 2009, as shown earlier in Table IV.1, and comparisons to model predictions are shown below in Figures IV.11 and IV.12. For the model simulation, a large domain model of the full Chesapeake Bay (Shen and Gong, 2009) was used to simulate tidal elevation in the Bay during this period and its output was used for the boundary condition of the present TB-TC model.
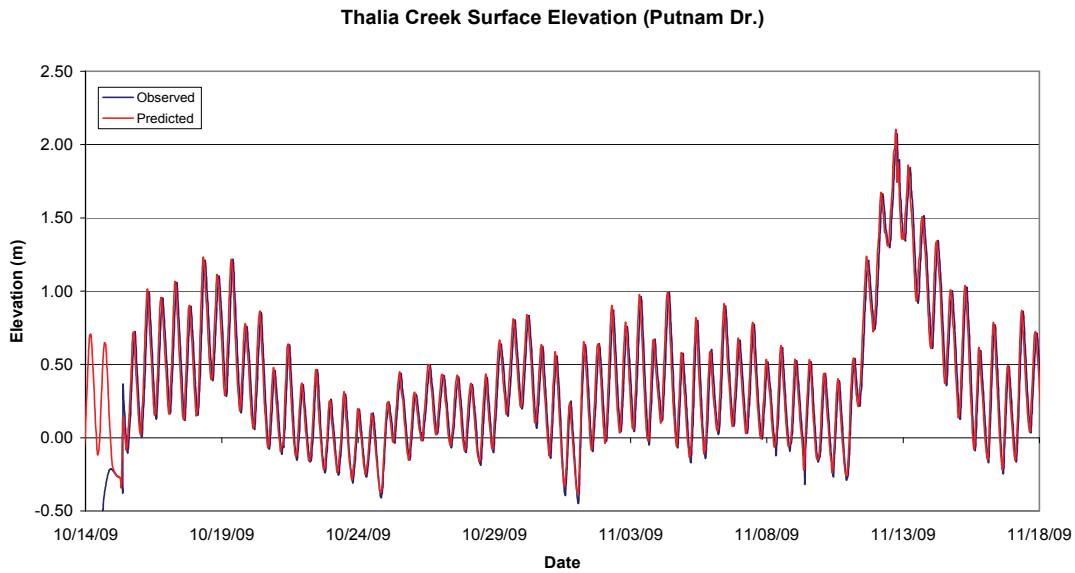

Figure IV.11. Predicted vs. observed surface elevation in Thalia Creek, October 14 – November 18, 2009.
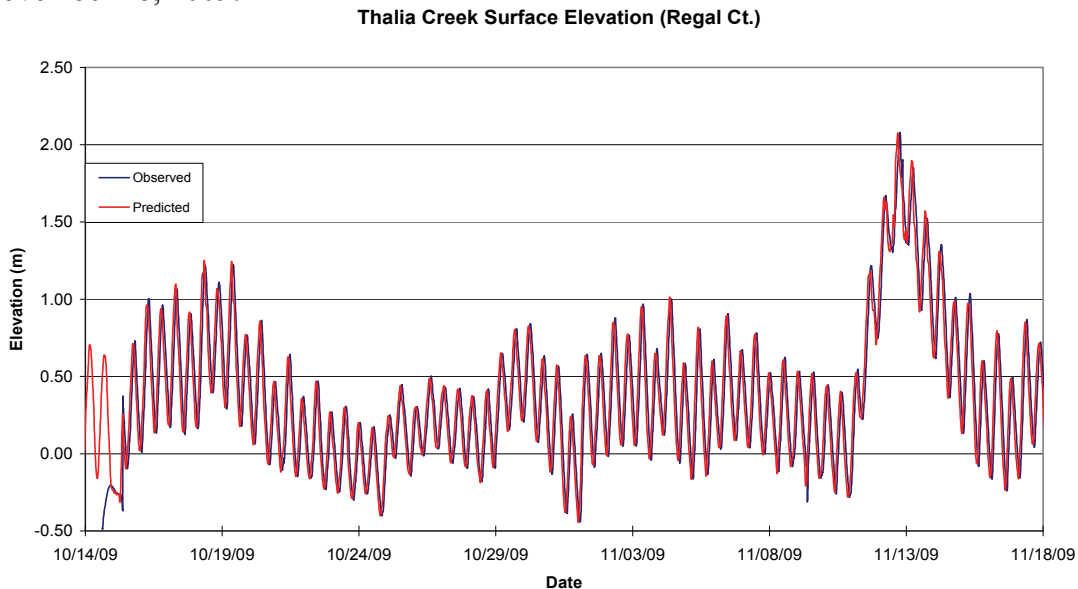

Figure IV.12. Predicted vs. observed surface elevation near mouth of Buchanan Creek, October 14 – November 18, 2009.

130

IV-2 Calibration of the Water Quality Model

The overall objective of the model calibration is to compare the water quality model results to the observed data utilizing a set of model coefficients and parameters that are consistent with field measurements and are within the general ranges of values accepted by the modeling community as reported in the literature.

The main steps involved in the calibration of the water quality model are: 1) the appropriate boundary condition has to be chosen, 2) the verified external nutrient loads have to be included, 3) the correct initial condition has to be specified, and 4) the suitable parameter values have to be estimated.

IV-2-1 Boundary condition

The boundary conditions for the TB–TC were taken from both observed and predicted values of the VIMS Lynnhaven River model for the area along the north boundary of the model domain shown in Figure IV.1.

IV-2-2 External loading

There is no point source input into the TB–TC system. The non-point nutrient loadings from the watershed discharged to TB-TC were obtained from the watershed model developed by URS Corporation of Virginia Beach (see Chapter III, Section III-3). Nonpoint source loads enter the water quality model through specification of the loading at model grid cells adjacent to the land. The procedure involves mapping of the model grid with watershed catchment areas adjacent to the receiving waters. These nonpoint source inputs are specified at the surface of the model cell at the location of discharge.

The external nutrient loads also include the atmospheric loads that are included in the total watershed model outputs. The time increment for loading input from the watershed model is daily.

IV-2-3 Initial condition

For the water quality modeling of the Thurston Branch – Thalia Creek system, the initial conditions were obtained by running the model with URS freshwater and nutrient loadings for a sufficient duration to populate the interior model cells with reasonable concentrations. This method of "spinning up" the model typically required only a few months of simulation to reach dynamic equilibrium. Upon attaining dynamic equilibrium, the values of all computed model cell output from prior model results were used to specify a suitable initial condition.

131

IV-2-4 Estimation of parameters

Most of the values of the parameters in the HEM-3D water quality model were adopted from the default parameters for the Chesapeake Bay and Lynnhaven models (Cerco and Cole, 1994; Sisson et al., 2008; Li, 2006). The modification of parameters depended on the comparison with measured data or unique features of the TB-TC system.

IV-2-5 Model Calibration Results

Calibration of the water quality model of Thurston Branch – Thalia Creek is shown by the comparison of time series plots of chlorophyll-a and dissolved oxygen. These comparisons were made at the locations of high-frequency measurements shown earlier in Figure II.1. Figures IV.13 through IV.15 show time series for the observed vs. predicted chlorophyll-a levels at all 5 high-frequency ConMon water quality measurement stations. For these figures, differences in the modeled and observed chlorophyll-a values remained within a few $\mu g \cdot L^{-1}$. Examination of Figures IV.13 through IV.15 reveals that the model catches the trend well throughout the deployments at the Thurston Branch and Thalia Creek stations.

Figures IV.16 through IV.18 show time series for the observed vs. predicted dissolved oxygen (DO) at all 5 high-frequency ConMon measurement stations. For these figures, differences in modeled and observed DO values generally remained within 1-2 $mg \cdot L^{-1}$. Examination of Figures IV.16 through IV.18 reveals that the model catches the overall trend well throughout the deployments at stations in Thurston Branch and Thalia Creek.

The rainfall event is a critical time for oxygen levels, dominated by two factors: 1) the photosynthesis process has been suppressed without sufficient sunlight, depleting oxygen in the water column, and 2) the heterotrophic respiration, sediment oxygen demand (SOD), and increased influx of organic matters continue to consume the water column oxygen. The decrease in oxygen due to the 2-cm rainfall on Julian Day 243 has a significant signature on the system. As can be seen in Figure IV.18, the observed DO shows a minimum in upper Thalia Creek (ConMon Station 5), while salinity (Figure IV.7) and temperature (Figure IV.10) decreased. For dissolved oxygen, the model results simulate this event reasonably well. The model predicts that chlorophyll should decrease (Figure IV.15) while the observed data showed values higher than 100 $\mu g \cdot L^{-1}$. Judging from these spiky data points, it is believed that the chlorophyll sensor may have mal-functioned from that date onward.

IV-2-6 Water Quality Model Validation Results

After calibrating the water quality model by comparing its predictions to the high-frequency observations conducted by VIMS in the summer of 2009, a validation of the model was performed by conducting a model simulation over the period 2003-2006 and comparing its predictions to the water quality observations made at DEQ station THA000.76 (coincident with VIMS ConMon Station 4). The comparison of several key water quality parameters over this 4-year period are shown for this location in Figure IV.19.
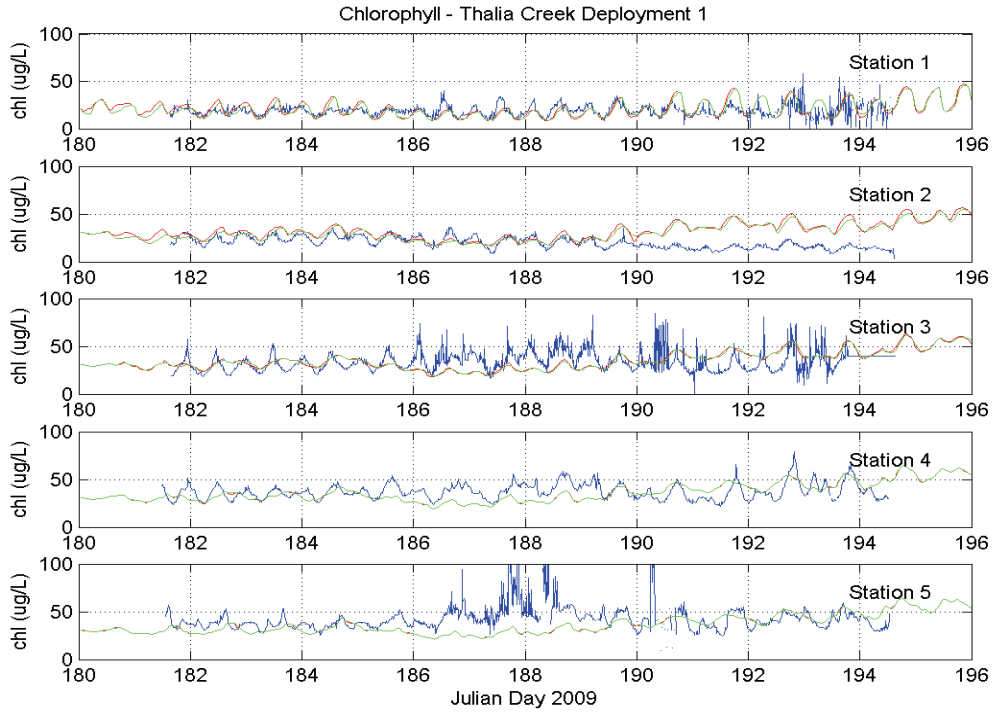
Figure IV.13. Predicted (red for surface, green for bottom) vs. observed (blue) chlorophyll-a - Thalia Creek Deployment 1, June 30 to July 13, 2009.
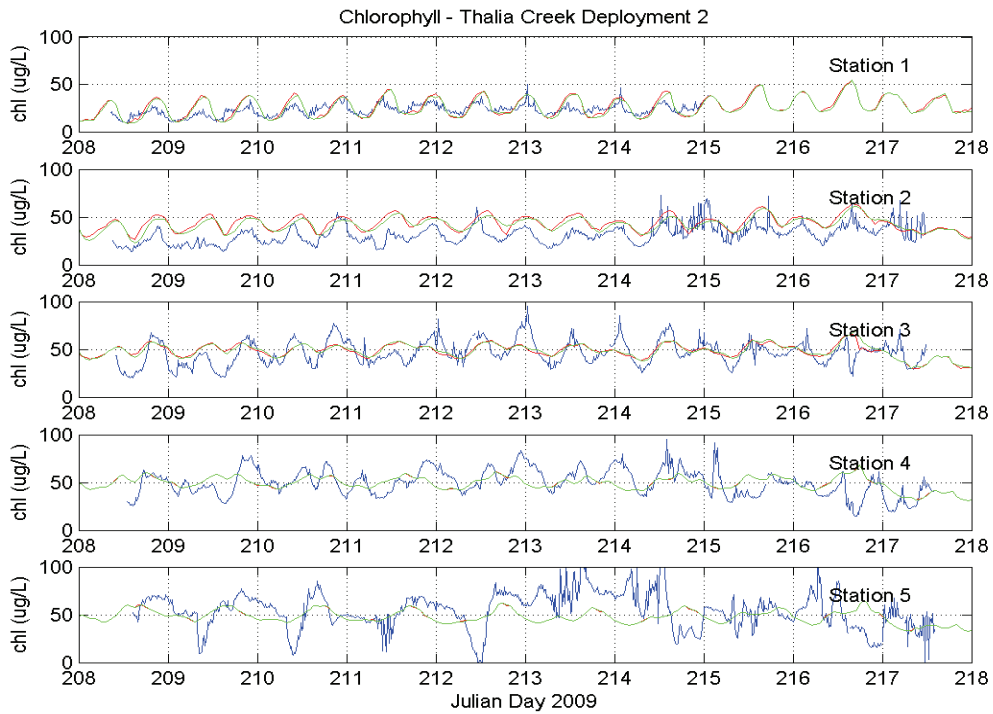

Figure IV.14. Predicted (red for surface, green for bottom) vs. observed (blue) chlorophyll-a - Thalia Creek Deployment 2, July 27 to August 5, 2009.
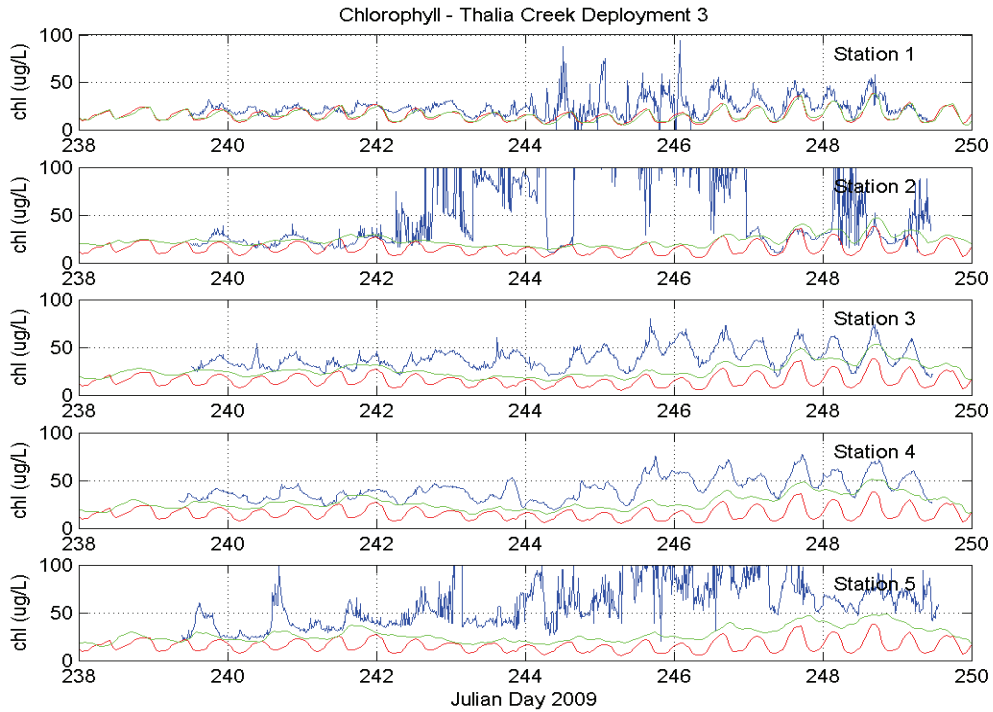
Figure IV.15. Predicted (red for surface, green for bottom) vs. observed (blue) chlorophyll-a - Thalia Creek Deployment 3, August 27 to September 6, 2009.
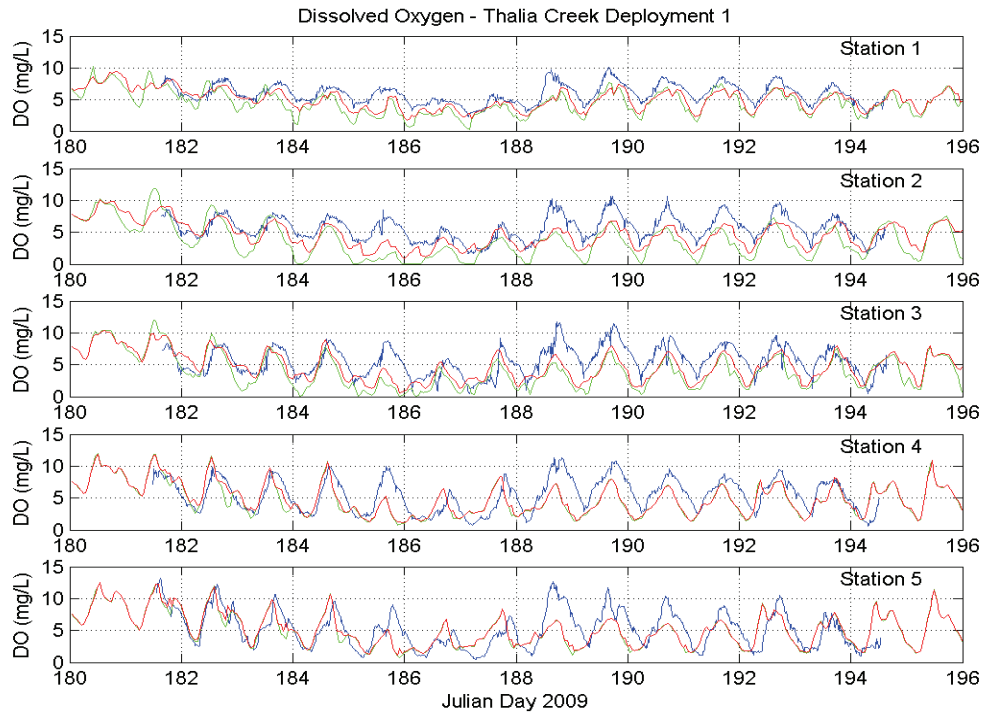

Figure IV.16. Predicted (red for surface, green for bottom) vs. observed (blue) dissolved oxygen - Thalia Creek Deployment 1, June 30 to July 13, 2009.
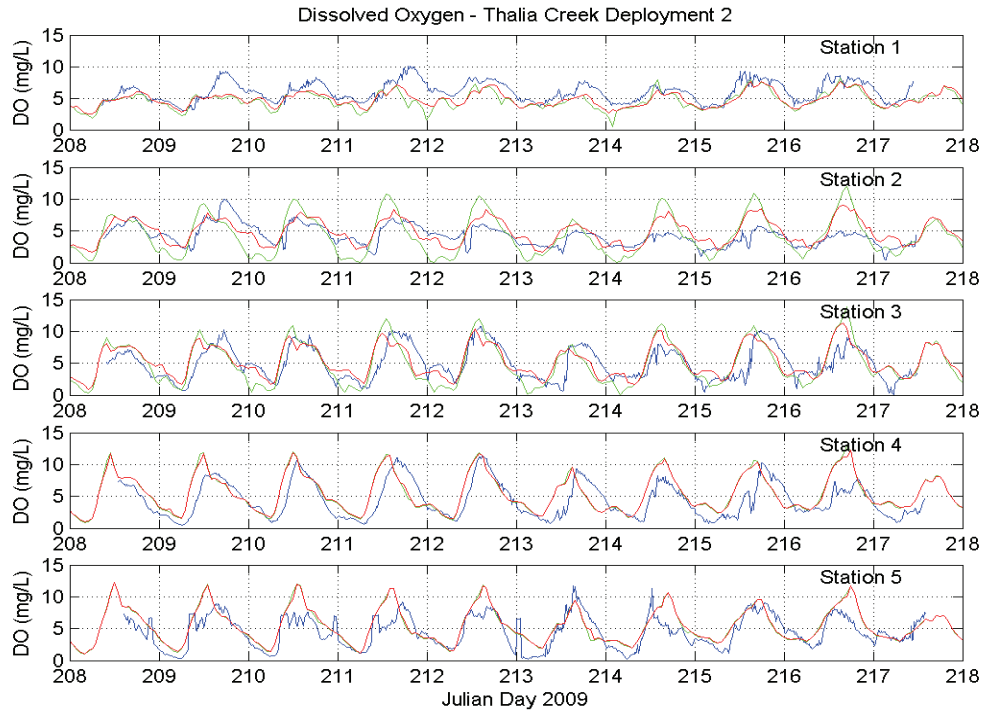
134

Figure IV.17. Predicted (red for surface, green for bottom) vs. observed (blue) dissolved oxygen - Thalia Creek Deployment 2, July 27 to August 5, 2009.
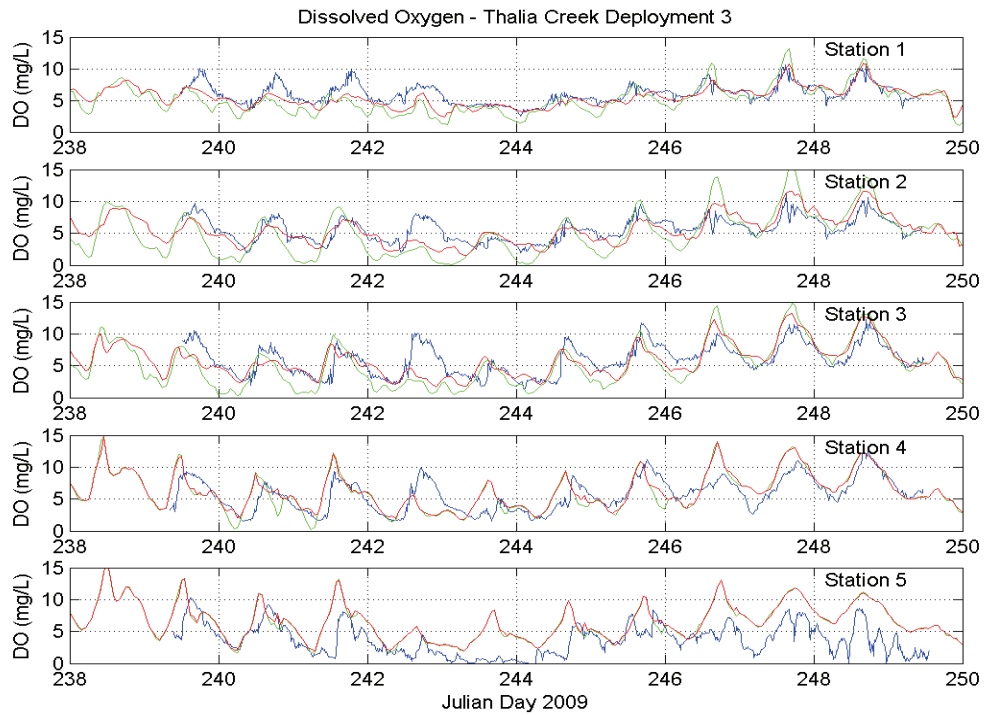

Figure IV.18. Predicted (red for surface, green for bottom) vs. observed (blue) dissolved oxygen - Thalia Creek Deployment 3, August 27 to September 6, 2009.
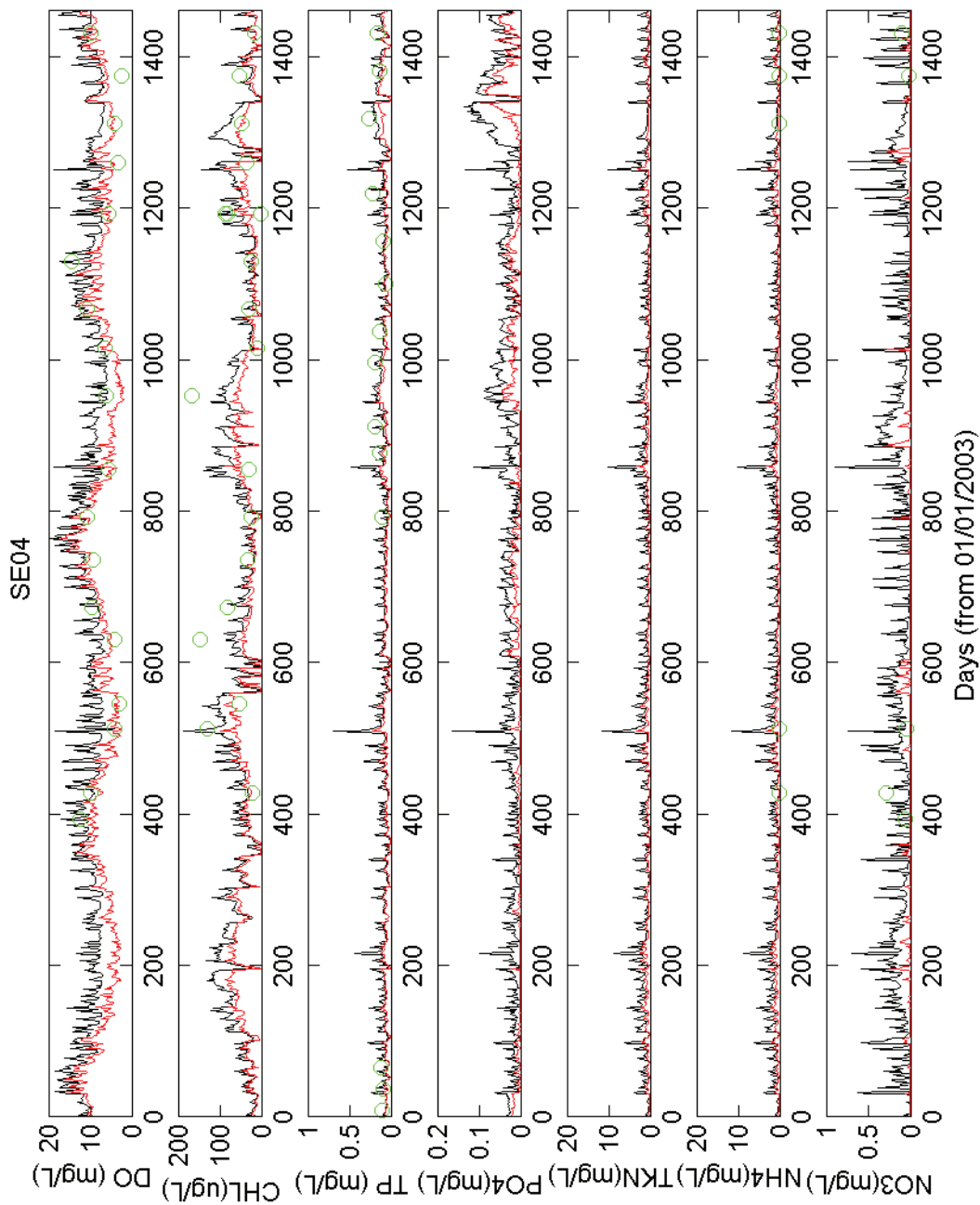
Figure IV.19. Predicted (black for maximum, red for minimum) *vs.* observed values of DO, chl-a, TP, PO_4, TKN, NH_4, and NO_3 measured at DEQ Station 7-THA000.76 from 2003–2006.

CHAPTER V. FECAL COLIFORM MODELING

The Thurston Branch – Thalia Creek system is on the 303D List (2004) as impaired for fecal coliform (City of Virginia Beach, List of Impaired Waters 2008). Suitable observation data for Thalia Creek included only one long-term monitoring station (VA-DEQ monitoring Station 7-THA000.76), which is coincident with VIMS ConMon Water Quality Station 4 of this project. For this project, the strategy was to compare model predictions to the long-term observations at 7-THA000.76 and then to compare spatially the model's predictions of fecal coliform against the fecal coliform observations made during VIMS grab sample surveys for this project in the summer of 2009.

V-1 Calibration of fecal coliform model

The overall objective of the model calibration is to compare the model simulated fecal coliform levels to the observed data utilizing a set of model coefficients and parameters that are consistent with field measurements and are within the general ranges of values accepted by the modeling community as reported in the literature.

The main steps involved in the calibration of the fecal coliform model are: the appropriate boundary condition has to be chosen, the external fecal coliform loads have to be included, the reasonable initial condition has to be specified, and the suitable parameter values have to be estimated.

V-1-1 Boundary condition

The boundary condition used for the numerical modeling of fecal coliform in Thalia Creek is a radiation boundary condition specified along the downstream boundary of the model domain. Average long-term values of fecal coliform as measured by VA-DSS and VA-DEQ at the northernmost exterior (i.e., concentrations on the order of 20 MPN·100 ml^{-1}) were then specified as boundary conditions. As the model open boundary extends downstream from Thalia Creek, the specification of the open boundary condition has less influence on the interior of the modeling domain.

V-1-2 External loading

There is no specific point source input into the TB-TC system. The non-point fecal coliform loadings from the watershed were obtained from the watershed model developed by URS Corporation of Virginia Beach. Nonpoint source loads enter the fecal coliform model through specification of total fecal coliform loading calculated through freshwater discharge and the concentration of fecal coliform at model grid cells adjacent to the land. The procedure involves mapping of the model grid with 44 watershed catchment areas adjacent to the receiving waters. These nonpoint source inputs are specified at the surface of the model cells at the locations of discharge. The time increment for loading input from the watershed model is daily.

V-1-3 Initial condition

As simulations for fecal coliform are long-term (i.e., multi-year) and, as the model domain responds reasonably rapidly to external loading inputs, it was sufficient to specify initial concentration of 0 MPN·100 ml^{-1} throughout the computational domain. Upon attaining dynamic equilibrium, the values of all computed model cell output from prior model results were used to specify a suitable initial condition. In our simulation, a value of 20 MPN·100 ml^{-1} was used.

V-1-4 Estimation of parameters

The major parameters used for the fecal coliform model are the decay rate and the mixing parameter. The survival of bacteria in natural waters depends on the particular type of water body and associated phenomena that influence the growth, death, and total loss of organisms. In general, the factors that influence the decay rate include: sunlight, temperature, salinity, predation, nutrient, settling, resuspension and after-growth. In the previous fecal coliform simulations in Lynnhaven River and the adjacent Back Bay, we have tested the various decay rates and found that 1.0 day^{-1} during the summer generates reasonable results. This value is consistent with estimated values from previous extensive surveys of fecal coliform in the Lynnhaven River. This same value is used in the Thalia Creek and Thurston Branch fecal coliform simulations. The major mixing parameter is the eddy diffusivity, which is calculated by a two-equation turbulence closure scheme using the Mellor-Yamada formulation.

V-1-5 Model Calibration Results

The calibration of the fecal coliform model in Thurston Branch – Thalia Creek included a full 3-year (i.e., 2003-2005) comparison of model predictions to observations made at Station 7-THA000.76, one of 16 primary Lynnhaven stations monitored every other month by the Virginia Department of Environmental Quality (VA-DEQ). It should be noted that Station 7-THA000.76 is the same location as ConMon Water Quality Station 4 referenced throughout this report. This comparison of predicted vs. observed values of fecal coliform is shown in Figure V.1. Data analysis shows that the fecal coliform distribution is similar during these years with fecal coliform values ranging from approximately 100 to 1600 MPN·100 ml^{-1}. The simulation of the period 2003-2005 is representative of the current condition.

Figure V.1 displays the customary log-scale for the fecal coliform values. It can be seen that the model predictions (shown in blue) vary over several orders of magnitude (from 1 to 10000 MPN·100 ml^{-1}) over short periods of time. Similarly, observed data values from this station (shown by the red circles) vary from 10 MPN·100 ml^{-1} to 1200 MPN·100 ml^{-1}, with the latter being the maximum observation detection limit using current measurement procedures. This is partly due to the fact that fecal coliform concentrations are often event-driven, with high concentrations following significant rainfall that delivers fecal pollutants from the watershed to the receiving waters. In the shallow Lynnhaven system, these events can occur with as little as 0.5 inches of rainfall. The 30-

day geometric mean (green line) is also plotted, as are the criteria values of 200 MPN·100 ml^{-1} (safe swimming standard) and 14 MPN·100 ml^{-1} (shellfish harvesting standard).

A comparison of the geometric mean with the 200 MPN·100 ml^{-1} criterion shows that the latte values is often exceeded, indicating that conditions for safe swimming in Thalia Creek often are not met. As the shellfish harvesting criterion is much more stringent, meeting this standard in Thalia Creek without load reductions appears to be not possible at this time.

V-1-6 Fecal Coliform Model Validation Results

To validate the Thalia Creek fecal coliform model, it was necessary to compare predictions to an entirely independent data set. These data were those collected during the July and August grab sample surveys of this project reported on in Chapter II (see Figures II.56 and II.57). The "snapshots" of model predictions throughout the domain are compared to the grab sample survey data for July 27, 2009 and August 27, 2009 in Figures V.2 and V.3, respectively. It is noted that, in these figures, the observed values are printed out adjacent to sampling locations (red squares) whereas the predicted values are shown throughout the model domain by the circles with a color-coding indicating their values, as shown by the figure legend.

Figure V.2 shows generally good overall agreement between predicted and observed values of fecal coliform. The highest observations of fecal coliform (generally between 900 and 1600 MPN·100 ml^{-1}) correspond closely with the darkest coloration of the legend. Figure V.3 shows high observed values throughout upper Thalia Creek (1600 MPN·100 ml^{-1} at nearly every station) and the corresponding predictions are in that range as well.

V-2 Fecal coliform load reduction sensitivity

Using the current fecal coliform calibration predictions in the Thurston Branch – Thalia Creek system as the base condition, a series of sensitivity runs were made using 70%, 90%, 95%, and 99% reduction scenarios over the 2003-2005 calibration period. The predictions of these scenarios, along with their associated 30-day geometric means, are shown in Figures V.4 through V.7, respectively, for the 70%, 90%, 95%, and 99% reductions.

On each of these figures, the associated 30-day geometric mean of model predictions is plotted and can be easily compared to the 200 MPN·100 ml^{-1} and 14 MPN·100 ml^{-1} criteria. Figure V.4 shows these geometric means exceeding the 200 MPN·100 ml^{-1} criterion for safe swimming for the 70% reduction scenario. Figures V.5 and V.6 (i.e., 90% and 95% reduction scenarios) show their maximum geometric means reaching approximately 100 MPN·100 ml^{-1} and 25 MPN·100 ml^{-1}, respectively. Lastly, Figure V.7 (99% reduction scenario) shows that the geometric mean of model predictions never exceeds even 10 MPN·100 ml^{-1}.

The TMDL study of the Lynnhaven River (HRPDC, 2006) concluded that a reduction of 81.5% was needed for the entire Lynnhaven watershed to bring the fecal coliform concentrations in the receiving waters into compliance with state regulations. This number represents a spatial average over the entire Lynnhaven. However, because Thalia Creek is located at the extreme upstream portion of the Western Branch and, subsequently, a large portion of the bacteria loadings pass through Thalia Creek, an even larger percentage reduction is necessary to meet the shellfish harvesting criteria in Thalia.

It is important to note that, unlike the criterion for safe swimming (a geometric mean of 200 MPN·100 ml^{-1}), there are, in fact, two criteria for shellfish harvesting for Virginia State water quality standards. As mentioned earlier, the 30-day geometric mean must not exceed 14 MPN·100 ml^{-1}. But an additional criterion for shellfish harvesting is that the 90th percentile of the data must not exceed 43 MPN·100 ml^{-1}. This second criterion is usually the most stringent. For that reason, this criterion of 43 MPN·100 ml^{-1} and the 90th percentile values for the model predictions are both shown in Figure V.7. It can be seen that the 90th percentile values fall below this criterion.
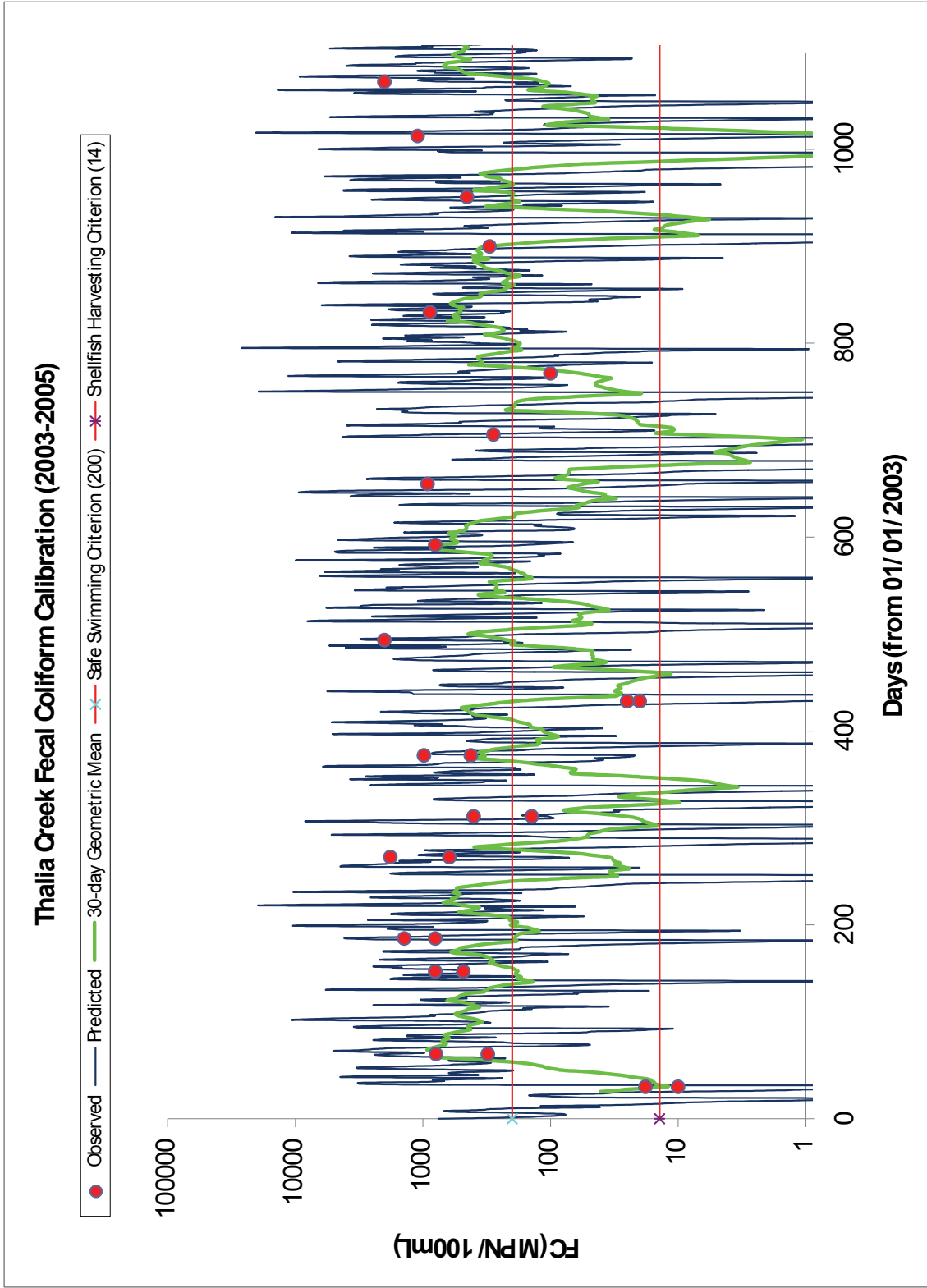
Figure V.1. Observed *vs.* predicted fecal coliform at DEQ Station 7-THA000.76 for 2003-2005 simulation.
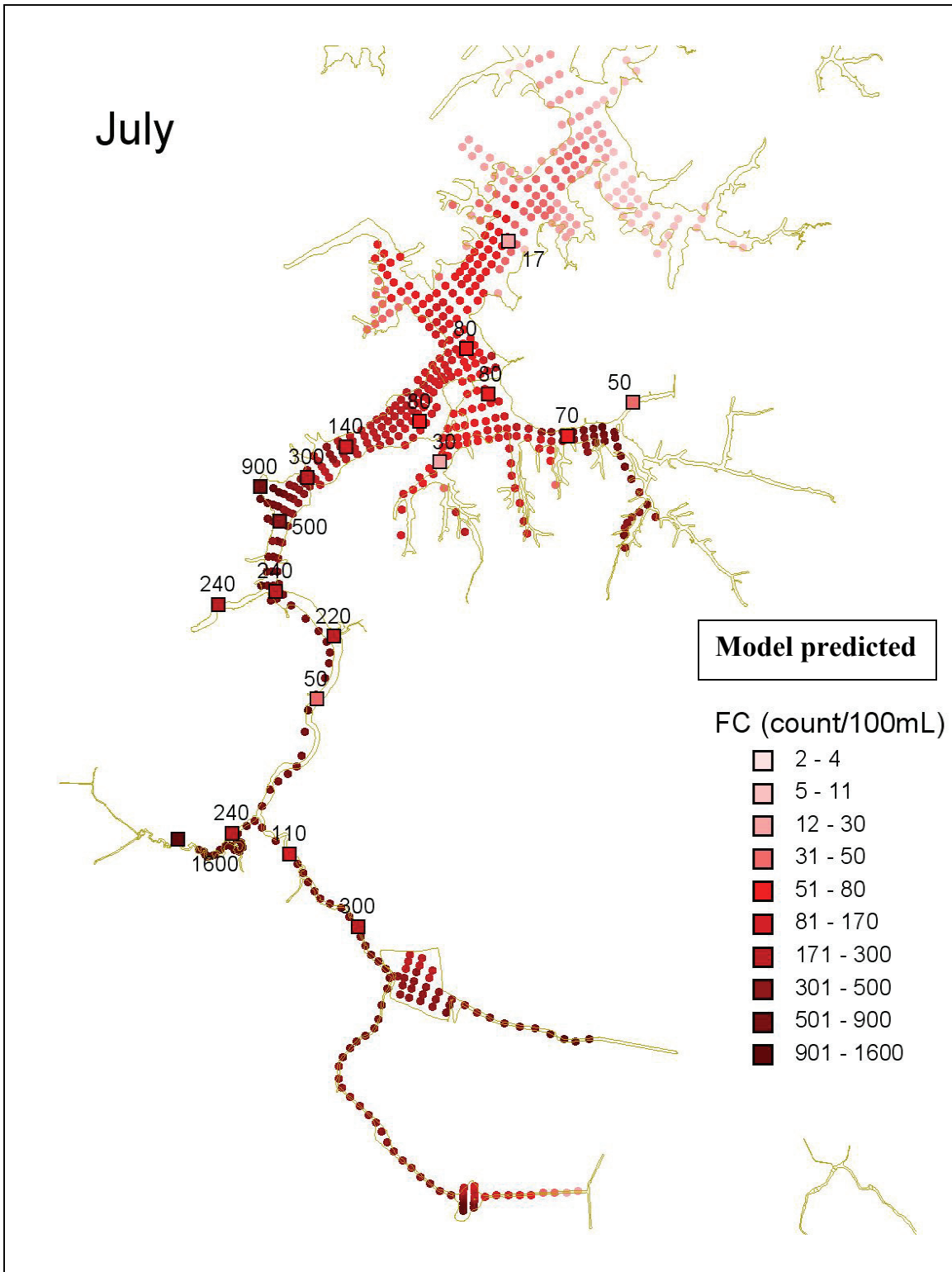
141

Figure V.2. Observed vs. predicted fecal coliform concentrations throughout Thurston Branch - Thalia Creek on July 27, 2009 [Note: observed values printed, predicted values color-coded to legend].
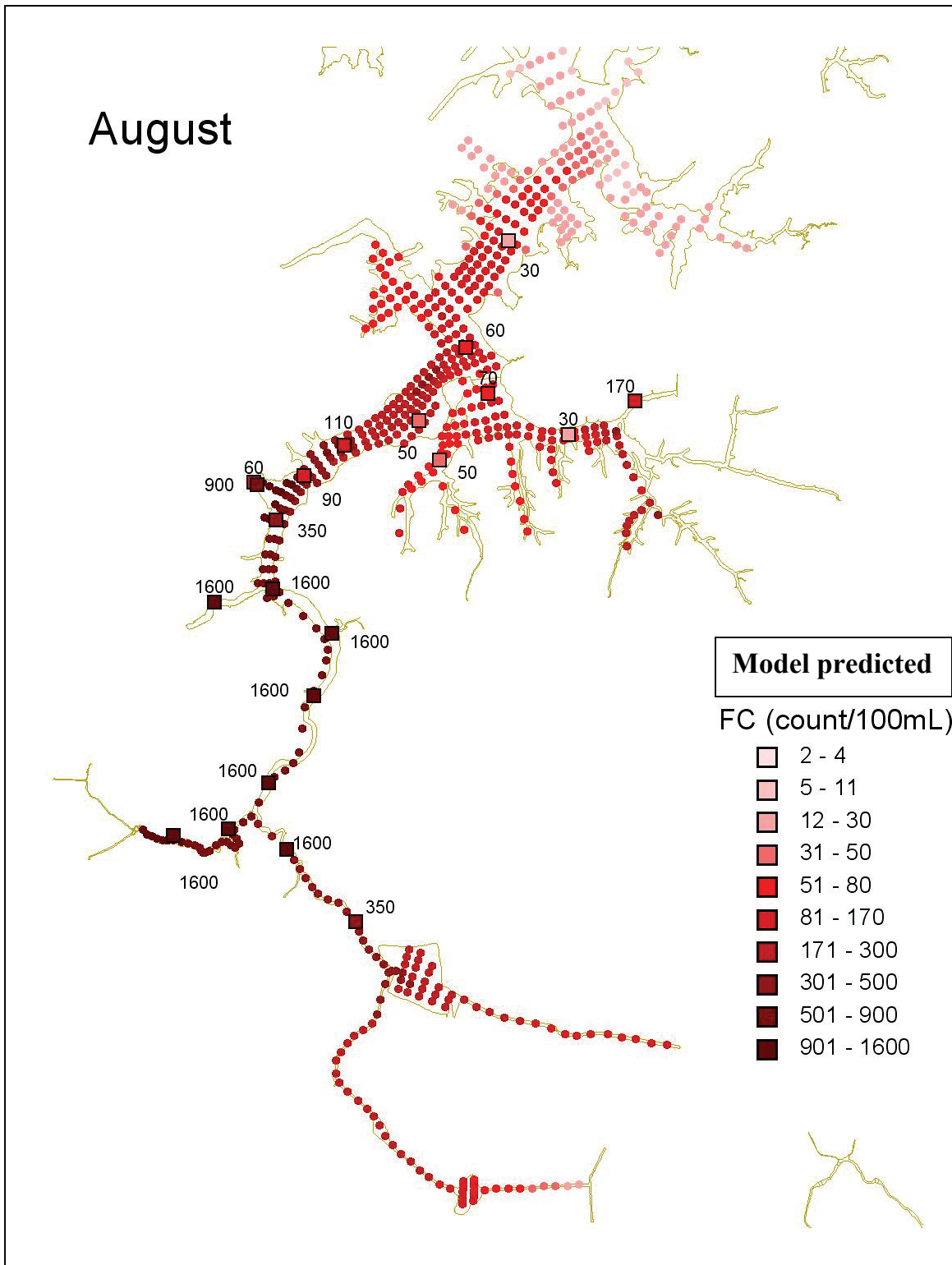
Figure V.3. Observed vs. predicted fecal coliform concentrations throughout Thurston Branch - Thalia Creek on August 30, 2009. [Note: observed values printed, predicted values color-coded to legend].
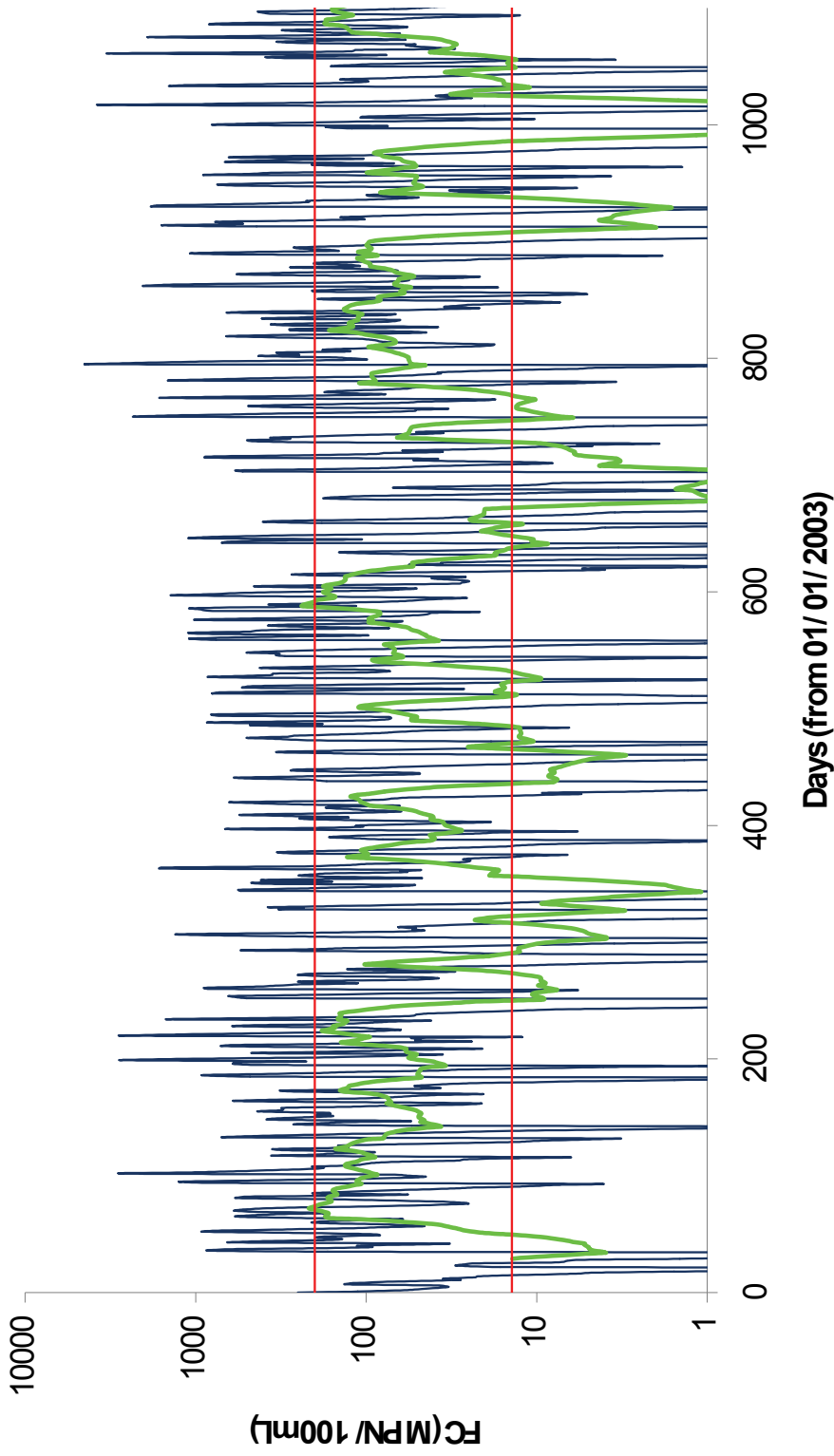
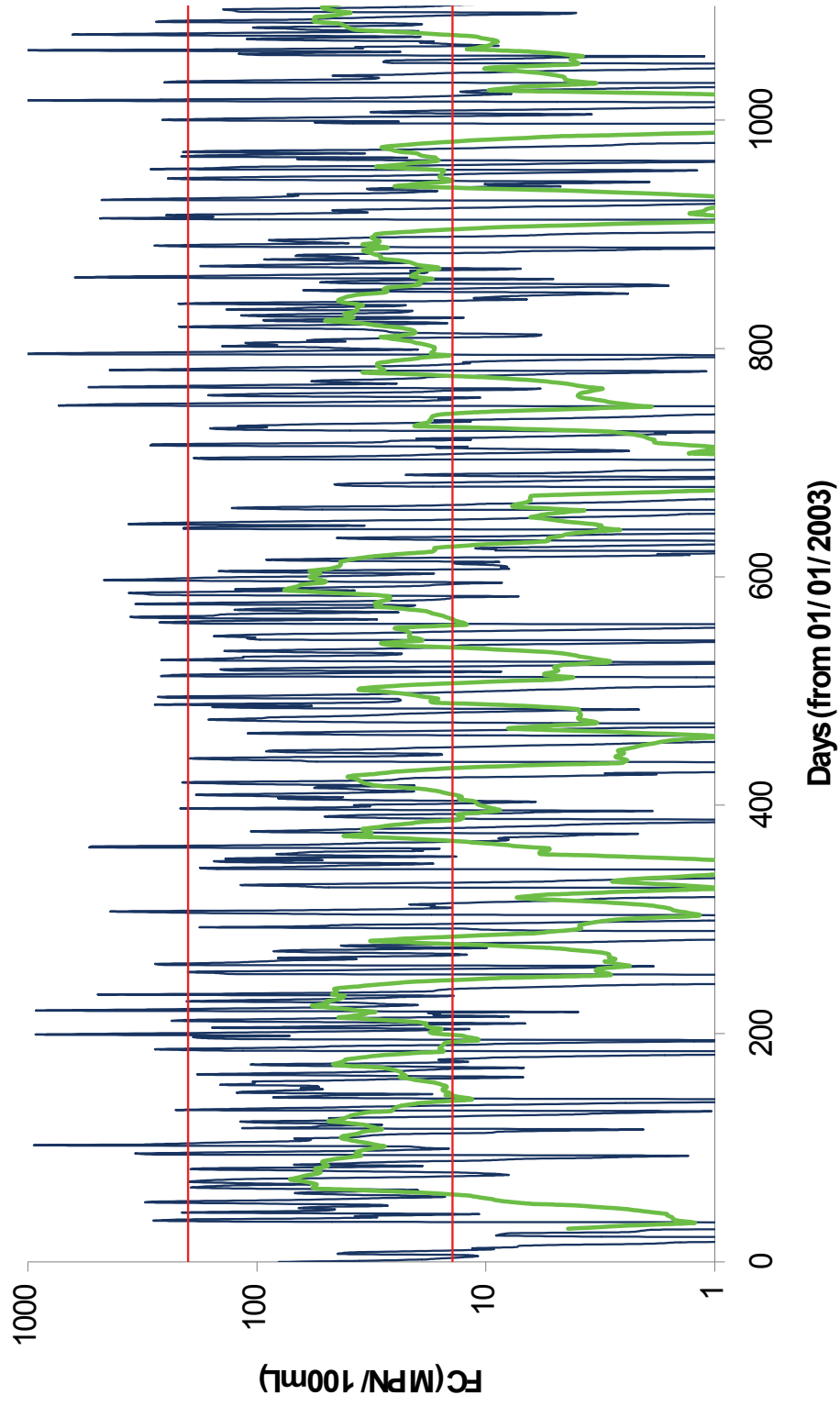Figure V.4. Fecal coliform predictions using a 70% load reduction for the 2003-2005 simulation.

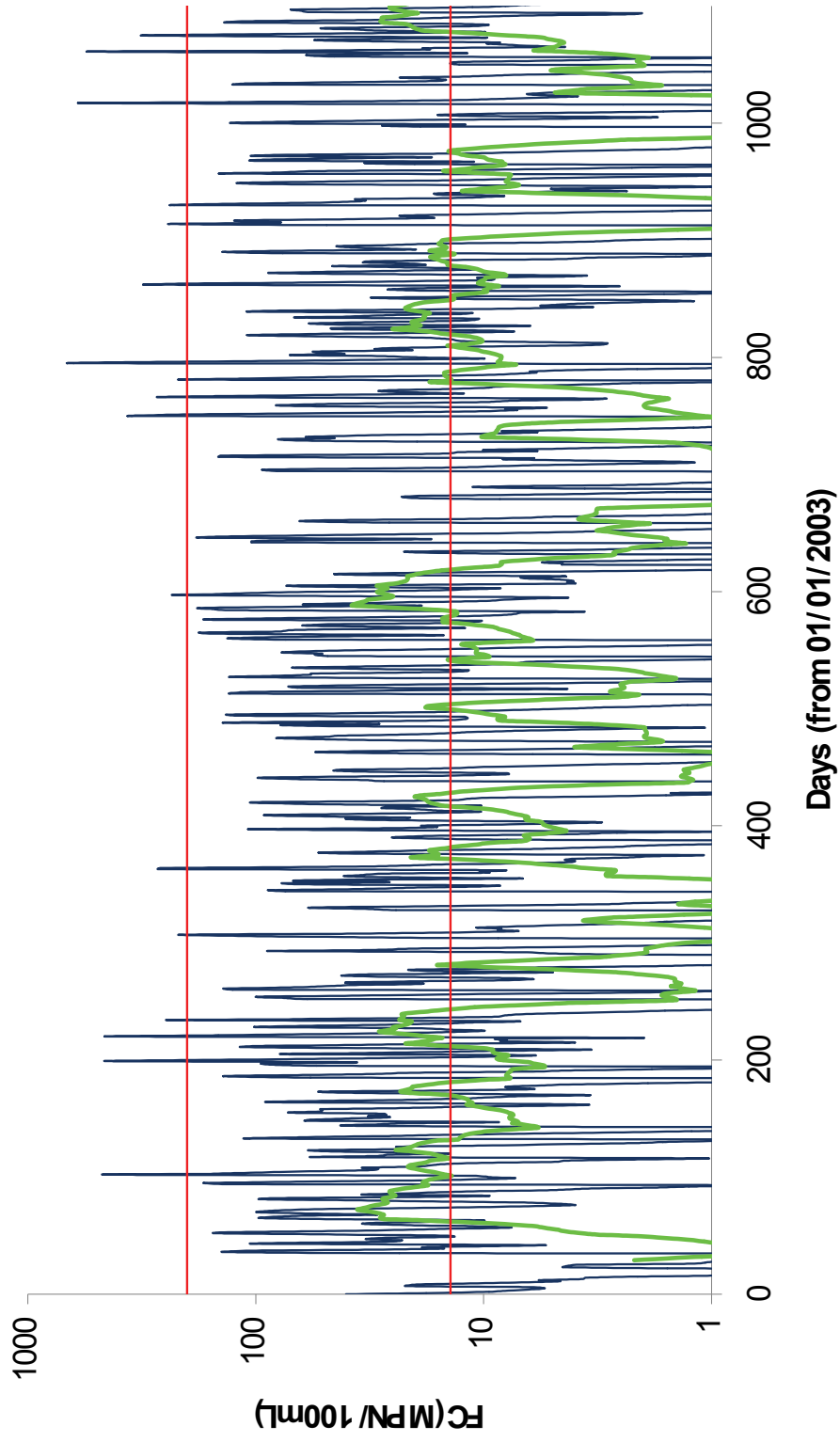Figure V.5. Fecal coliform predictions using a 90% load reduction for the 2003-2005 simulation.

Figure V.6. Fecal coliform predictions using a 95% load reduction for the 2003-2005 simulation.
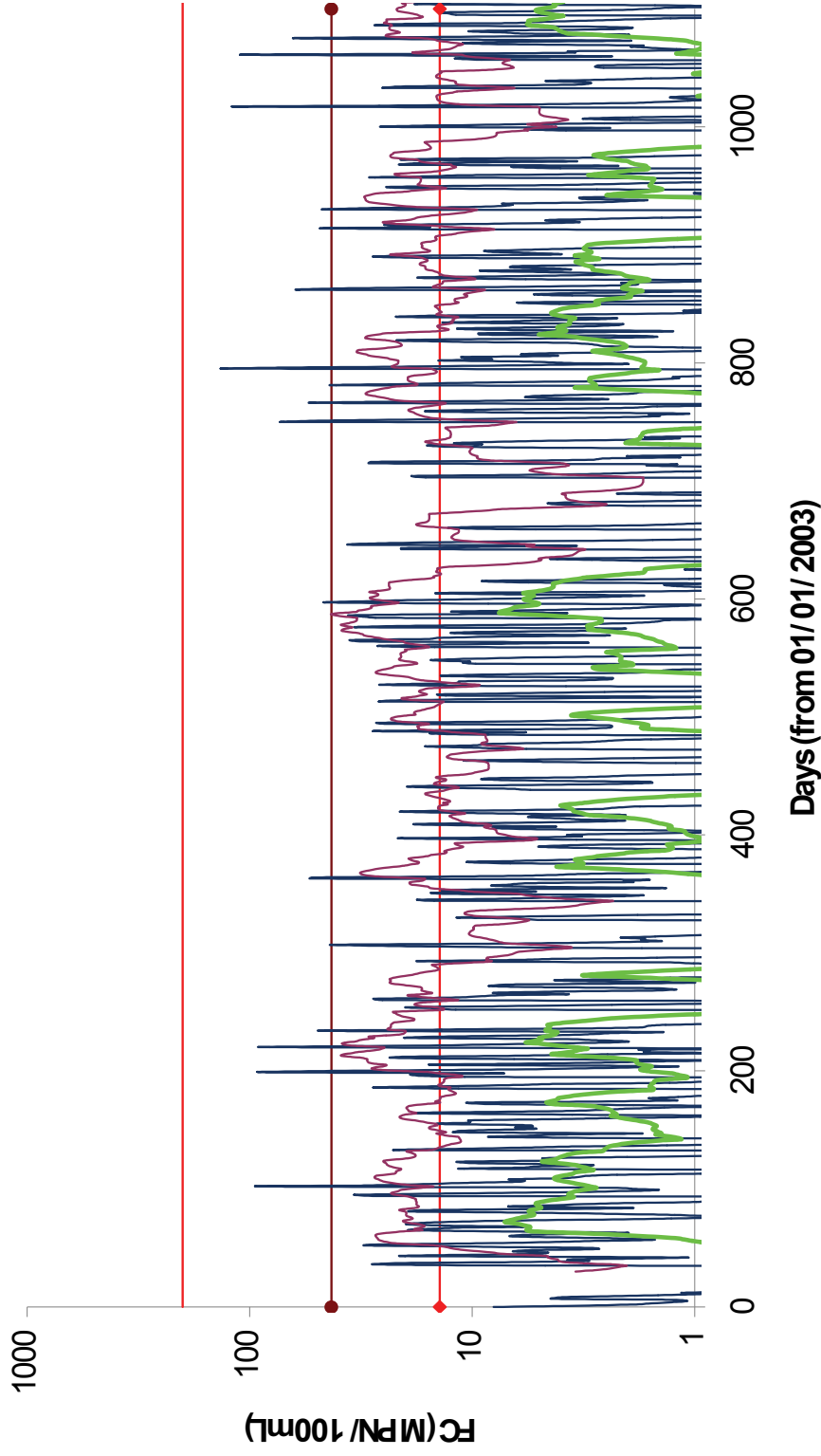
Figure V.7. Fecal coliform predictions using a 99% load reduction for the 2003-2005 simulation.

CHAPTER VI. MODEL APPLICATIONS

With the modeling framework in place and the model having undergone calibration and validation, one of the most advantageous elements of the modeling is the ability to simulate hypothetical conditions. In the case of water quality, designs of Best Management Practices (BMPs) can thereby be assessed prior to any implementation.

A good example of how the model, once calibrated and validated, can be applied is through *sensitivity* testing. Model inputs can be individually assessed by comparing model results with and without these inputs.

One immediate question that arises concerning Thurston Branch – Thalia Creek is how much of the water quality problems results from the present non-point source loadings and how much are from legacy sediment problems.

VI-1 Model sensitivity to a 100% non-point source (NPS) load reduction over an 80-day period

A sensitivity test was conducted with the NPS runoff from the 44 sub-watersheds (catchment areas) provided by URS completely eliminated. The resulting impacts on chlorophyll-a and dissolved oxygen levels of this pollutant load reduction were then examined.

Figures VI.1 through VI.5 show the hypothetical model predictions of the key water quality parameters for the 5 ConMon stations that result from the complete elimination of non-point source pollutant loading. These predictions span the period of the 3 VIMS deployments of 2009. The water quality parameters plotted at each station include dissolved oxygen, chlorophyll-a, total phosphorus, phosphate, TKN, ammonia, and nitrate. On each station plot, a red line is used to denote the instantaneous open water minimum criterion (VAC 25260-185, 2009) for dissolved oxygen, which is 4.3 mg·L^{-1} (>29C^{o}).

A comparison of chlorophyll and DO values with those shown earlier in Figures IV.13 – IV.18 show lower levels of chlorophyll and higher DO levels. Furthermore, a comparison of the nutrient levels in Figure VI.4 with the long-term nutrient levels from this location, VA-DEQ Station 7-THA000.76, shows significantly lower values for total phosphorus and TKN, as expected. However, the dissolved oxygen predictions frequently fall below the 4.3 mg·L^{-1} instantaneous criterion consistently at all 5 stations during this critical summer period. The complete removal of the non-point source loading will not show a quick improvement. Rather, it will require a long time because of sediment legacy due to the bottom deposition of nitrogen and phosphorus.

From this sensitivity test, we conclude that even complete nutrient load removal from the Thalia Creek watershed would not bring the receiving waters into compliance with the state water quality regulations within a short period.
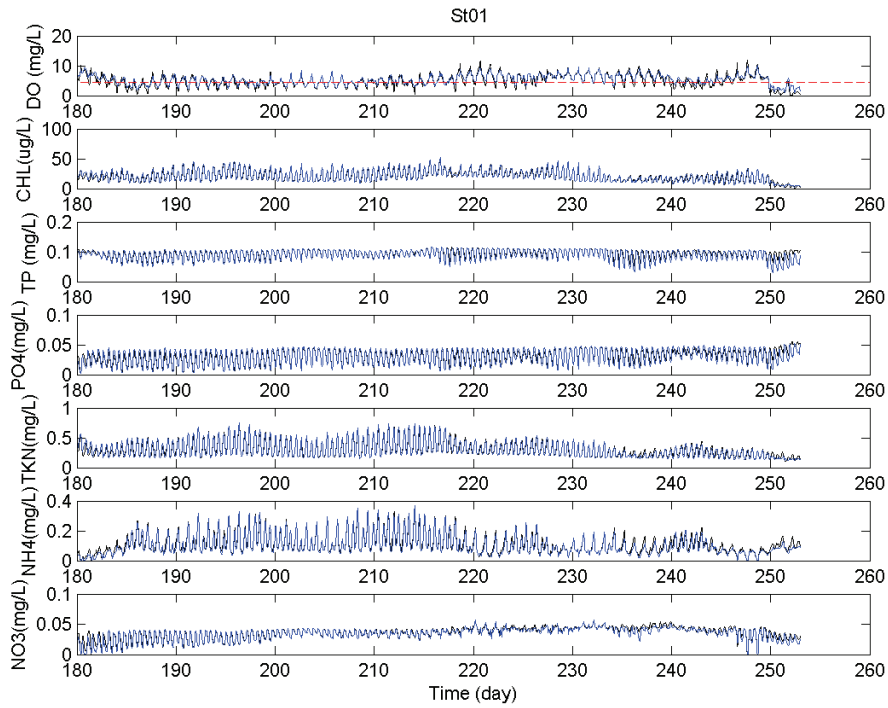
Figure VI.1. Model predictions at ConMon Station 1 (Thurston Branch) resulting from a total elimination of non-point source loading in Thalia Creek for June - August 2009.
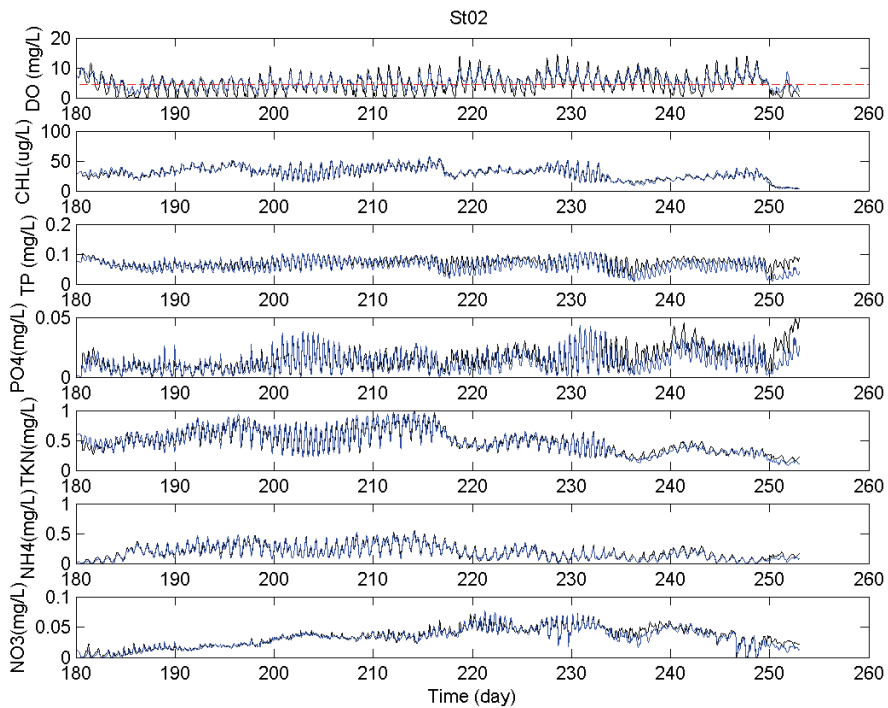

Figure VI.2. Model predictions at ConMon Station 2 (Thurston Branch) resulting from a total elimination of non-point source loading in Thalia Creek for June - August 2009.
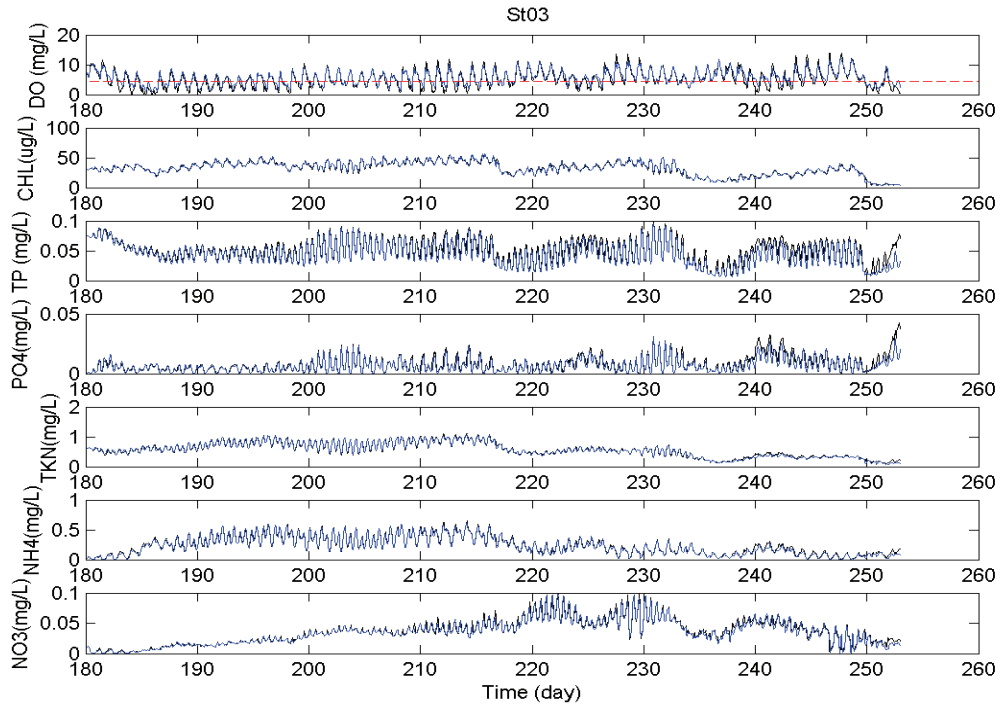
Figure VI.3. Model predictions at ConMon Station 3 (Thalia Creek) resulting from a total elimination of non-point source loading in Thalia Creek for June - August 2009.
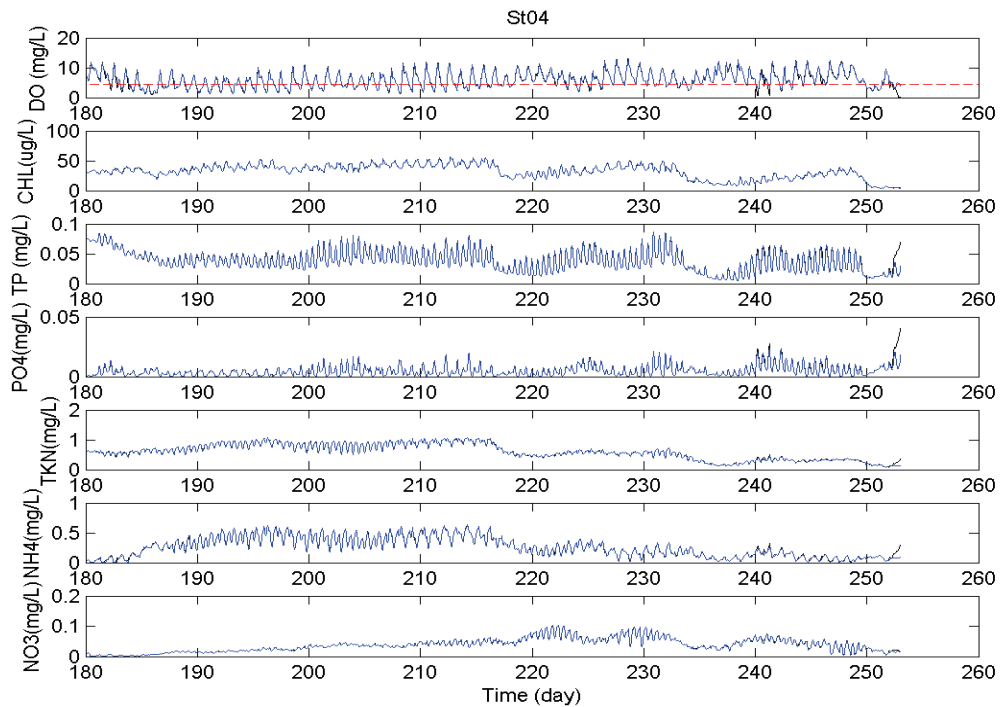

Figure VI.4. Model predictions at ConMon Station 4 (Thalia Creek) resulting from a total elimination of non-point source loading in Thalia Creek for June - August 2009.
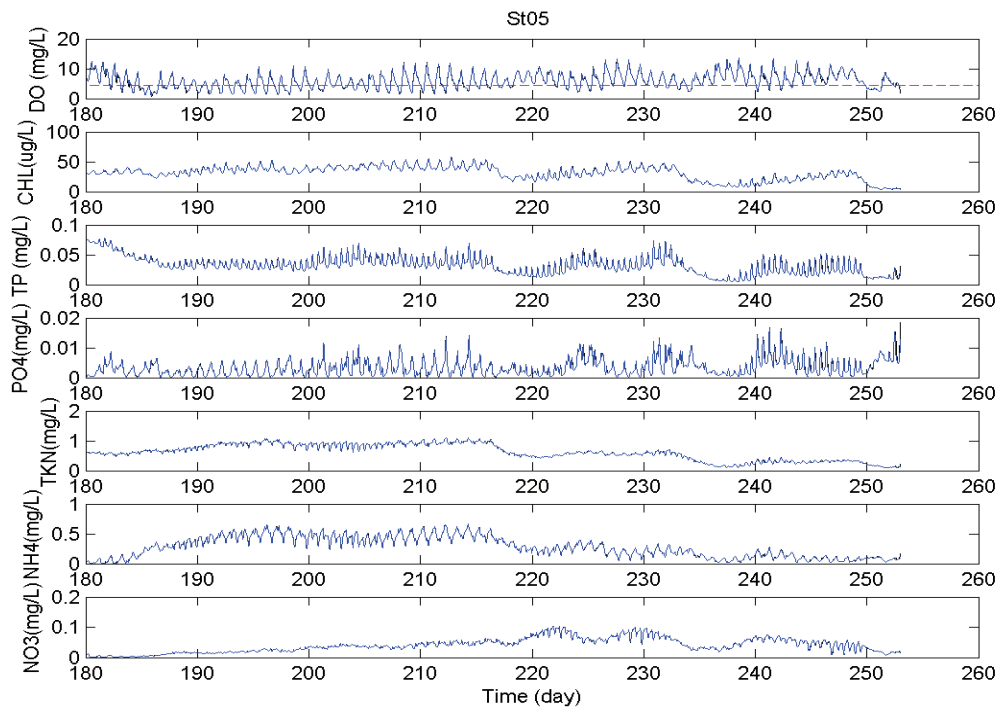
Figure VI.5. Model predictions at ConMon Station 5 (Thalia Creek) resulting from a total elimination of non-point source loading in Thalia Creek for June - August 2009.

VI-2 Model sensitivity to the "clean bottom" initial condition over an 80-day period

The second model application was to run a sensitivity test simulating clean sediment as an initial condition for the real-time model run over this 80-day period spanning the VIMS 2009 surveys. Sediment deposition rates for ammonia (NH_4), nitrate (NO_3), and phosphate (PO_4) are shown for the 5 ConMon stations in Figures VI.6 through VI.10. These rates increase for the most upstream stations (Stations 4 and 5 shown in Figures VI.9 and VI.10) and as this 80-day simulation progresses.

All fluxes start with a value of zero, and then increase as the non-point source loadings into the water column begin to deposit onto the sediment. The rates of several important fluxes between the water column and sediment layer, i.e., sediment oxygen demand (SOD), ammonia (NH_4), nitrate (NO_3), and phosphate (PO_4), are shown for the 5 ConMon stations in Figures VI.11 through VI.15. It should be noted that the convention is such that a negative flux is from the water column to the sediment, as can be seen for the SOD and PO_4 fluxes at all stations. Conversely, ammonia and nitrate fluxes were from the sediment to the water column. The full suite of predictions for the key water quality state variables of DO, chl, TP, PO_4, TKN, NH_4, and NO_3 is shown for the 5 ConMon stations in Figures VI.16 through VI.20. Overall, the concentrations are low compared to observations. Most importantly, however, the DO levels are usually above the 4.3 mg·L^{-1}criterion marked in red on these figures, indicating that the sediment removal sensitivity test has even more impact than the complete removal of non-point source loadings. However, this model sensitivity test also suggests that nutrients will continually build up on the bottom sediment without the removal of NPS loading.
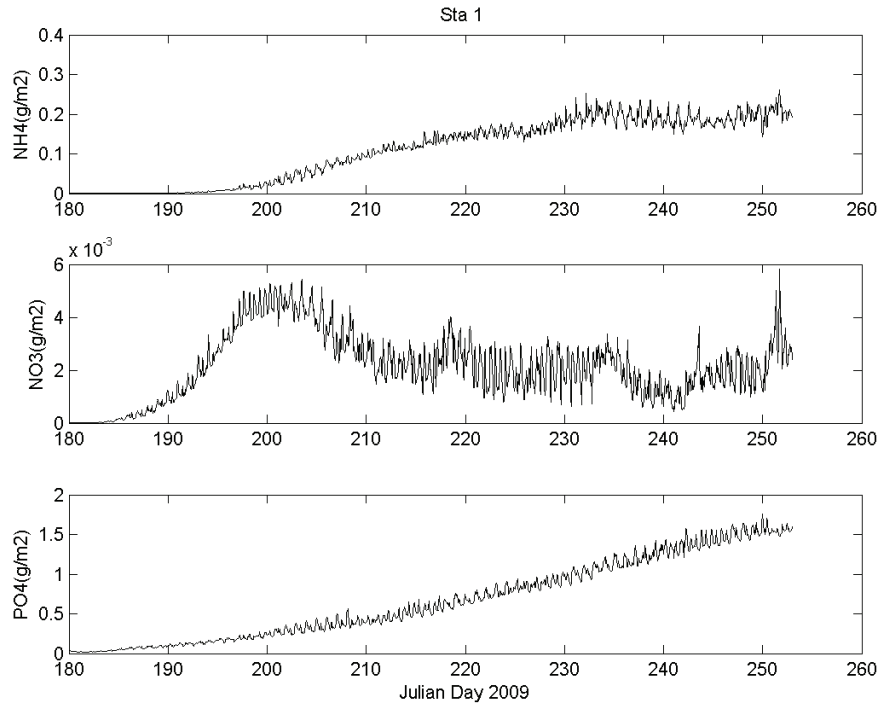
151

Figure VI.6. Sediment deposition for ammonia (NH$_4$), nitrate (NO$_3$), and phosphate (PO$_4$) at Thalia Creek ConMon Station 1 in a sensitivity test of a clean bottom condition for sediment.

Figure VI.7. Sediment deposition for ammonia (NH$_4$), nitrate (NO$_3$), and phosphate (PO$_4$) at Thalia Creek ConMon Station 2 in a sensitivity test of a clean bottom condition for sediment.
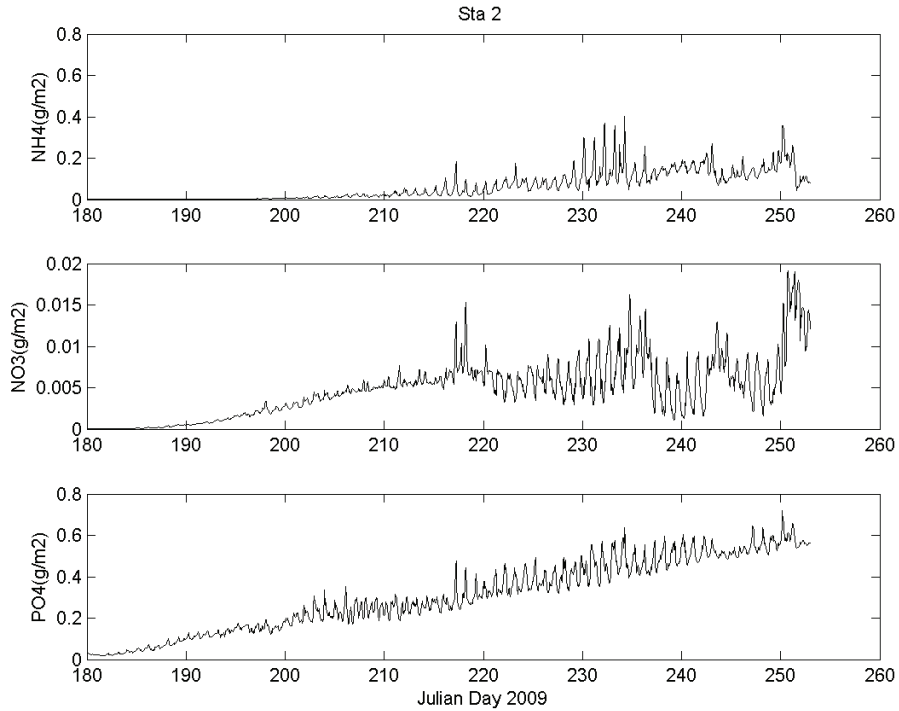
152

Figure VI.8. Sediment deposition for ammonia (NH$_4$), nitrate (NO$_3$), and phosphate (PO$_4$) at Thalia Creek ConMon Station 3 in a sensitivity test of a clean bottom condition for sediment.

Figure VI.9. Sediment deposition for ammonia (NH$_4$), nitrate (NO$_3$), and phosphate (PO$_4$) at Thalia Creek ConMon Station 4 in a sensitivity test of a clean bottom condition for sediment.
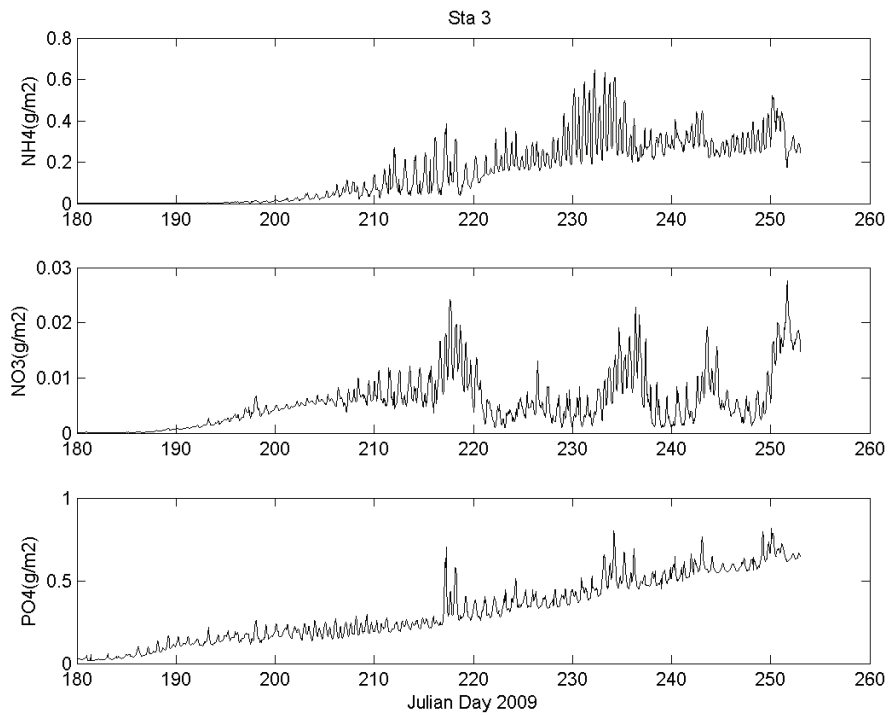
153

Figure VI.10. Sediment deposition for ammonia (NH$_4$), nitrate (NO$_3$), and phosphate (PO$_4$) at Thalia Creek ConMon Station 5 in a sensitivity test of a clean bottom condition for sediment.
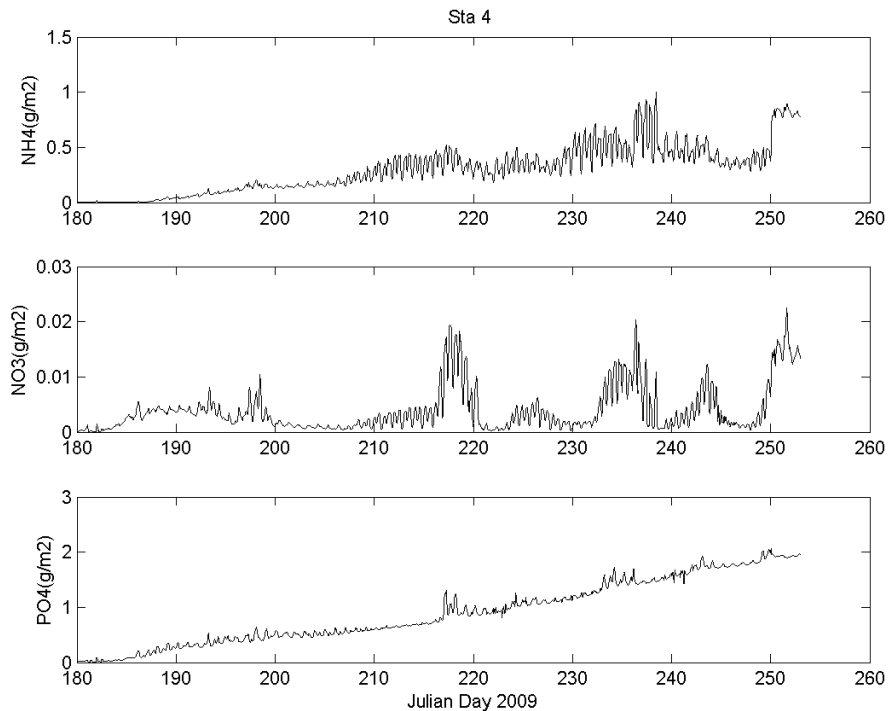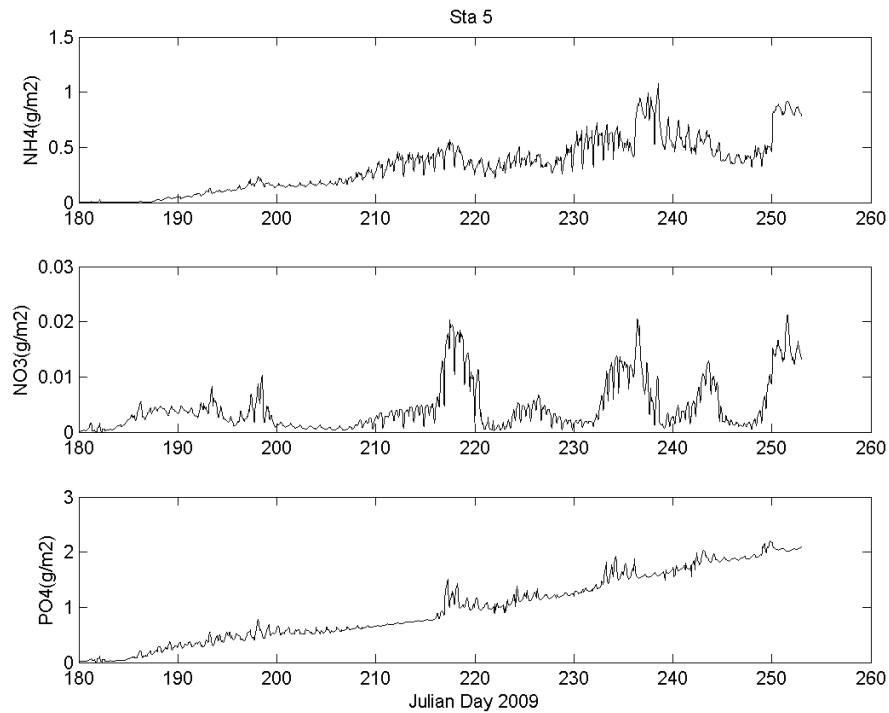

Figure VI.11. Flux rates for sediment oxygen demand (SOD), ammonia (NH$_4$), nitrate (NO$_3$), and phosphate (PO$_4$) at Thalia Creek ConMon Station 1 in a sensitivity test of an initially clean bottom condition for sediment. {Note: positive denotes from sediment to water column and negative denotes from water column to sediment}.

Figure VI.12. Flux rates for sediment oxygen demand (SOD), ammonia (NH_4), nitrate (NO_3), and phosphate (PO_4) at Thalia Creek ConMon Station 2 in a sensitivity test of an initially clean bottom condition for sediment. {Note: positive denotes from sediment to water column and negative denotes from water column to sediment}.
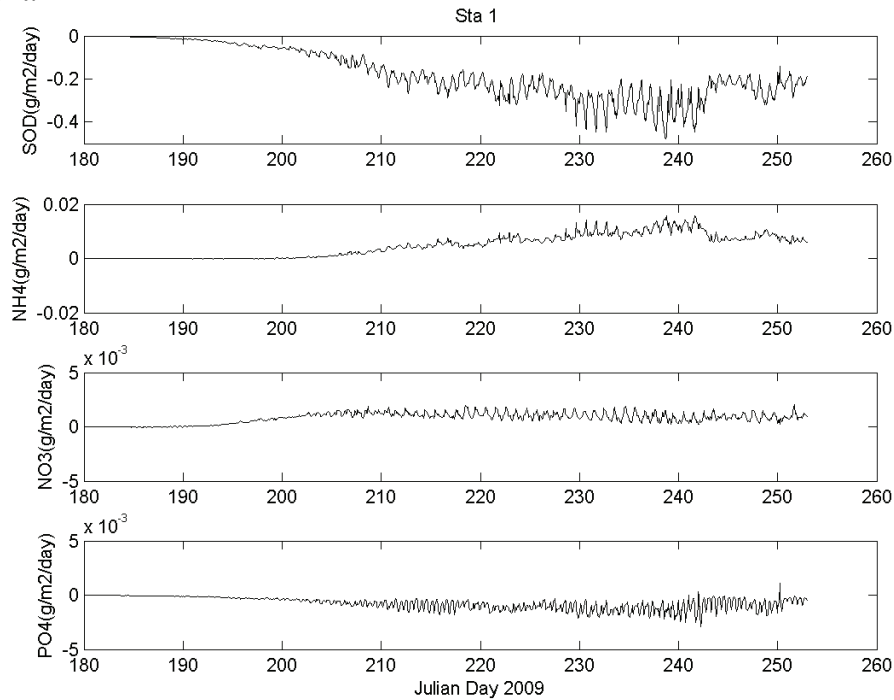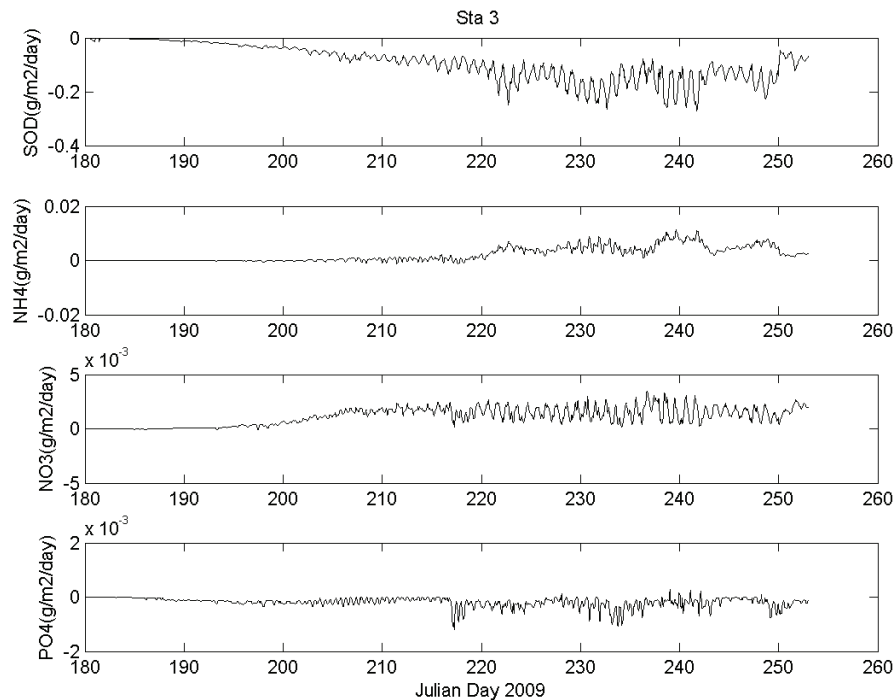

Figure VI.13. Flux rates for sediment oxygen demand (SOD), ammonia (NH_4), nitrate (NO_3), and phosphate (PO_4) at Thalia Creek ConMon Station 3 in a sensitivity test of an initially clean bottom condition for sediment. {Note: positive denotes from sediment to water column and negative denotes from water column to sediment}.
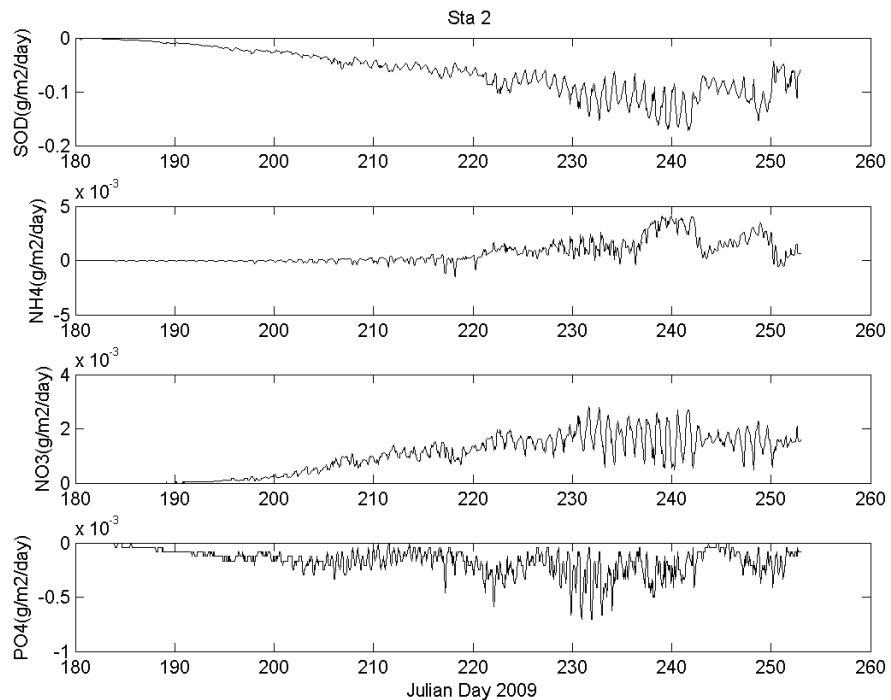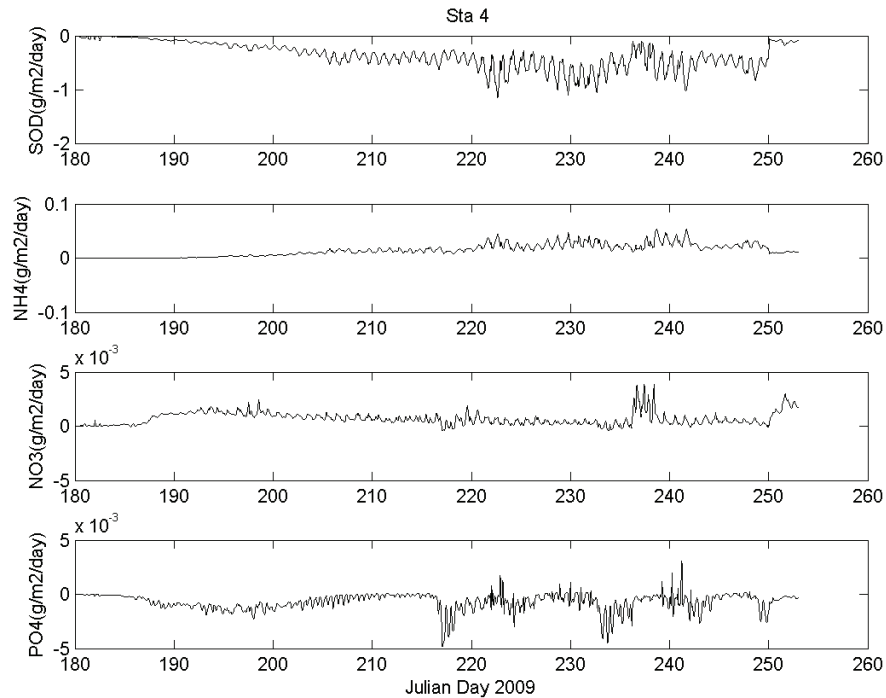
Figure VI.14. Flux rates for sediment oxygen demand (SOD), ammonia (NH$_4$), nitrate (NO$_3$), and phosphate (PO$_4$) at Thalia Creek ConMon Station 4 in a sensitivity test of an initially clean bottom condition for sediment. {Note: positive denotes from sediment to water column and negative denotes from water column to sediment}.
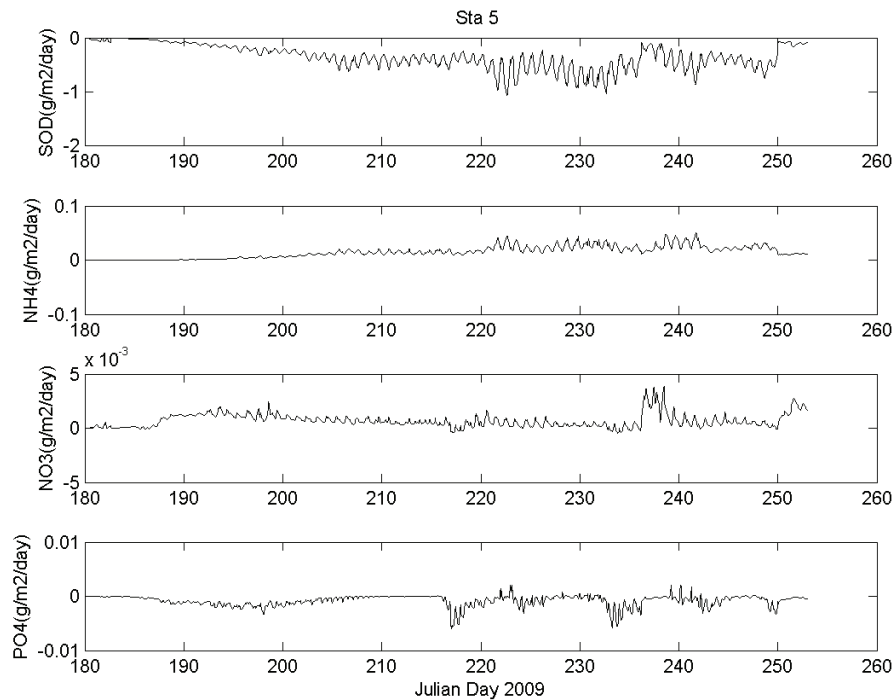
Figure VI.15. Flux rates for sediment oxygen demand (SOD), ammonia (NH$_4$), nitrate (NO$_3$), and phosphate (PO$_4$) at Thalia Creek ConMon Station 5 in a sensitivity test of an initially clean bottom condition for sediment. {Note: positive denotes from sediment to water column and negative denotes from water column to sediment}.

156

Figure VI.16. Predictions for the key water quality state variables of DO, chl, TP, PO$_4$, TKN, NH$_4$, and NO$_3$ at Thalia Creek ConMon Station 1 in a sensitivity test of a clean bottom condition for sediment.

Figure VI.17. Predictions for the key water quality state variables of DO, chl, TP, PO$_4$, TKN, NH$_4$, and NO$_3$ at Thalia Creek ConMon Station 2 in a sensitivity test of a clean bottom condition for sediment.

Figure VI.18. Predictions for the key water quality state variables of DO, chl, TP, PO$_4$, TKN, NH$_4$, and NO$_3$ at Thalia Creek ConMon Station 3 in a sensitivity test of a clean bottom condition for sediment.

Figure VI.19. Predictions for the key water quality state variables of DO, chl, TP, PO$_4$, TKN, NH$_4$, and NO$_3$ at Thalia Creek ConMon Station 4 in a sensitivity test of a clean bottom condition for sediment.

Figure VI.20. Predictions for the key water quality state variables of DO, chl, TP, PO$_4$, TKN, NH$_4$, and NO$_3$ at Thalia Creek ConMon Station 5 in a sensitivity test of a clean bottom condition for sediment.

VI-3 Model sensitivity to a combined 50% NPS reduction and clean bottom initial condition

The next scenario of the model applications was designed to assess the combined effects of reducing the NPS loadings by 50% and applying the no sediment (i.e., "clean bottom") initial condition. For this test, the simulation was conducted over the 80-day period from late June to early September (Julian days 180 – 260) 2009.

The full suite of predictions for the key water quality state variables of DO, chl, TP, PO$_4$, TKN, NH$_4$, and NO$_3$ is shown for the 5 ConMon stations in Figures VI.21 through VI.25. Overall, DO levels are above the instantaneous water quality criterion and chlorophyll concentration levels are reduced substantially. The model results suggest that, with clean sediment and reduction of non-point source loading, the water quality condition can be improved.
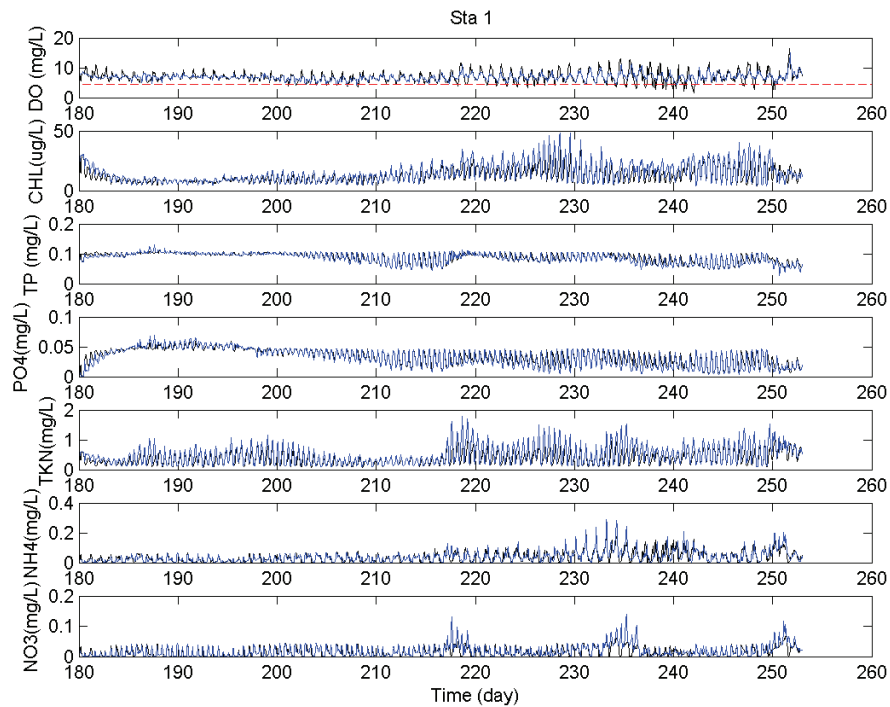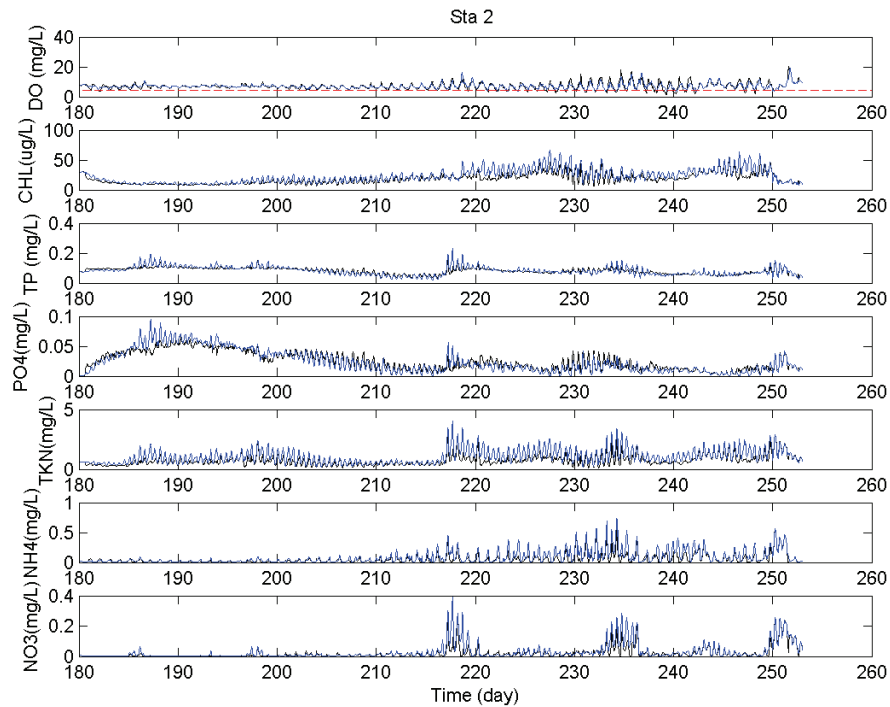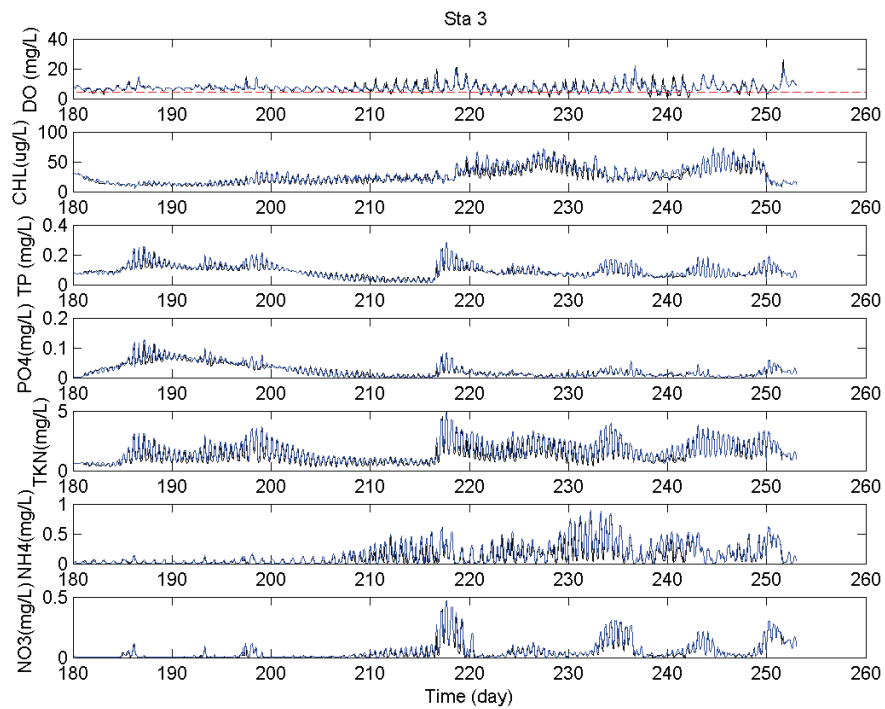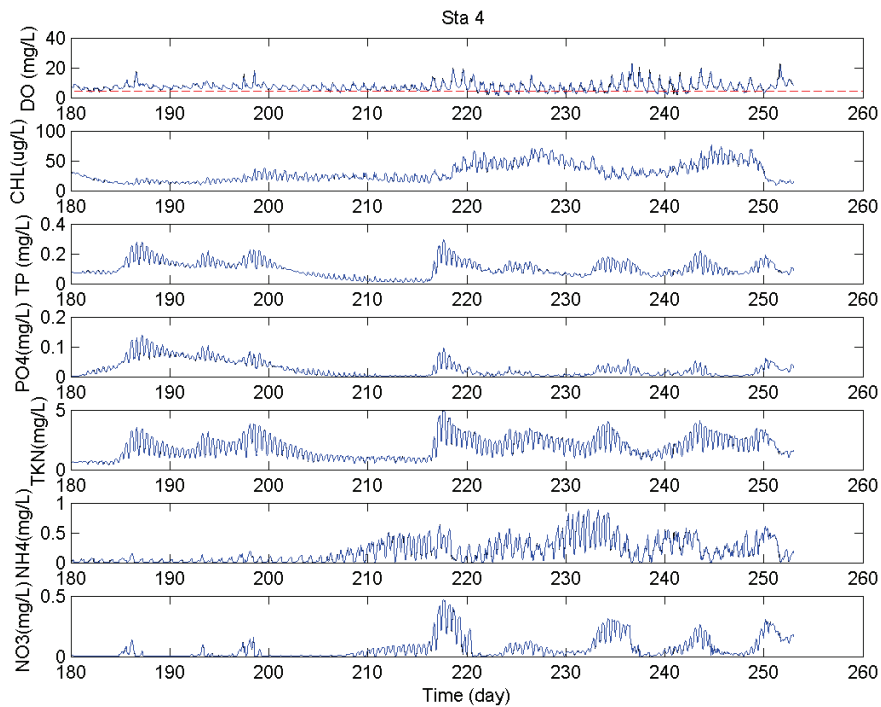
159

Figure VI.21. Predictions for the key water quality state variables of DO, chl, TP, PO₄, TKN, NH₄, and NO₃ at Thalia Creek ConMon Station 1 in a sensitivity test combining 50% NPS removal and a clean bottom initial condition for sediment.
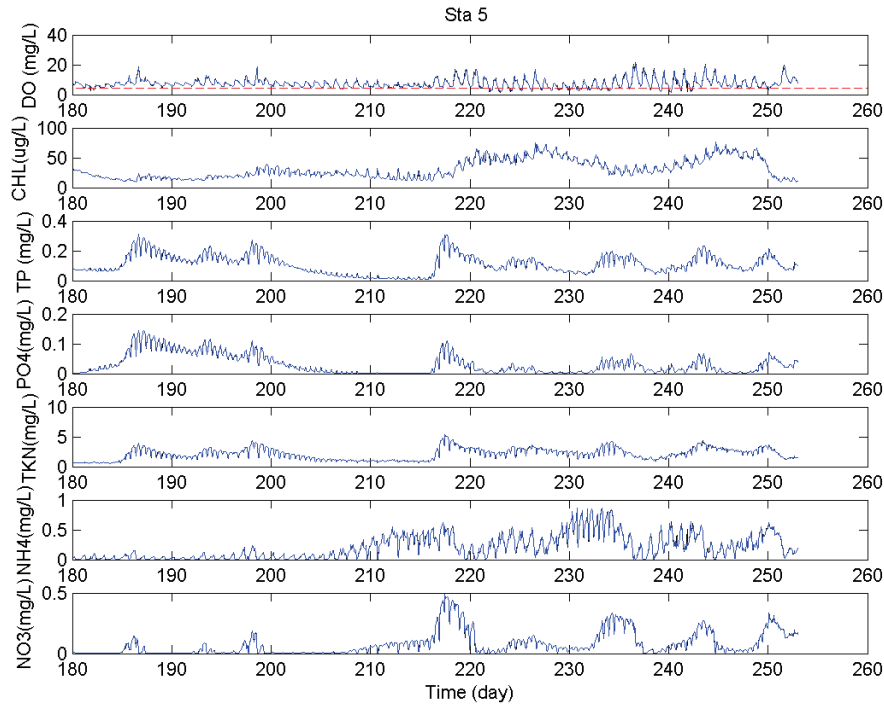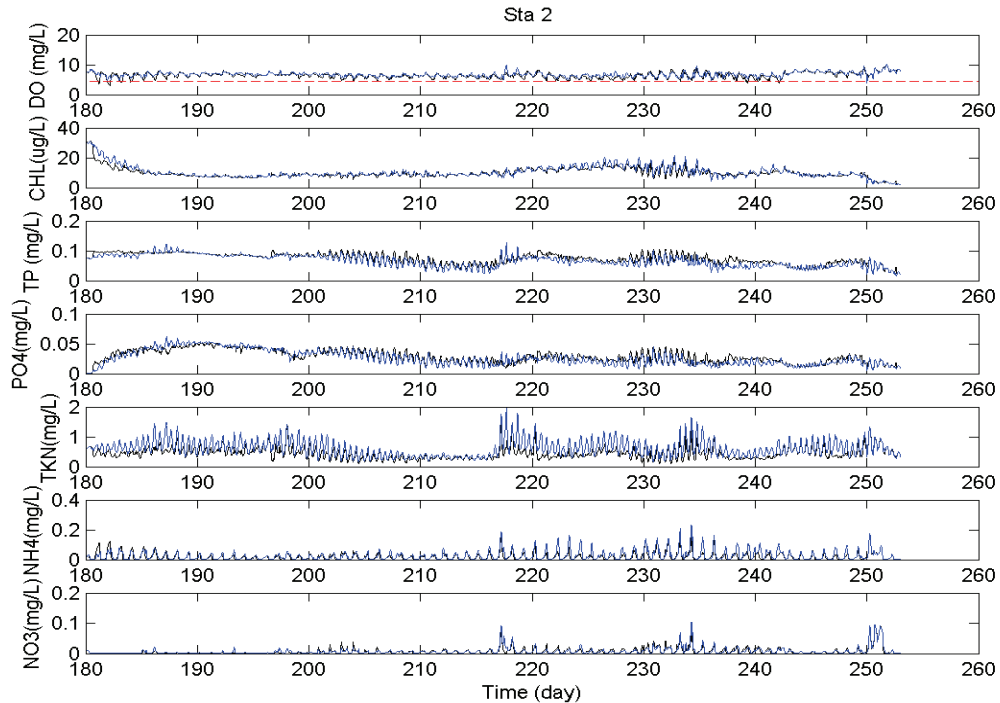

Figure VI.22. Predictions for the key water quality state variables of DO, chl, TP, PO₄, TKN, NH₄, and NO₃ at Thalia Creek ConMon Station 2 in a sensitivity test combining 50% NPS removal and a clean bottom initial condition for sediment.

160
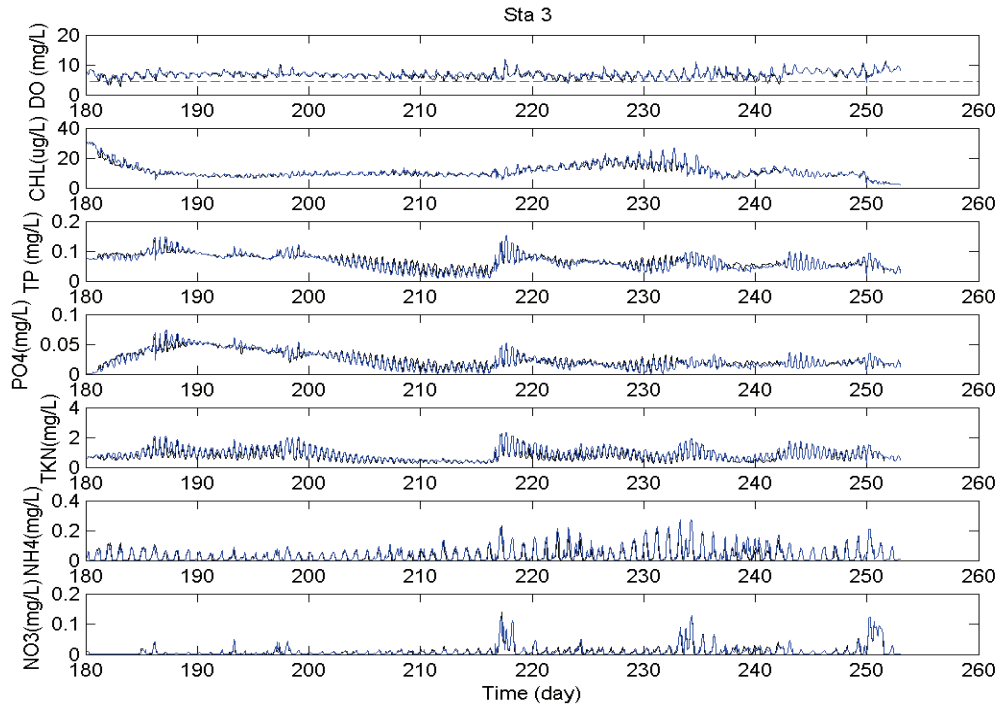
Figure VI.23. Predictions for the key water quality state variables of DO, chl, TP, PO$_4$, TKN, NH$_4$, and NO$_3$ at Thalia Creek ConMon Station 3 in a sensitivity test combining 50% NPS removal and a clean bottom initial condition for sediment.

Figure VI.24. Predictions for the key water quality state variables of DO, chl, TP, PO$_4$, TKN, NH$_4$, and NO$_3$ at Thalia Creek ConMon Station 4 in a sensitivity test combining 50% NPS removal and a clean bottom initial condition for sediment.
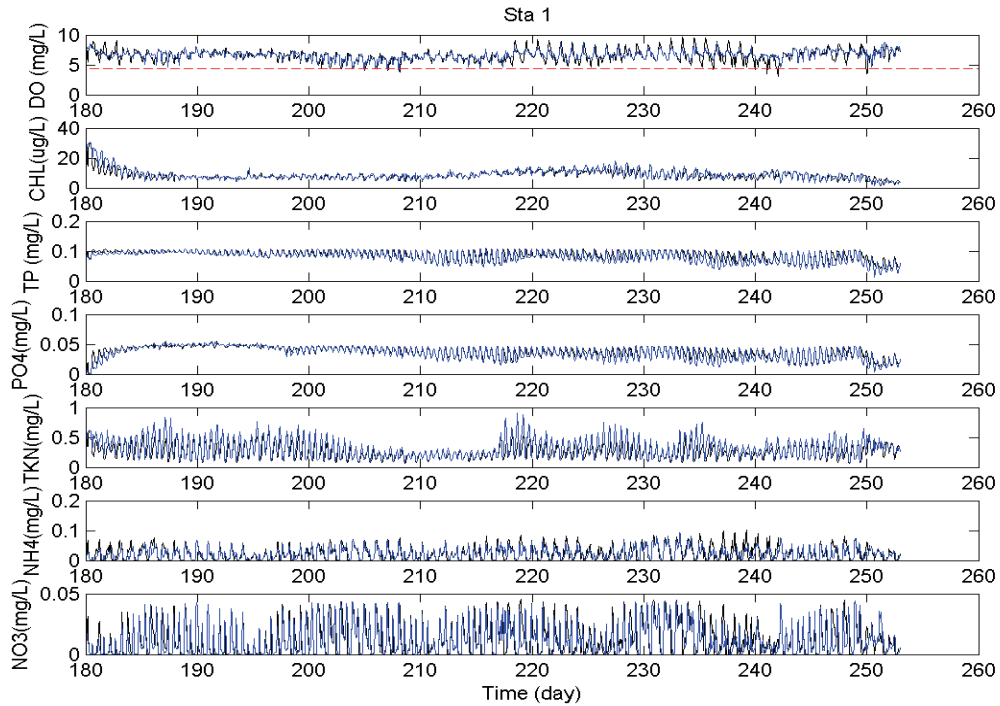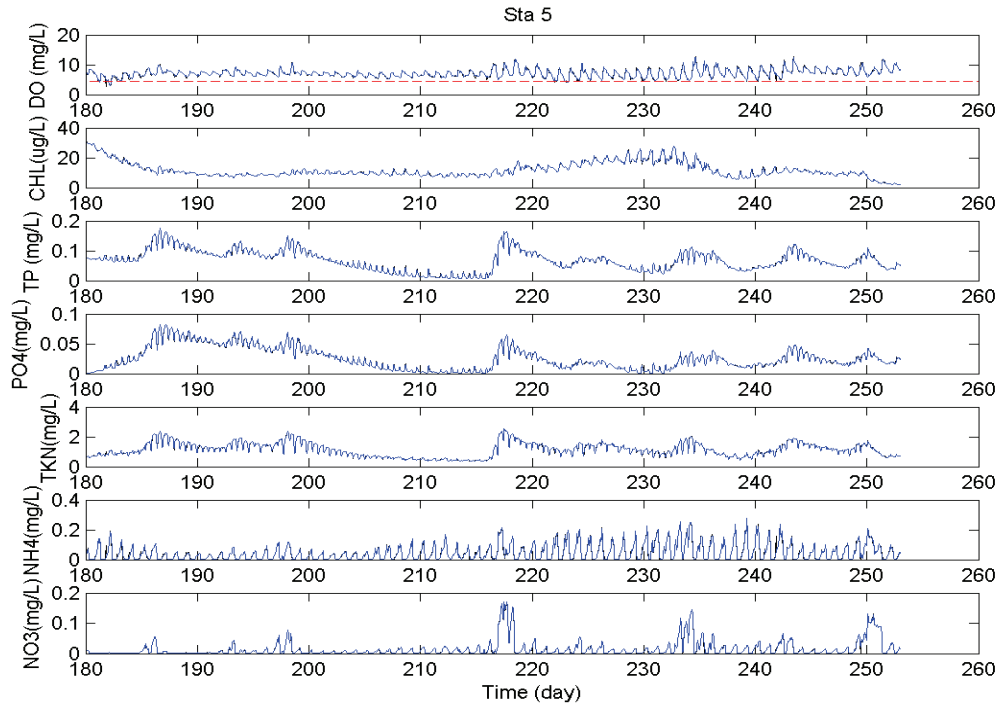
Figure VI.25. Predictions for the key water quality state variables of DO, chl, TP, PO$_4$, TKN, NH$_4$, and NO$_3$ at Thalia Creek ConMon Station 5 in a sensitivity test combining 50% NPS removal and a clean bottom initial condition for sediment.
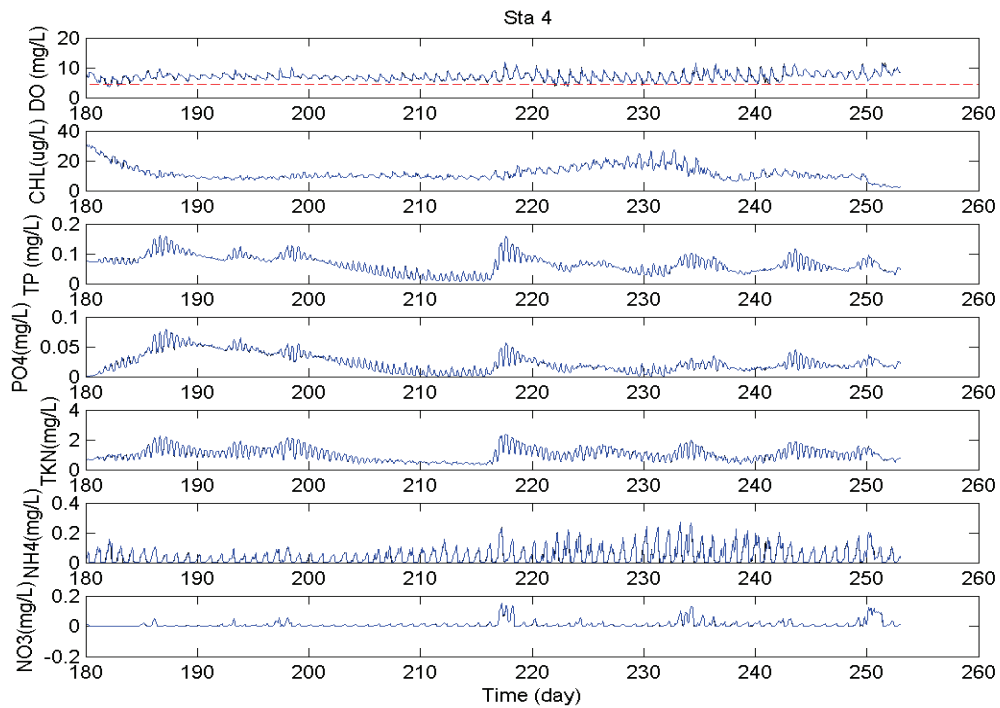
VI-4 Model sensitivity to combined 50% NPS reduction from 4 selected subwatersheds and clean bottom initial condition

The loading analysis shows that a large amount of nonpoint source loading is discharged into the stream from the watershed upstream of the Creek and from watersheds upstream of the tributary. The next scenario of the model applications was designed to assess the combined effects of a selective reduction of the NPS loadings at 4 subwatersheds by 50% and applying the no sediment (i.e., "clean bottom") initial condition. For this test, the simulation was conducted over the 80-day period from late June-early September (Julian days 180 – 260) 2009.

Of the 44 Thalia Creek subwatersheds delineated by URS Corporation, 4 subwatersheds (i.e., subwatersheds 68, 62, 61, and 196) are included in this sensitivity test. Figure VI.26 shows their locations, as well as a spatial distribution of TKN loadings throughout the Thalia Creek watershed. The heavy loadings and large acreage of subwatershed 196 should be noted.

The full suite of predictions for the key water quality state variables of DO, chl, TP, PO$_4$, TKN, NH$_4$, and NO$_3$ is shown for the 5 ConMon stations in Figures VI.27 through VI.31. It can be seen the results are almost the same as those of the previous sensitivity test in the reduction of non-point source loading from the entire watershed. This sensitivity test

162

suggests that, using new technologies (such as BMPs) at key subwatershed locations, water quality conditions in Thalia Creek can be improved in a more efficient and cost-effective manner.
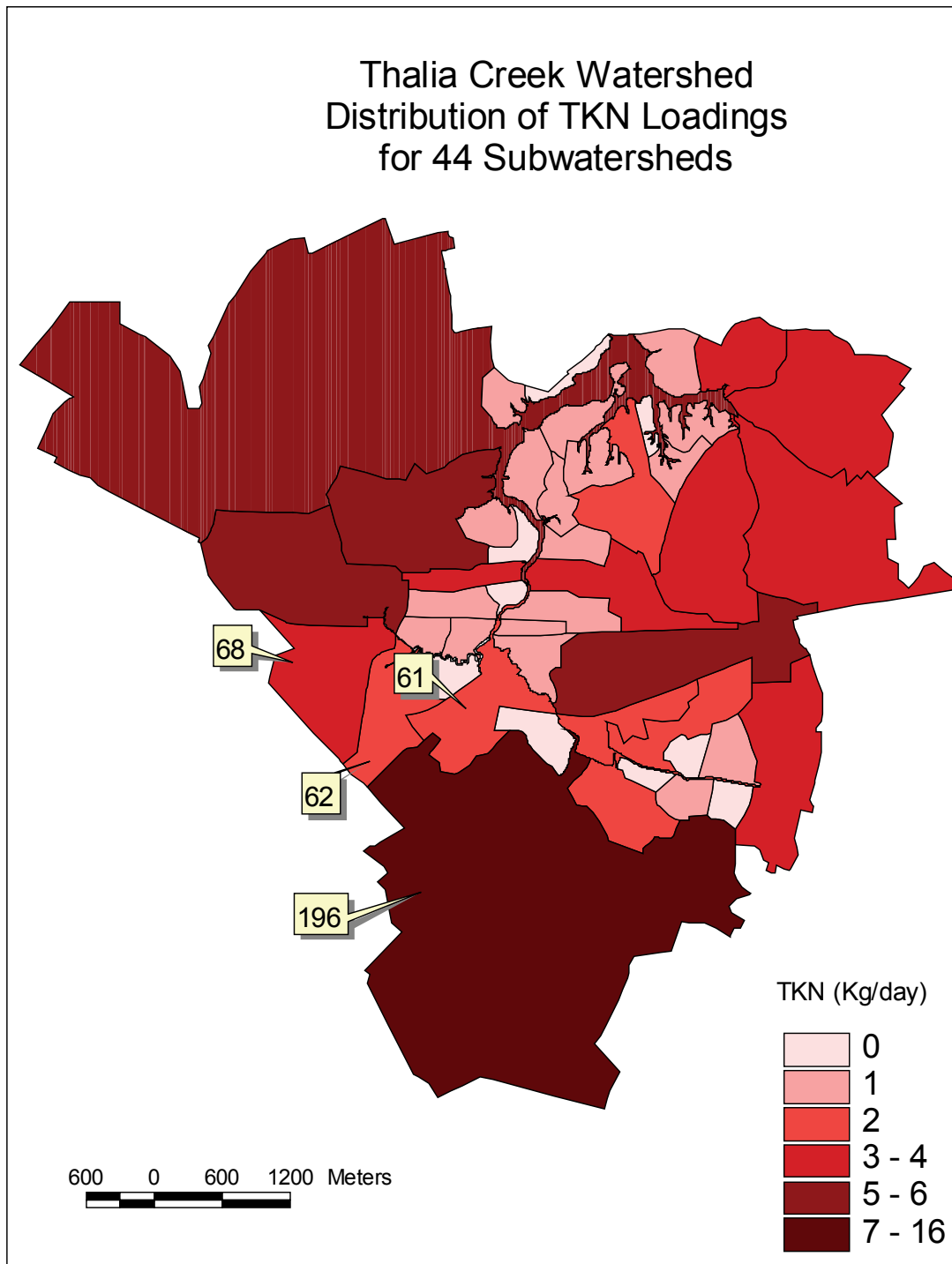
Figure VI.26. Locations of 4 subwatersheds selected for sensitivity testing and the spatial distribution of TKN loads for the 44 Thalia Creek subwatersheds.
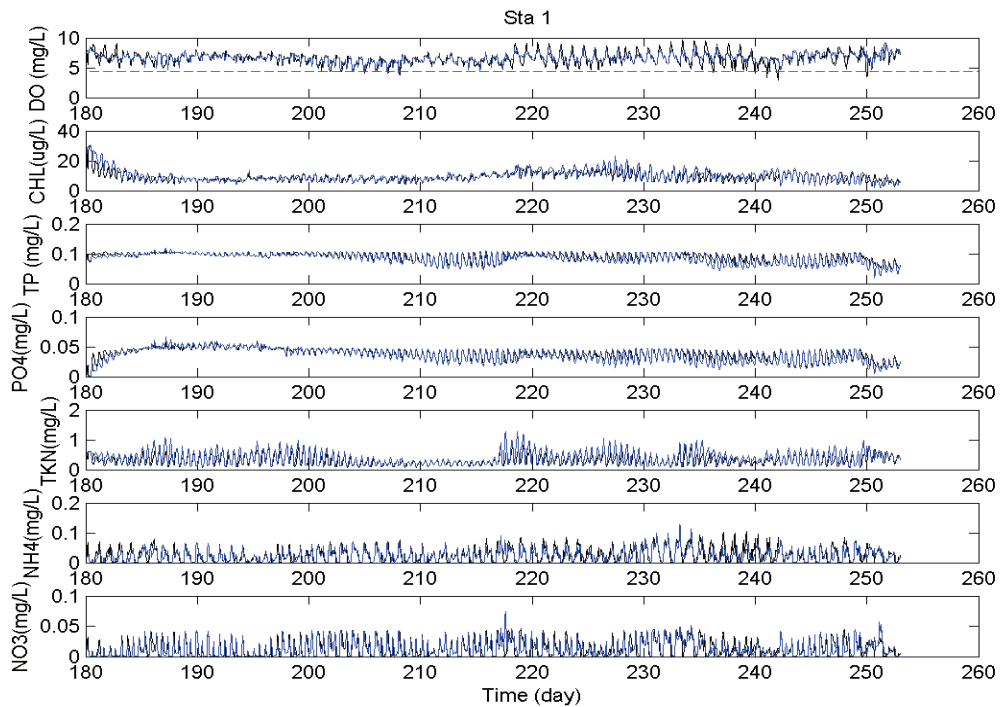
Figure VI.27. Predictions of DO, chl, TP, PO₄, TKN, NH₄, and NO₃ at Thalia Creek ConMon Station 1 in a sensitivity test combining 50% NPS removal from 4 selected subwatersheds and a clean bottom initial condition for sediment.
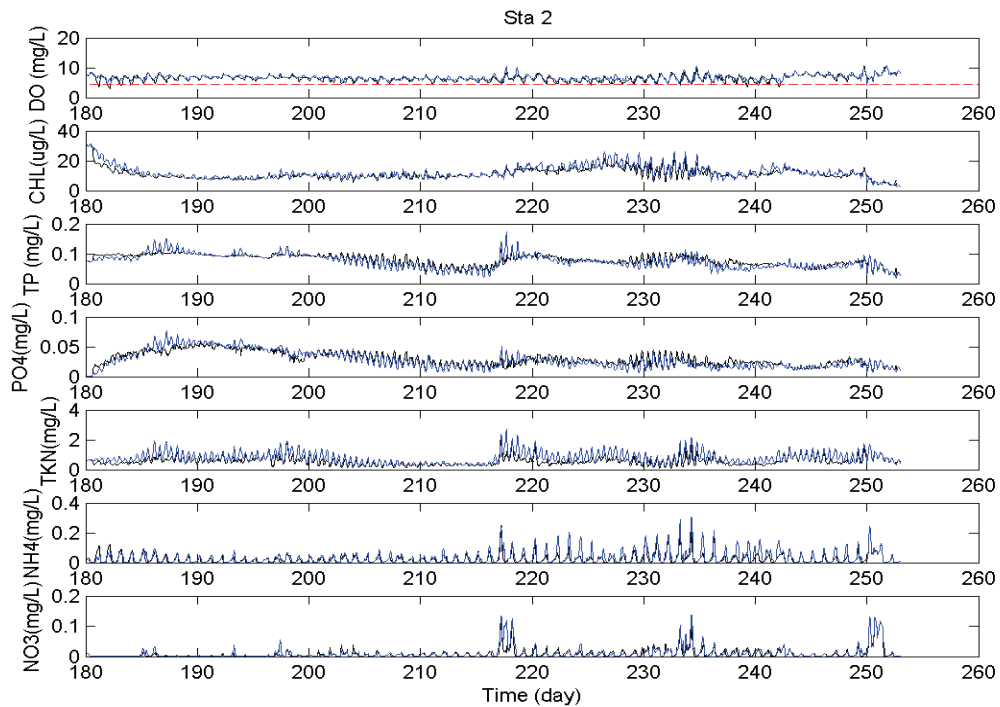
Figure VI.28. Predictions of DO, chl, TP, PO₄, TKN, NH₄, and NO₃ at Thalia Creek ConMon Station 2 in a sensitivity test combining 50% NPS removal from 4 selected subwatersheds and a clean bottom initial condition for sediment.
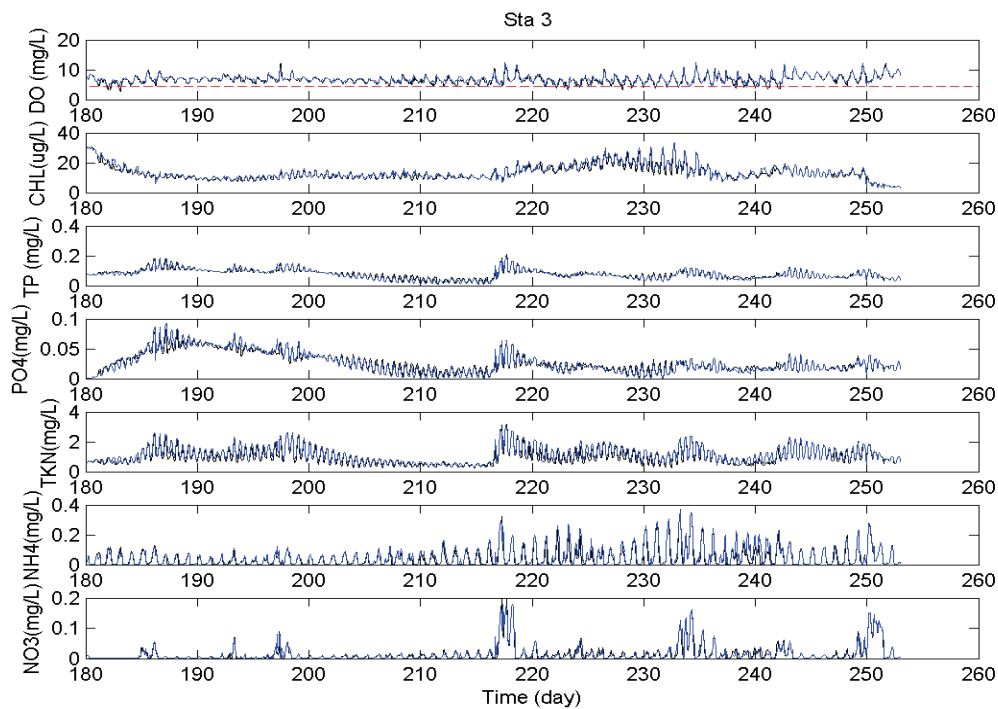
Figure VI.29. Predictions of DO, chl, TP, PO₄, TKN, NH₄, and NO₃ at Thalia Creek ConMon Station 3 in a sensitivity test combining 50% NPS removal from 4 selected subwatersheds and a clean bottom initial condition for sediment.

Figure VI.30. Predictions of DO, chl, TP, PO₄, TKN, NH₄, and NO₃ at Thalia Creek ConMon Station 4 in a sensitivity test combining 50% NPS removal from 4 selected subwatersheds and a clean bottom initial condition for sediment.

Figure VI.31. Predictions of DO, chl, TP, PO$_4$, TKN, NH$_4$, and NO$_3$ at Thalia Creek ConMon Station 5 in a sensitivity test combining 50% NPS removal from 4 selected subwatersheds and a clean bottom initial condition for sediment.

VI-5 Model sensitivity to a 50% non-point source load reduction over a 4-yr period

The sensitivity tests shown earlier indicated that the total elimination of the non-point source loadings in Thalia Creek would apparently require much more than the 80-day simulation periods described in Sections VI-1 through VI-3 to bring dissolved oxygen levels into compliance. At that point, the question arose: "how long a period of non-point source load reduction, and what percentage reduction, would cause notable increases in dissolved oxygen levels and decreases in chlorophyll-a levels"?

A sensitivity test reducing the NPS loadings throughout the Thalia Creek watershed was conducted over a 4-year period (from 2003-2006). Results of this simulation at the 5 ConMon water quality stations for the water quality parameters predictions of DO, chl, TP, PO$_4$, TKN, NH$_4$, and NO$_3$ are shown in Figures VI.32 through VI.36. In these figures, the black and green lines represent, respectively, the daily maximum and minimum predicted values.

It can be seen that DO levels in this simulation seldom fall below the 4.3 mg·L^{-1} instantaneous criterion (red line) shown on the top panel of each of Figures VI.32 through VI.36. However, chlorophyll levels associated with this simulation of 50% NPS loading reduction over this 4-year period generally remain high, and are shown to exceed 50 ug·L^{-1} at all stations.

166

Figure VI.32. Predictions of DO, chl, TP, PO₄, TKN, NH₄, and NO₃ at Thalia Creek ConMon Station 1 in a sensitivity test using 50% NPS removal extended over a 4-year period.
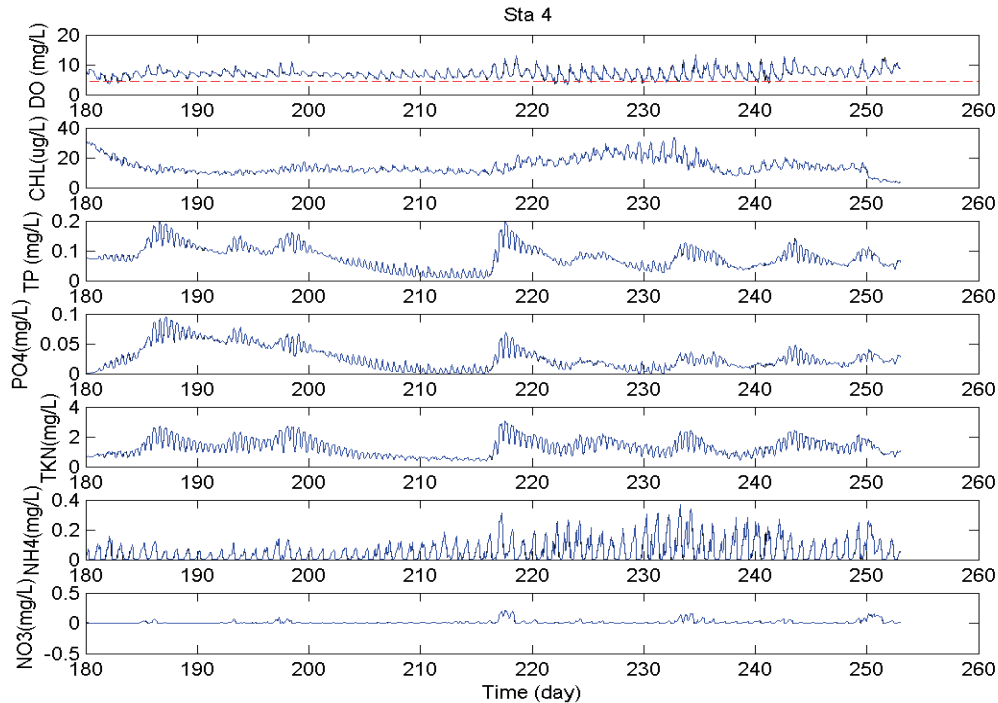

Figure VI.33. Predictions of DO, chl, TP, PO₄, TKN, NH₄, and NO₃ at Thalia Creek ConMon Station 2 in a sensitivity test using 50% NPS removal extended over a 4-year period.

Figure VI.34. Predictions of DO, chl, TP, PO₄, TKN, NH₄, and NO₃ at Thalia Creek ConMon Station 3 in a sensitivity test using 50% NPS removal extended over a 4-year period.
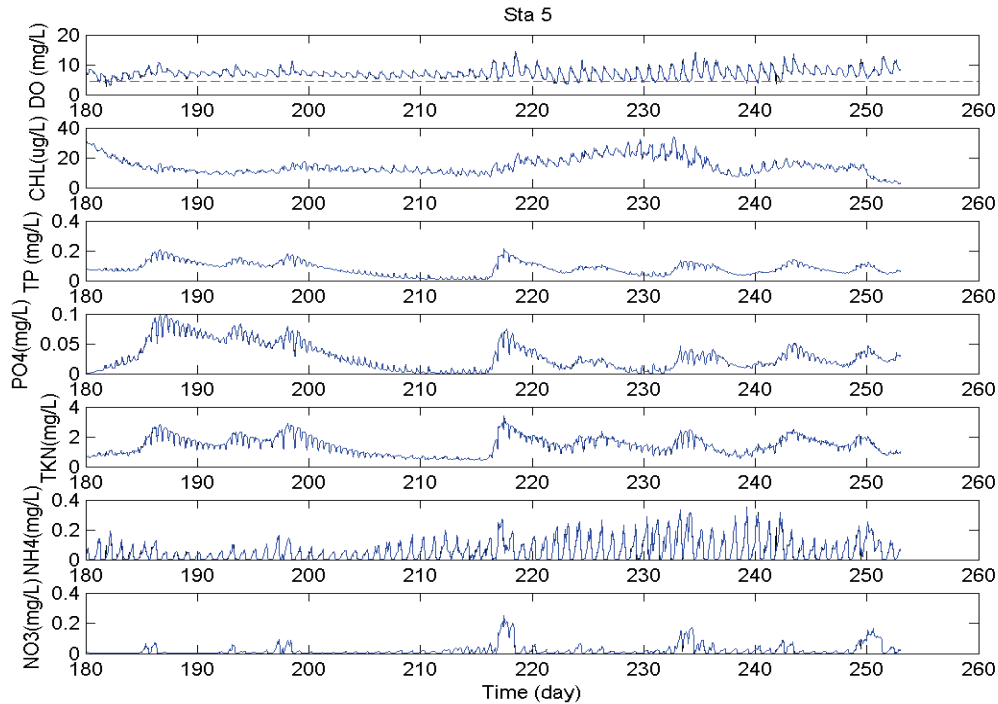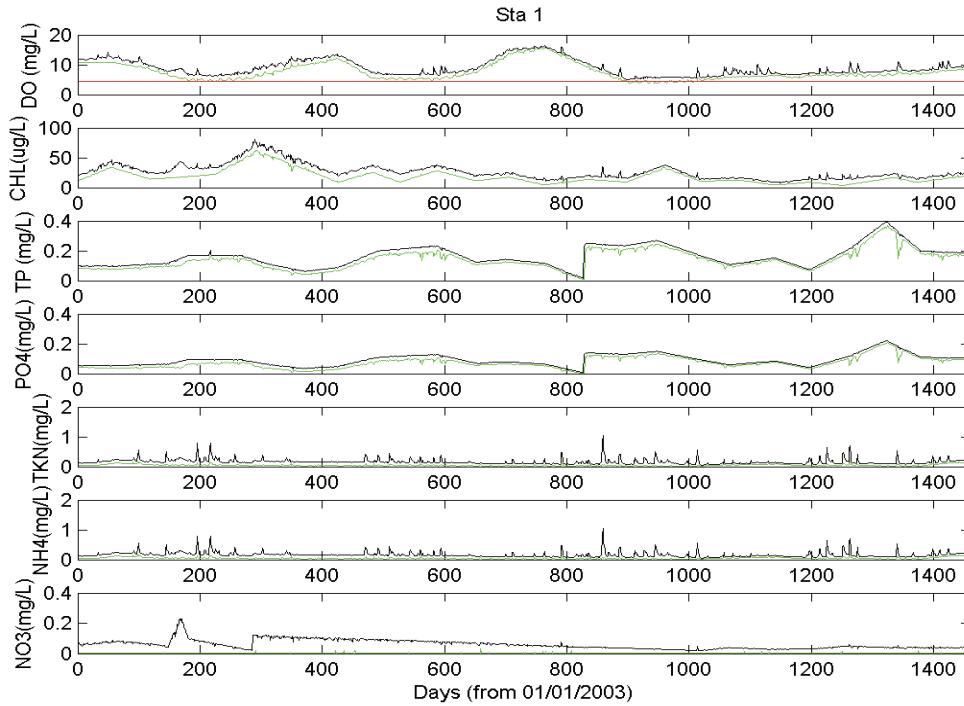

Figure VI.35. Predictions of DO, chl, TP, PO₄, TKN, NH₄, and NO₃ at Thalia Creek ConMon Station 4 in a sensitivity test using 50% NPS removal extended over a 4-year period.

168

Figure VI.36. Predictions of DO, chl, TP, PO$_4$, TKN, NH$_4$, and NO$_3$ at Thalia Creek ConMon Station 5 in a sensitivity test using 50% NPS removal extended over a 4-year period.

VI-6 Model sensitivity to a 70% non-point source load reduction over a 4-yr period

The next sensitivity test to be shown is identical to that described in Section VI-5, except that the NPS load reductions were increased from 50% to 70%. The results of this simulation at the 5 ConMon water quality stations are shown in Figures VI.37 through VI.41. In these figures, the black and green lines represent the daily maximum and minimum model predictions, respectively.

From these figures, it can be seen that the DO levels consistently remain above the 4.3 mg·L^{-1} instantaneous criterion shown by the red line in each top panel. Additionally, the chlorophyll levels are lower than those shown earlier in Figures VI.32 through VI.36 for the 50% NPS load reduction simulation. In particular, the chlorophyll levels from this 70% NPS load reduction simulation are further reduced from the 50% NPS load reduction simulation as the 4-year simulation progresses into years 2, 3, and 4 and as one compares the stations further upstream (i.e., Stations 4 and 5 shown in Figures VI.40 and VI.41).

169

Figure VI.37. Predictions of DO, chl, TP, PO$_4$, TKN, NH$_4$, and NO$_3$ at Thalia Creek ConMon Station 1 in a sensitivity test using 70% NPS removal extended over a 4-year period.

Figure VI.38. Predictions of DO, chl, TP, PO$_4$, TKN, NH$_4$, and NO$_3$ at Thalia Creek ConMon Station 2 in a sensitivity test using 70% NPS removal extended over a 4-year period.

Figure VI.39. Predictions of DO, chl, TP, PO₄, TKN, NH₄, and NO₃ at Thalia Creek ConMon Station 3 in a sensitivity test using 70% NPS removal extended over a 4-year period.
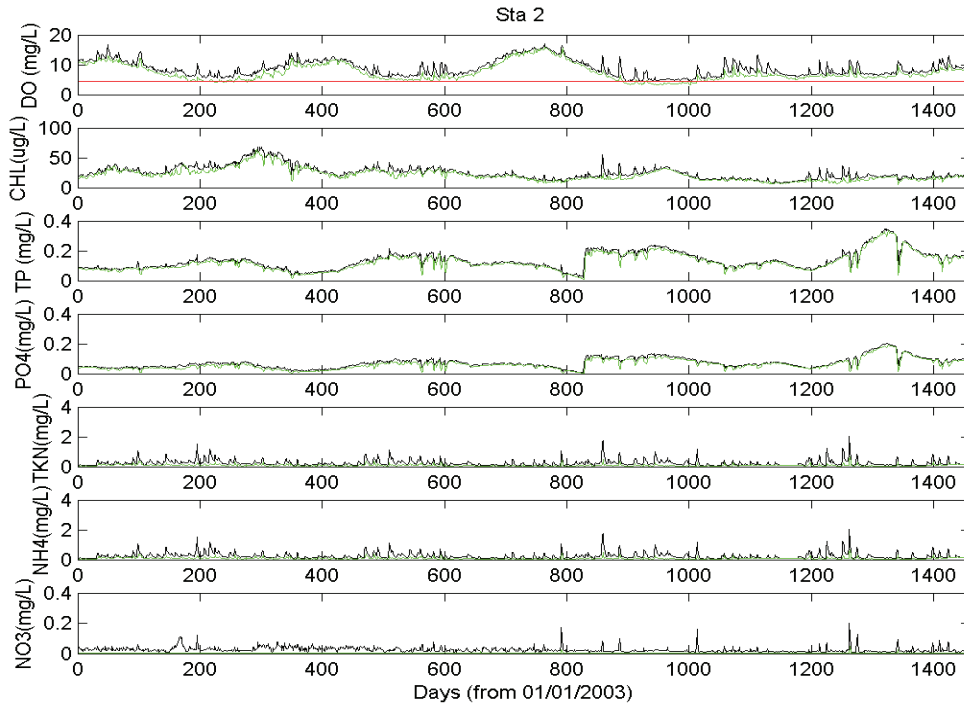

Figure VI.40. Predictions of DO, chl, TP, PO₄, TKN, NH₄, and NO₃ at Thalia Creek ConMon Station 4 in a sensitivity test using 70% NPS removal extended over a 4-year period.
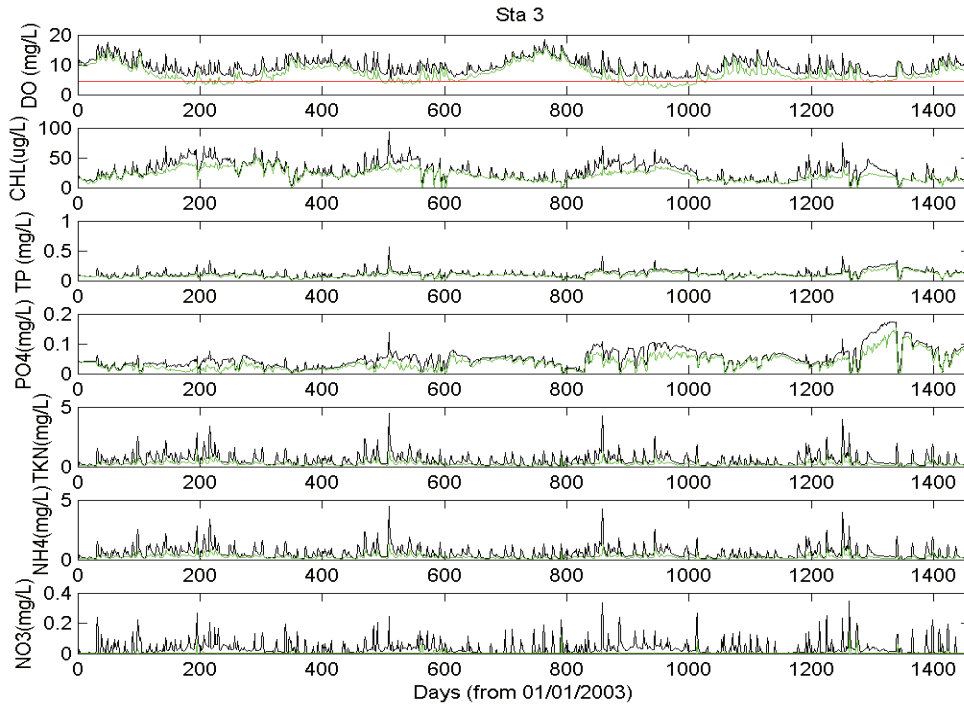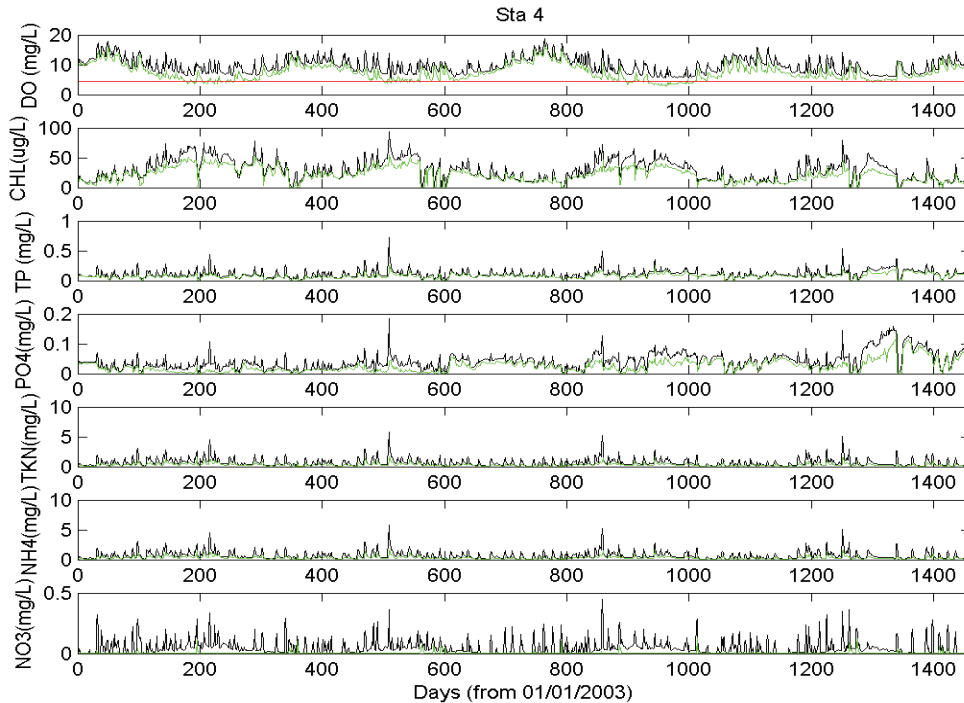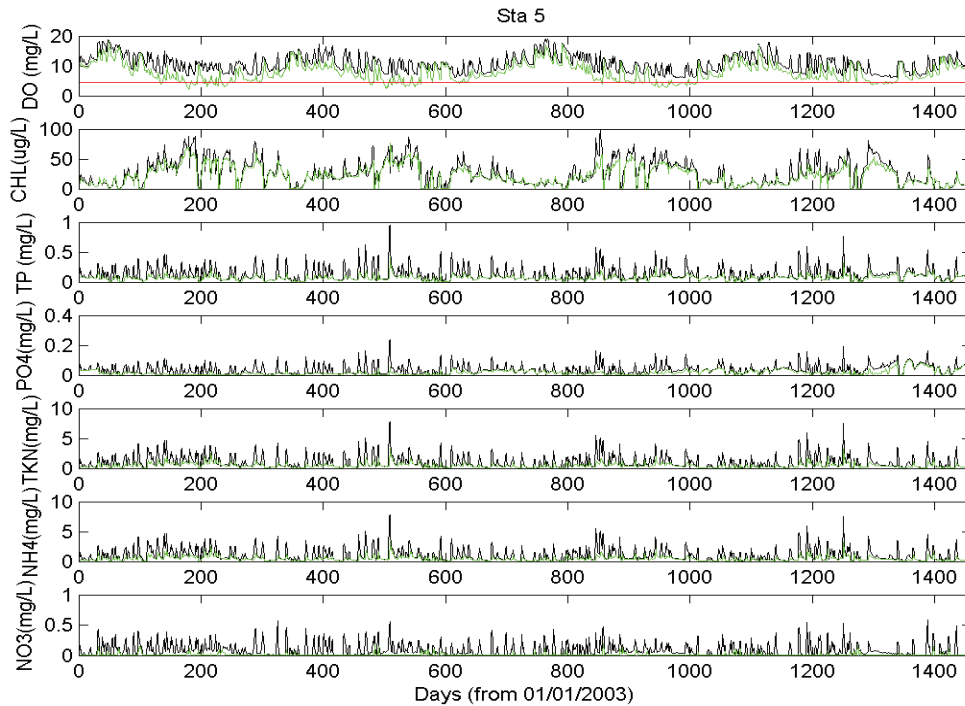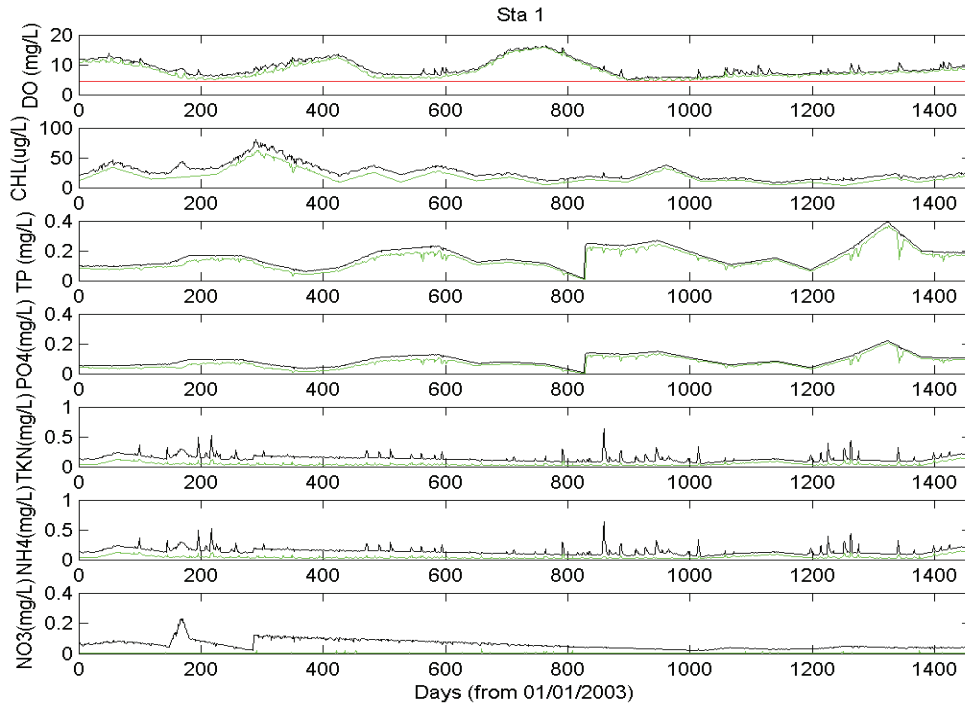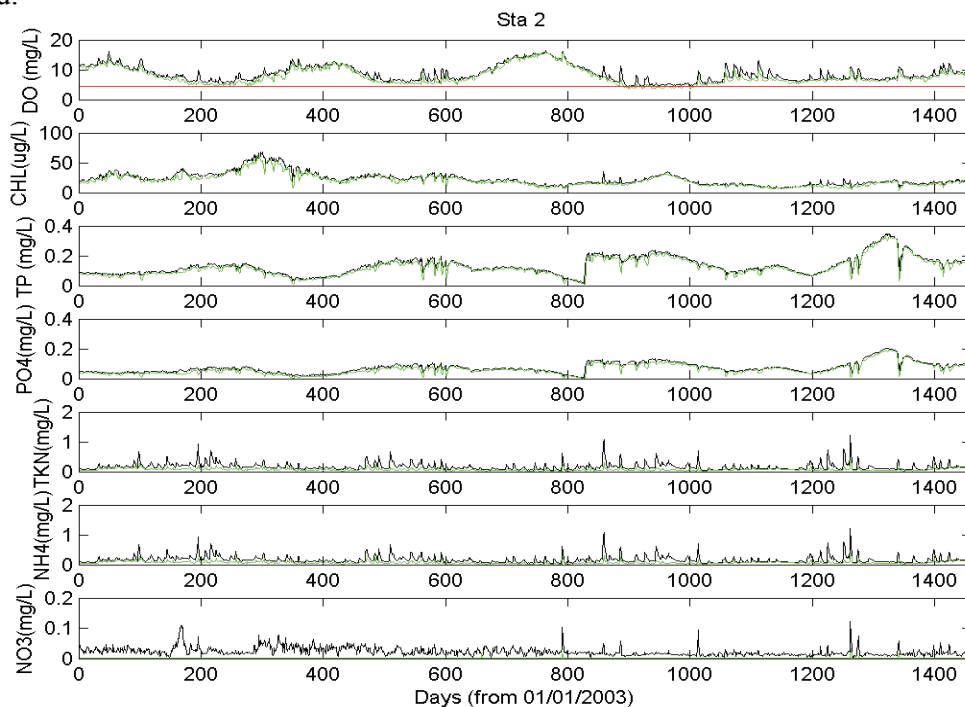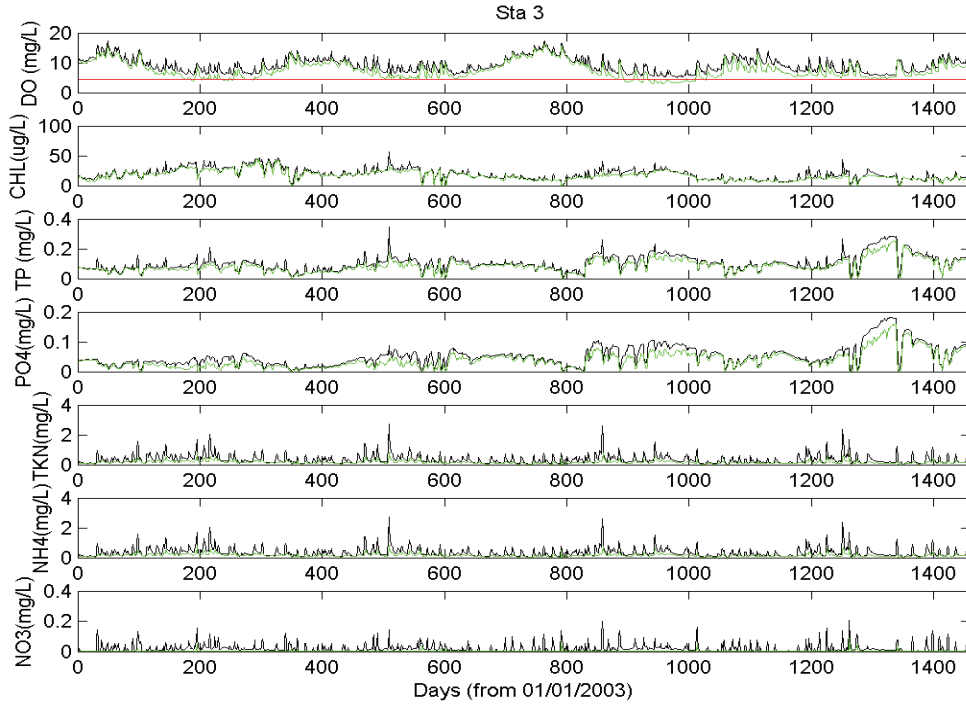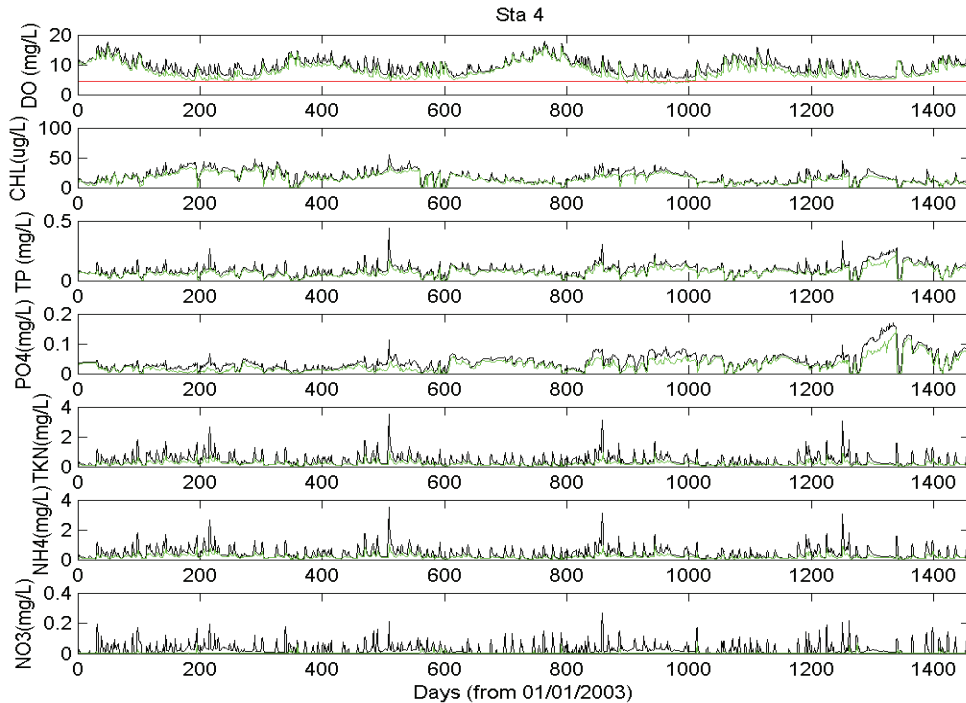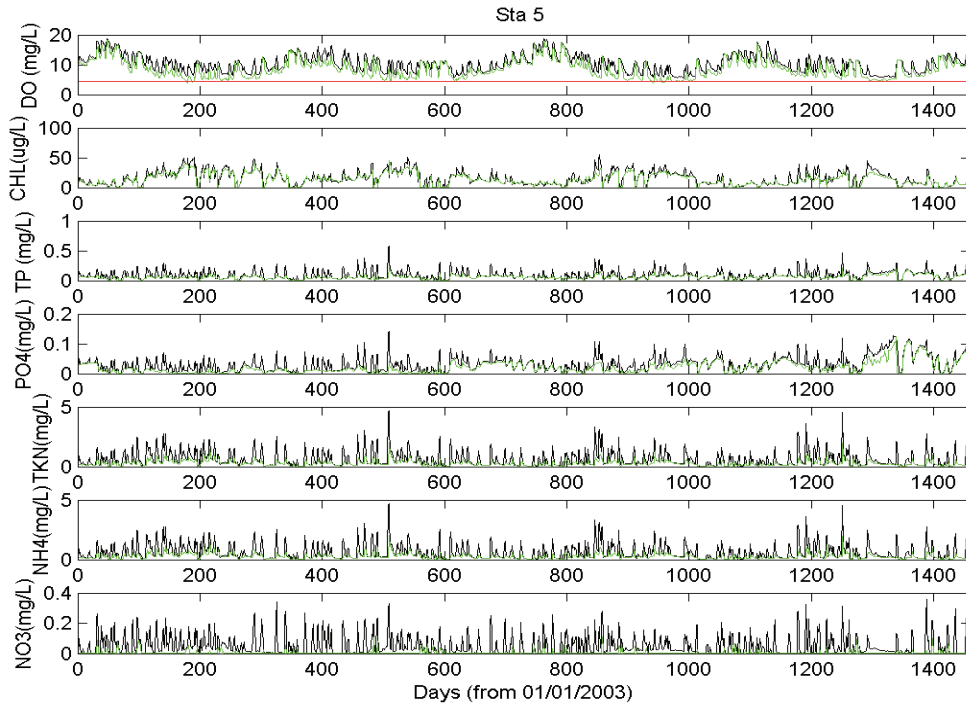
171

Figure VI.41. Predictions of DO, chl, TP, PO$_4$, TKN, NH$_4$, and NO$_3$ at Thalia Creek ConMon Station 5 in a sensitivity test using 70% NPS removal extended over a 4-year period.

CHAPTER VII. SUMMARY AND CONCLUSIONS

This report provides the results of VIMS efforts as related to the collection of temporally high-resolution water quality data, grab sample surveys for key water quality parameters, sediment characterization and sediment oxygen demand (SOD) studies, and the physical-water quality integrated numerical modeling exercises. The objectives of these efforts were to assess the roles of non-point source and internal loadings of nutrients and FCB in support of efforts to reduce eutrophic and microbiological water quality issues within the TB-TC system.

VIMS performed field surveys in summer 2009 spanning the TC-TB regions. High-frequency measurements of depth (surface elevation), salinity, water temperature, dissolved oxygen, chlorophyll, and turbidity were made at 5 locations in this region for periods of approximately ten days to two weeks each commencing in June, July, and August of 2009. Grab sample surveys were conducted at over 20 locations spanning this region on June 30, July 27, and August 27, 2009. These grab samples were each analyzed for water temperature, salinity, pH, dissolved oxygen, dissolved oxygen percent saturation, phosphate (PO_4), total dissolved phosphorus (TDP), ammonium (NH_4), nitrite (NO_2), nitrate-nitrite (NO_{23}), total dissolved nitrogen (TDN), the ratio of DIN:DIP, chlorophyll-a, pheo, fecal coliform, and *E. Coli*. It is noted that the parameters of dissolved organic phosphorus (DOP), nitrate (NO_3), dissolved inorganic nitrogen (DIN), and dissolved organic nitrogen (DON) were then calculated from these measurements. Two 30-day, high-frequency tide gauge deployments were conducted at locations in TC-TB in the latter part of 2009. All these data were added to the VIMS Lynnhaven River database. Additionally, sediment oxygen demand was measured and an additional grab sample survey was used to characterize the grain size distributions for more than 20 locations throughout the TB-TC system.

High (>20 to $\leq$ 60 ug·L^{-1}) to hyper-eutrophic (>60 ug·L^{-1}) concentrations of chl *a* were observed within the TB-TC system. Mean chl *a* concentrations and variability of measurements increased with distance upstream. High pheopigment to chl *a* ratios, particularly in the upper TC reaches, suggested a relatively degraded phytoplankton population possibly due to stress (e.g., light, salt) or elevated grazing pressures.

Dissolved oxygen patterns within the TB-TC system was highly dynamic and exhibited a strong diurnal signal driven by water temperature variation and biological activities. While most severe and chronic in the upper reaches, hypoxia (defined as $DO_{conc} \leq 2$ mg·L^{-1}) was observed throughout the TB-TC system. The duration of hypoxia ranged from 15 minutes to over 34 hours for a single event. The set-up and duration of severe hypoxia was influenced by solar insolation, timing of ebb-tide and freshwater input derived from storms. We have found that the oxygen and chlorophyll-a do not oscillate in the same frequency. DO is dominated by diurnal oscillations, while chlorophyll-a is more semi-diurnal. These observations indicate that benthic or attached algae may contribute to the DO diurnal oscillation which is less influenced by the tide.

All high-frequency monitoring stations exhibited negative mean net ecosystem metabolism (NEM) values ranging from -1.8 to -0.5 g O_2 m^{-2}·day^{-1} and respiration rates varying from 10.09-16.97 g O_2 m^{-2}·day^{-1}. Net summer heterotrophy increased with distance upstream and suggests that significant amounts of allochthonous sources of carbon are helping to fuel the high respiration rates. Sediment oxygen demand accounted for between 10-15% of open water respiration rates in the upper TC reach. Water column vertical light extinction coefficient (k_e) within the TB-TC system varied from 2.8 to 6.3 m^{-1} with corresponding $z_{1\%}$ depths (depths at which 1% of surface light is transmitted) ranging from 0.7 to 1.6 m, suggesting a limited role of benthic primary production in the channel regions in contrast to the shallower, broad shoal regions.

VIMS has completed a successful development of an integrated numerical modeling framework for the TB-TC system. This framework combines a high-resolution 3D hydrodynamic model (HEM-3D hydro) that provides the required transport for a water quality model (HEM-3D water quality) that, in turn, provides intra-tidal predictions of 23 water quality state variables. The hydrodynamic model underwent an extensive calibration for surface elevation, salinity, and temperature and the water quality model was calibrated for dissolved oxygen and chl-a.

Using the calibrated water quality model for the TB – TC system in the short-term (Julian Days 180 through 260 of 2009) simulations, several sensitivity tests were performed to assess the roles of non-point source (NPS) loadings and inputs from the bottom sediments. In these 80-day simulations, it was determined that even the total elimination of the NPS nutrients loadings could not bring the TC water quality for dissolved oxygen into compliance with state water quality standards within a short period due to high deposition of organics. An 80-day sensitivity test of a clean ("no sediment") river bottom was also conducted, and again DO levels often fell below the instantaneous criterion for DO (i.e., 4.3 mg·L^{-1}). The sensitivity test suggests that removal of sediment deposition without reducing nonpoint source loading will not solve the DO problem as nutrients can be quickly deposited to the bottom during high runoff events. Next, sensitivity tests were run that combined the clean river bottom and a 50% NPS reduction, and the results of these tests were that DO levels consistently exceeded the 4.3 mg·L^{-1} instantaneous minimum. Lastly, NPS loadings reductions were run as long-term (i.e., 4-year) simulations testing both 50% and 70% reductions from the TC watershed. It was determined that the DO criterion can be attained with approximately 70% reduction of nitrogen and carbon, and 40% reduction of phosphorus.

Fecal coliform bacteria (FCB) densities exceeded Commonwealth contact standards (> 200 MPN 100· ml^{-1}) in the upper reaches of TC on a routine basis while the lower and more open reaches of TB typically exhibited FCB densities between shellfish waters and recreational contact standards (> 14 MPN to ≤ 200 MPN·100 ml^{-1}). Findings are consistent with an increased "land effect" due to increases in the ratio of shoreline to water volume in the upper tidal reaches. Elevated FCB densities were also observed after periods of high rainfall. The relationship between FCB and *E. coli* density was strong (r^2 ≥ 0.95) for two of the three surveys; heavy rainfall and loadings of ubiquitous FC positive microbes may explain discrepancies with the third survey. Sources of FCB to the TB-TC

system would include nonpoint source runoff from urbanized and natural lands, and direct domestic and wild animal loadings. Additional study is required to source track and differentiate FCB loadings and to determine if true health concerns exist.

A fecal coliform model was also developed throughout the TB–TC system and simulations were performed for the fecal coliform load reductions. A long-term calibration was performed comparing model predictions with bi-monthly observations at VA-DEQ Station 7-THA000.76 for the period 2003-2006. Additionally, spatial comparisons were made between fecal coliform model predictions and the observations at more than 20 grab sample locations for two surveys (July 27, 2009 and August 30, 2009). The calibrated model was then used to assess fecal coliform loading reductions of 70%, 90%, 95% and 99%. It was determined that the swimming criterion (200 MPN·100 ml^{-1}) could be attained with approximately 90-95% reduction, whereas the shellfish harvesting criteria (14 MPN·100 ml^{-1} for 30-day geometric mean and 43 MPN·100 ml^{-1} for the 90th percentile) required a fecal coliform reduction of 99%.

VIII. REFERENCES

Alderisio, K. and N. deLuca. 1999. Seasonal enumeration of fecal coliform bacteria from the feces of Ring-billed Gulls (*Larus delawarensis*) and Canada Geese (*Branta Canadensis*). Applied and Environmental Microbiology 65(12): 5628-5630.

American Public Health Association. 1992. Standard Methods for the Examination of Water and Wastewater, 18th ed. American Public Health Association, Washington, D.C.

Bricker, S.B., C.G. Clement, D.E. Pirhalla, S.P. Orlando, and D.R.G. Farrow. 1999. National Estuarine Eutrophication Assessment: Effects of Nutrient Enrichment in the Nation's Estuaries. NOAA, National Ocean Service, Special Projects Office and the National Centers for Coastal Ocean Science. Silver Spring, MD: 71 pp.

Caffrey, J.M. 2004. Factors controlling net ecosystem metabolism in U.S. estuaries. Estuaries 27(1): 90-101.

Cerco, C.F., and Cole, T. 1994. Three-Dimensional Eutrophication Model of Chesapeake Bay. *Technical Report* EL-94-4, U.S. Army Engineer Waterways Experiment Station, Vicksburg, MS, 658.

D'Avanzo and J.N. Kremer. 1994. Diel oxygen dynamics and anoxic events in an eutrophic estuary of Waquoit Bay, Massachusetts. Estuaries 17(No. 1B): 131-139.

D'Avanzo, C., J.N. Kremer and S.C. Wainright. 1996. Ecosystem production and respiration in response to eutrophication in shallow temperate estuaries. Marine Ecology Progress Report 141: 263-274.

Dean, W.E., Jr. 1974. Determination of carbonate and organic matter in calcareous sediments and sedimentary rocks by loss on ignition: Comparison of methods. Journal of Sedimentary Petrology 44(1): 242-248.

D'Elia, C.F., P.A. Steudler, and N. Corwin. 1977. Determination of total nitrogen in aqueous samples using persulfate digestion. Limnology and Oceanography 22: 760-764.

DiToro, D. M., and J. J. Fitzpatrick. 1993. Chesapeake Bay sediment flux model, Contract Report EL-93-2, U. S. Army Engineer Waterways Experiment Station, Vicksburg, MS.

Engelsen, A., S. Hulth, L. Pihl, and K. Sundback. 2008. Benthic trophies status and nutrient fluxes in shallow-water sediments. Estuarine, Coastal and Shelf Science 78: 783-795.

Feng, P.C. and P.A. Hartman. 1982. Fluorogenic assays for immediate confirmation of *Escherichia coli*. Applied and Environmental Microbiology 43(6): 1320-1329.

Folk, R.L. 1980. Petrology of Sedimentary Rocks. Austin, Texas: Hemphill Publishing Company.

Genet, L., Smith, D., and M. Sonnen. 1974. Computer program documentation for the dynamic estuary model. U.S. Environmental Protection Agency, Systems Development Branch, Washington, DC.

Hamrick, J. M. 1994. Linking hydrodynamic and biogeochemical transport model s for estuarine and coastal waters. Estuarine and Coastal Modeling, Proceedings of the 3rd International Conference, M. L. Spaulding et al., Eds., American Society of Civil Engineers, New York, 591-608.

Hamrick, J. M. 1992. A three-dimensional environmental fluid dynamics computer code: theoretical and computational aspects. Special Report in Applied Marine Science and Ocean Engineering (SRAMSOE) # 317, Virginia Institute of Marine Science, Gloucester Pt., VA. 63 pp.

Hamrick, J. M. and Z. Yang. 1995. Lagrangian mean descriptions of long-term estuarine mass transport. Proceedings of the 1994 International Conference on the Physics of Estuaries and Bays. D. Aubrey, ED., American Geophysical Union.

Ho, G.C., A.Y. Kuo, and B.J. Neilson. 1977. A water quality study of Buchanan Creek, a small tributary of the Lynnhaven Bay system. Special Report No. 127 in Applied Marine Science and Ocean Engineering. Virginia Institute of Marine Science, Gloucester Point, VA. 47 pp.

HRPDC (Hampton Roads Planning District Commission). 2006. Draft Implementation Plan for the Fecal Coliform TMDL (Total Maximum Daily Load) for Shellfish Areas of Lynnhaven Bay, Broad Bay, and Linkhorn Bay Watersheds.

Hussong, D., J. Damare, R. Limpert, W. Sladen, R. Weiner, and R. Colwell. 1979. Microbial impact of Canada Geese (*Branta Canadensis*) and Whistling Swans (*Cygnus columbianus columbianus*) on aquatic ecosystems. Applied and Environmental Microbiology 37(1): 14-20.

Jassby, A., and T. Platt. 1976. Mathematical formulation of the relationship between photosynthesis and light for phytoplankton. Limnology and Oceanography, 21: 540–547.

Jeffrey, S.W., R.F. Mantoura, and S.W. Wright. 1996. Phytoplankton pigments in oceanography. UNESCO Publication. Paris, FR.

Kemp, W.M., P.A. Sampou, J. Tuttle and W.R. Boynton. 1992. Seasonal depletion of oxygen from bottom waters of Chesapeake Bay: Roles of benthic and planktonic respiration and physical exchange processes. Marine Ecology Progress Report 85: 2137-157.

Kemp, W.M., R. Batiuk, R. Bartleson, P. Bergstrom, V. Carter, C.L Gallegos, W. Hunley, L. Karrh, E.W. Koch, J.M. Landwehr, K.A. Moore, L. Murray, M. Naylor, N.B. Rybicki, J.C. Stevenson, and D.J. Wilcox. 2004. Habitat requirements for submerged aquatic vegetation in Chesapeake Bay: Water quality, light regime, and physical-chemical factors: Estuaries, v. 27, no. 3, p. 363–377.

Li, Y. 2006. Development of an Unstructured Grid, Finite Volume Eutrophication Model for the Shallow Water Coastal Bay: Application in the Lynnhaven River Inlet System. Ph.D. dissertation. Virginia Institute of Marine Science, College of William and Mary, 305 pp.

Malcolm Pirnie Engineers, Inc. 1980. Conditions in the Lynnhaven Estuarine System, Virginia Beach, Virginia. Prepared for Norfolk District Army Corps of Engineers.

Odum, H.T. 1956. Primary production in flowing waters. Limnology and Oceanography 1: 102-117.

Odum, E. 1971. Fundamentals of Ecology, 3rd ed. W. B. Saunders. Philadelphia, Pennsylvania.

Park, K., Kuo, A.Y., Shen, J., and J. M. Hamrick. 1995. A three-dimensional hydrodynamic-eutrophication model (HEM-3D): Description of water quality and sediment process sub-models. Special Report in Applied Marine Science and Ocean Engineering (SRAMSOE) # 327, Virginia Institute of Marine Science, Gloucester Pt., VA, 102 pp. and Appendices.

Parsons, T., Takahashi, M., and B. Hargrave. 1984. Biological oceanography processes, 3rd edition, Permagon Press, Oxford.

Redfield, A., B. Ketchum, and F. Richards. 1963. The influence of organisms on the composition of sea water. In: The Sea, Vol. 2. M. Hill (ed.). Wiley-Interscience. New York, NY. pp. 276-297.

Scavia, D. and S.B. Bricker. 2006. Coastal eutrophication assessment in the United States. Biogeochemistry 79: 187-208.

Shen, J. and W. Gong. 2009. Influence of model domain size, wind directions and Ekman transport on storm surge development inside the Cheasapeake Bay: a case study of extratropical cyclone Ernesto. Journal of Marine Systems, 75, 198-215.

Shima, F., W. Reay, D. Gallagher, G. Simmons, J. Waldon and K. Reay. 1994. Groundwater transport of fecal coliform bacteria to open coastal waters of Virginia's Coastal Plain: A GIS approach. Final report. Virginia Department of Environmental Quality, Coastal Resources Management Program. Richmond, VA.

Siewicki, T., T. Pullaro, W. Pan, S. McDaniel, R. Glenn, and J. Stewart. 2007. Models of total and presumed wildlife sources of fecal coliform bacteria in coastal ponds. Journal of Environmental Management 82: 120-132.

Simmons. G., S. Herbein, and C. James. 1995. Managing nonpoint fecal coliform sources to tidal inlets. Journal of Contemporary Water research and Education 100: 64-74.

Sisson, M., Wang, H., Li, Y., Shen, J., Kuo, A., and W. Gong. 2008. Technical Support in Engineering Construction Phase of Craney Island Eastward Expansion. Final Report to Craney Island Design Partners and the U.S. Army Corps of Engineers, Norfolk District. Virginia Institute of Marine Science. Special Report No. 400 in Applied Marine Science and Ocean Engineering. 156 pp. & Appendices.

Solorzano, L. 1969. Determination of ammonia in natural waters by the phenol hypochlorite method. Limnology and Oceanography 14: 799-801.

Thomann, R., and J. Fitzpatrick. 1982. Calibration and verification of a mathematical model of the eutrophication of the Potomac Estuary. HydroQual Inc., Mahwah, NJ.

Thomann, R.V. and J.A. Mueller. 1987. Principles of Surface Water Quality Modeling and Control. Harper and Row, Publishers. New York. 644 pp.

Tyler, R.M., D.C. Brady, and T.E. Targett. 2009. Temporal and spatial dynamics of diel-cycling hypoxia in estuarine tributaries. Estuaries and Coasts 32: 123-145.

URS Corporation, Virginia Beach Office. 2006. Hydrologic Concepts and Parameter Development. Work Order 8B, URS Project No. 11656274. Technical Memorandum. Prepared for City of Virginia Beach. 5 pp. and Appendices.

URS Corporation, Virginia Beach Office. 2007. Historic Water Quality Monitoring Data Evaluation. A&E Contract PWCN-6-0026. Technical Memorandum. Prepared for City of Virginia Beach. 18 pp. and Appendices.

U. S. Army Corps of Engineers. 2002. Lynnhaven River Restoration – Reconnaissance Report. Fort Norfolk District. 18 pp. Available at Website:http://www.nao.usace.army.mil/Projects/Lynnhaven/Lynnhaven.html

U.S. Environmental Protection Agency. 1983. Methods for Chemical Analysis of Water and Wastes. Washington, D.C.: EPA-600/4-79-020.

U.S. Environmental Protection Agency. 1988. Water Quality Standards Criteria Summaries: A Compilation of State/Federal Criteria. Office of Water Regulations and Standards, Washington, DC. EPA/440/5-88-023. 84pp.

Valiela, I., M. Alber, and M. LaMontagne. 1991. Fecal coliform loadings and stocks in Buttermilk Bay, Massachusetts, USA, and Management Implications. Environmental Management 15(5): 659-674.

Virginia State Water Control Board. 2009. 9 VAC 25-260 Virginia Water Quality Standards. Statutory Authority: § 62.1-44.15 3a of the Code of Virginia, with amendments effective August 20, 2009.

VaDEQ/VaDCR. 2004. Virginia water quality assessment 305(b)/303(d) integrated report. Virginia Departments of Environmental Quality and Conservation and Recreation. Richmond, VA, 505p. plus appendices.

Wezernak, C. T., and J. J. Gannon. 1968. Evaluation of nitrification in streams. Journal of the Sanitary Engineering Division, ASCE, 94(SA5): 883-895.